Electronic Supplementary Information (ESI)

Click-tambjamines as efficient and tunable bioactive anion transporters

Israel Carreira-Barral,[a] Marcin Mielczarek,[a] Daniel Alonso-Carrillo,[a] Valeria Capurro,[b] Vanessa Soto-Cerrato,[c] Ricardo Pérez-Tomás,[c] Emanuela Caci,[b] María García-Valverde[a] and Roberto Quesada[a]*

[a] Departamento de Química, Universidad de Burgos, Burgos, 09001, Spain. E-mail: rquesada@ubu.es
[b] UOC Genetica Medica, IRCSS Istituto Giannina Gaslini, Genova, Italy.
[c] Department of Pathology and Experimental Therapeutics, Faculty of Medicine, Universitat de Barcelona, Barcelona, Spain.

Contents

1. STRUCTURES OF THE STUDIED COMPOUNDS

(a)

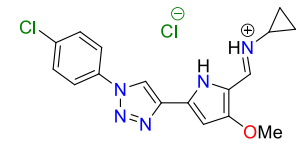

1

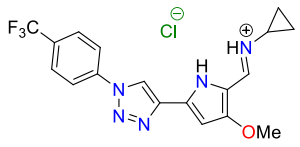

4

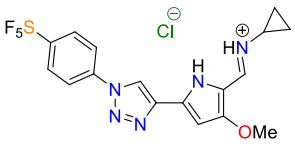

7

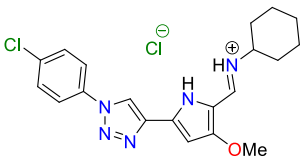

2

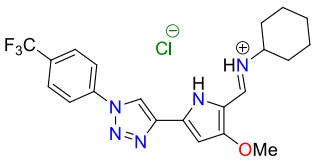

5

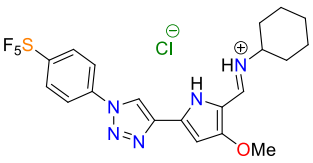

8

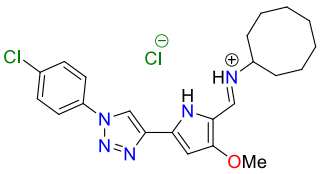

3

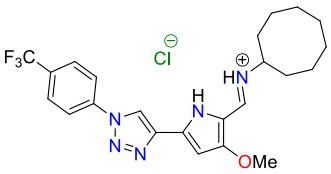

6

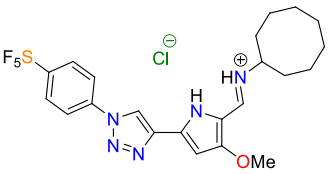

9

(b)

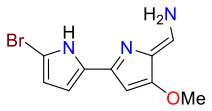

Tambjamine B

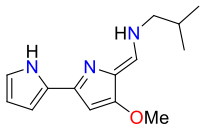

Tambjamine C

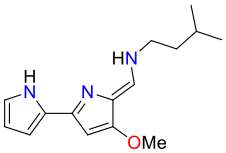

Tambjamine K

Chart 1. (a) Structures of the studied compounds. (b) Three representative examples of natural tambjamines.

2. SYNTHESES AND CHARACTERISATION DATA

2.1. General procedures and methods

Commercial reagents were employed as received without any further purification. NMR spectra were recorded at 298 K on a Varian Mercury-300 MHz spectrometer, employing $CDCl_3$ or DMSO-d_6 as solvents, with their residual signals being used to reference the spectra. High-resolution mass spectra were performed on an Agilent 6545 Q-TOF mass spectrometer coupled to a 1260 Infinity liquid chromatographer from the same brand; the ionisation source employed was electrospray in its positive mode. Absorption and emission spectra were recorded in Hitachi U-3900 and F-7000 spectrophotometers, respectively. X-ray diffraction studies were carried out at 298 or 100 K on Bruker Smart APEX CCD or Bruker D8 VENTURE diffractometers.

2.2. Precursors and intermediates

2.2.1. Compound A1

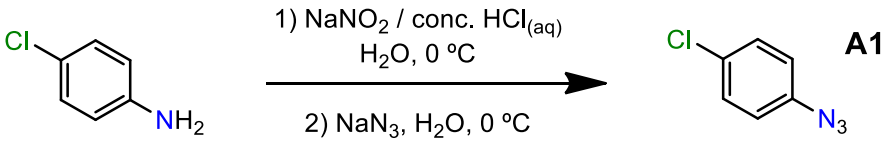

4-Chloroaniline (2.51 g, 19.7 mmol) was mixed with conc. HCl aqueous solution (20 mL) and the obtained mixture was stirred vigorously at 0 °C (ice bath) for 15 min. Note 1: the aniline was not dissolved. A solution of sodium nitrite (2.04 g, 29.6 mmol, 1.5 equiv.) in water (15 mL) was added in a dropwise manner over a period of 5 min. Note 2: formation of a yellow solution was observed. The mixture was stirred at 0 °C for an additional 30 min. A solution of sodium azide (2.56 g, 39.4 mmol, 2.0 equiv.) in water (15 mL) was added dropwise at 0 °C within 5 min and the resulting reaction mixture was stirred vigorously at room temperature for a further 3 h. Note 3: addition of the sodium azide solution resulted in the disappearance of the yellow colour. The mixture was extracted with ethyl acetate (3 × 35 mL), the extracts were combined, washed with water (1 × 50 mL), dried over anhydrous sodium sulphate, filtered and concentrated under reduced pressure to give compound **A1** as a yellow liquid (2.80 g, 93%).[1] ^{1}H NMR (300 MHz, $CDCl_3$): δ (ppm) = 7.34-7.28 (m, 2H), 6.99-6.92 (m, 2H). ^{13}C NMR (75 MHz, $CDCl_3$): δ (ppm) = 138.7 (ArC), 130.3 (ArC), 129.9 (ArCH), 120.4 (ArCH). No satisfactory HR-MS (+ESI) analysis result was obtained for **A1**.

[1] Z.-C. Dai, Y.-F. Chen, M. Zhang, S.-K. Li, T.-T. Yang, L. Shen, J.-X. Wang, S.-S. Qian, H.-L. Zhu and Y.-H. Ye, *Org. Biomol. Chem.*, 2015, **13**, 477-486.

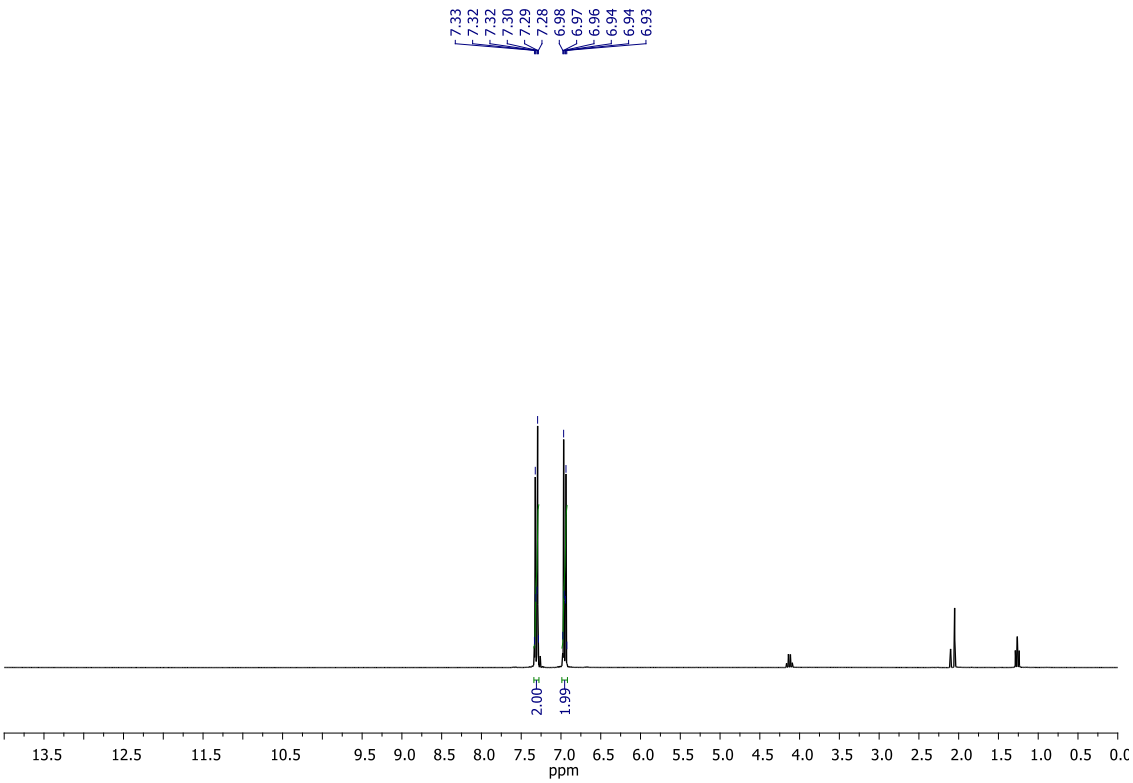

Figure S1. ^{1}H NMR spectrum (300 MHz, $CDCl_3$) for compound **A1**.

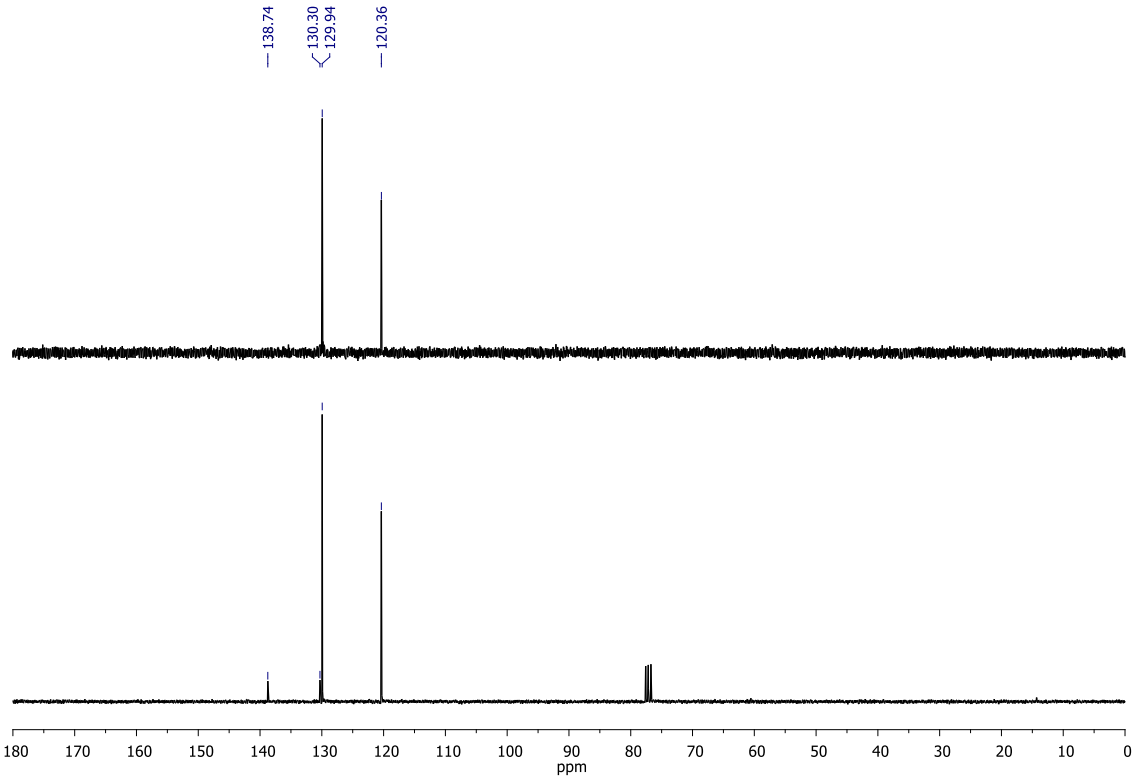

Figure S2. ^{13}C NMR and DEPT spectra (75 MHz, $CDCl_3$) for compound **A1**.

2.2.2. Compound A2

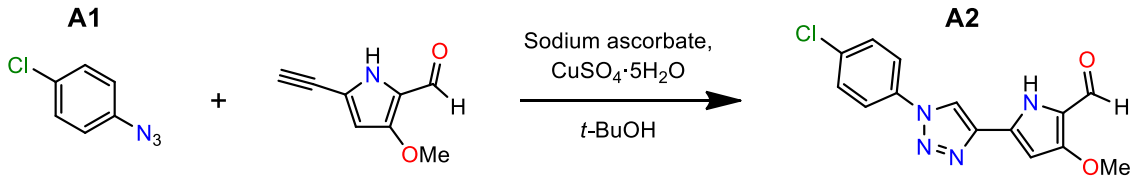

5-ethynyl-3-methoxy-1H-pyrrole-2-carbaldehyde (1.01 g, 6.77 mmol) and compound **A1** (1.05 g, 6.84 mmol, 1.0 equiv.) were dissolved partially in *tert*-butanol (20 mL) in a 250 mL Schlenk tube. A solution of (+)-sodium L-ascorbate (271 mg, 1.37 mmol, 0.2 equiv.) in water (10 mL) and a solution of $CuSO_4 \cdot 5H_2O$ (168 mg, 0.67 mmol, 0.1 equiv.) in water (10 mL) were subsequently added to the resulting suspension. Note: a gradual change of colour from dark brown to pale brown was observed upon addition of the $CuSO_4$ solution. The tube was closed with a stopper and the reaction mixture was stirred at room temperature for 18 h. The content of the flask was poured into water (100 mL), the precipitate was filtered out, washed with water (3 × 30 mL), diethyl ether (3 × 50 mL) and air-dried to give compound **A2** as a brown powder (1.41 g, 69%).[1,2] ^{1}H NMR (300 MHz, DMSO-d_6): δ (ppm) = 12.07 (s, 1H, NH), 9.48 (s, 1H, CHO), 9.12 (s, 1H, triazole CH), 7.96-7.65 (m, 4H), 6.52 (s, 1H), 3.89 (s, 3H). ^{13}C NMR (75 MHz, DMSO-d_6): δ (ppm) = 173.9 (CHO), 140.4 (ArC), 135.1 (ArC), 133.3 (ArC), 130.0 (ArCH), 129.1 (ArC), 121.8 (ArCH), 120.2 (ArCH), 118.8 (ArC), 93.8 (ArCH), 58.0 (CH_3). HR-MS (+ESI): found *m/z* 303.0647 ($[M+H]^+$), $[C_{14}H_{11}ClN_4O_2H]^+$ requires *m/z* 303.0643 (monoisotopic mass).

[2] (a) A. J. McCarroll, C. S. Matthews, G. Wells, T. D. Bradshaw and M. F. G. Stevens, *Org. Biomol. Chem.*, 2010, **8**, 2078-2084; (b) R. J. Detz, S. A. Heras, R. de Gelder, P. W. N. M. van Leeuwen, H. Hiemstra, J. N. H. Reek and J. H. van Maarseveen, *Org. Lett.*, 2006, **8**, 3227-3230.

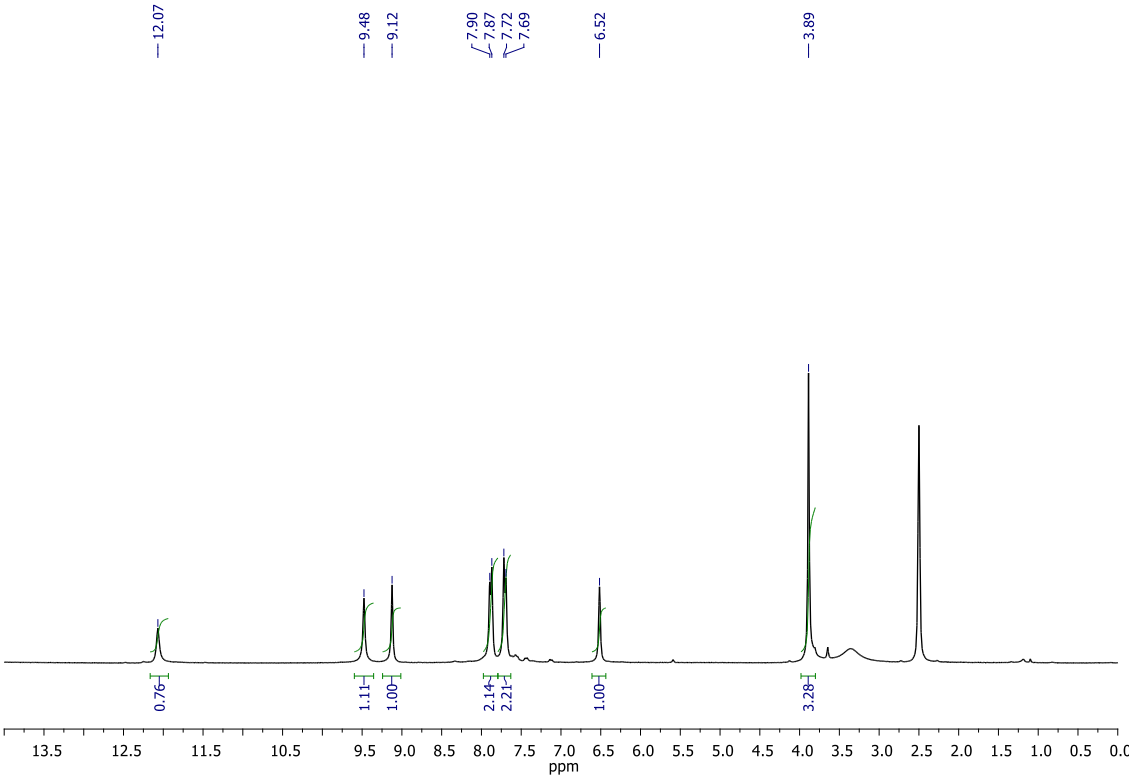

Figure S3. ^{1}H NMR spectrum (300 MHz, DMSO-d_6) for compound **A2**.

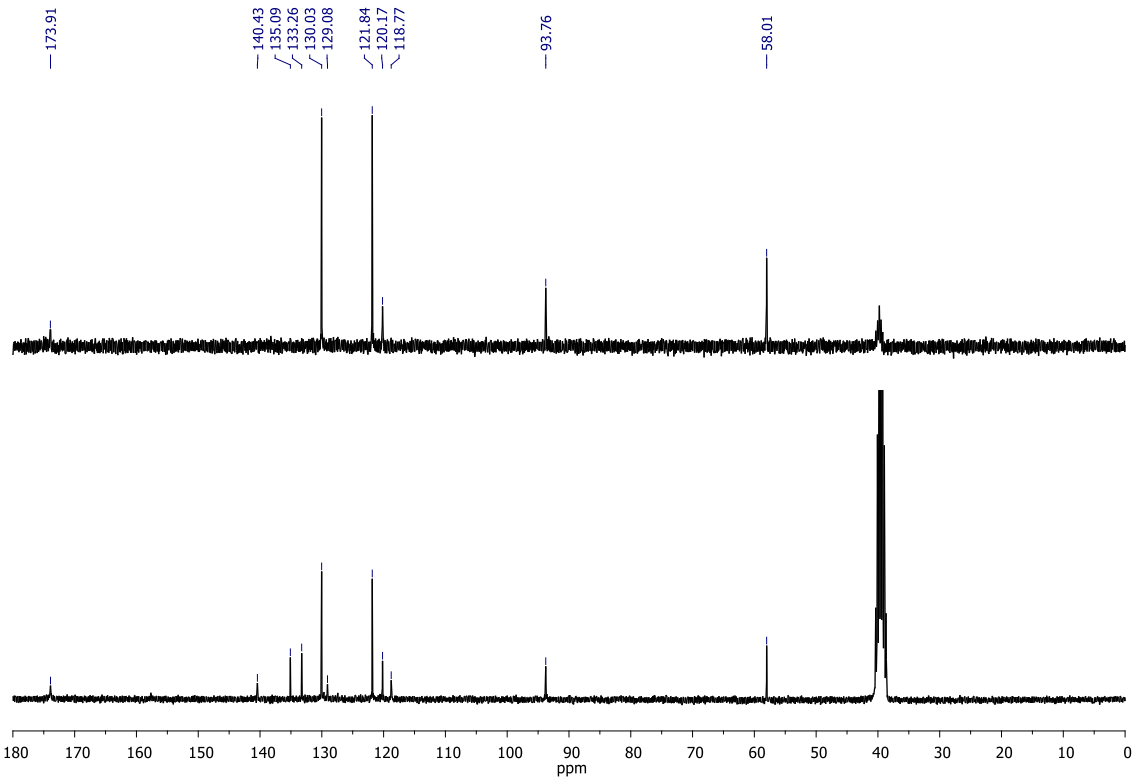

Figure S4. ^{13}C NMR and DEPT spectra (75 MHz, DMSO-d_6) for compound **A2**.

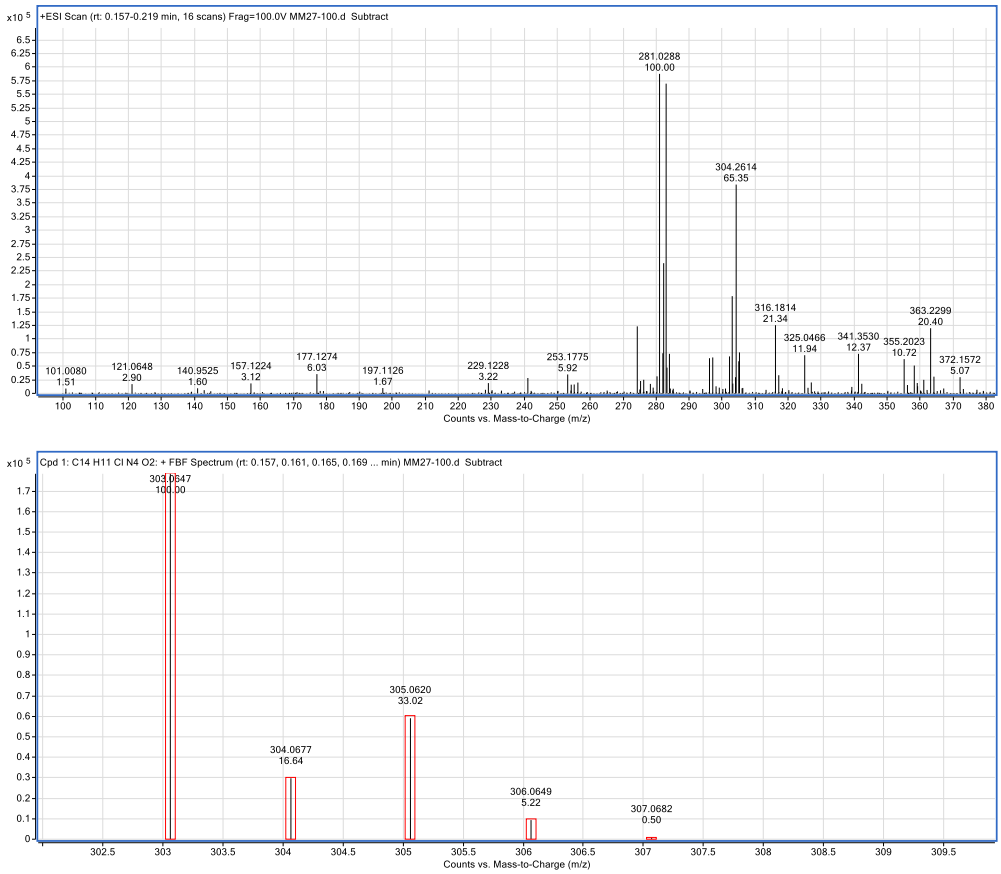

Figure S5. HR-MS (ESI^+) spectrum for compound **A2**.

2.2.3. Compound B1

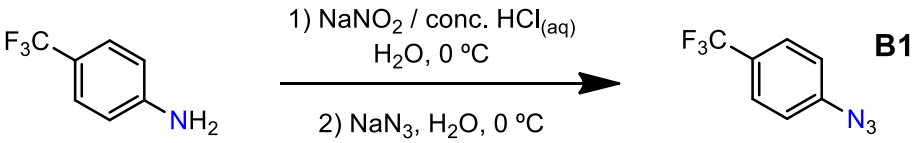

4-(trifluoromethyl)aniline (3.0 mL, 24.0 mmol) was mixed with conc. HCl aqueous solution (20 mL) and the obtained mixture was stirred vigorously at 0 °C (ice bath) for 15 min. Note 1: the aniline was not dissolved. A solution of sodium nitrite (2.55 g, 37.0 mmol, 1.5 equiv.) in water (15 mL) was added in a dropwise manner over a period of 5 min. Note 2: formation of a yellow solution was observed. The mixture was stirred at 0 °C for an additional 30 min. A solution of sodium azide (3.13 g, 48.1 mmol, 2.0 equiv.) in water (15 mL) was added dropwise at 0 °C within 5 min and the resulting reaction mixture was stirred vigorously at room temperature for a further 3 h. Note 3: addition of the sodium azide solution resulted in the disappearance of the yellow colour. The mixture was extracted with ethyl acetate (3 × 35 mL), the extracts were combined, washed with water (1 × 50 mL), dried over anhydrous sodium sulphate, filtered and concentrated under reduced pressure to give compound **B1** as a yellow liquid (1.94 g, 43%). ^{1}H NMR (300 MHz, $CDCl_3$): δ (ppm) = 7.62-7.54 (m, 2H), 7.09-7.01 (m, 2H). ^{13}C NMR (75 MHz, $CDCl_3$): δ (ppm) = 143.9 (ArC), 127.1 (q, ^{3}J = 3.8 Hz, ArCH), 124.1 (q, ^{1}J = 272 Hz, CF_3), 119.3 (ArCH). No satisfactory HR-MS (+ESI) analysis result was obtained for **B1**.

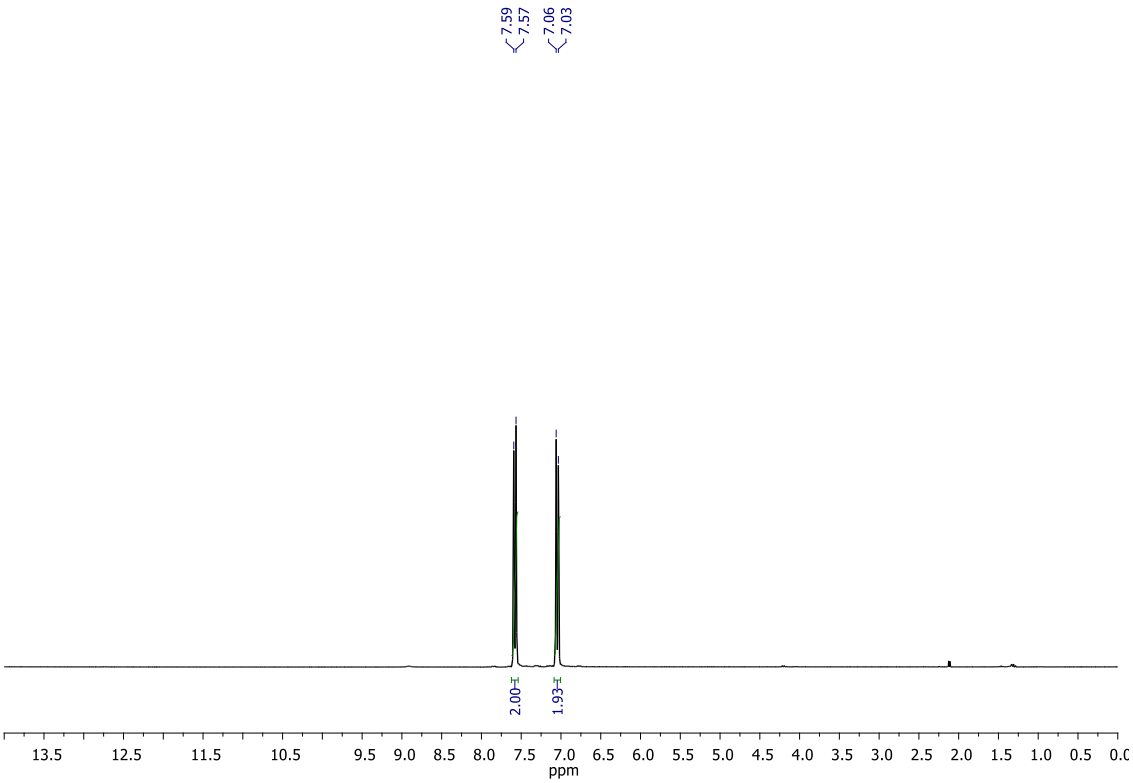

Figure S6. ^{1}H NMR spectrum (300 MHz, $CDCl_3$) for compound **B1**.

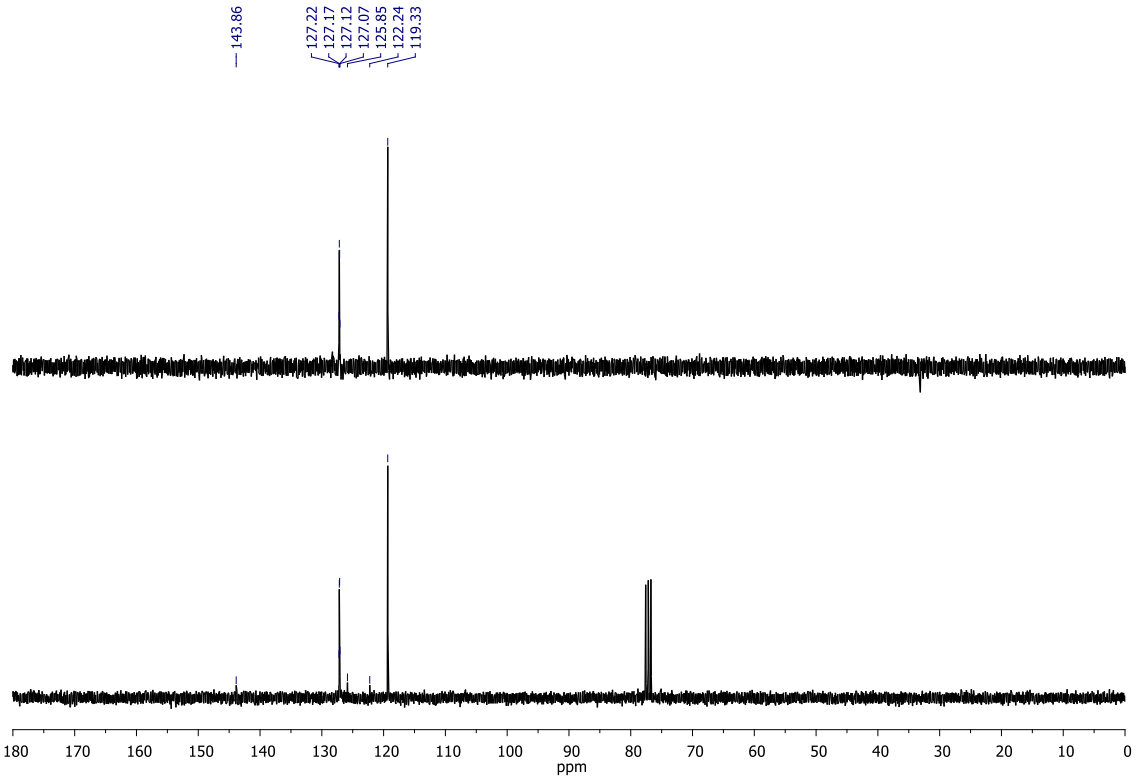

Figure S7. ^{13}C NMR and DEPT spectra (75 MHz, $CDCl_3$) for compound **B1**.

2.2.4. Compound B2

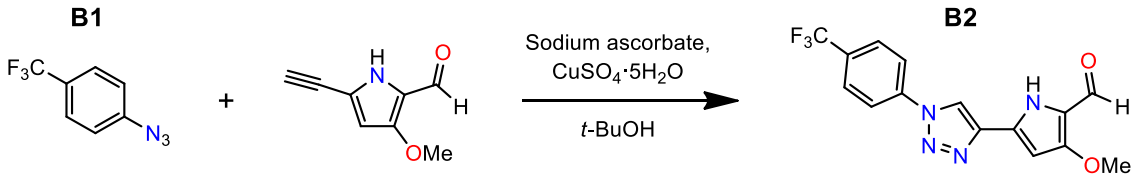

5-ethynyl-3-methoxy-1H-pyrrole-2-carbaldehyde (1.71 g, 11.5 mmol, 1.0 equiv.) and compound **B1** (2.14 g, 11.4 mmol) were dissolved partially in *tert*-butanol (20 mL) in a 250 mL Schlenk tube. A solution of (+)-sodium L-ascorbate (434 mg, 2.19 mmol, 0.2 equiv.) in water (10 mL) and a solution of $CuSO_4 \cdot 5H_2O$ (286 mg, 1.15 mmol, 0.1 equiv.) in water (10 mL) were subsequently added to the resulting suspension. Note: a gradual change of colour from dark brown to pale brown was observed upon addition of the $CuSO_4$ solution. The tube was closed with a stopper and the reaction mixture was stirred at room temperature for 4 days. The content of the flask was poured into water (100 mL), the precipitate was filtered out, washed with water (3 × 30 mL), diethyl ether (3 × 50 mL) and air-dried to give compound **B2** as a brown non-crystalline solid (1.37 g, 36%). ^{1}H NMR (300 MHz, DMSO-d_6): δ (ppm) = 12.13 (s, 1H, NH), 9.48 (s, 1H, CHO), 9.25 (s, 1H, triazole CH), 8.18-7.98 (m, 4H), 6.55 (s, 1H), 3.90 (s, 3H). HR-MS (+ESI): found *m/z* 337.0909 ($[M+H]^+$), $[C_{15}H_{11}F_3N_4O_2H]^+$ requires *m/z* 337.0907 (monoisotopic mass). Note: no suitable ^{13}C NMR spectrum could be obtained due to the low solubility of the compound in the selected solvent.

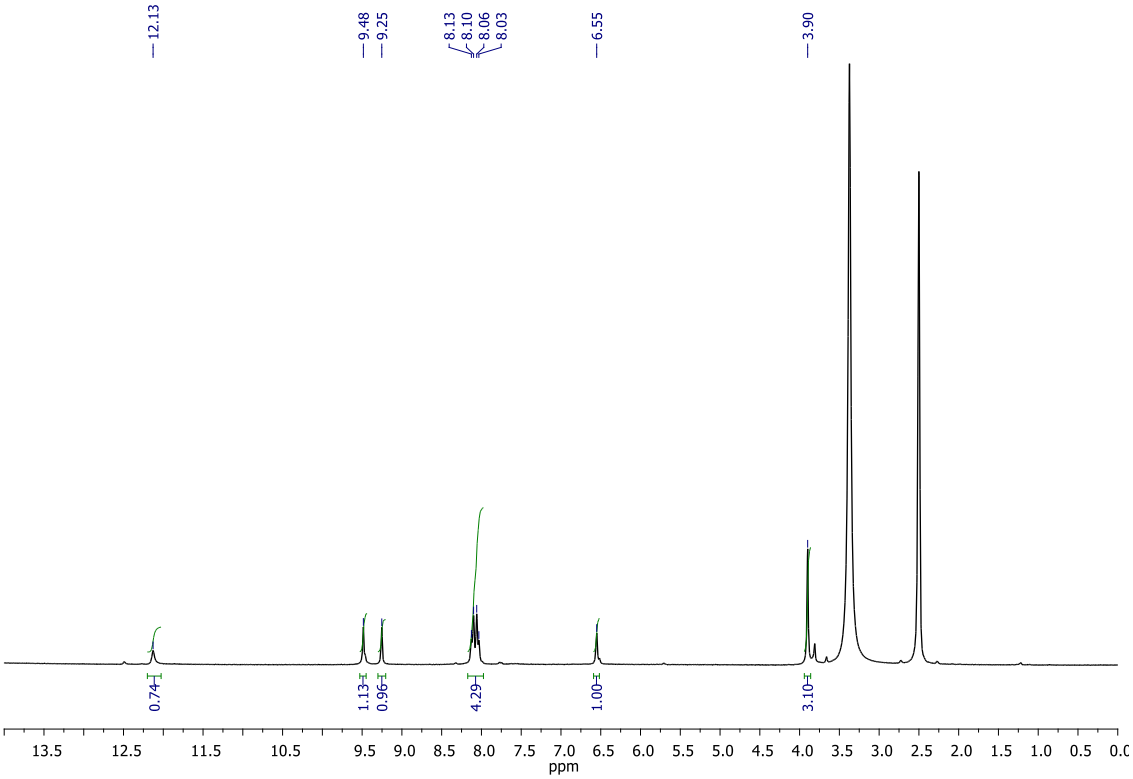

Figure S8. ^{1}H NMR spectrum (300 MHz, DMSO-d_6) for compound **B2**.

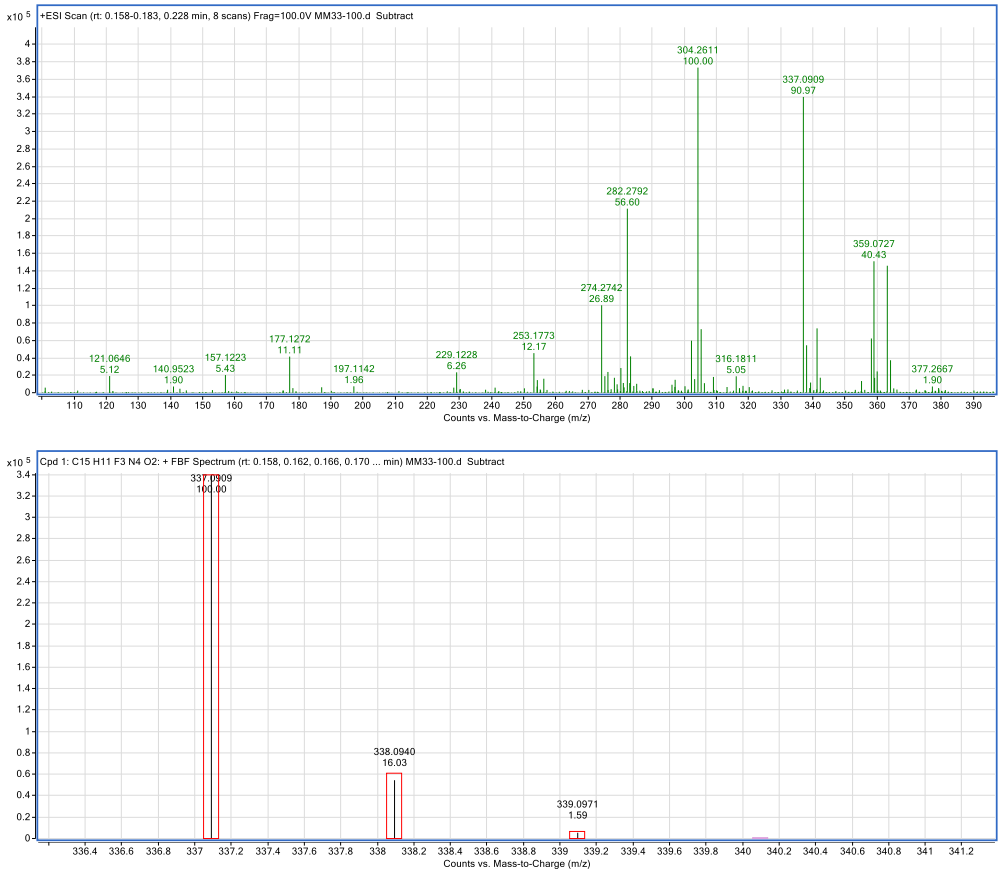

Figure S9. HR-MS (ESI^{+}) spectrum for compound **B2**.

2.2.5. Compound C1

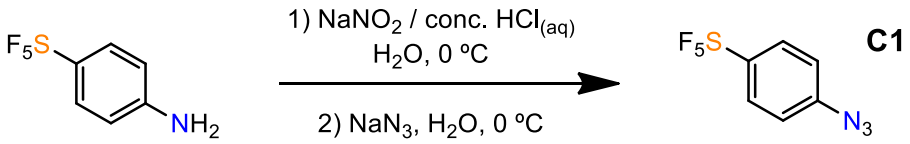

4-(pentafluoro-λ^6-sulfanyl)aniline (3.51 g, 16.0 mmol) was mixed with conc. HCl aqueous solution (20 mL) and the obtained mixture was stirred vigorously at 0 °C (ice bath) for 15 min. Note 1: the aniline was not dissolved. A solution of sodium nitrite (1.66 g, 24.1 mmol, 1.5 equiv.) in water (15 mL) was added in a dropwise manner over a period of 5 min. Note 2: formation of a yellow solution was observed. The mixture was stirred at 0 °C for an additional 30 min. A solution of sodium azide (2.08 g, 32.0 mmol, 2.0 equiv.) in water (15 mL) was added dropwise at 0 °C within 5 min and the resulting reaction mixture was stirred vigorously at room temperature for a further 3 h. Note 3: addition of the sodium azide solution resulted in the disappearance of the yellow colour. The mixture was extracted with ethyl acetate (3 × 35 mL), the extracts were combined, washed with water (1 × 50 mL), dried over anhydrous sodium sulphate and concentrated under reduced pressure to give compound **C1** as a yellow liquid (3.67 g, 93%). ^{1}H NMR (300 MHz, $CDCl_3$): δ (ppm) = 7.77-7.69 (m, 2H), 7.11-7.03 (m, 2H). ^{13}C NMR (75 MHz, $CDCl_3$): δ (ppm) = 150.3 (quint, ^{2}J = 19 Hz, ArC), 143.6 (ArC), 127.9 (quint, ^{3}J = 4.5 Hz, ArCH), 119.0 (ArCH). No satisfactory HR-MS (+ESI) analysis result was obtained for **C1**.

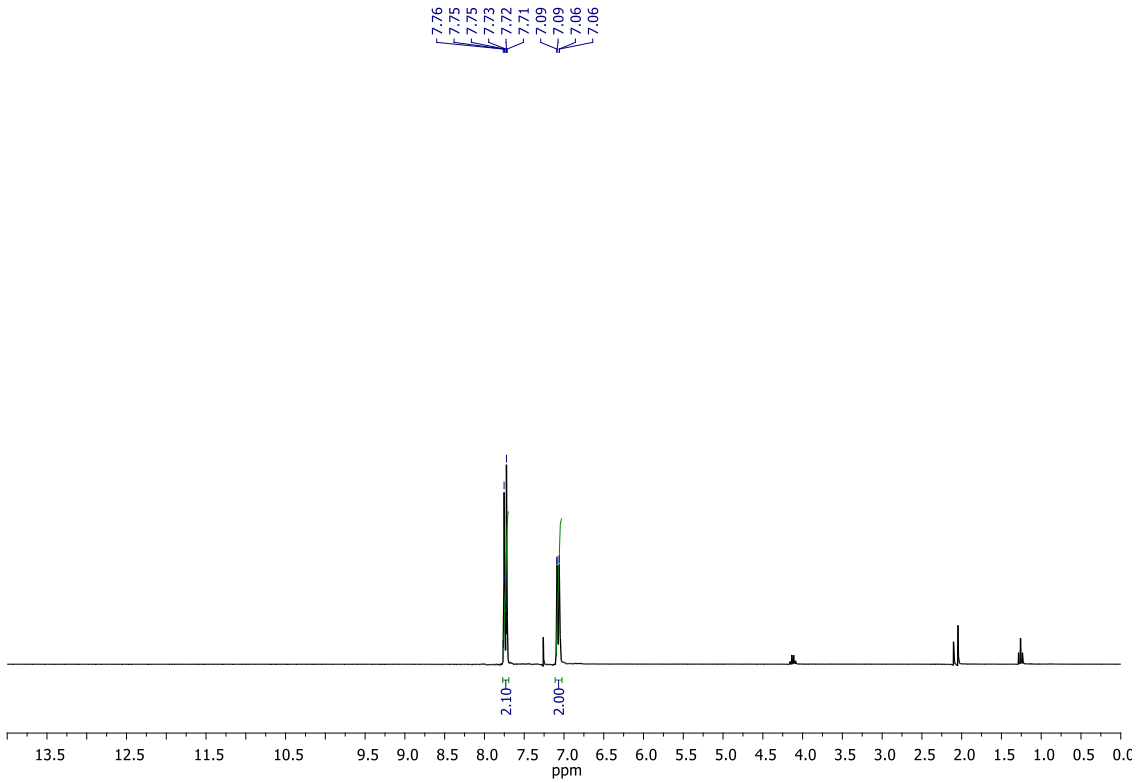

Figure S10. ^{1}H NMR spectrum (300 MHz, $CDCl_3$) for compound **C1**.

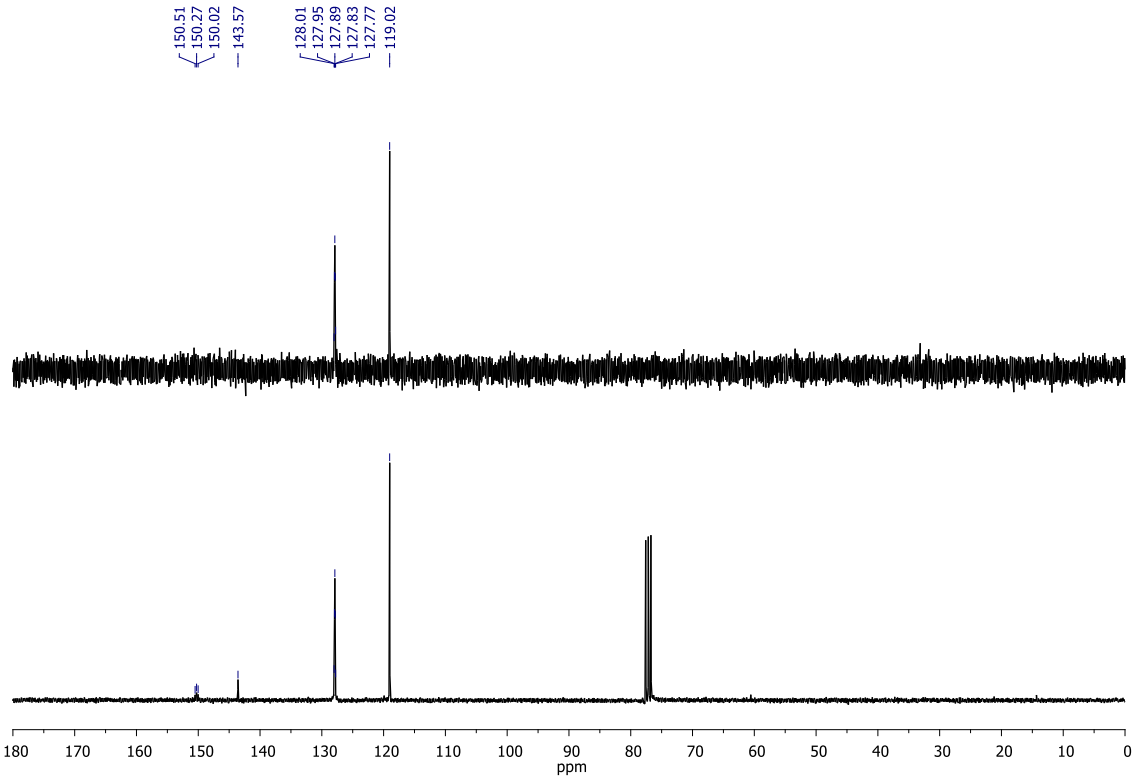

Figure S11. ^{13}C NMR and DEPT spectra (75 MHz, $CDCl_3$) for compound **C1**.

2.2.6. Compound C2

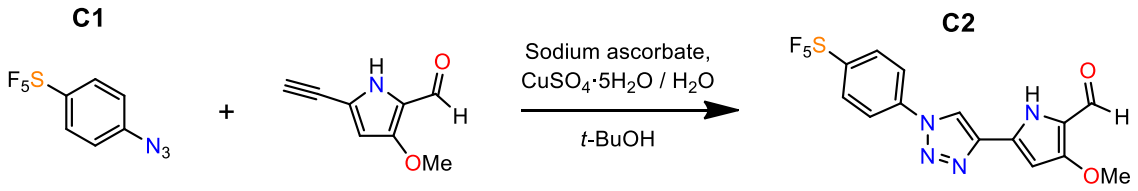

5-ethynyl-3-methoxy-1H-pyrrole-2-carbaldehyde (2.24 g, 15.0 mmol) and compound **C1** (3.67 g, 15.0 mmol, 1.0 equiv.) were dissolved partially in *tert*-butanol (20 mL) in a 250 mL Schlenk tube. A solution of (+)-sodium L-ascorbate (596 mg, 3.01 mmol, 0.2 equiv.) in water (10 mL) and a solution of $CuSO_4 \cdot 5H_2O$ (379 mg, 1.52 mmol, 0.1 equiv.) in water (10 mL) were subsequently added to the resulting suspension. Note: a gradual change of colour from dark brown to pale brown was observed upon addition of the $CuSO_4$ solution. The tube was closed with a stopper and the reaction mixture was stirred at room temperature for 3 days. The content of the flask was poured into water (100 mL), the precipitate was filtered out, washed with water (3 × 30 mL), diethyl ether (3 × 50 mL) and air-dried to give compound **C2** as a brown non-crystalline solid (3.79 g, 64%). ^{1}H NMR (300 MHz, DMSO-d_6): δ (ppm) = 12.12 (s, 1H, NH), 9.48 (s, 1H, CHO), 9.26 (s, 1H, triazole CH), 8.28-8.04 (m, 4H), 6.55 (s, 1H), 3.89 (s, 3H). ^{13}C NMR (75 MHz, DMSO-d_6): δ (ppm) = 174.0 (CHO), 157.6 (ArC), 151.9 (quint, ^2J = 17 Hz, ArC), 140.7 (ArC), 138.6 (ArC), 128.8 (ArC), 128.1 (quint, ^3J = 4.5 Hz, ArCH), 120.6 (ArCH), 120.4 (ArCH), 118.9 (ArC), 94.0 (ArCH), 58.1 (CH_3). HR-MS (+ESI): found *m/z* 395.0606 ($[M+H]^+$), $[C_{14}H_{11}F_5N_4O_2SH]^+$ requires *m/z* 395.0596 (monoisotopic mass).

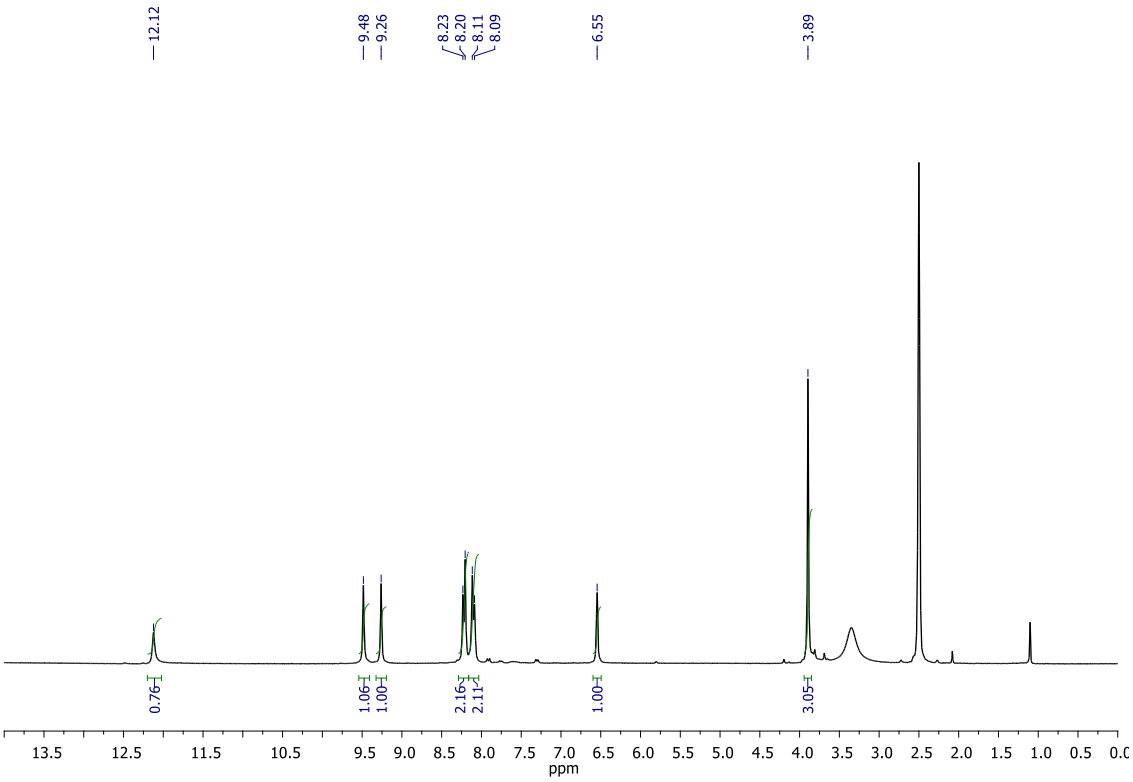

Figure S12. ^{1}H NMR spectrum (300 MHz, DMSO-d_6) for compound **C2**.

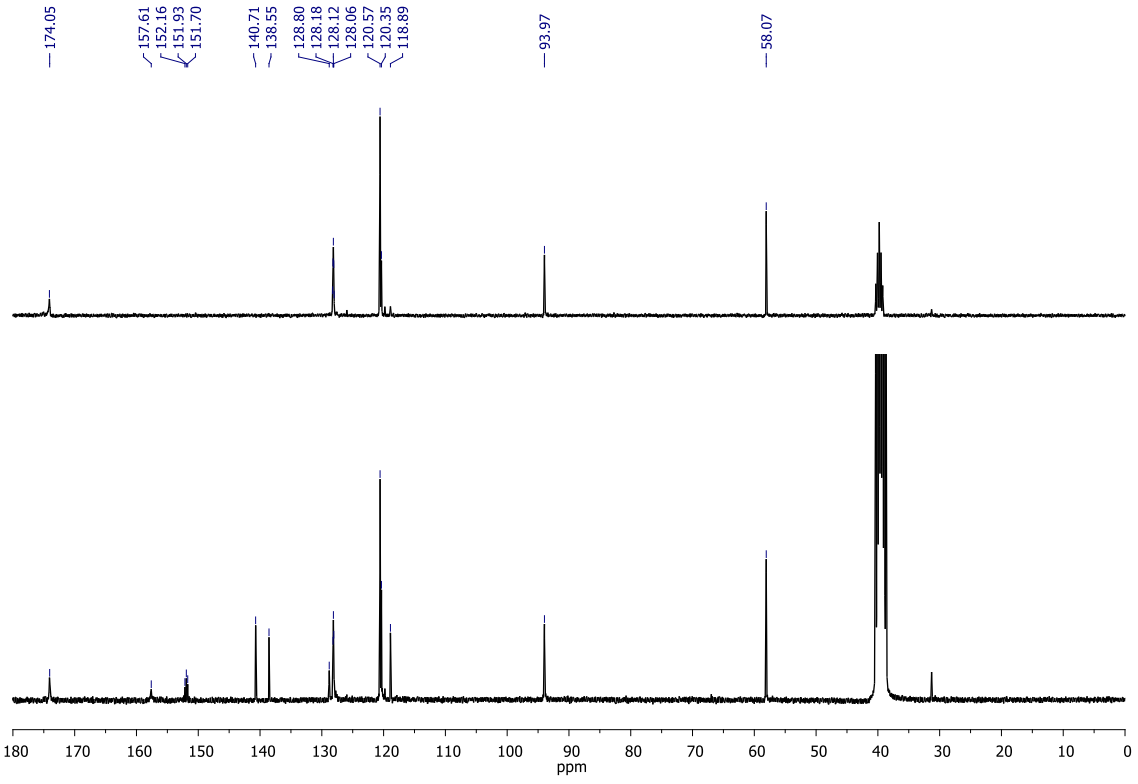

Figure S13. ^{13}C NMR and DEPT spectra (75 MHz, DMSO-d_6) for compound **C2**.

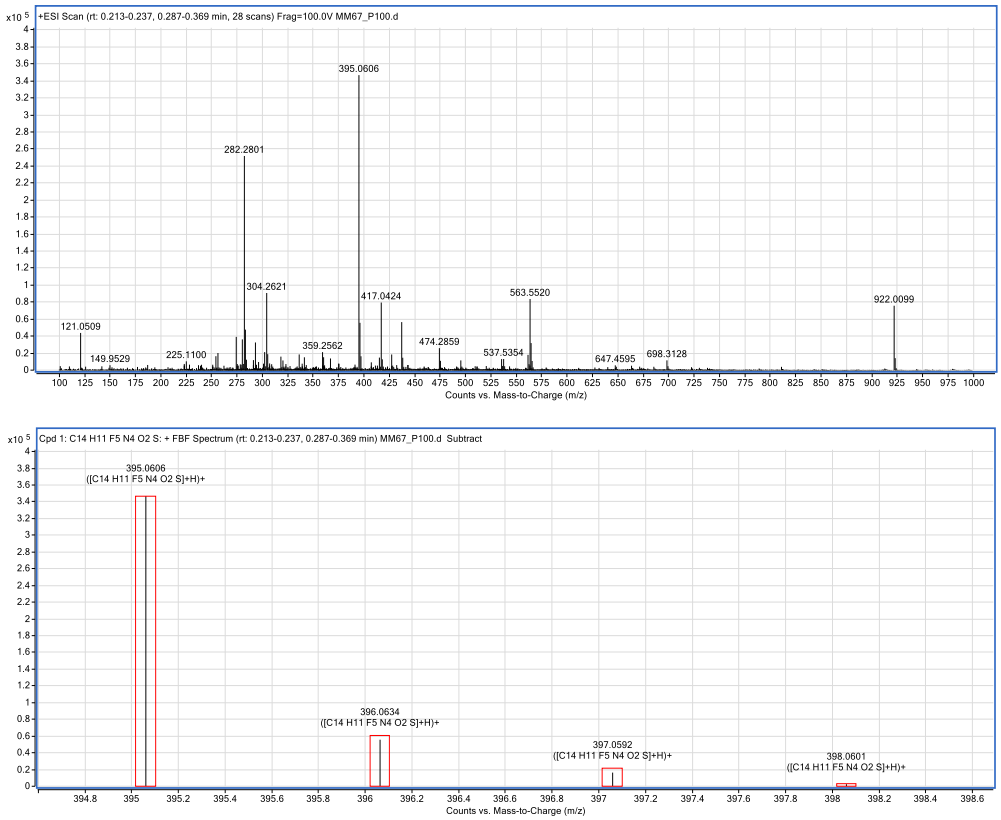

Figure S14. HR-MS (ESI$^+$) spectrum for compound **C2**.

2.3. Click tambjamines

2.3.1. Compound 1

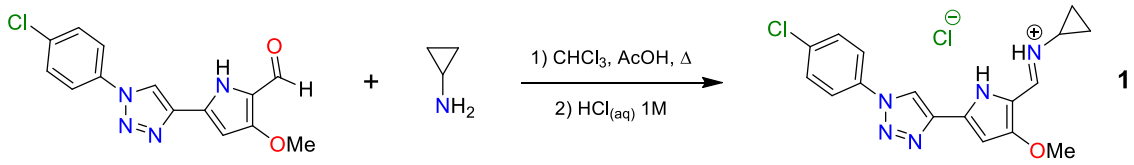

A mixture of aldehyde **A2** (454 mg, 1.50 mmol), cyclopropylamine (207 µL, 2.99 mmol, 2.0 equiv.) and glacial acetic acid (50 µL) in chloroform (10 mL) was stirred at 45 °C for 6 hours. Upon cooling to room temperature the chloroform was evaporated under reduced pressure and the residue was redissolved in dichloromethane (30 mL). The solution of the crude compound was washed with a 1 M aqueous HCl solution (3 × 20 mL), dried over anhydrous sodium sulphate, filtered and evaporated to dryness under reduced pressure. The residue was recrystallised from a mixture of dichloromethane and *n*-hexane to give compound **1** as dark brown crystals (294 mg, 52%). Slow evaporation of a solution of the compound in *n*-butanol provided dark brown single crystals, suitable for X-ray diffraction analysis. ^{1}H NMR (300 MHz, $CDCl_3$): δ (ppm) = 13.78 (s, 1H, NH), 11.26 (d, J = 15 Hz, 1H, NH), 9.09 (s, 1H, triazole CH), 7.83-7.75 (m, 2H), 7.76 (d, J = 15 Hz, 1H, overlapped with phenyl ArH), 7.56-7.48 (m, 2H), 6.56 (d, J = 1.8 Hz, 1H), 3.99 (s, 3H), 3.18-3.06 (m, 1H), 1.15-0.96 (m, 4H). ^{13}C NMR (75 MHz, $CDCl_3$): δ (ppm) = 163.4 (ArC), 144.2 (imine CH), 140.0 (ArC), 139.2 (ArC), 135.2 (ArC), 134.9 (ArC), 130.2 (ArCH), 122.0 (ArCH), 121.4 (ArCH), 111.8 (ArC), 93.8 (ArCH), 58.9 (CH_3), 32.5 (CH), 7.0 (CH_2). HR-MS (+ESI): found m/z 342.1125 ($[M+H]^+$), $[C_{17}H_{16}ClN_5OH]^+$ requires m/z 342.1116 (monoisotopic mass).

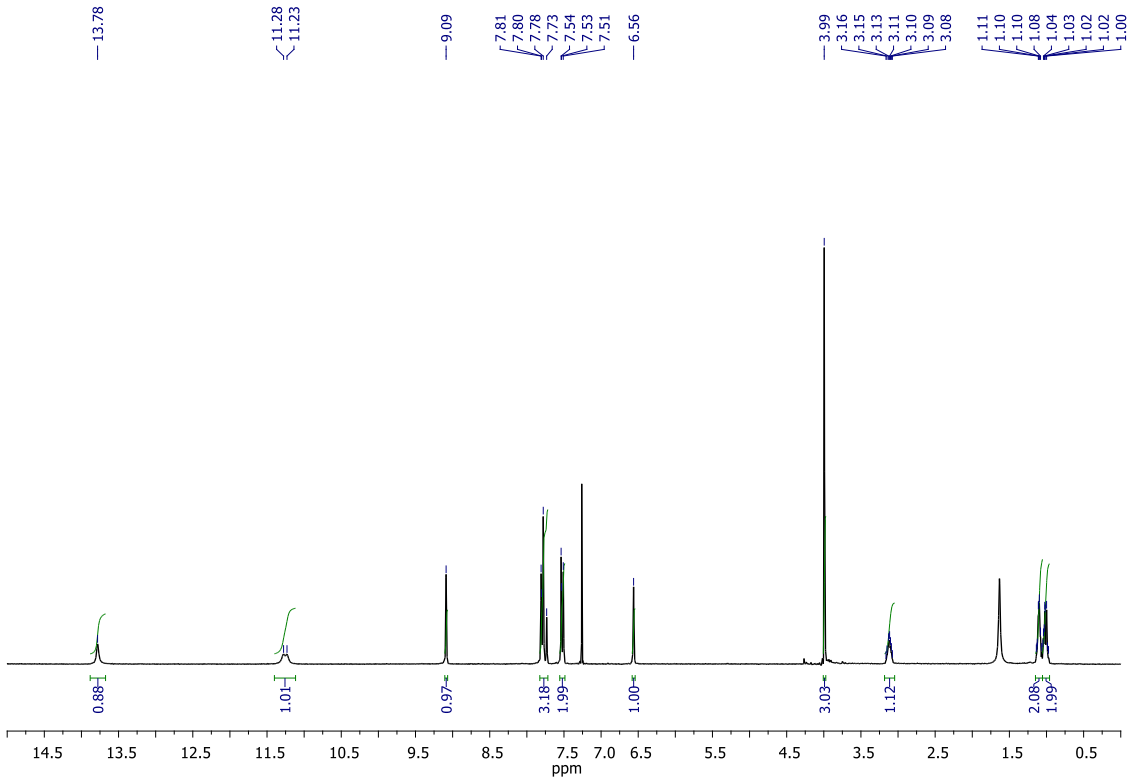

Figure S15. ^{1}H NMR spectrum (300 MHz, $CDCl_3$) for compound **1**.

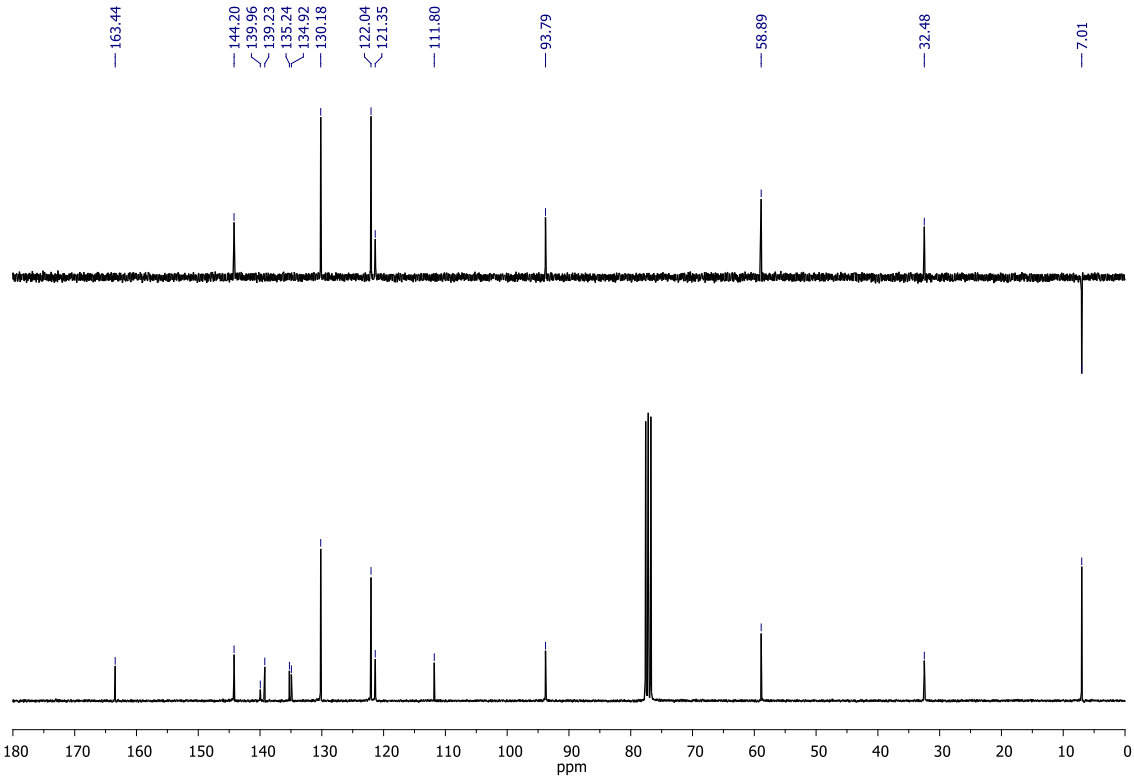

Figure S16. ^{13}C NMR and DEPT spectra (75 MHz, $CDCl_3$) for compound **1**.

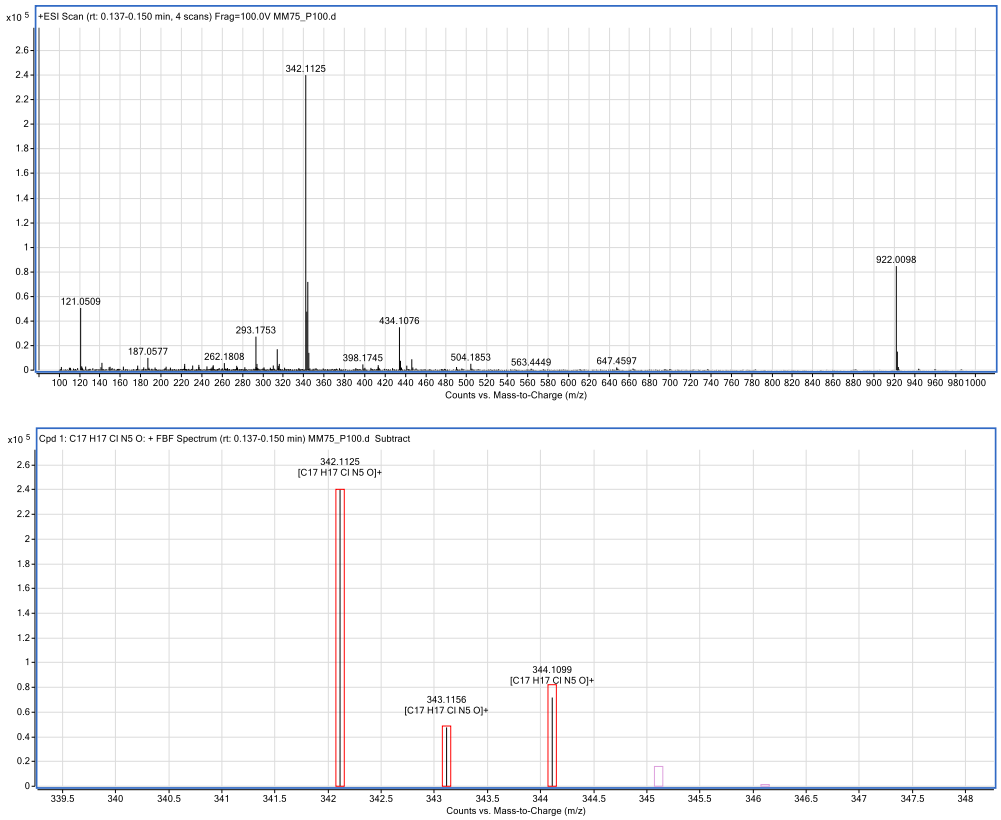

Figure S17. HR-MS (ESI^+) spectrum for compound **1**.

2.3.2. Compound 2

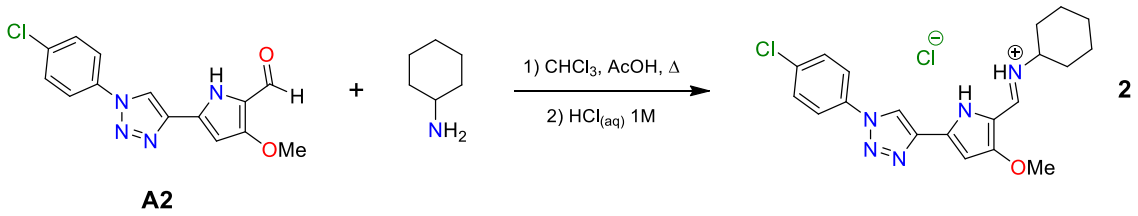

A mixture of aldehyde **A2** (253 mg, 0.84 mmol), cyclohexylamine (191 µL, 1.67 mmol, 2.0 equiv.) and glacial acetic acid (50 µL) in chloroform (10 mL) was stirred at 60 °C for 5.5 hours. Upon cooling to room temperature the chloroform was evaporated under reduced pressure and the residue was redissolved in dichloromethane (30 mL). The solution of the crude compound was washed with a 1 M aqueous HCl solution (3 × 20 mL), dried over anhydrous sodium sulphate, filtered and evaporated to dryness under reduced pressure. The residue was recrystallised from a mixture of dichloromethane and *n*-hexane to give compound **2** as a brown non-crystalline solid (100 mg, 29%). Slow evaporation of a solution of the compound in *n*-butanol provided orange single crystals, suitable for X-ray diffraction analysis. ^{1}H NMR (300 MHz, $CDCl_3$): δ (ppm) = 13.79 (s, 1H, NH), 11.28-11.05 (m, 1H, NH), 9.09 (s, 1H, triazole CH), 7.82-7.74 (m, 2H), 7.66 (d, J = 15 Hz, 1H), 7.54-7.46 (m, 2H), 6.52 (d, J = 3.0 Hz, 1H), 3.95 (s, 3H), 3.54-3.38 (m, 1H), 2.14-2.00 (m, 2H), 1.95-1.82 (m, 2H), 1.75-1.55 (m, 3H), 1.43-1.16 (m, 3H). ^{13}C NMR (75 MHz, $CDCl_3$): δ (ppm) = 163.1 (ArC), 142.1 (imine CH), 140.0 (ArC), 138.4 (ArC), 135.1 (ArC), 134.9 (ArC), 130.1 (ArCH), 122.0 (ArCH), 121.2 (ArCH), 111.4 (ArC), 93.6 (ArCH), 60.7 (CH), 58.8 (CH_3), 32.9 (CH_2), 24.7 (CH_2), 24.6 (CH_2). HR-MS (+ESI): found m/z 384.1578 ($[M+H]^+$), $[C_{20}H_{22}ClN_5OH]^+$ requires m/z 384.1586 (monoisotopic mass).

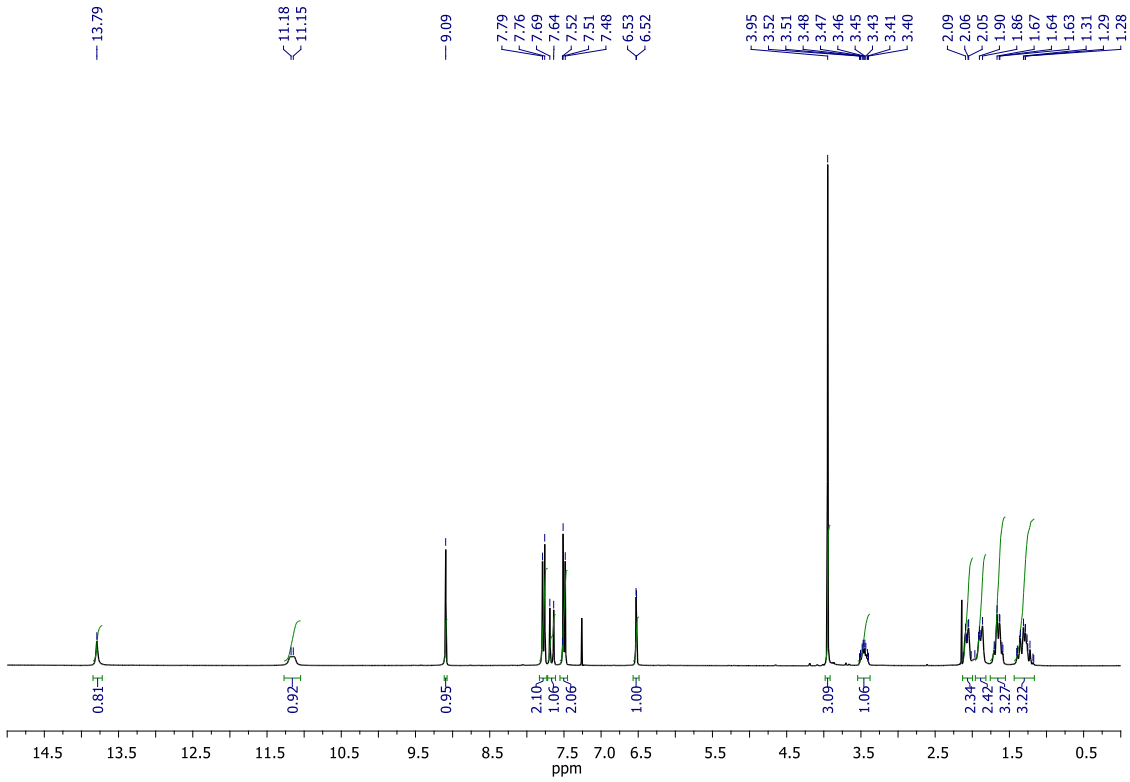

Figure S18. ^{1}H NMR spectrum (300 MHz, $CDCl_3$) for compound **2**.

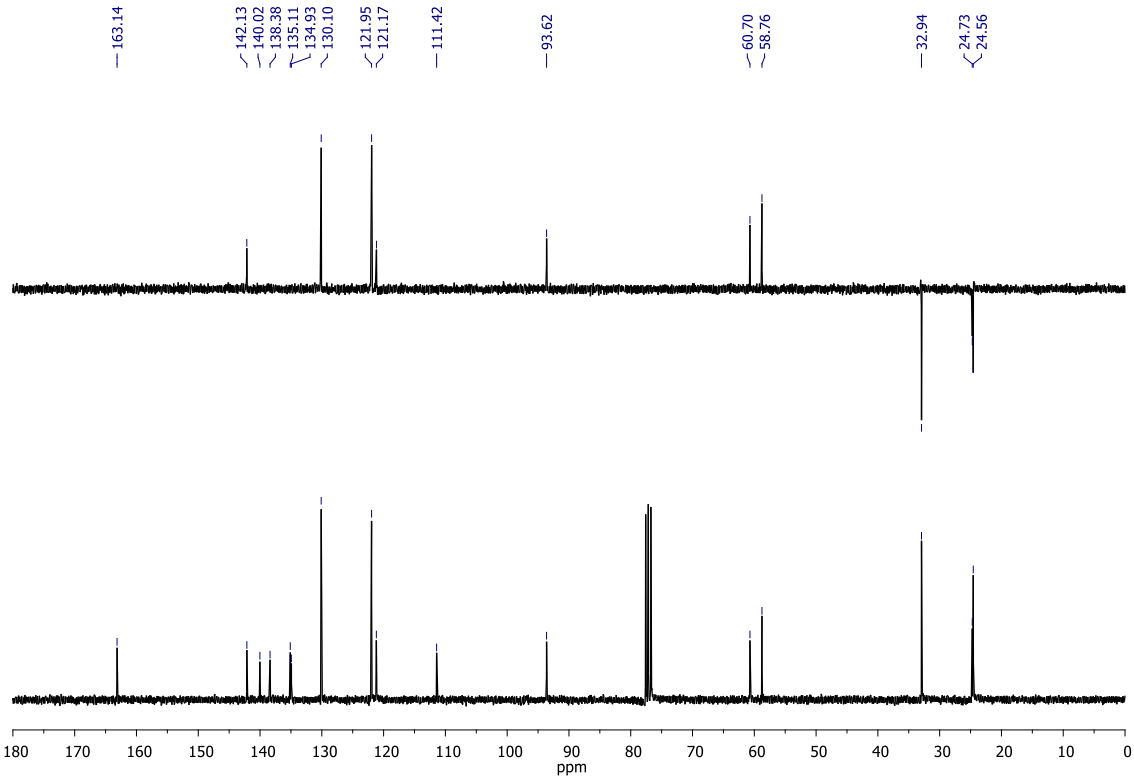

Figure S19. ^{13}C NMR and DEPT spectra (75 MHz, $CDCl_3$) for compound **2**.

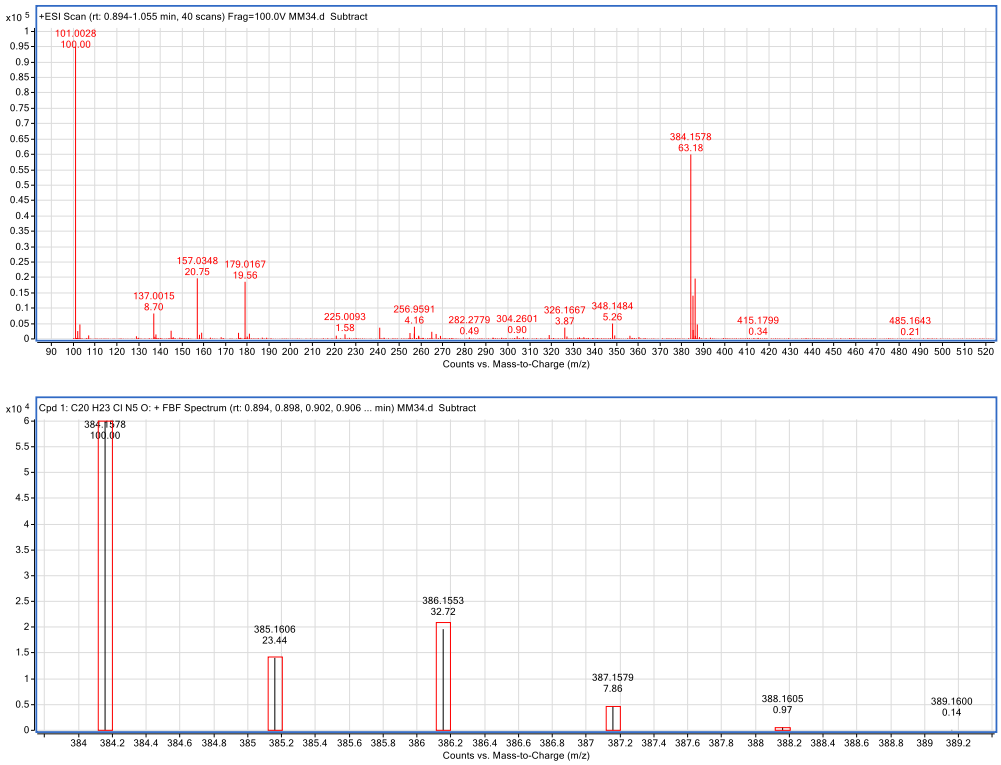

Figure S20. HR-MS (ESI$^+$) spectrum for compound **2**.

2.3.3. Compound 3

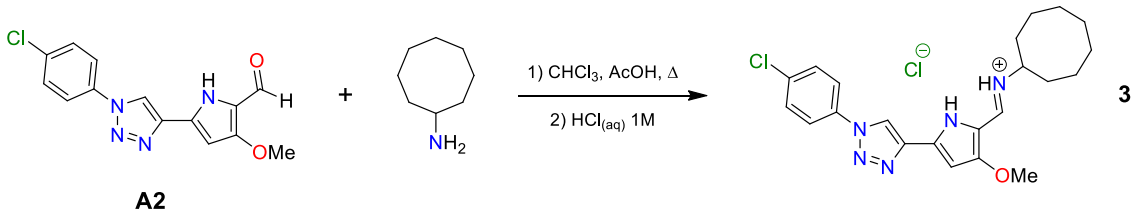

A mixture of aldehyde **A2** (430 mg, 1.42 mmol), cyclooctylamine (389 µL, 2.84 mmol, 2.0 equiv.) and glacial acetic acid (50 µL) in chloroform (10 mL) was stirred at 60 °C for 8 hours. Upon cooling to room temperature the chloroform was evaporated under reduced pressure and the residue was redissolved in dichloromethane (30 mL). The solution of the crude compound was washed with a 1 M aqueous HCl solution (3 × 20 mL), dried over anhydrous sodium sulphate, filtered and evaporated to dryness under reduced pressure. The residue was recrystallised from a mixture of dichloromethane and *n*-hexane to give compound **3** as a brown non-crystalline powder (364 mg, 57%). ^{1}H NMR (300 MHz, $CDCl_3$): δ (ppm) = 13.90 (s, 1H, NH), 11.30-11.04 (m, 1H, NH), 9.15 (s, 1H, triazole CH), 7.84-7.76 (m, 2H), 7.66 (d, J = 15 Hz, 1H), 7.56-7.48 (m, 2H), 6.56 (d, J = 3.0 Hz, 1H), 3.98 (s, 3H), 3.78-3.64 (m, 1H), 2.12-1.45 (m, 14H). ^{13}C NMR (75 MHz, $CDCl_3$): δ (ppm) = 163.1 (ArC), 142.3 (imine CH), 140.1 (ArC), 138.4 (ArC), 135.1 (ArC), 135.0 (ArC), 130.1 (ArCH), 121.9 (ArCH), 121.3 (ArCH), 111.4 (ArC), 93.6 (ArCH), 62.9 (CH), 58.8 (CH_3), 32.3 (CH_2), 27.0 (CH_2), 25.4 (CH_2), 23.5 (CH_2). HR-MS (+ESI): found m/z 412.1911 ($[M+H]^+$), $[C_{22}H_{26}ClN_5OH]^+$ requires m/z 412.1899 (monoisotopic mass).

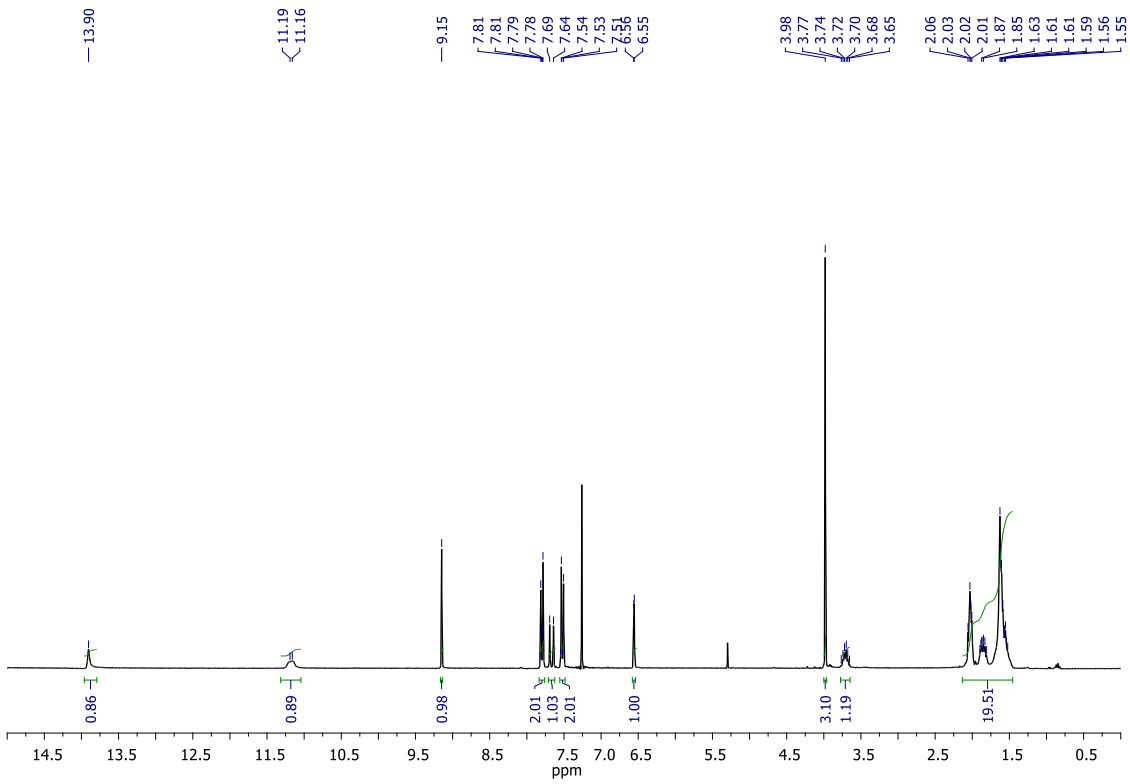

Figure S21. ^{1}H NMR spectrum (300 MHz, $CDCl_3$) for compound **3**.

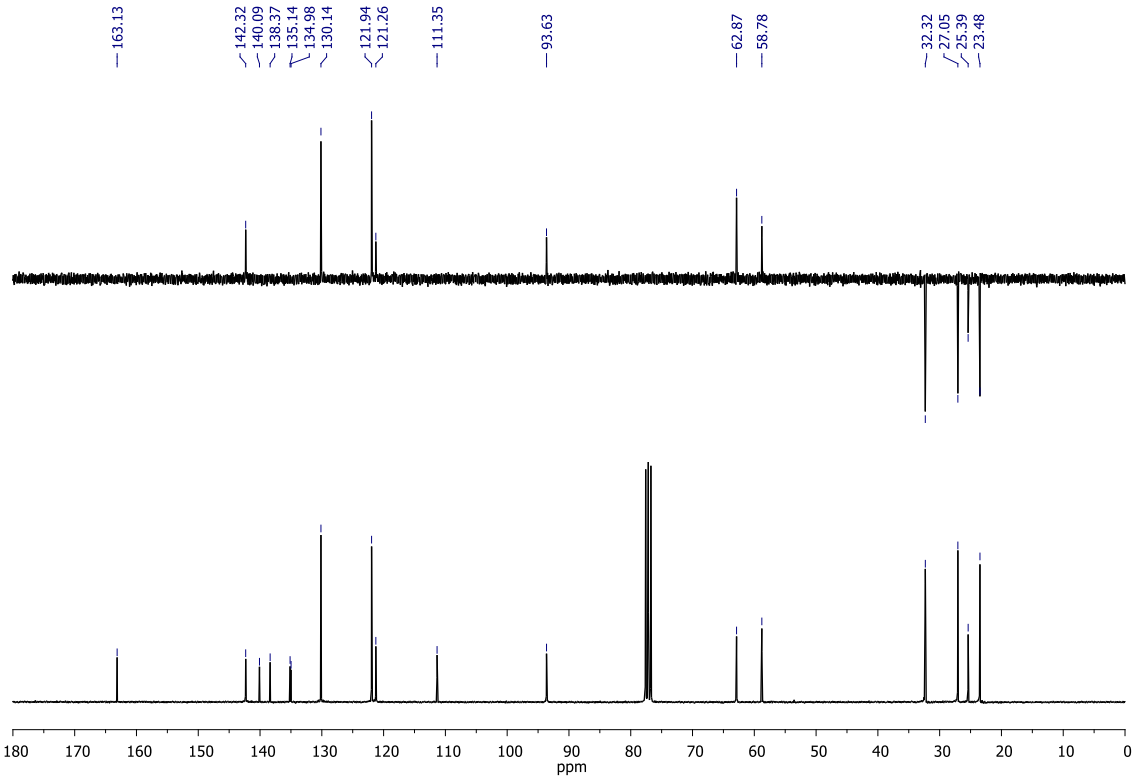

Figure S22. ^{13}C NMR and DEPT spectra (75 MHz, $CDCl_3$) for compound **3**.

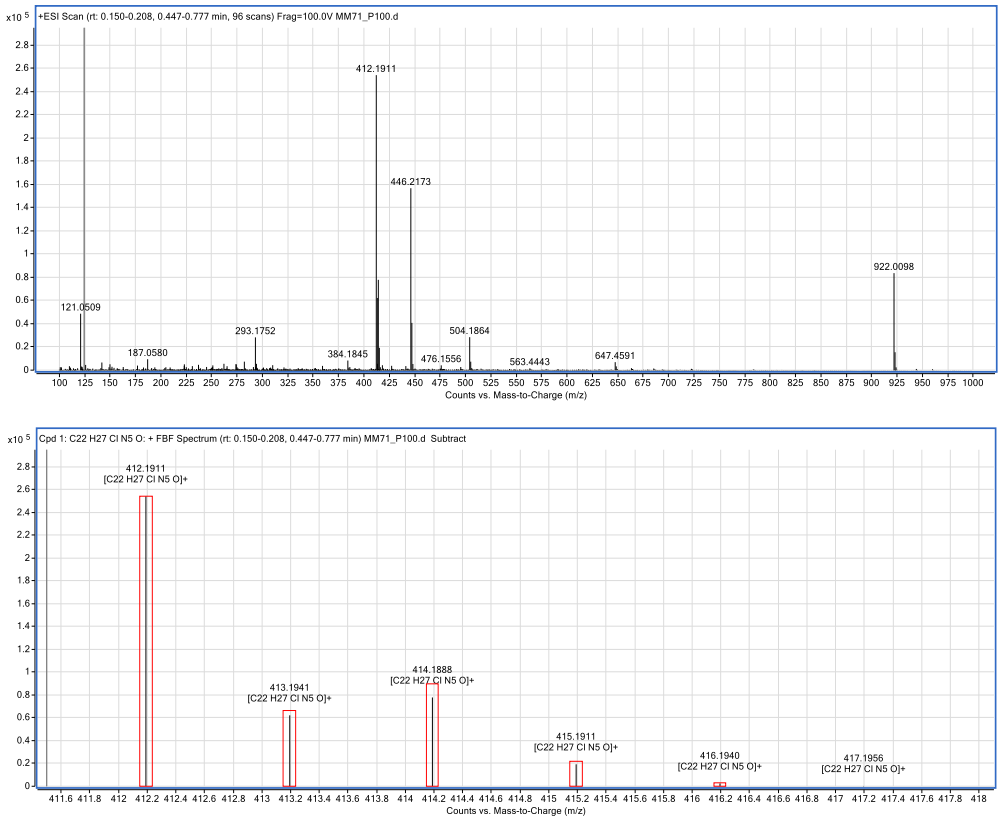

Figure S23. HR-MS (ESI^+) spectrum for compound **3**.

2.3.4. Compound 4

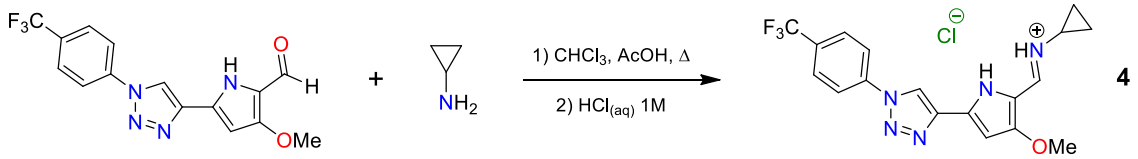

A mixture of aldehyde **B2** (452 mg, 1.34 mmol), cyclopropylamine (186 µL, 2.68 mmol, 2.0 equiv.) and glacial acetic acid (50 µL) in chloroform (10 mL) was stirred at 45 °C for 8 hours. Upon cooling to room temperature the chloroform was evaporated under reduced pressure and the residue was redissolved in dichloromethane (30 mL). The solution of the crude compound was washed with a 1 M aqueous HCl solution (3 x 20 mL), dried over anhydrous sodium sulphate, filtered and evaporated to dryness under reduced pressure. The residue was recrystallised from a mixture of dichloromethane and *n*-hexane to give compound **4** as a dark brown non-crystalline powder (390 mg, 70%). ^{1}H NMR (300 MHz, $CDCl_3$): δ (ppm) = 13.82 (s, 1H, NH), 11.25 (d, J = 12 Hz, 1H, NH), 9.19 (s, 1H, triazole CH), 8.05-7.97 (m, 2H), 7.86-7.78 (m, 2H), 7.76 (d, J = 15 Hz, 1H, overlapped with phenyl ArH), 6.56 (d, J = 2.1 Hz, 1H), 3.99 (s, 3H), 3.19-3.06 (m, 1H), 1.16-0.96 (m, 4H). ^{13}C NMR (75 MHz, $CDCl_3$): δ (ppm) = 163.4 (ArC), 144.4 (imine CH), 140.2 (ArC), 139.0 (ArC), 138.9 (ArC), 131.3 (q, ^{2}J = 33 Hz, ArC), 127.3 (q, ^{3}J = 3.7 Hz, ArCH), 123.6 (q, ^{1}J = 271 Hz, CF_3), 121.4 (ArCH), 120.8 (ArCH), 111.9 (ArC), 93.9 (ArCH), 58.9 (CH_3), 32.6 (CH), 7.0 (CH_2). HR-MS (+ESI): found m/z 376.1392 ($[M+H]^+$), $[C_{18}H_{16}F_3N_5OH]^+$ requires m/z 376.1380 (monoisotopic mass).

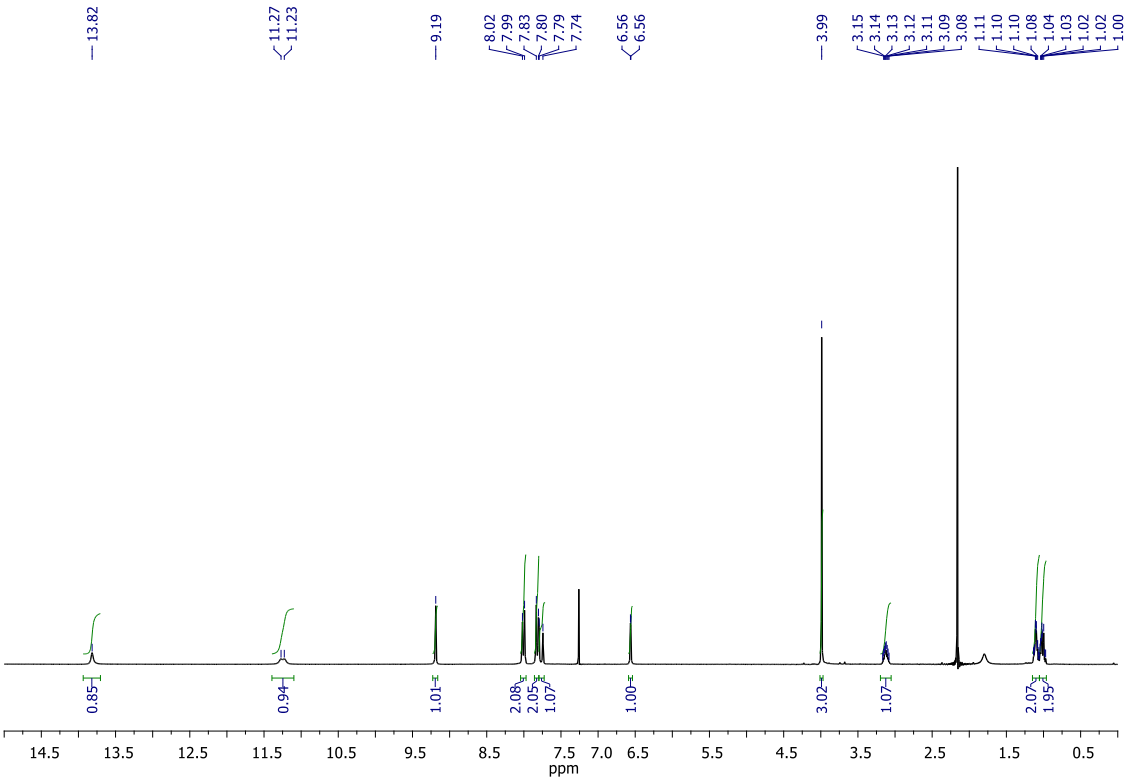

Figure S24. ^{1}H NMR spectrum (300 MHz, $CDCl_3$) for compound **4**.

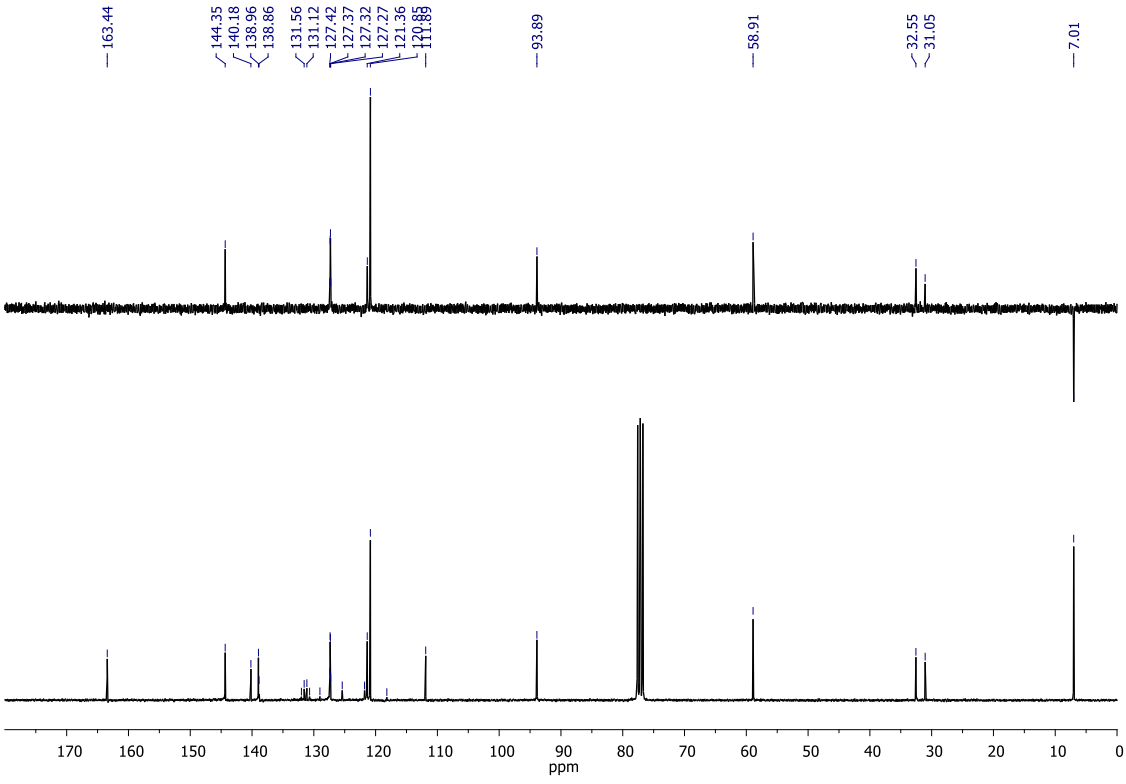

Figure S25. ^{13}C NMR and DEPT spectra (75 MHz, $CDCl_3$) for compound **4**.

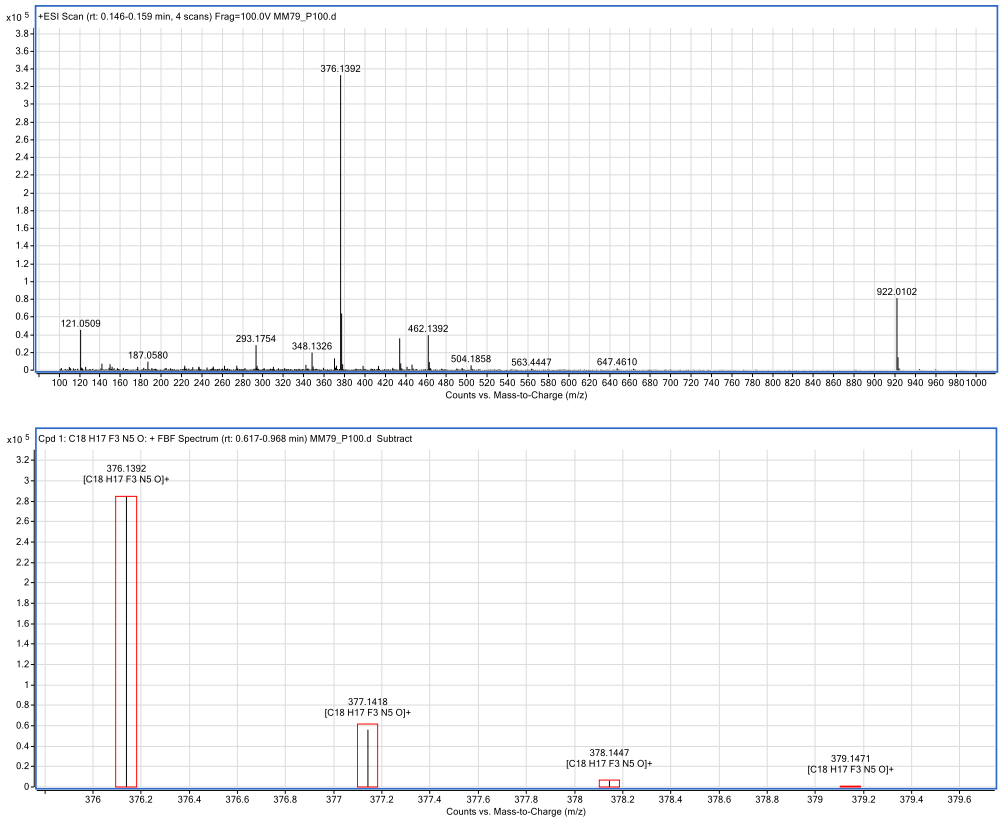

Figure S26. HR-MS (ESI^+) spectrum for compound **4**.

2.3.5. Compound 5

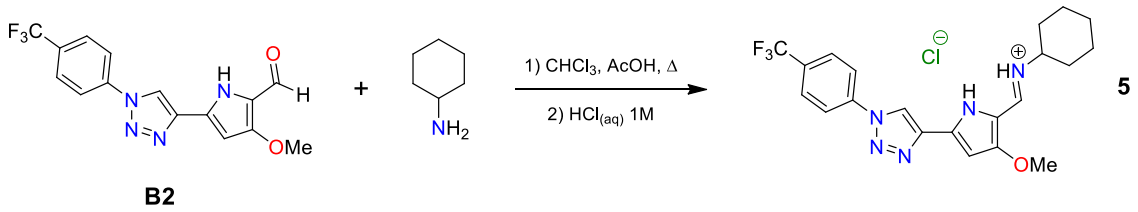

A mixture of aldehyde **B2** (200 mg, 0.59 mmol), cyclohexylamine (136 µL, 1.19 mmol, 2.0 equiv.) and glacial acetic acid (100 µL) in chloroform (20 mL) was stirred at 65 °C for 24 hours. Upon cooling to room temperature the chloroform was evaporated under reduced pressure and the residue was redissolved in dichloromethane (20 mL). The solution of the crude compound was washed with a 1 M aqueous HCl solution (3 × 20 mL), dried over anhydrous sodium sulphate, filtered and evaporated to dryness under reduced pressure. The residue was recrystallised from a mixture of dichloromethane and *n*-hexane to give compound **5** as a dark brown crystalline powder (58 mg, 21%). Slow evaporation of a solution of the compound in *n*-butanol provided orange single crystals, suitable for X-ray diffraction analysis. ^{1}H NMR (300 MHz, $CDCl_3$): δ (ppm) = 13.77 (s, 1H, NH), 11.12-11.09 (m, 1H, NH), 9.17 (s, 1H, triazole CH), 7.96 (d, J = 7.8 Hz, 2H), 7.76 (d, J = 7.7 Hz, 2H), 7.65 (d, J = 15 Hz, 1H), 6.48 (s, 1H), 3.90 (s, 3H), 3.53-3.35 (m, 1H), 2.05-2.02 (m, 2H), 1.86-1.82 (m, 2H), 1.67-1.55 (m, 3H), 1.35-1.18 (m, 3H). ^{13}C NMR (75 MHz, $CDCl_3$): δ (ppm) = 163.0 (ArC), 142.2 (imine CH), 140.1 (ArC), 138.7 (ArC), 137.9 (ArC), 131.0 (q, ^{2}J = 33 Hz, ArC), 127.1 (q, ^{3}J = 3.7 Hz, ArCH), 123.5 (q, ^{1}J = 273 Hz, CF_3), 121.0 (ArCH), 120.6 (ArCH), 111.3 (ArC), 93.6 (ArCH), 60.6 (CH), 58.7 (CH_3), 32.8 (CH_2), 24.6 (CH_2), 24.4 (CH_2). HR-MS (+ESI): found m/z 418.1832 ($[M+H]^+$), $[C_{21}H_{22}F_3N_5OH]^+$ requires m/z 418.1849 (monoisotopic mass).

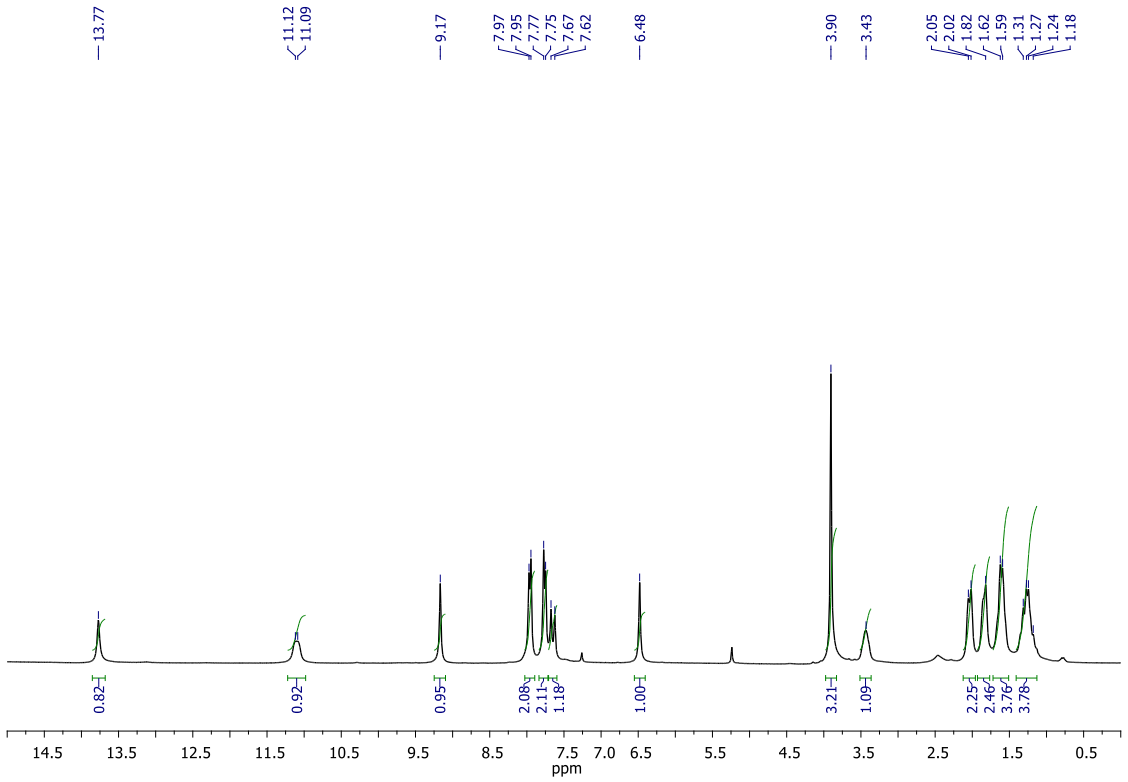

Figure S27. ^{1}H NMR spectrum (300 MHz, $CDCl_3$) for compound **5**.

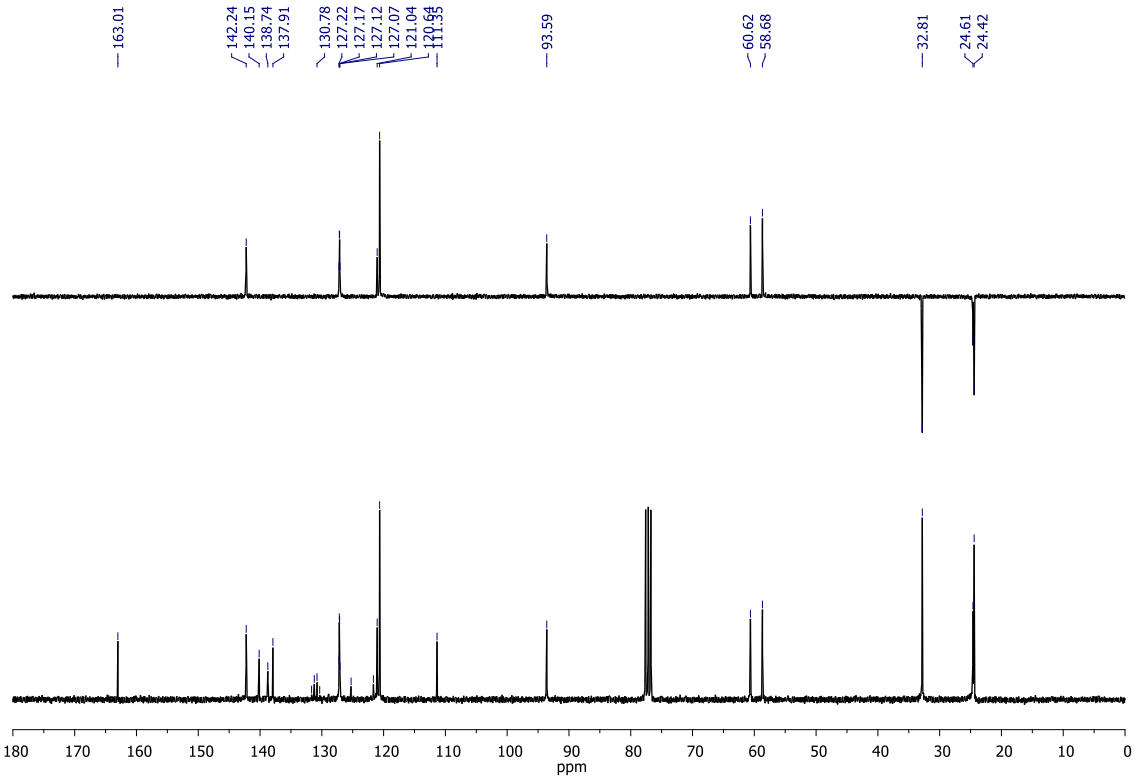

Figure S28. ^{13}C NMR and DEPT spectra (75 MHz, $CDCl_3$) for compound **5**.

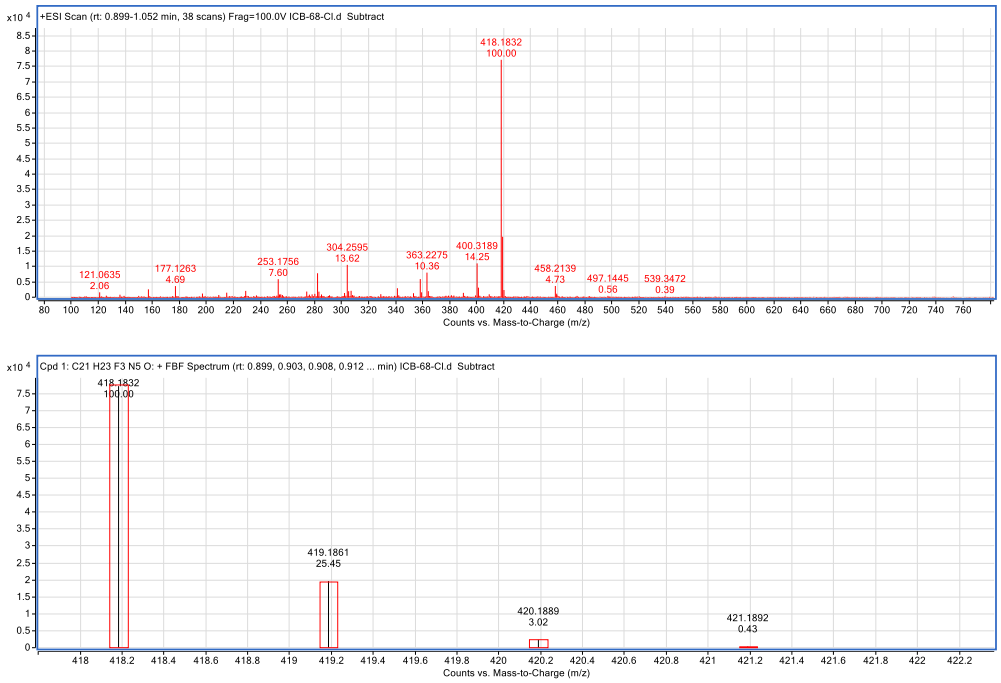

Figure S29. HR-MS (ESI^+) spectrum for compound **5**.

2.3.6. Compound 6

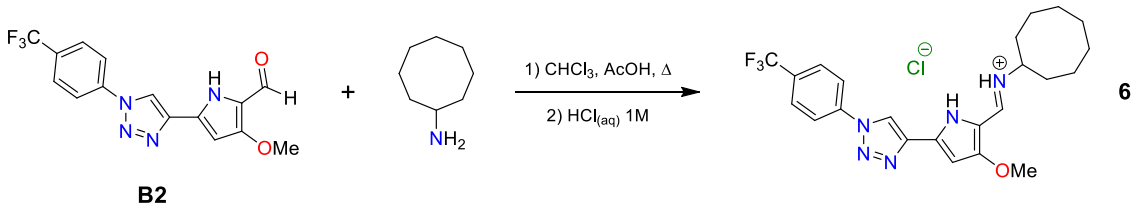

A mixture of aldehyde **B2** (428 mg, 1.27 mmol), cyclooctylamine (349 µL, 2.55 mmol, 2.0 equiv.) and glacial acetic acid (50 µL) in chloroform (10 mL) was stirred at 60 °C for 8 hours. Upon cooling to room temperature the chloroform was evaporated under reduced pressure and the residue was redissolved in dichloromethane (30 mL). The solution of the crude compound was washed with a 1 M aqueous HCl solution (3 × 20 mL), dried over anhydrous sodium sulphate, filtered and evaporated to dryness under reduced pressure. The residue was recrystallised from a mixture of dichloromethane and *n*-hexane to give compound **6** as a dark brown non-crystalline powder (475 mg, 77%). ^{1}H NMR (300 MHz, $CDCl_3$): δ (ppm) = 13.93 (s, 1H, NH), 11.31-11.00 (m, 1H, NH), 9.24 (s, 1H, triazole CH), 8.04-7.96 (m, 2H), 7.85-7.76 (m, 2H), 7.68 (d, J = 15 Hz, 1H), 6.54 (d, J = 3.0 Hz, 1H), 3.96 (s, 3H), 3.78-3.62 (m, 1H), 2.10-1.42 (m, 14H). ^{13}C NMR (75 MHz, $CDCl_3$): δ (ppm) = 163.1 (ArC), 142.5 (imine CH), 140.3 (ArC), 138.9 (q, J = 1.5 Hz, ArC), 138.0 (ArC), 131.2 (q, ^{2}J = 33 Hz, ArC), 127.3 (q, ^{3}J = 3.7 Hz, ArCH), 123.6 (q, ^{1}J = 271 Hz, CF_3), 121.2 (ArCH), 120.7 (ArCH), 111.4 (ArC), 93.7 (ArCH), 62.9 (CH), 58.8 (CH_3), 32.3 (CH_2), 27.0 (CH_2), 25.4 (CH_2), 23.4 (CH_2). HR-MS (+ESI): found m/z 446.2173 ($[M+H]^+$), $[C_{23}H_{26}F_3N_5OH]^+$ requires m/z 446.2162 (monoisotopic mass).

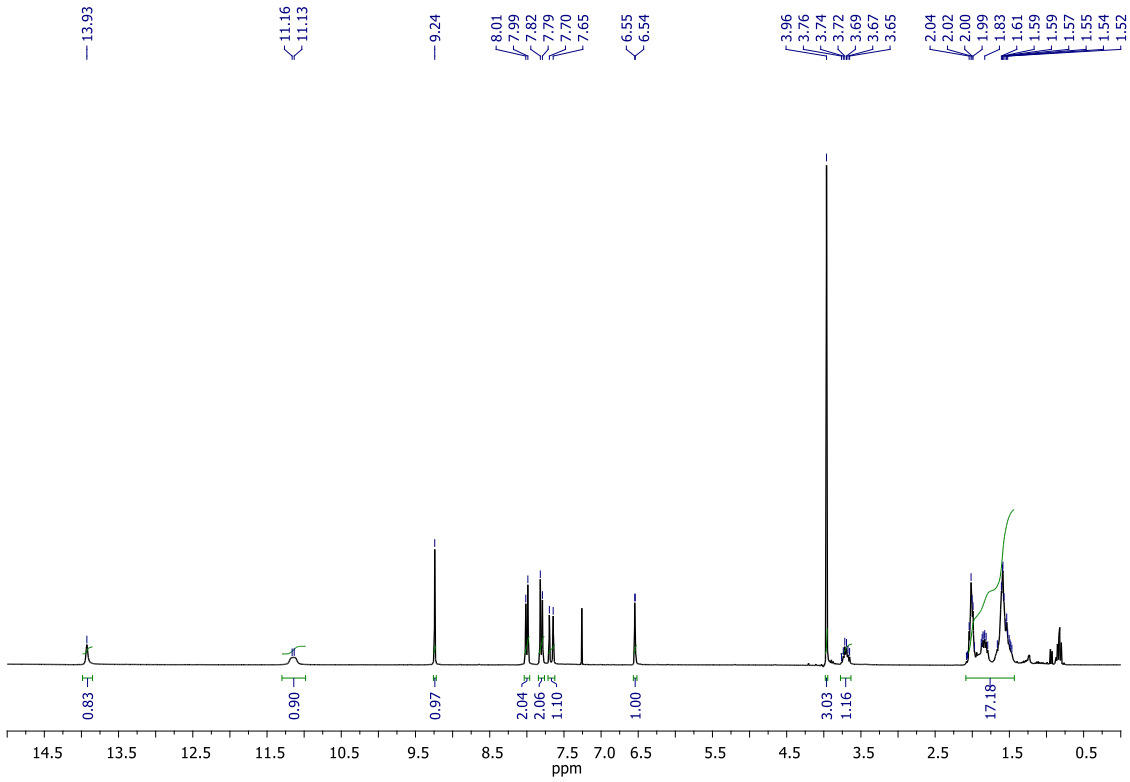

Figure S30. ^{1}H NMR spectrum (300 MHz, $CDCl_3$) for compound **6**.

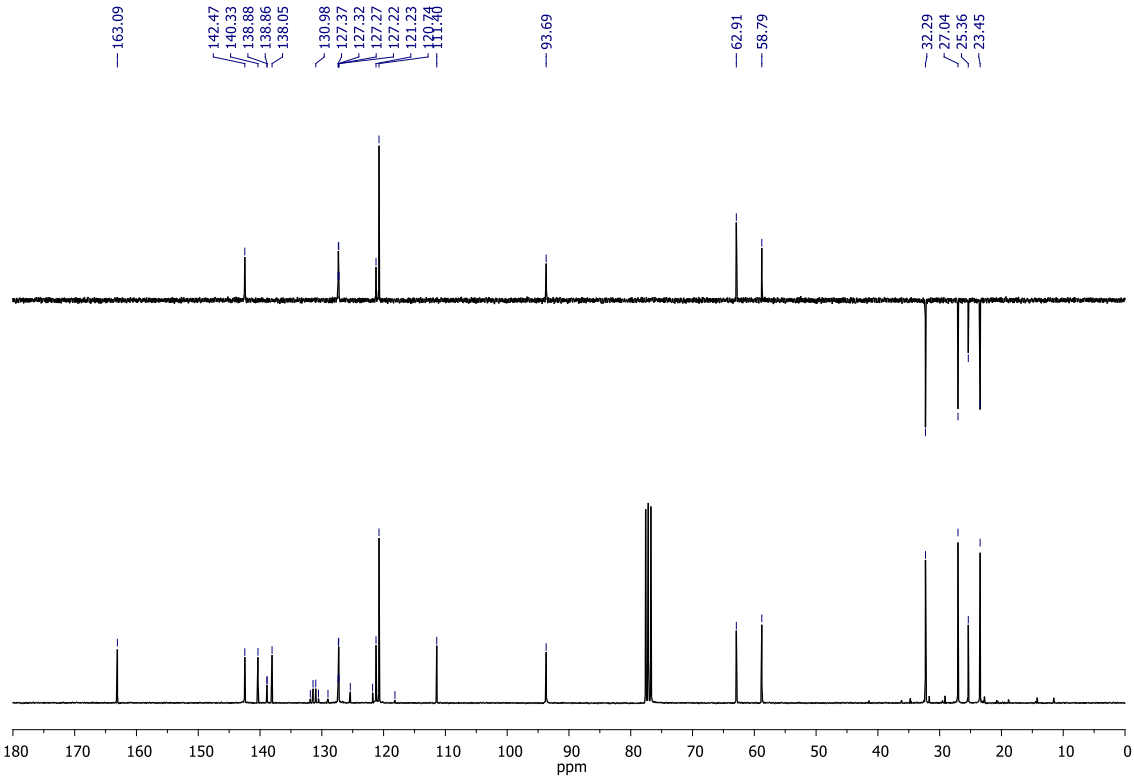

Figure S31. ^{13}C NMR and DEPT spectra (75 MHz, $CDCl_3$) for compound **6**.

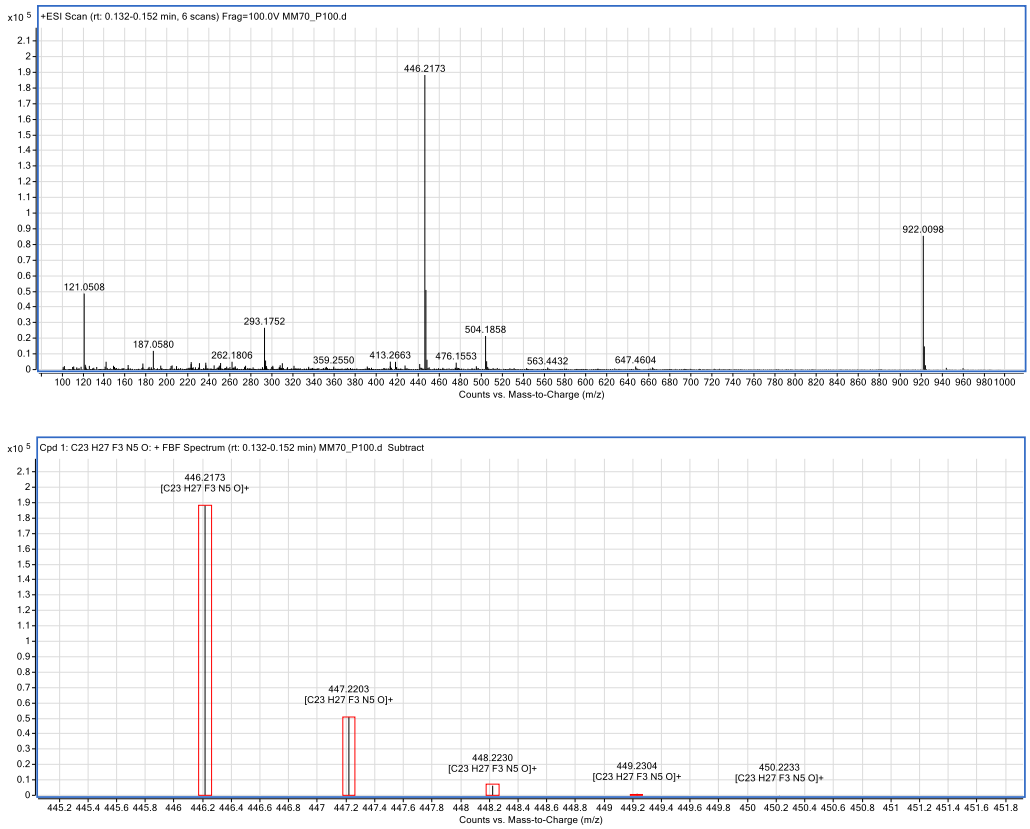

Figure S32. HR-MS (ESI^+) spectrum for compound **6**.

2.3.7. Compound 7

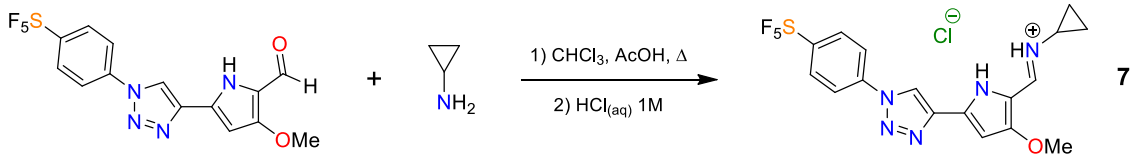

C2

A mixture of aldehyde **C2** (452 mg, 1.15 mmol), cyclopropylamine (159 µL, 2.29 mmol, 2.0 equiv.) and glacial acetic acid (50 µL) in chloroform (10 mL) was stirred at 45 °C for 6 hours. Upon cooling to room temperature the chloroform was evaporated under reduced pressure and the residue was redissolved in dichloromethane (30 mL). The solution of the crude compound was washed with a 1 M aqueous HCl solution (3 × 20 mL), dried over anhydrous sodium sulphate, filtered and evaporated to dryness under reduced pressure. The residue was recrystallised from a mixture of dichloromethane and *n*-hexane to give compound **7** as a dark brown powder (184 mg, 50%). ^{1}H NMR (300 MHz, $CDCl_3$): δ (ppm) = 13.83 (s, 1H, NH), 11.22 (d, J = 12 Hz, 1H, NH), 9.21 (s, 1H, triazole CH), 8.05-7.90 (m, 4H), 7.78 (d, J = 15 Hz, 1H), 6.55 (s, 1H), 3.99 (s, 3H), 3.20-3.05 (m, 1H), 1.18-0.95 (m, 4H). ^{13}C NMR (75 MHz, $CDCl_3$): δ (ppm) = 163.4 (ArC), 153.6 (quint, ^{2}J = 18 Hz, ArC), 144.4 (imine CH), 140.3 (ArC), 138.7 (ArC), 138.2 (ArC), 128.1 (quint, ^{3}J = 4.5 Hz, ArCH), 121.3 (ArCH), 120.5 (ArCH), 111.9 (ArC), 93.9 (ArCH), 58.9 (CH_3), 32.6 (CH), 7.0 (CH_2). HR-MS (+ESI): found m/z 434.1080 ($[M+H]^+$), $[C_{17}H_{16}F_5N_5OSH]^+$ requires m/z 434.1068 (monoisotopic mass).

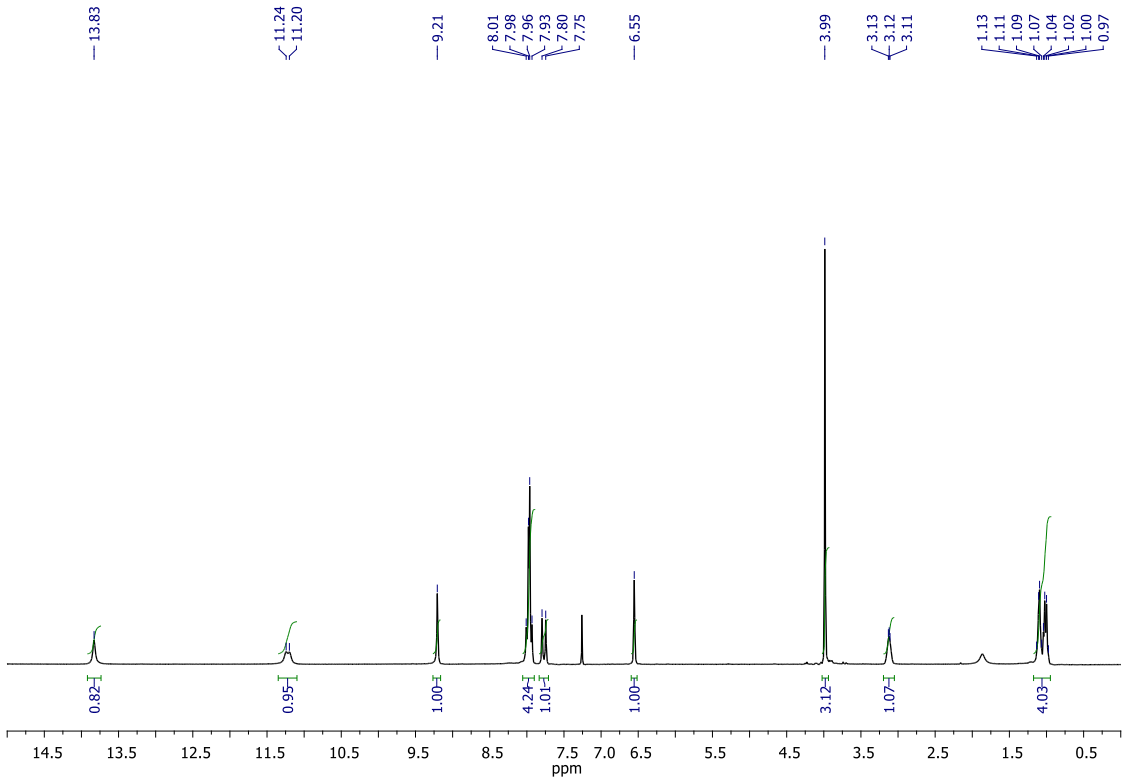

Figure S33. ^{1}H NMR spectrum (300 MHz, $CDCl_3$) for compound **7**.

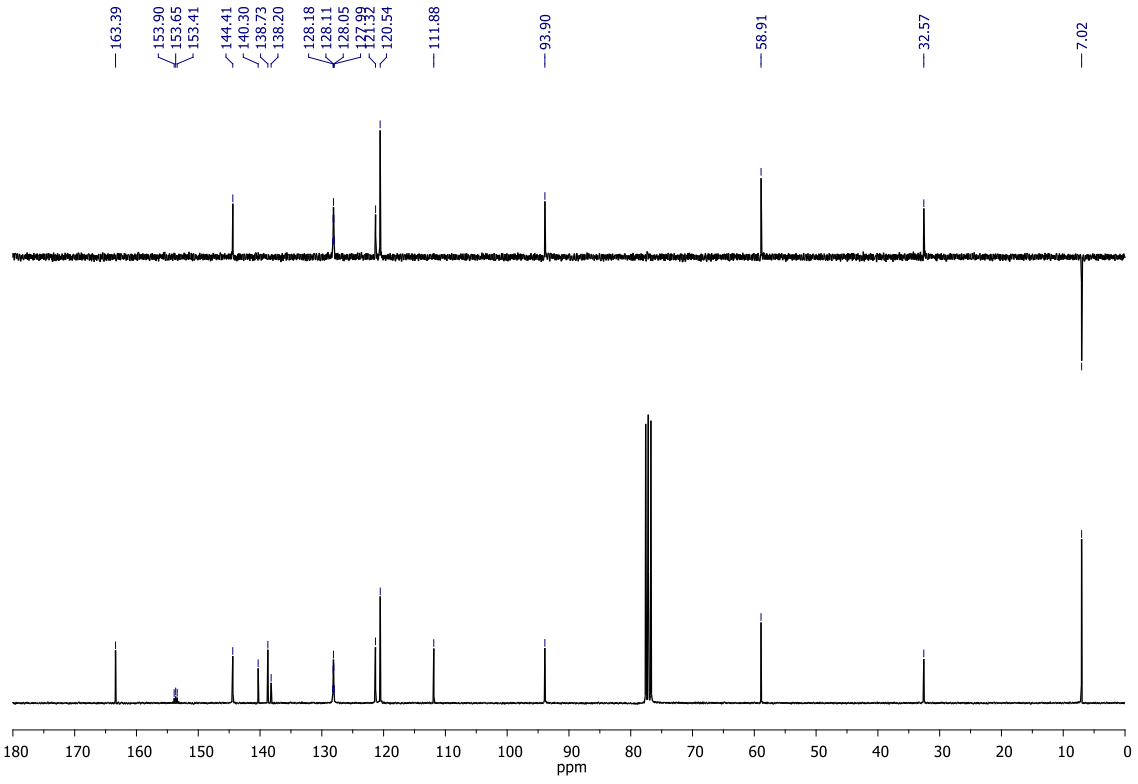

Figure S34. ^{13}C NMR and DEPT spectra (75 MHz, $CDCl_3$) for compound **7**.

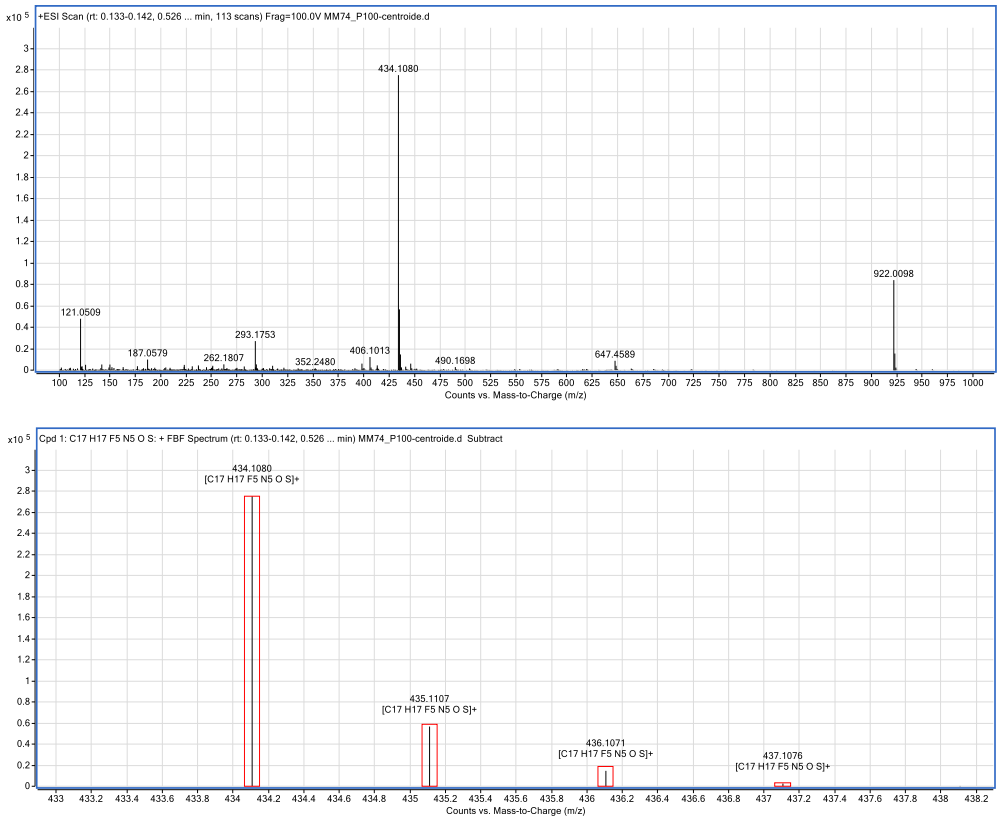

Figure S35. HR-MS (+ESI) spectrum for compound **7**.

2.3.8. Compound 8

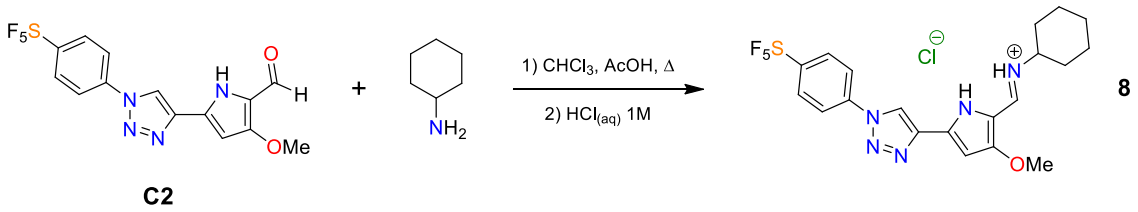

A mixture of aldehyde **C2** (377 mg, 0.96 mmol), cyclohexylamine (218 µL, 1.91 mmol, 2.0 equiv.) and glacial acetic acid (50 µL) in chloroform (10 mL) was stirred at 60 °C for 8 hours. Upon cooling to room temperature the chloroform was evaporated under reduced pressure and the residue was redissolved in dichloromethane (30 mL). The solution of the crude compound was washed with a 1 M aqueous HCl solution (3 × 20 mL), dried over anhydrous sodium sulphate, filtered and evaporated to dryness under reduced pressure. The residue was recrystallised from a mixture of dichloromethane and *n*-hexane to give compound **8** as a dark brown non-crystalline powder (347 mg, 71%). ^{1}H NMR (300 MHz, $CDCl_3$): δ (ppm) = 13.89 (s, 1H, NH), 11.16 (d, J = 15 Hz, 1H, NH), 9.24 (s, 1H, triazole CH), 8.04-7.90 (m, 4H), 7.70 (d, J = 15 Hz, 1H), 6.55 (s, 1H), 3.97 (s, 3H), 3.55-3.38 (m, 1H), 2.16-1.17 (m, 10H). ^{13}C NMR (75 MHz, $CDCl_3$): δ (ppm) = 163.2 (ArC), 153.6 (quint, ^{2}J = 19 Hz, ArC), 142.4 (imine CH), 140.4 (ArC), 138.2 (ArC), 138.0 (ArC), 128.1 (quint, ^{3}J = 4.5 Hz, ArCH), 121.2 (ArCH), 120.5 (ArCH), 111.6 (ArC), 93.8 (ArCH), 60.8 (CH), 58.8 (CH_3), 33.0 (CH_2), 24.7 (CH_2), 24.6 (CH_2). HR-MS (+ESI): found m/z 476.1550 ($[M+H]^+$), $[C_{20}H_{22}F_5N_5OSH]^+$ requires m/z 476.1538 (monoisotopic mass).

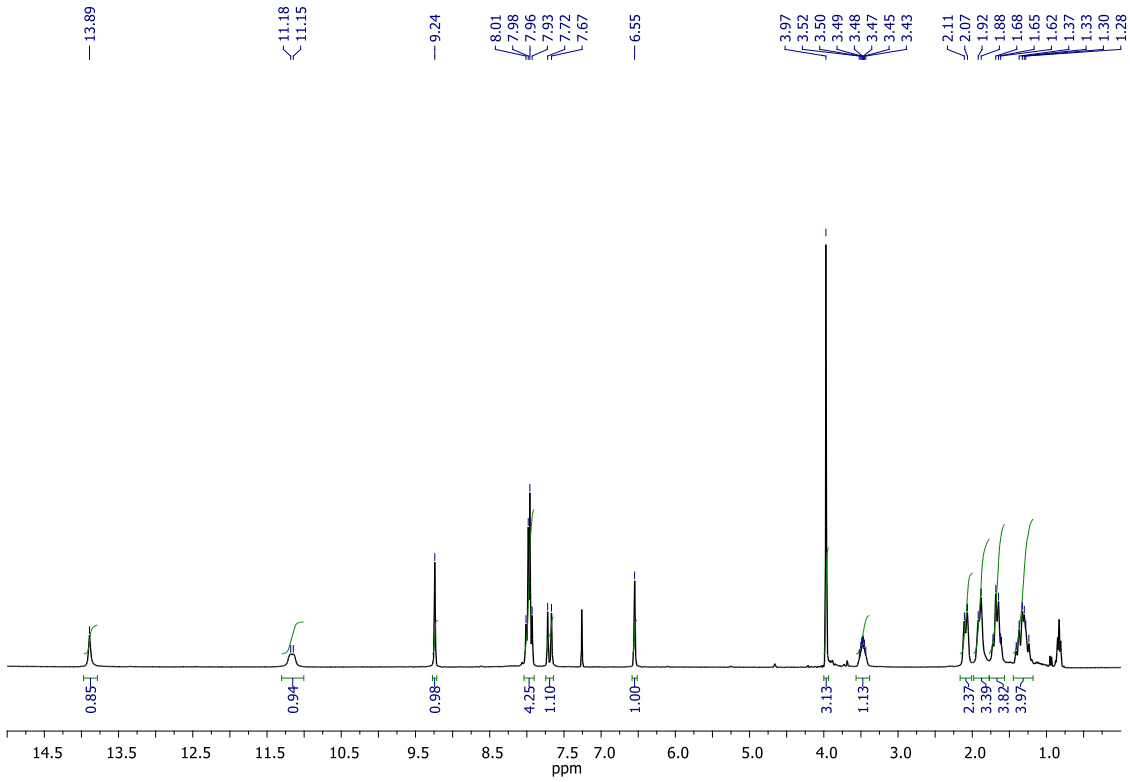

Figure S36. ^{1}H NMR spectrum (300 MHz, $CDCl_3$) for compound **8**.

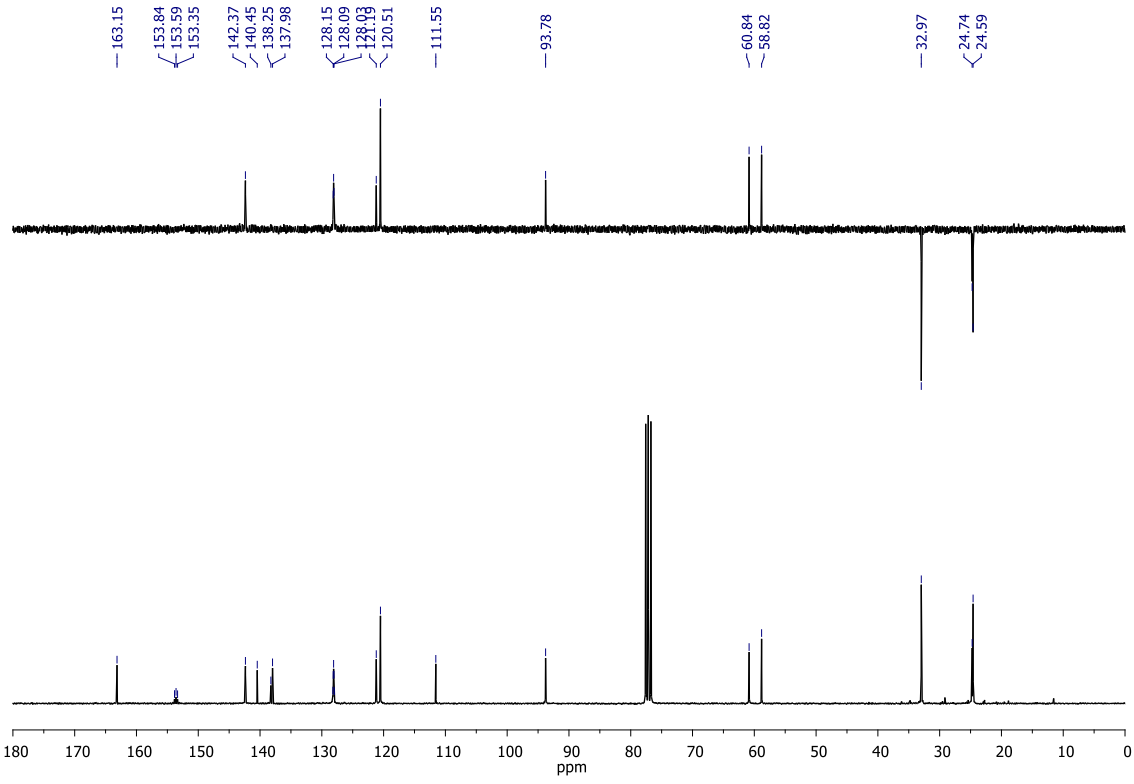

Figure S37. ^{13}C NMR and DEPT spectra (75 MHz, $CDCl_3$) for compound **8**.

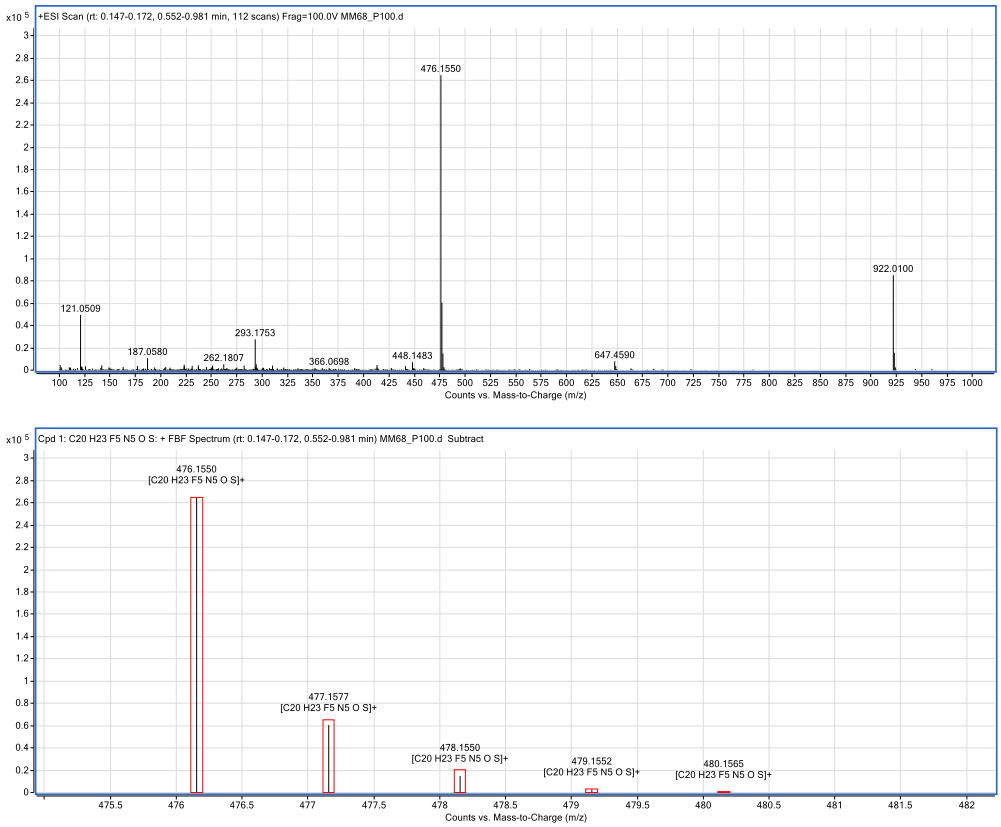

Figure S38. HR-MS (+ESI) spectrum for compound **8**.

2.3.9. Compound 9

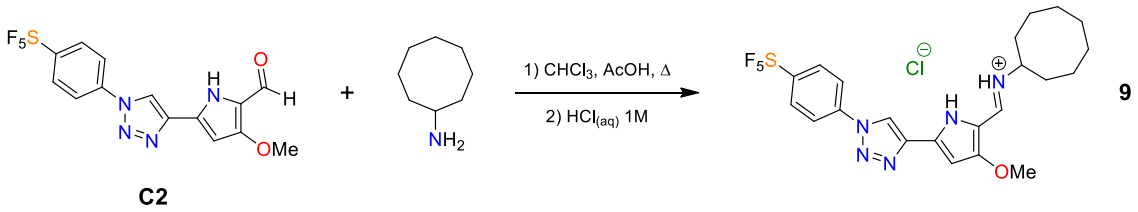

A mixture of aldehyde **C2** (359 mg, 0.91 mmol), cyclooctylamine (250 µL, 1.82 mmol, 2.0 equiv.) and glacial acetic acid (50 µL) in chloroform (10 mL) was stirred at 60 °C for 8 hours. Upon cooling to room temperature the chloroform was evaporated under reduced pressure and the residue was redissolved in dichloromethane (30 mL). The solution of the crude compound was washed with a 1 M aqueous HCl solution (3 × 20 mL), dried over anhydrous sodium sulphate, filtered and evaporated to dryness under reduced pressure. The residue was recrystallised from a mixture of dichloromethane and *n*-hexane to give compound **9** as a dark brown non-crystalline powder (329 mg, 67%). ^{1}H NMR (300 MHz, $CDCl_3$): δ (ppm) = 13.97 (s, 1H, NH), 11.29-11.02 (m, 1H, NH), 9.27 (s, 1H, triazole CH), 8.03-7.91 (m, 4H), 7.68 (d, J = 15 Hz, 1H), 6.56 (d, J = 3.0 Hz, 1H), 3.98 (s, 3H), 3.80-3.62 (m, 1H), 2.11-1.44 (m, 14H). ^{13}C NMR (75 MHz, $CDCl_3$): δ (ppm) = 163.0 (ArC), 153.5 (quint, ^{2}J = 19 Hz, ArC), 142.5 (imine CH), 140.4 (ArC), 138.2 (ArC), 137.8 (ArC), 128.0 (quint, ^{3}J = 4.5 Hz, ArCH), 121.2 (ArCH), 120.4 (ArCH), 111.4 (ArC), 93.7 (ArCH), 62.9 (CH), 58.8 (CH_3), 32.2 (CH_2), 27.0 (CH_2), 25.3 (CH_2), 23.4 (CH_2). HR-MS (+ESI): found m/z 504.1861 ($[M+H]^+$), $[C_{22}H_{26}F_5N_5OSH]^+$ requires m/z 504.1851 (monoisotopic mass).

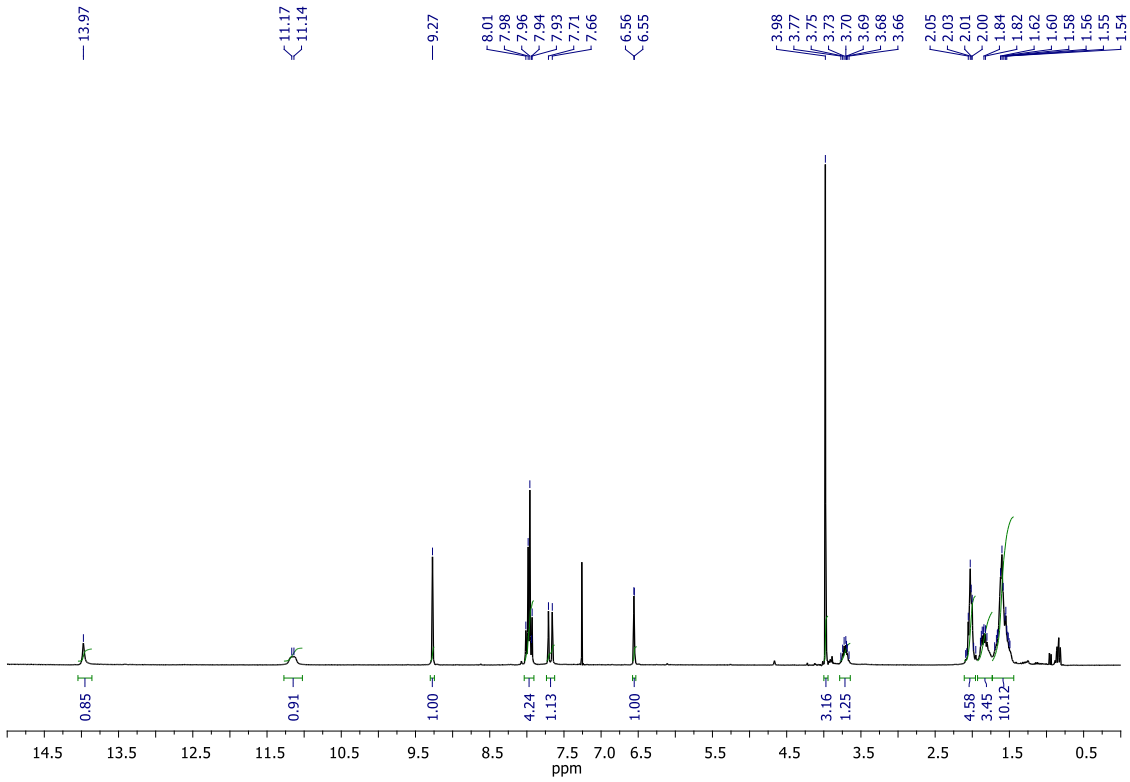

Figure S39. ^{1}H NMR spectrum (300 MHz, $CDCl_3$) for compound **9**.

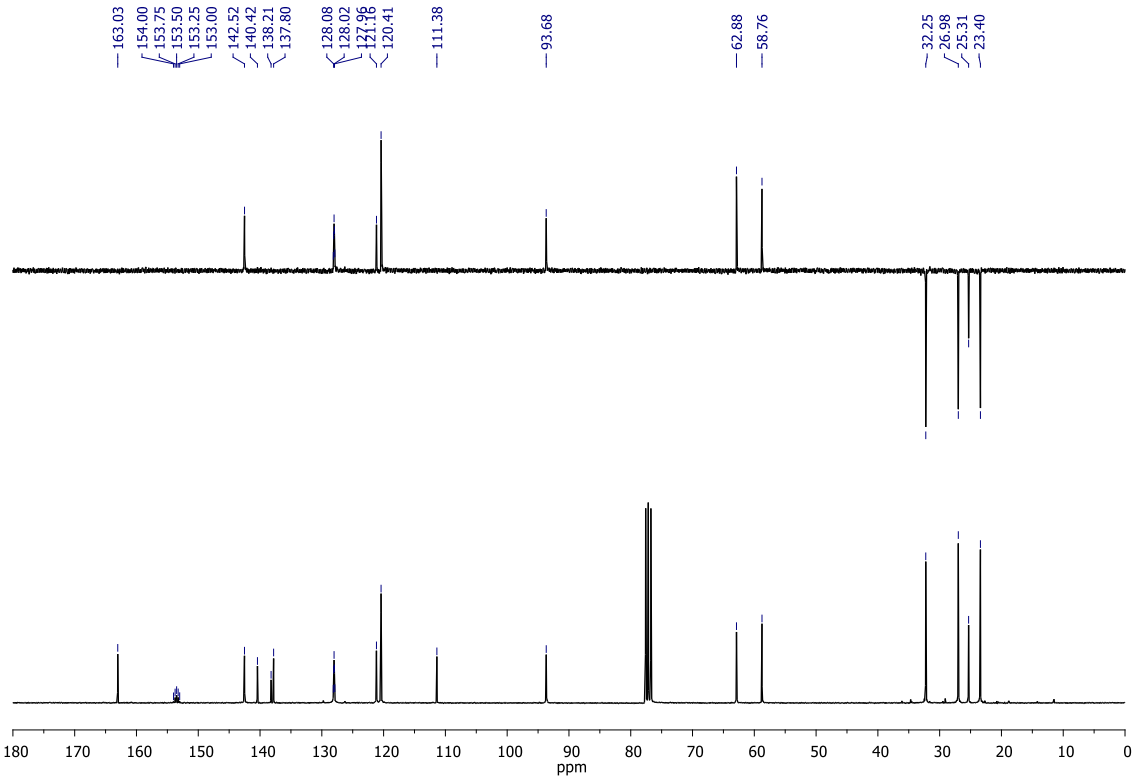

Figure S40. ^{13}C NMR and DEPT spectra (75 MHz, $CDCl_3$) for compound **9**.

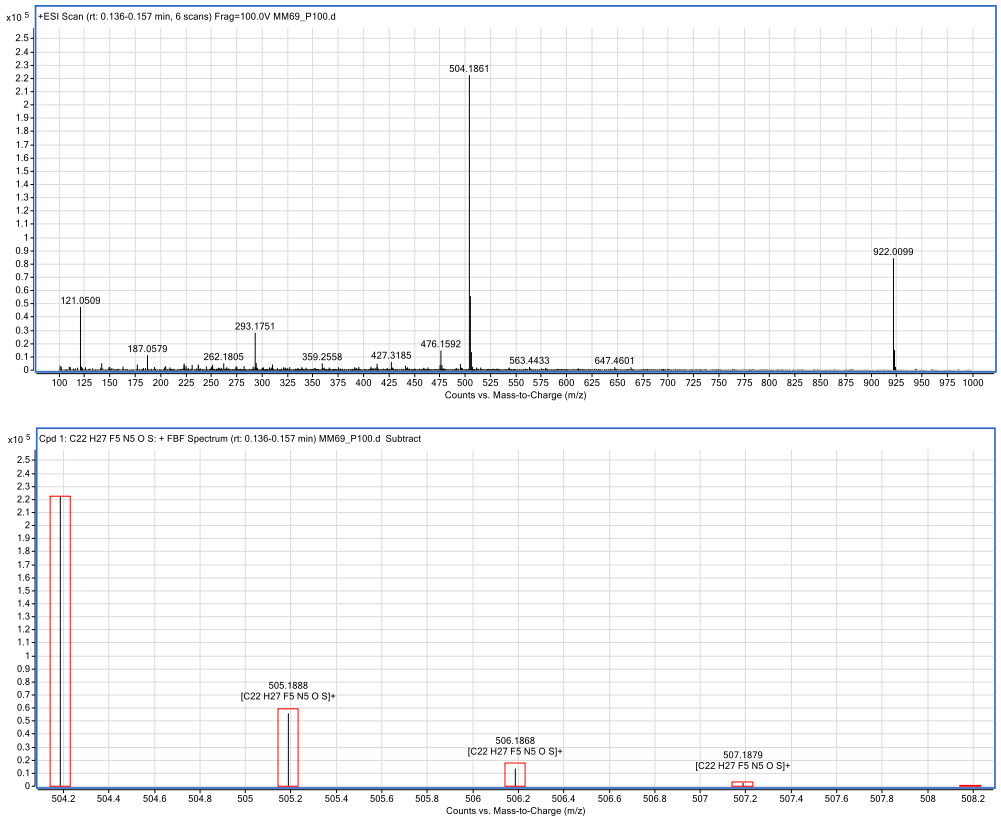

Figure S41. HR-MS (ESI^+) spectrum for compound **9**.

3. ABSORPTION AND EMISSION SPECTRA OF THE CLICK TAMBJAMINES

Absorption spectra

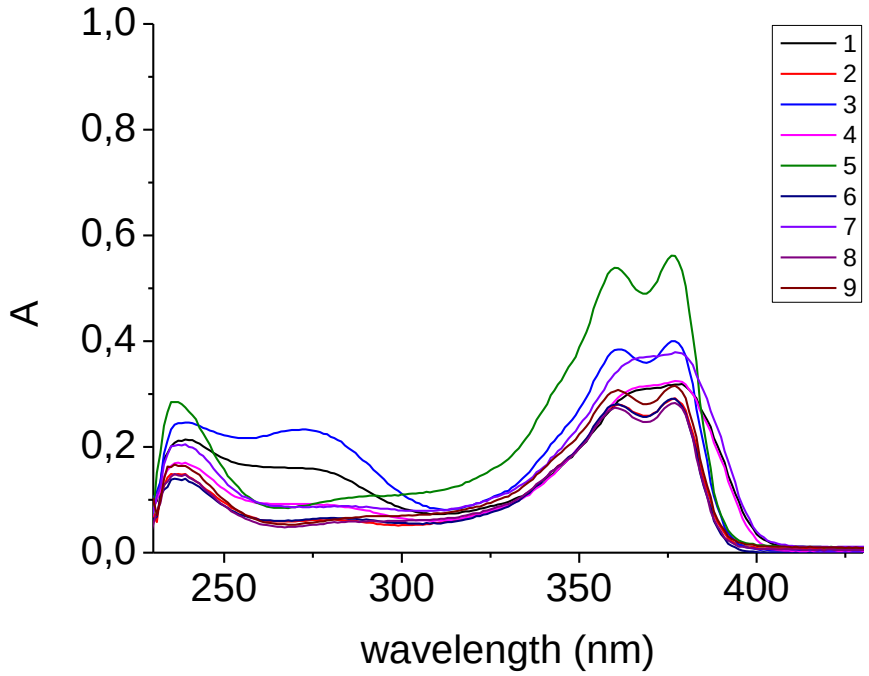

Figure S42. Absorption spectra recorded for 10^{-5} M solutions of the pure compounds in chloroform.

Emission spectra

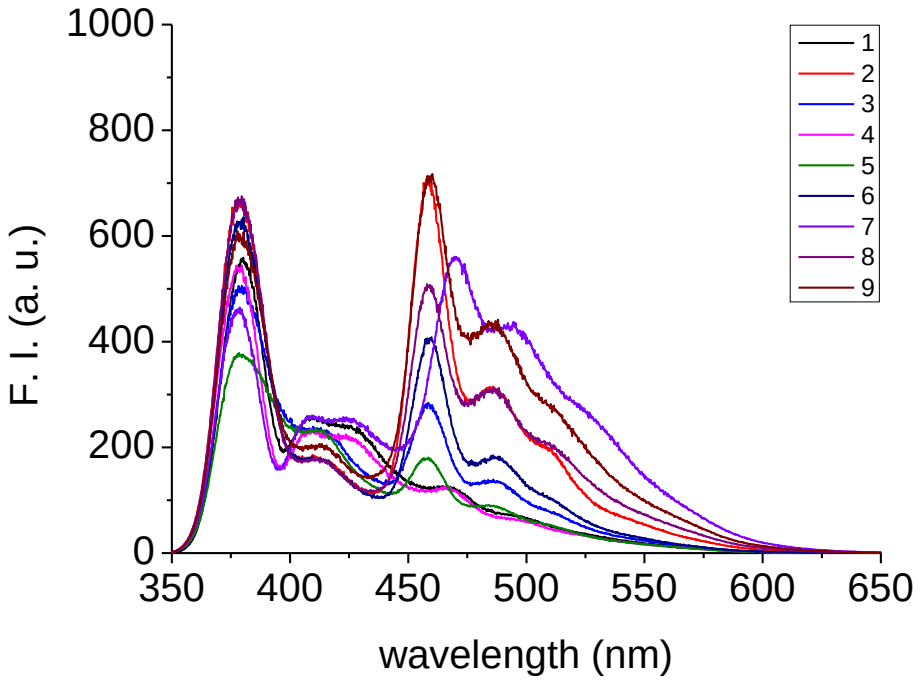

Figure S43. Emission spectra recorded for 10^{-5} M solutions of the pure compounds in chloroform. Each sample was excited at the wavelength of the maximum of its absorption spectrum.

4. X-RAY DIFFRACTION STUDIES

Solid state structures of compounds 1, 2 and 5

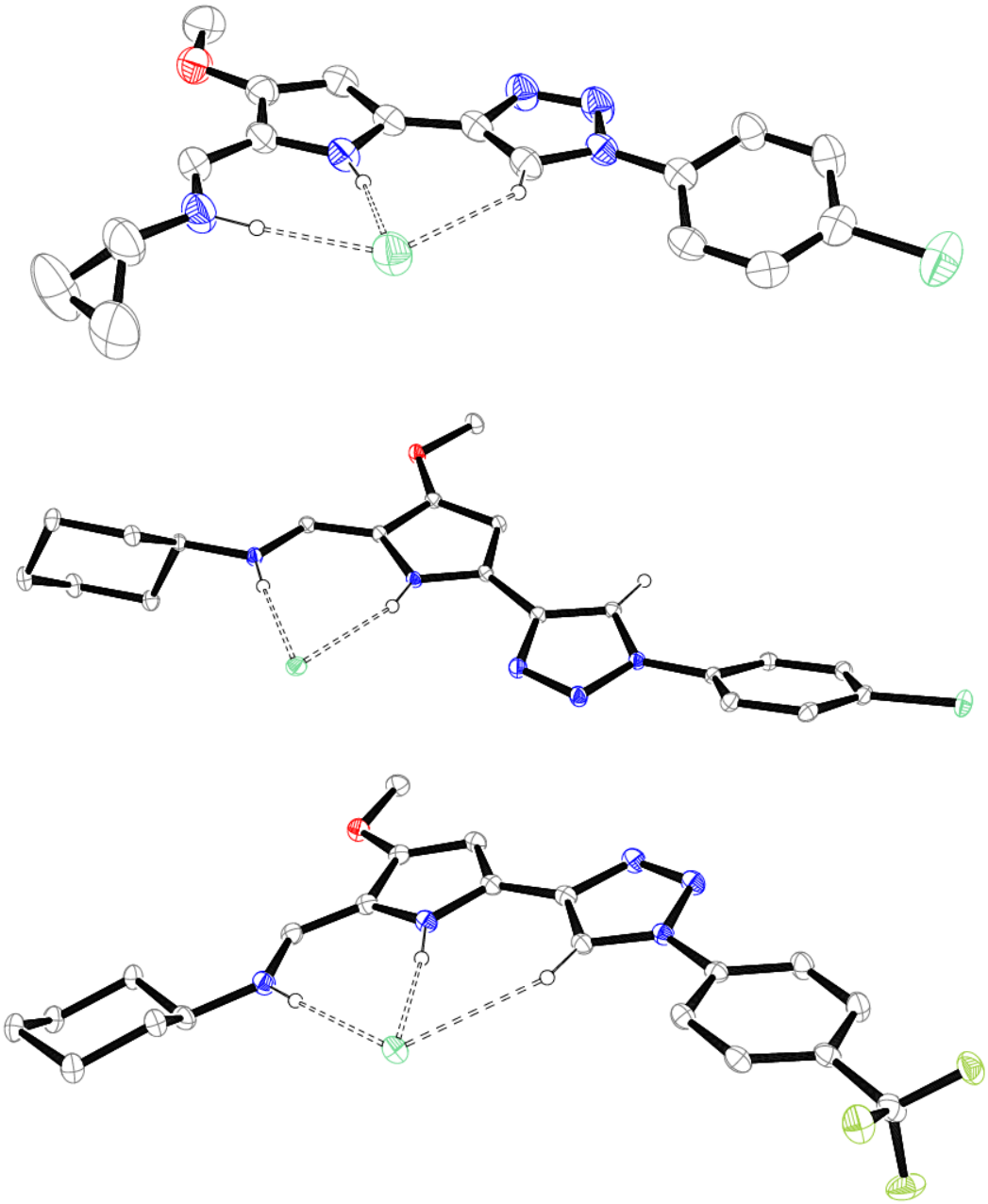

Figure S44. X-ray molecular structures of compounds **1** (top), **2** (middle) and **5** (bottom). Hydrogen atoms, except those involved in hydrogen-bonding interactions, are omitted for the sake of simplicity. In the case of **5** only one of the two molecules the asymmetric unit consists of is shown. The ORTEP plot is at the 30% probability level.

Table S1. Crystal data and refinement details for **1**, **2** and **5**.

	1	**2**	**5**
Empirical formula	$C_{17}H_{17}Cl_2N_5O$	$C_{24}H_{35}Cl_2N_5O_3$	$C_{21}H_{23}ClF_3N_5O$
MW	378.25	512.47	453.89
crystal system	Monoclinic	Triclinic	Monoclinic
space group	*P* $2_1/c$	*P* -1	*P* $2_1/n$
T/K	298(2)	100(2)	100(2)
a/Å	5.7035(14)	7.9219(2)	11.0699(4)
b/Å	20.182(5)	9.5881(2)	23.3590(9)
c/Å	15.891(4)	19.0533(5)	16.6594(6)
α/deg	90	99.4900(10)	90
β/deg	96.478(4)	91.0580(10)	96.992(2)
γ/deg	90	110.6260(10)	90
V/Å^3	1817.5(8)	1331.31(6)	4275.8(3)
F(000)	784	544	1888
Z	4	2	8
λ, Å	0.71073 (MoKα)	1.54178 (CuKα)	1.54178 (CuKα)
D_{calc}/g cm^{-3}	1.382	1.278	1.410
μ/mm^{-1}	0.373	2.469	2.022
θ range/deg	1.64 – 28.29	2.36 – 67.72	3.27 – 66.59
R_{int}	0.1077	0.0486	0.0610
reflections measured	20460	17573	34141
unique reflections	4221	4815	7537
reflections observed	2758	4232	5627
GOF on F^2	1.023	1.061	1.037
$R1^a$	0.0517	0.0356	0.0532
$wR2^b$	0.1537	0.0869	0.1593
Largest ≠ peak & hole/eÅ^{-3}	0.401 and -0.283	0.286 and -0.310	0.832 and -0.592

^{a} $R1 = \sum \big| |F_0| - |Fc| \big| / \sum |F_0|$. ^{b} w$R2$ (all data) = $\{\sum[w(|F_0|^2 - |Fc|^2)^2]/\sum[w(F_0^4)]\}^{1/2}$

X-ray diffraction studies. Single crystals were obtained by slow evaporation of solutions of the isolated compounds in *n*-butanol. Three dimensional X-ray data were collected on a Bruker D8 VENTURE (**2** and **5**) or a Bruker KAPPA APEXII CCD (**1**) diffractometers. In the case of **2** and **5**, data were corrected for absorption effects using the multi-scan method (SADABS)[3]; no absorption correction was applied in the case of **1**. Complex scattering factors were taken from the program SHELXL-2014[4] (**5**) or SHELXL-2016[4] (**1** and **2**) running under the Olex2 program[5] (**5**) or the WinGX program system[6] (**1** and **2**). The structure of **5** was solved with ShelXT,[7] whereas those of **1** and **2** were solved with SIR92.[8] The three structures were refined by full-matrix least-squares on F^2. For **1** and **2** all hydrogen atoms, except those corresponding to the N-H fragments of the imine function and the pyrrole ring and that of the C-H fragment of the triazole ring, which were refined freely in the final stages of the refinement, were included in calculated positions and refined in riding mode; in the case of **5** all hydrogen atoms were included in calculated positions. Finally, refinement converged with anisotropic displacement parameters for all non-hydrogen atoms for the three crystals. Crystal data and details on data collection and refinement are summarised in Table S1. Note: the crystallographic service did not provide the dimensions of the **2** measured crystal.

[3] SADABS 2016: L. Krause, R. Herbst-Irmer, G. M. Sheldrick and D. Stalke, *J. Appl. Cryst.*, 2015, **48**, 3-10.

[4] SHELXL: G. M. Sheldrick, *Acta Cryst.*, 2008, **A64**, 112-122.

[5] OLEX2: O. V. Dolomanov, L. J. Bourhis, R. J. Gildea, J. A. K. Howard and H. Puschmann, *J. Appl. Cryst.*, 2009, **42**, 339-341.

[6] WinGX: L. J. Farrugia, *J. Appl. Cryst.*, 1999, **32**, 837-838.

[7] SHELXT: G. M. Sheldrick, *Acta Cryst.*, 2015, **A71**, 3-8.

[8] SIR92: A. Altomare, G. Cascarano, C. Giacovazzo, A. Guagliardi, M. C. Burla, G. Polidori and M. Camalli, *J. Appl. Cryst.*, 1994, **27**, 435-435.

5. ^{1}H NMR TITRATIONS

5.1. Titration procedure and titration data fitting

Dichloromethane solutions of the hydrochloric salts of the nine compounds were washed three times with a 1 M sodium hydroxide aqueous solution and, after that, they were rinsed, also three times, with a 1 M perchloric acid aqueous solution, yielding the corresponding hydroperchloric salts. 2 mL of a DMSO-d_6 stock solution of the corresponding click tambjamine in its perchlorate form (host) were prepared (0.01 M). From this solution, 1 mL was taken to prepare the solution of the titrating agent (guest; the corresponding tetrabutylammonium –chloride or nitrate– or tetraethylammonium –bicarbonate– salt); in this way the dilution effect is avoided. 0.5 mL of the solution of the host were put into an NMR tube, which was capped with a septum, and the ^{1}H NMR spectrum was recorded. Subsequently, an aliquot of the solution of the guest was added with a proper microsyringe through the septum, the solution homogenised and the spectrum recorded. This process was repeated 20 times.

For each ^{1}H NMR titration, the signals of the protons of the imine and pyrrole NH and the triazole CH groups of the molecules were monitored for changes in chemical shift, which provided several data sets that were employed in the determination of the association constants K_a. The fitting, performed with the Bindfit software,[9] takes into account all data sets at the same time, thus improving the quality of the non-linear curve fitting. The data for both the chloride and nitrate adducts were fitted satisfactorily to the 1:1 (LH:A) binding model, LH being the protonated receptor and A the anion.

[9] (a) P. Thordarson, *Chem. Soc. Rev.*, 2011, **40**, 1305-1323; (b) www.supramolecular.org (last access: October 2019).

5.2. ^{1}H NMR titration spectra and fitted binding isotherms

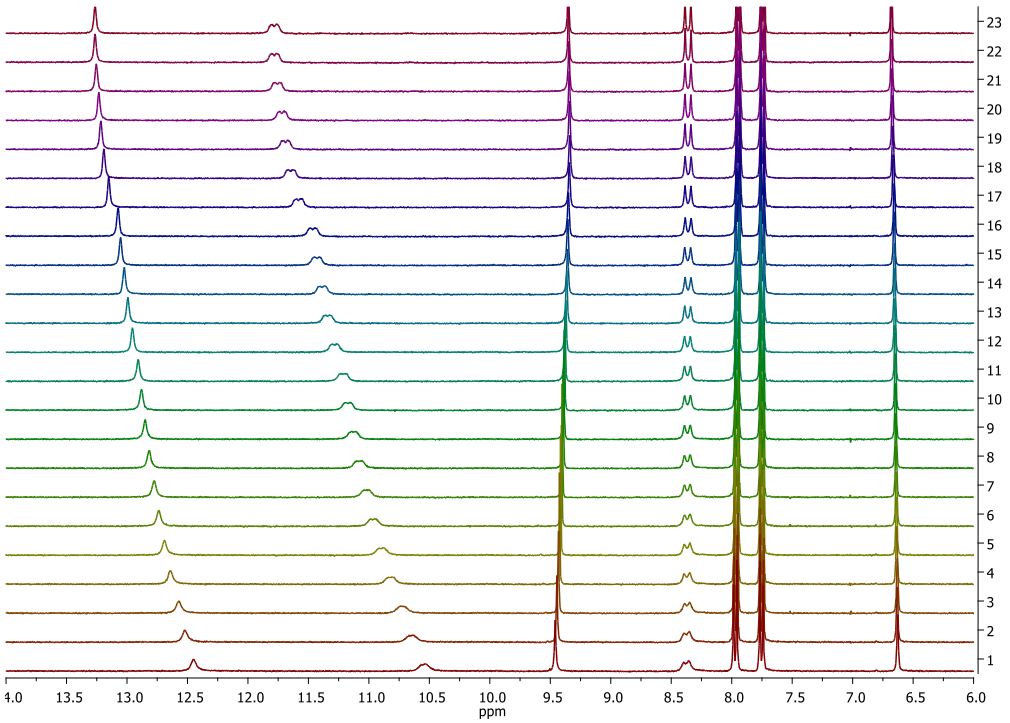

Figure S45. Excerpt of the ^{1}H NMR spectra (300 MHz, DMSO-d_6) obtained upon addition of different aliquots of a 0.1 M solution of TBACl, prepared with a 0.01 M solution of **1**·$HClO_4$, to a 0.01 M solution of **1**·$HClO_4$.

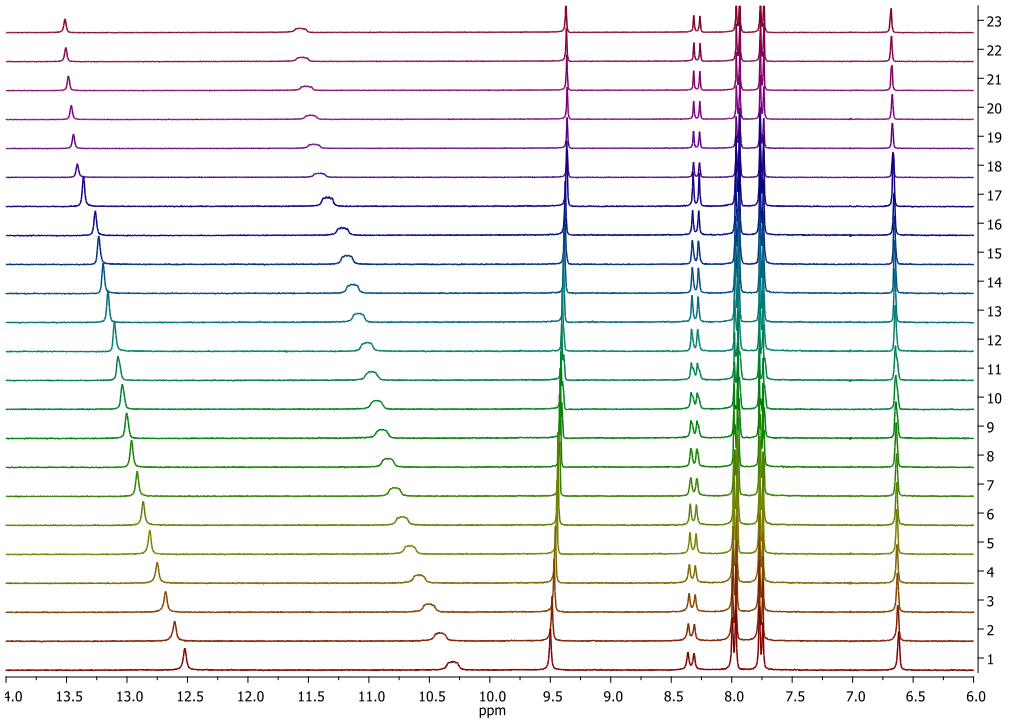

Figure S46. Excerpt of the ^{1}H NMR spectra (300 MHz, DMSO-d_6) obtained upon addition of different aliquots of a 0.1 M solution of TBACl, prepared with a 0.01 M solution of **2**·$HClO_4$, to a 0.01 M solution of **2**·$HClO_4$.

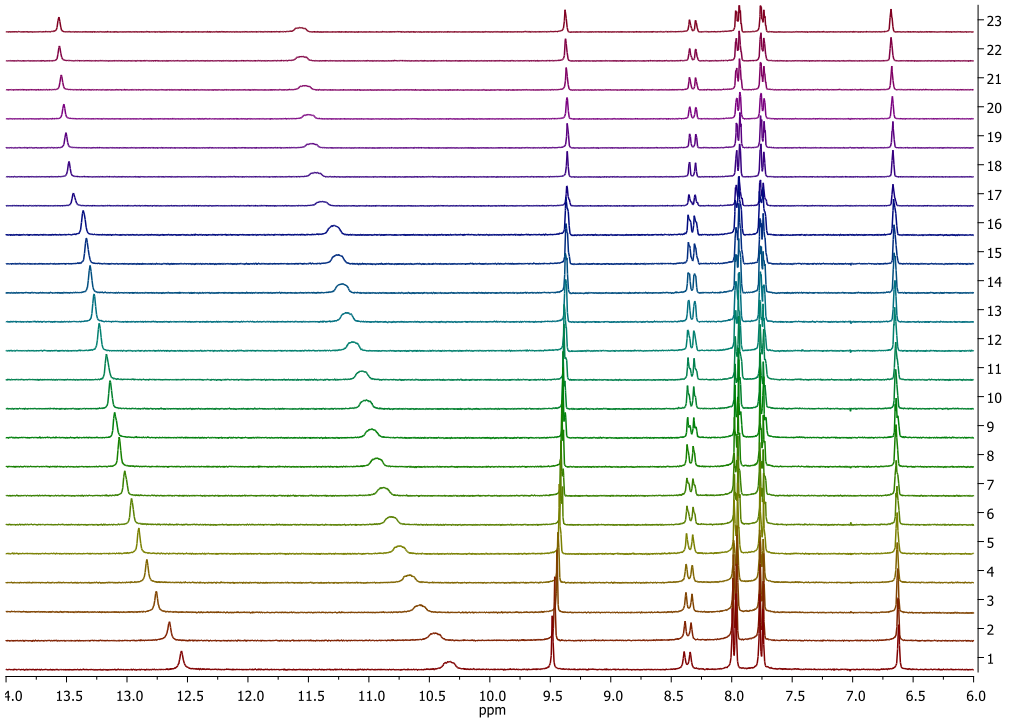

Figure S47. Excerpt of the ^{1}H NMR spectra (300 MHz, DMSO-d_6) obtained upon addition of different aliquots of a 0.1 M solution of TBACl, prepared with a 0.01 M solution of **3**·$HClO_4$, to a 0.01 M solution of **3**·$HClO_4$.

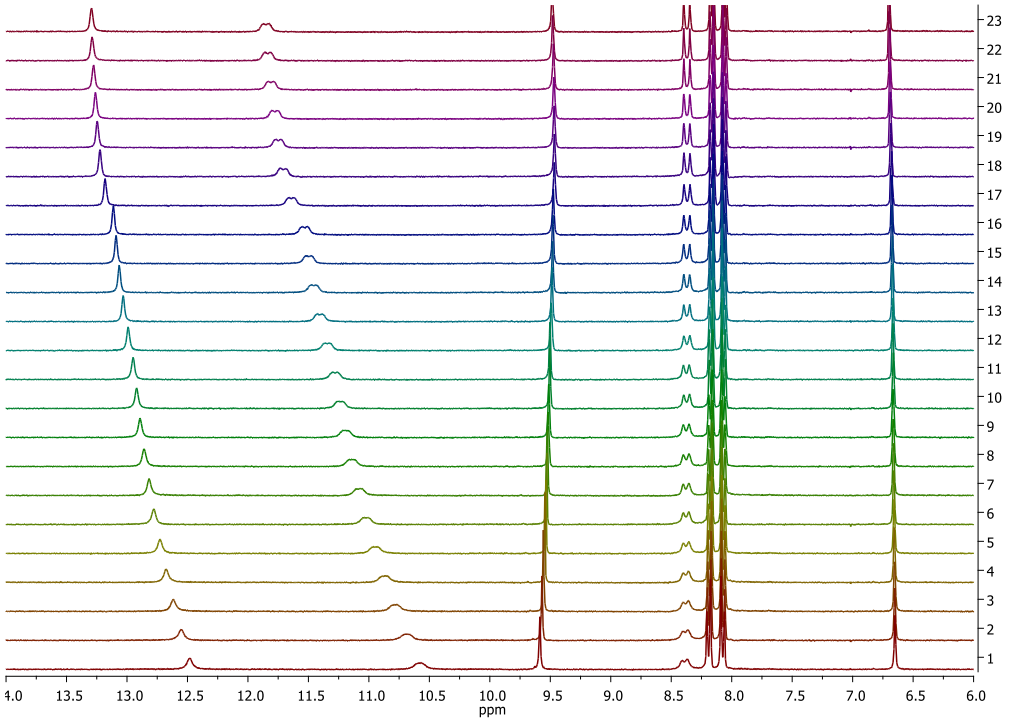

Figure S48. Excerpt of the ^{1}H NMR spectra (300 MHz, DMSO-d_6) obtained upon addition of different aliquots of a 0.1 M solution of TBACl, prepared with a 0.01 M solution of **4**·$HClO_4$, to a 0.01 M solution of **4**·$HClO_4$.

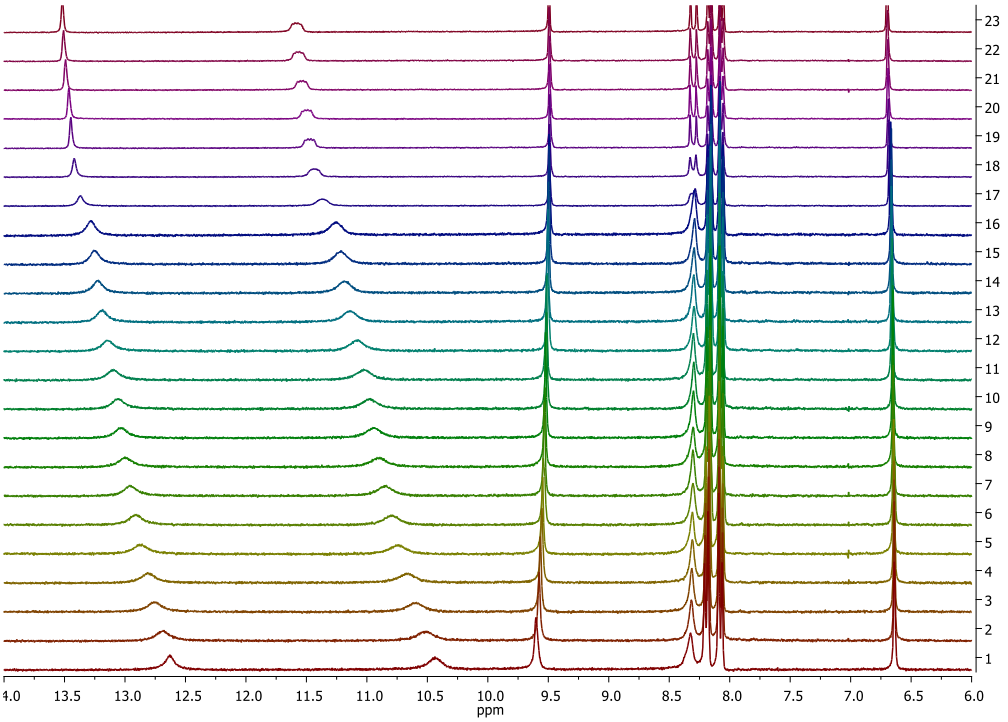

Figure S49. Excerpt of the ^{1}H NMR spectra (300 MHz, DMSO-d_6) obtained upon addition of different aliquots of a 0.1 M solution of TBACl, prepared with a 0.01 M solution of **5**·$HClO_4$, to a 0.01 M solution of **5**·$HClO_4$.

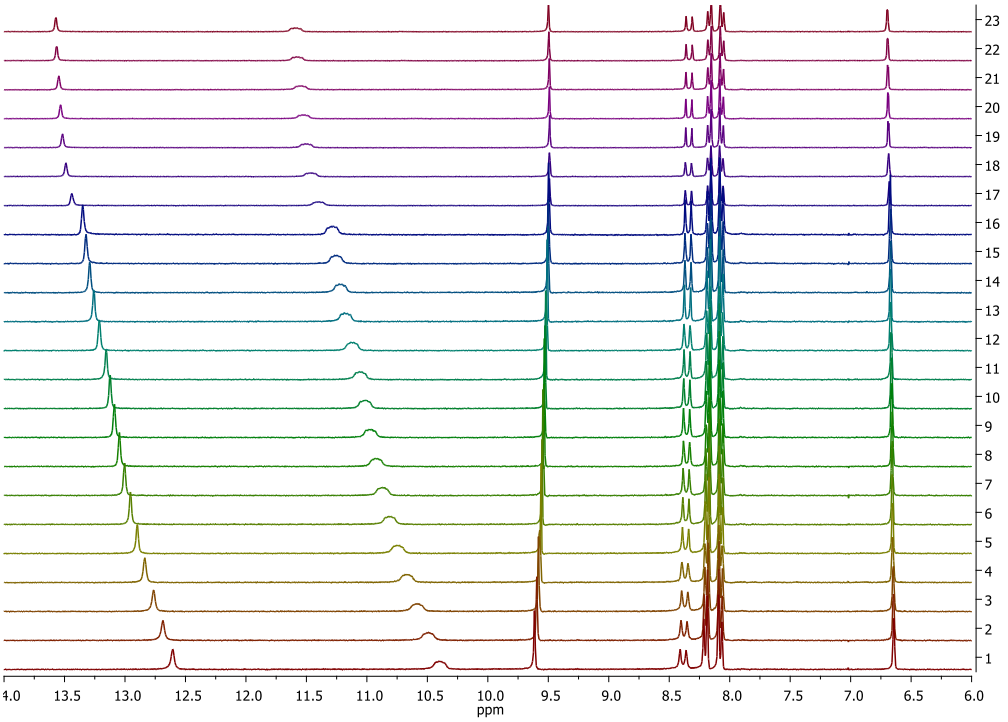

Figure S50. Excerpt of the ^{1}H NMR spectra (300 MHz, DMSO-d_6) obtained upon addition of different aliquots of a 0.1 M solution of TBACl, prepared with a 0.01 M solution of **6**·$HClO_4$, to a 0.01 M solution of **6**·$HClO_4$.

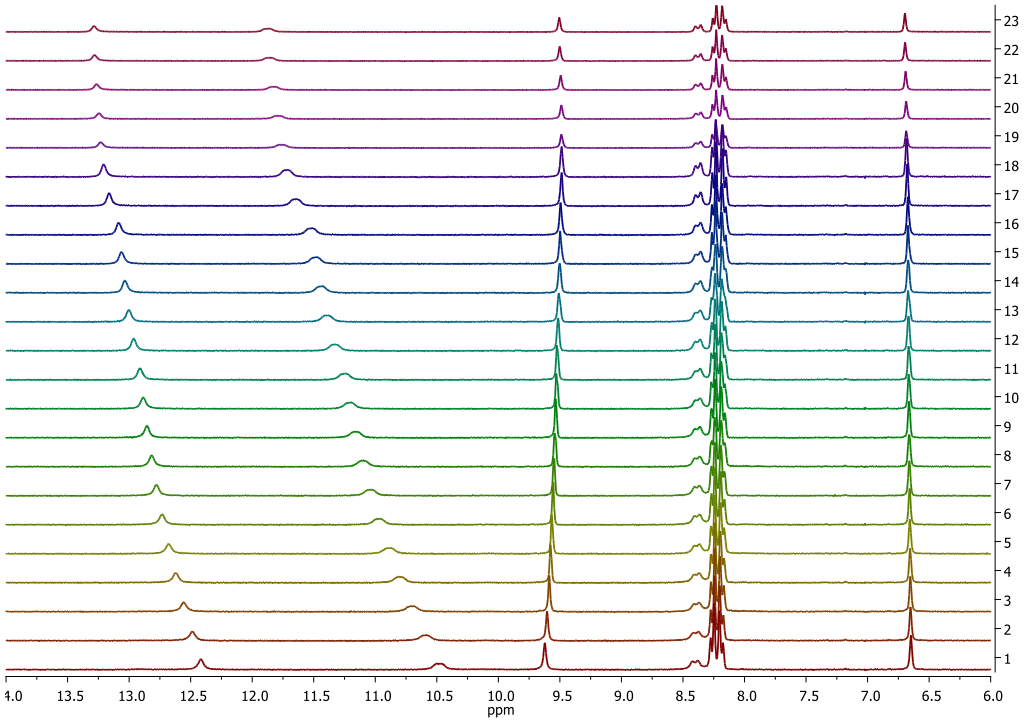

Figure S51. Excerpt of the ^{1}H NMR spectra (300 MHz, DMSO-d_6) obtained upon addition of different aliquots of a 0.1 M solution of TBACl, prepared with a 0.01 M solution of **7**·$HClO_4$, to a 0.01 M solution of **7**·$HClO_4$.

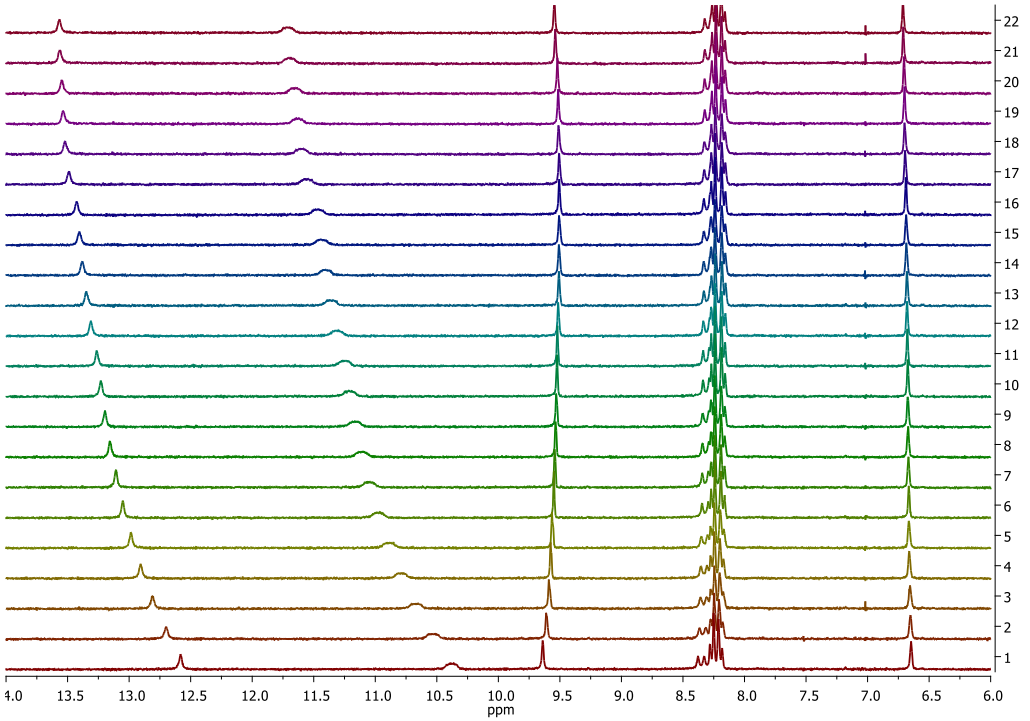

Figure S52. Excerpt of the ^{1}H NMR spectra (300 MHz, DMSO-d_6) obtained upon addition of different aliquots of a 0.1 M solution of TBACl, prepared with a 0.01 M solution of **8**·$HClO_4$, to a 0.01 M solution of **8**·$HClO_4$.

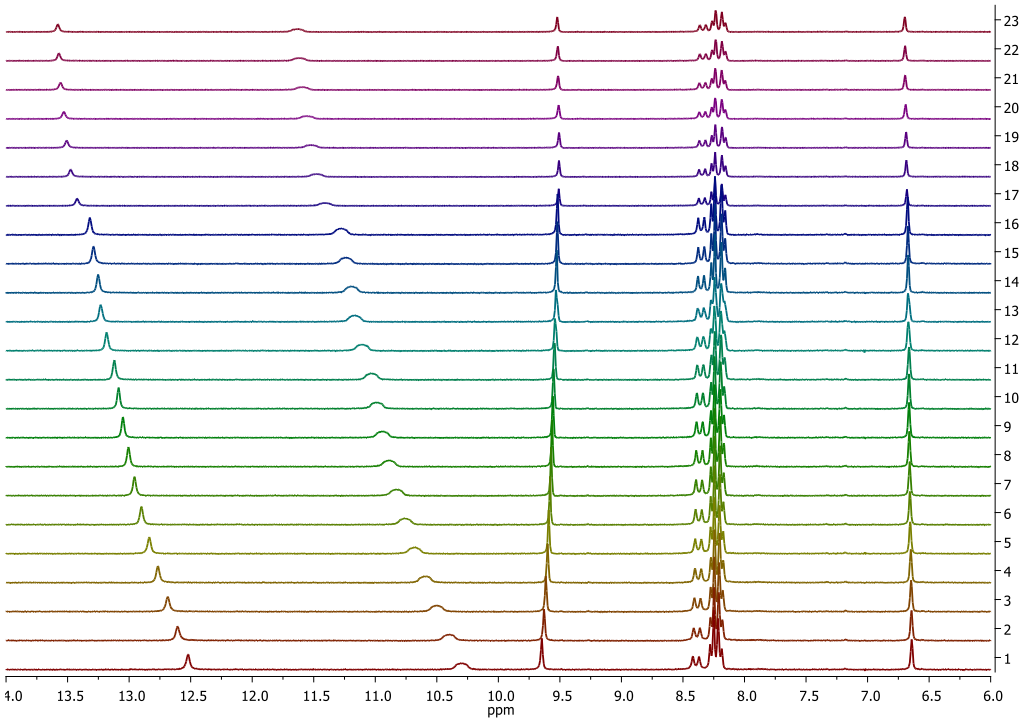

Figure S53. Excerpt of the ^{1}H NMR spectra (300 MHz, DMSO-d_6) obtained upon addition of different aliquots of a 0.1 M solution of TBACl, prepared with a 0.01 M solution of **9**·$HClO_4$, to a 0.01 M solution of **9**·$HClO_4$.

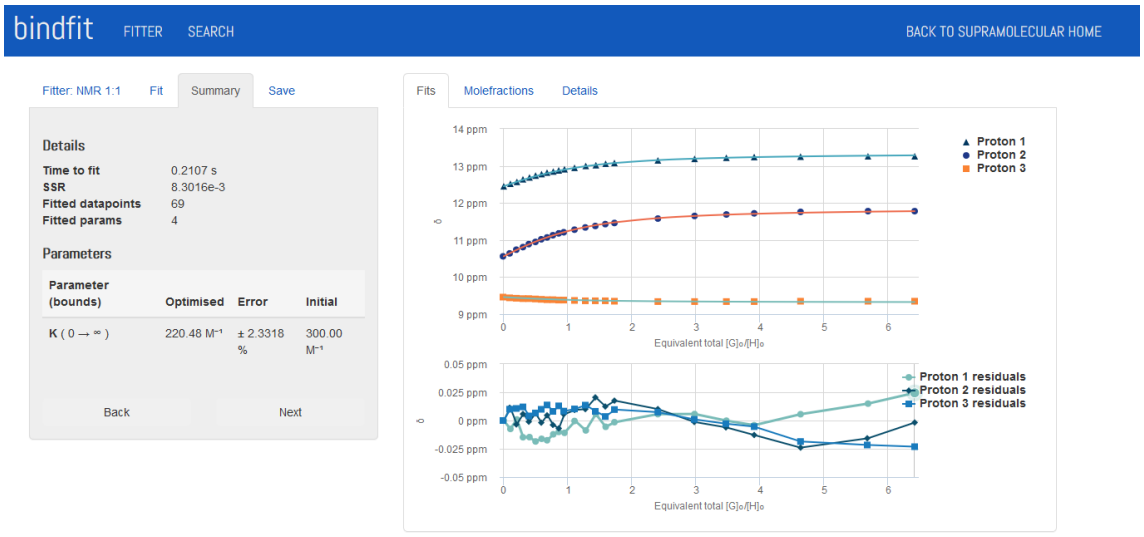

Figure S54. Fitted binding isotherm obtained for the titration of a 0.01 M solution of compound **1**·$HClO_4$ with a 0.1 M solution of TBACl (DMSO-d_6). In order to avoid the dilution effect, the latter was prepared with the former. The graph shows the change in chemical shift of the signals due to the pyrrole and imine NH protons and the triazole CH proton of the molecule, fitted to the 1:1 (LH:Cl) binding model. K_a = 220 ± 5 M^{-1}.

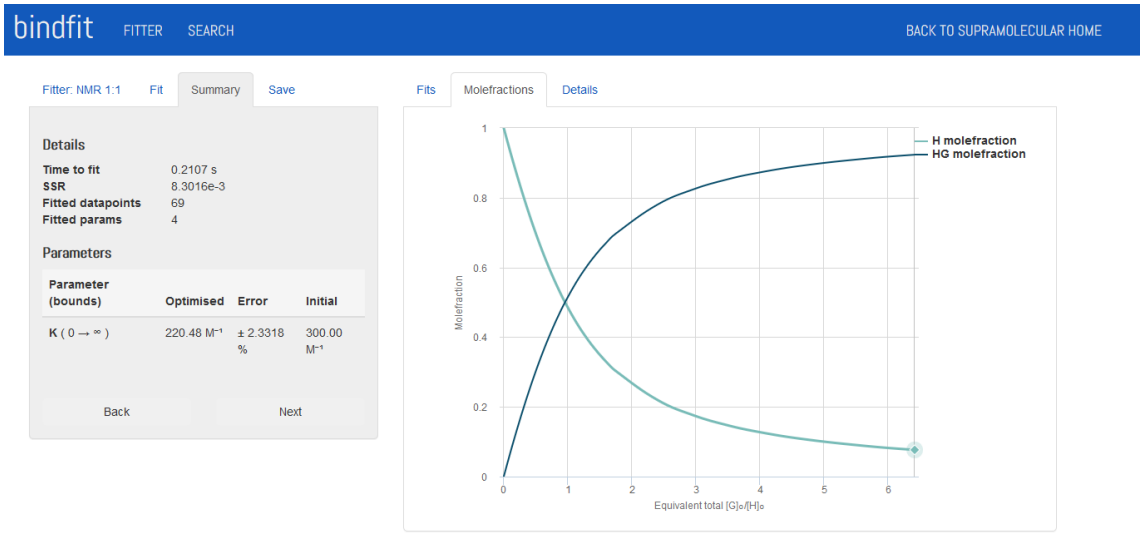

Figure S55. Species distribution diagram obtained for the titration of a 0.01 M solution of compound **1**·$HClO_4$ with a 0.1 M solution of TBACl (DMSO-d_6), to show how the composition of the mixture changes over the course of the titration. *H* corresponds to the host, the protonated click tambjamine, and *G* to the guest, the chloride anion.

Figure S56. Fitted binding isotherm obtained for the titration of a 0.01 M solution of compound **2**·$HClO_4$ with a 0.1 M solution of TBACl (DMSO-d_6). In order to avoid the dilution effect, the latter was prepared with the former. The graph shows the change in chemical shift of the signals due to the pyrrole and imine NH protons and the triazole CH proton of the molecule, fitted to the 1:1 (LH:Cl) binding model. K_a = 240 ± 8 M^{-1}.

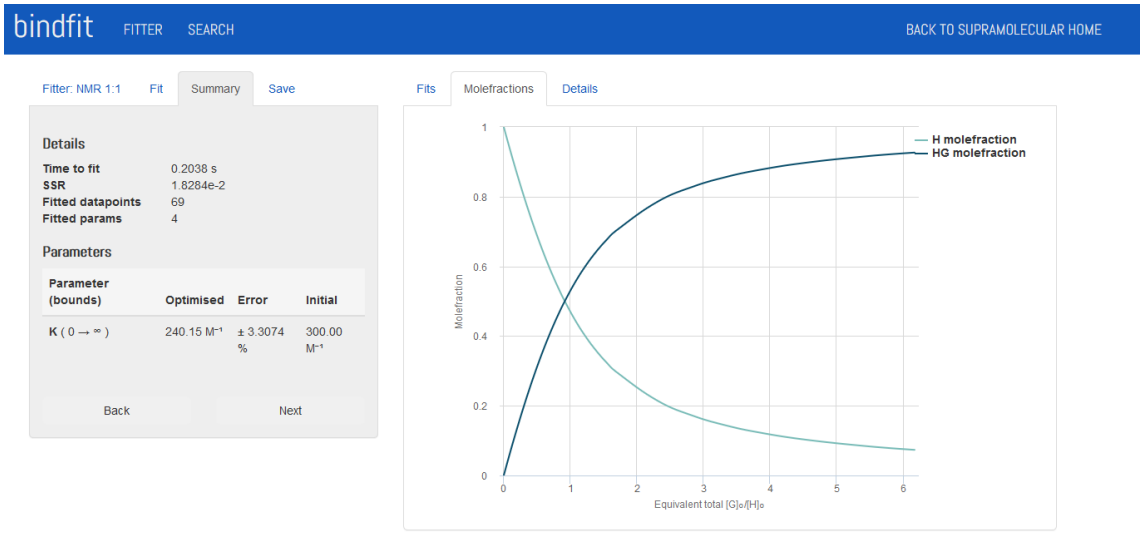

Figure S57. Species distribution diagram obtained for the titration of a 0.01 M solution of compound **2**·$HClO_4$ with a 0.1 M solution of TBACl (DMSO-d_6), to show how the composition of the mixture changes over the course of the titration. *H* corresponds to the host, the protonated click tambjamine, and *G* to the guest, the chloride anion.

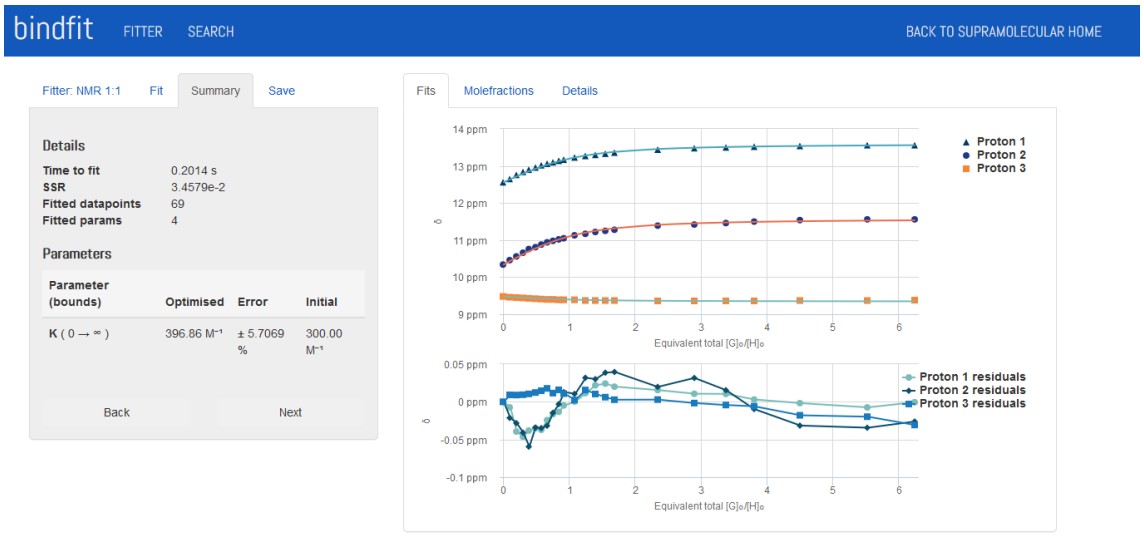

Figure S58. Fitted binding isotherm obtained for the titration of a 0.01 M solution of compound **3**·$HClO_4$ with a 0.1 M solution of TBACl (DMSO-d_6). In order to avoid the dilution effect, the latter was prepared with the former. The graph shows the change in chemical shift of the signals due to the pyrrole and imine NH protons and the triazole CH proton of the molecule, fitted to the 1:1 (LH:Cl) binding model. K_a = 397 ± 23 M^{-1}.

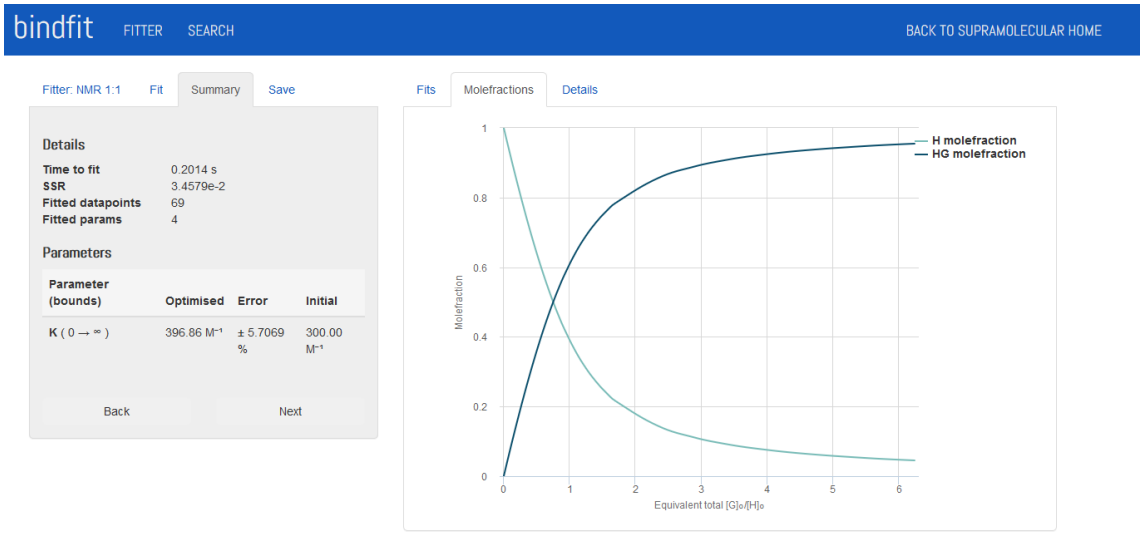

Figure S59. Species distribution diagram obtained for the titration of a 0.01 M solution of compound **3**·$HClO_4$ with a 0.1 M solution of TBACl (DMSO-d_6), to show how the composition of the mixture changes over the course of the titration. *H* corresponds to the host, the protonated click tambjamine, and *G* to the guest, the chloride anion.

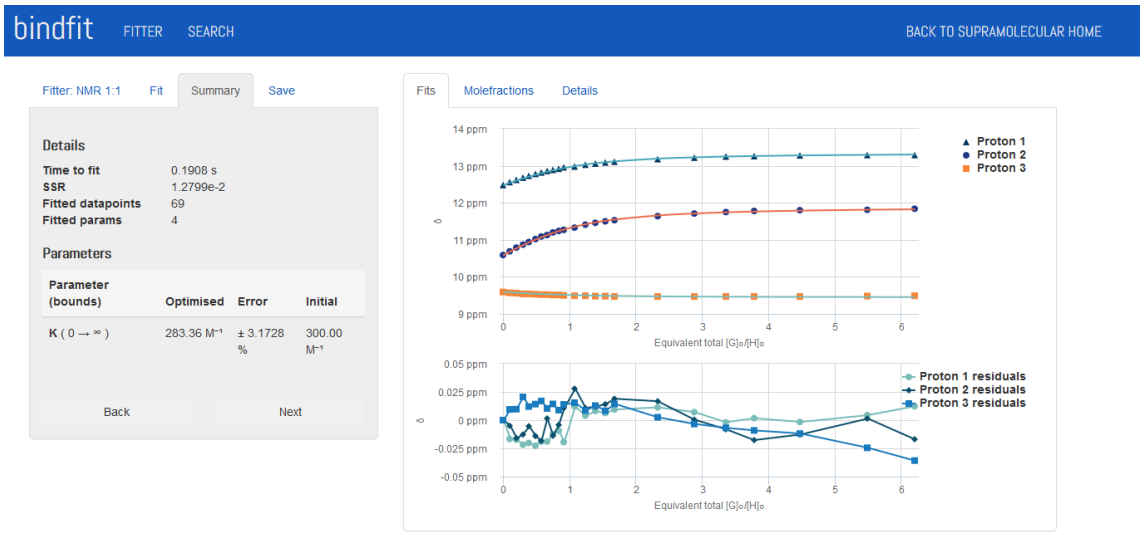

Figure S60. Fitted binding isotherm obtained for the titration of a 0.01 M solution of compound **4**·$HClO_4$ with a 0.1 M solution of TBACl (DMSO-d_6). In order to avoid the dilution effect, the latter was prepared with the former. The graph shows the change in chemical shift of the signals due to the pyrrole and imine NH protons and the triazole CH proton of the molecule, fitted to the 1:1 (LH:Cl) binding model. K_a = 283 ± 9 M^{-1}.

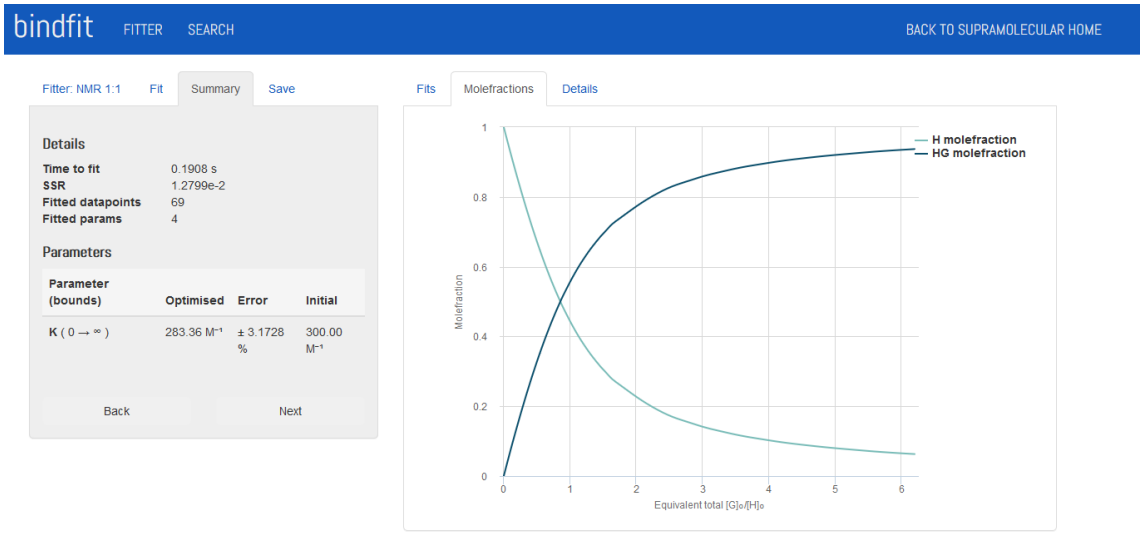

Figure S61. Species distribution diagram obtained for the titration of a 0.01 M solution of compound **4**·$HClO_4$ with a 0.1 M solution of TBACl (DMSO-d_6), to show how the composition of the mixture changes over the course of the titration. *H* corresponds to the host, the protonated click tambjamine, and *G* to the guest, the chloride anion.

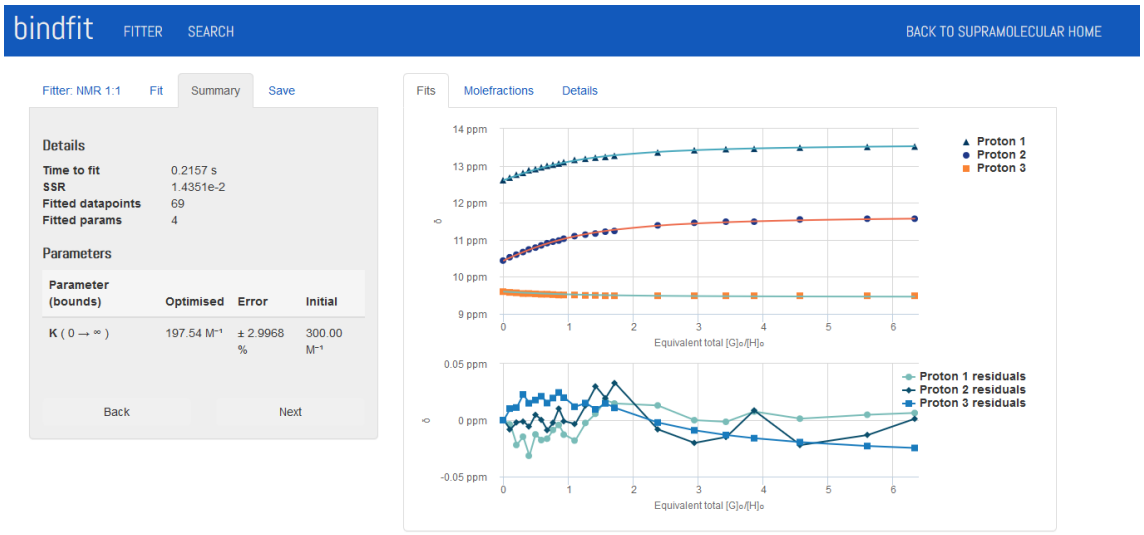

Figure S62. Fitted binding isotherm obtained for the titration of a 0.01 M solution of compound **5**·$HClO_4$ with a 0.1 M solution of TBACl (DMSO-d_6). In order to avoid the dilution effect, the latter was prepared with the former. The graph shows the change in chemical shift of the signals due to the pyrrole and imine NH protons and the triazole CH proton of the molecule, fitted to the 1:1 (LH:Cl) binding model. K_a = 197 ± 6 M^{-1}.

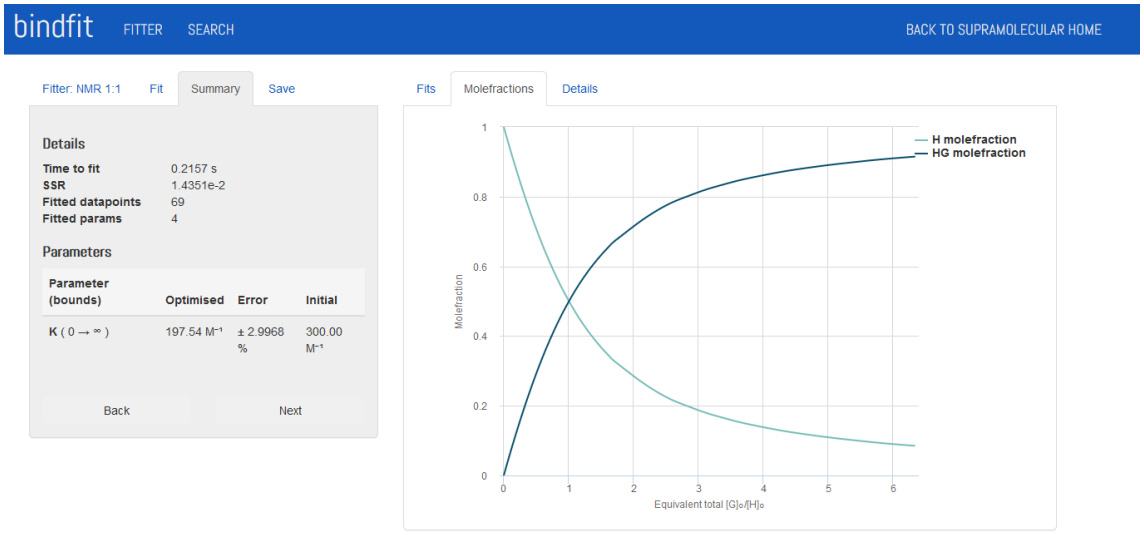

Figure S63. Species distribution diagram obtained for the titration of a 0.01 M solution of compound **5**·$HClO_4$ with a 0.1 M solution of TBACl (DMSO-d_6), to show how the composition of the mixture changes over the course of the titration. *H* corresponds to the host, the protonated click tambjamine, and *G* to the guest, the chloride anion.

Figure S64. Fitted binding isotherm obtained for the titration of a 0.01 M solution of compound **6**·$HClO_4$ with a 0.1 M solution of TBACl (DMSO-d_6). In order to avoid the dilution effect, the latter was prepared with the former. The graph shows the change in chemical shift of the signals due to the pyrrole and imine NH protons and the triazole CH proton of the molecule, fitted to the 1:1 (LH:Cl) binding model. K_a = 281 ± 7 M^{-1}.

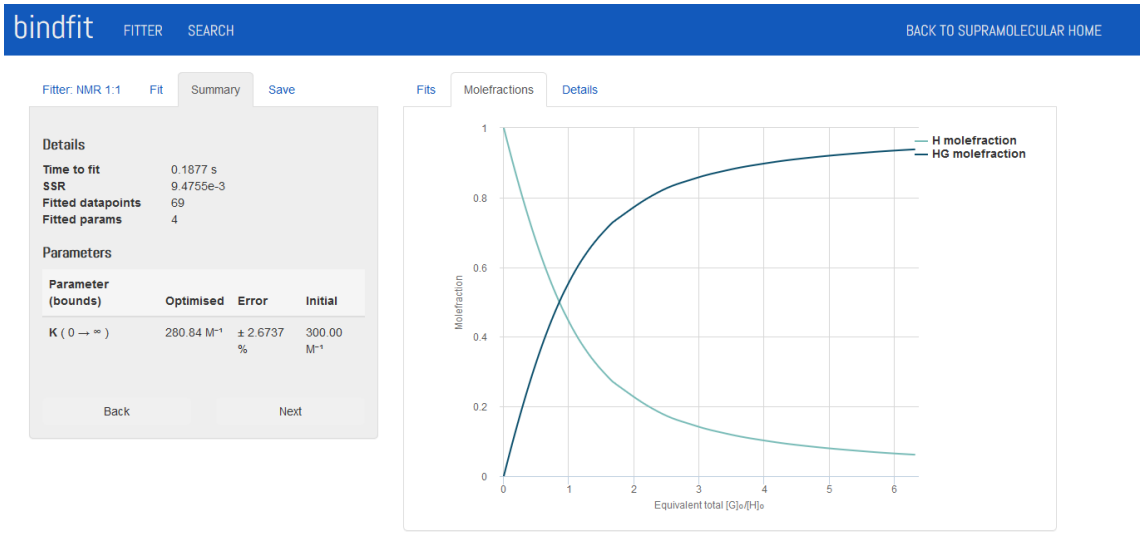

Figure S65. Species distribution diagram obtained for the titration of a 0.01 M solution of compound **6**·$HClO_4$ with a 0.1 M solution of TBACl (DMSO-d_6), to show how the composition of the mixture changes over the course of the titration. *H* corresponds to the host, the protonated click tambjamine, and *G* to the guest, the chloride anion.

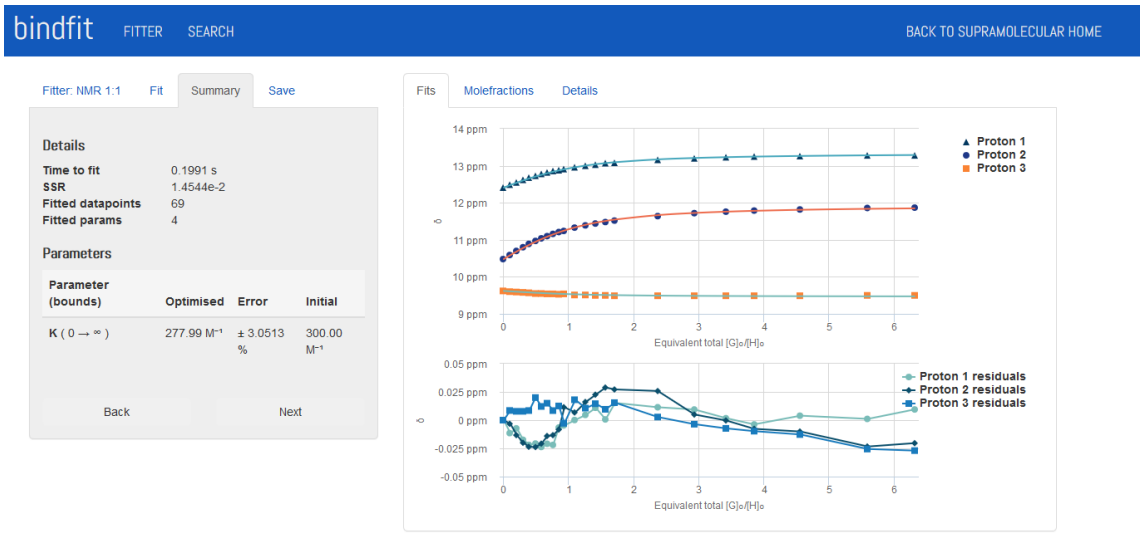

Figure S66. Fitted binding isotherm obtained for the titration of a 0.01 M solution of compound **7**·$HClO_4$ with a 0.1 M solution of TBACl (DMSO-d_6). In order to avoid the dilution effect, the latter was prepared with the former. The graph shows the change in chemical shift of the signals due to the pyrrole and imine NH protons and the triazole CH proton of the molecule, fitted to the 1:1 (LH:Cl) binding model. K_a = 278 ± 8 M^{-1}.

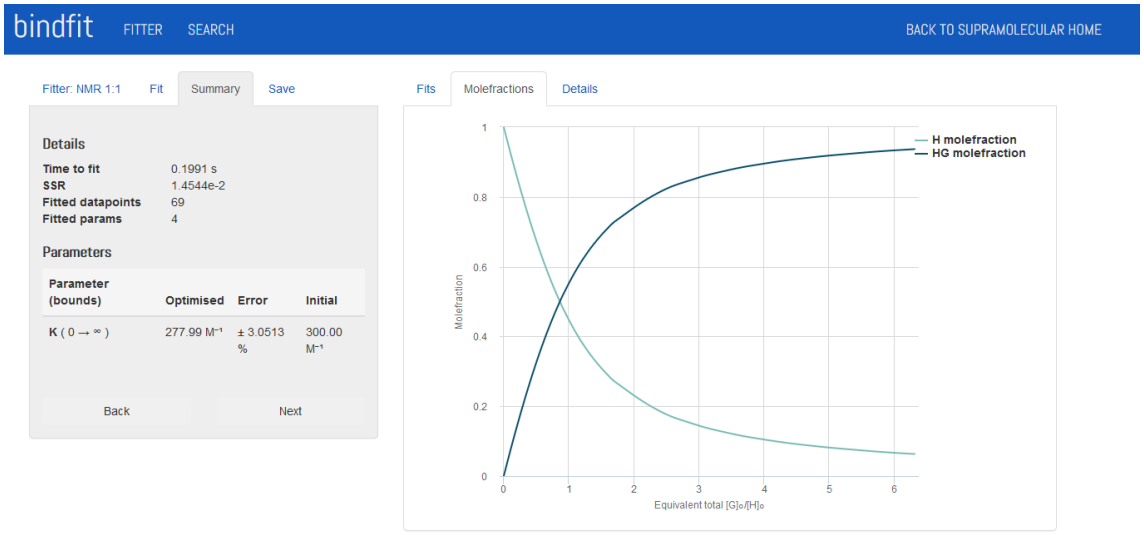

Figure S67. Species distribution diagram obtained for the titration of a 0.01 M solution of compound **7**·$HClO_4$ with a 0.1 M solution of TBACl (DMSO-d_6), to show how the composition of the mixture changes over the course of the titration. *H* corresponds to the host, the protonated click tambjamine, and *G* to the guest, the chloride anion.

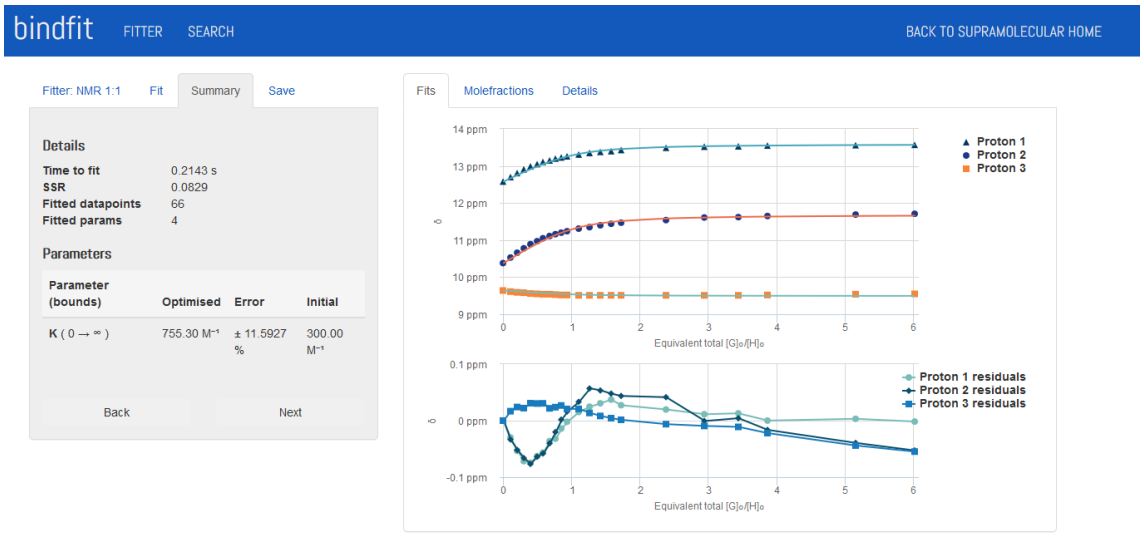

Figure S68. Fitted binding isotherm obtained for the titration of a 0.01 M solution of compound **8**·$HClO_4$ with a 0.1 M solution of TBACl (DMSO-d_6). In order to avoid the dilution effect, the latter was prepared with the former. The graph shows the change in chemical shift of the signals due to the pyrrole and imine NH protons and the triazole CH proton of the molecule, fitted to the 1:1 (LH:Cl) binding model. K_a = 755 ± 87 M^{-1}.

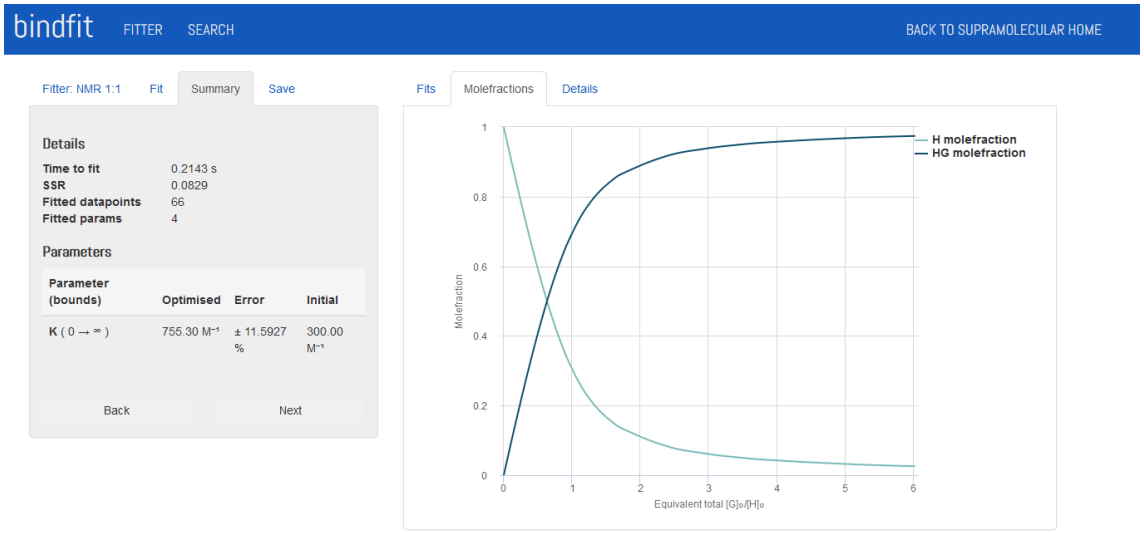

Figure S69. Species distribution diagram obtained for the titration of a 0.01 M solution of compound **8**·$HClO_4$ with a 0.1 M solution of TBACl (DMSO-d_6), to show how the composition of the mixture changes over the course of the titration. *H* corresponds to the host, the protonated click tambjamine, and *G* to the guest, the chloride anion.

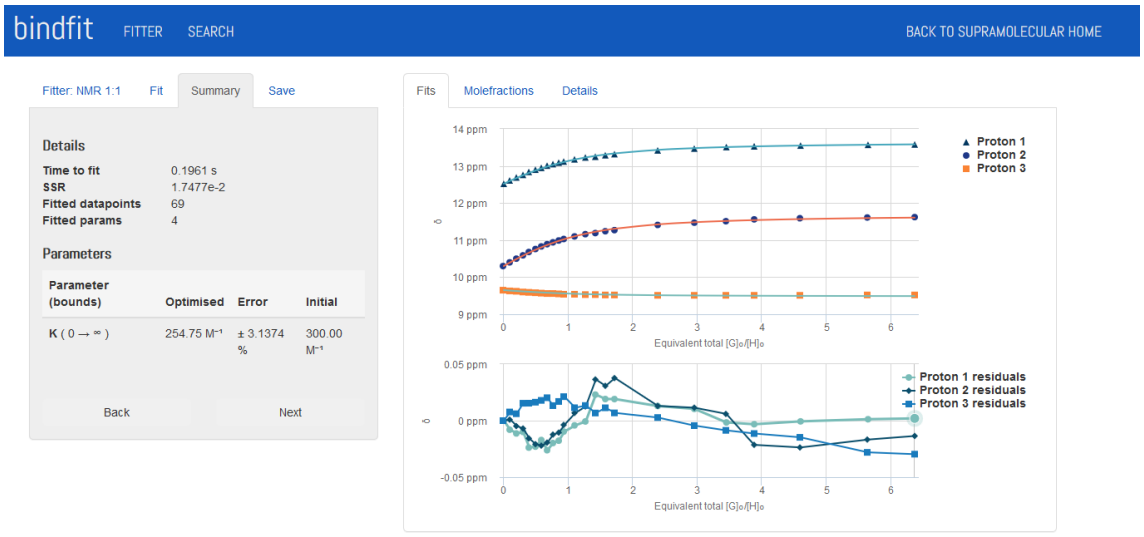

Figure S70. Fitted binding isotherm obtained for the titration of a 0.01 M solution of compound **9**·$HClO_4$ with a 0.1 M solution of TBACl (DMSO-d_6). In order to avoid the dilution effect, the latter was prepared with the former. The graph shows the change in chemical shift of the signals due to the pyrrole and imine NH protons and the triazole CH proton of the molecule, fitted to the 1:1 (LH:Cl) binding model. K_a = 255 ± 8 M^{-1}.

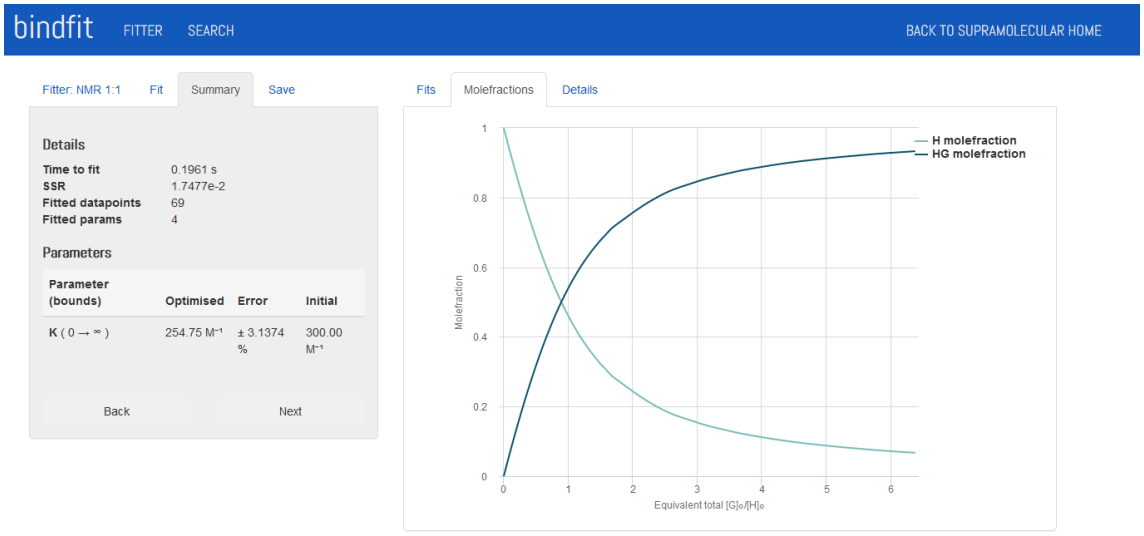

Figure S71. Species distribution diagram obtained for the titration of a 0.01 M solution of compound **9**·$HClO_4$ with a 0.1 M solution of TBACl (DMSO-d_6), to show how the composition of the mixture changes over the course of the titration. *H* corresponds to the host, the protonated click tambjamine, and *G* to the guest, the chloride anion.

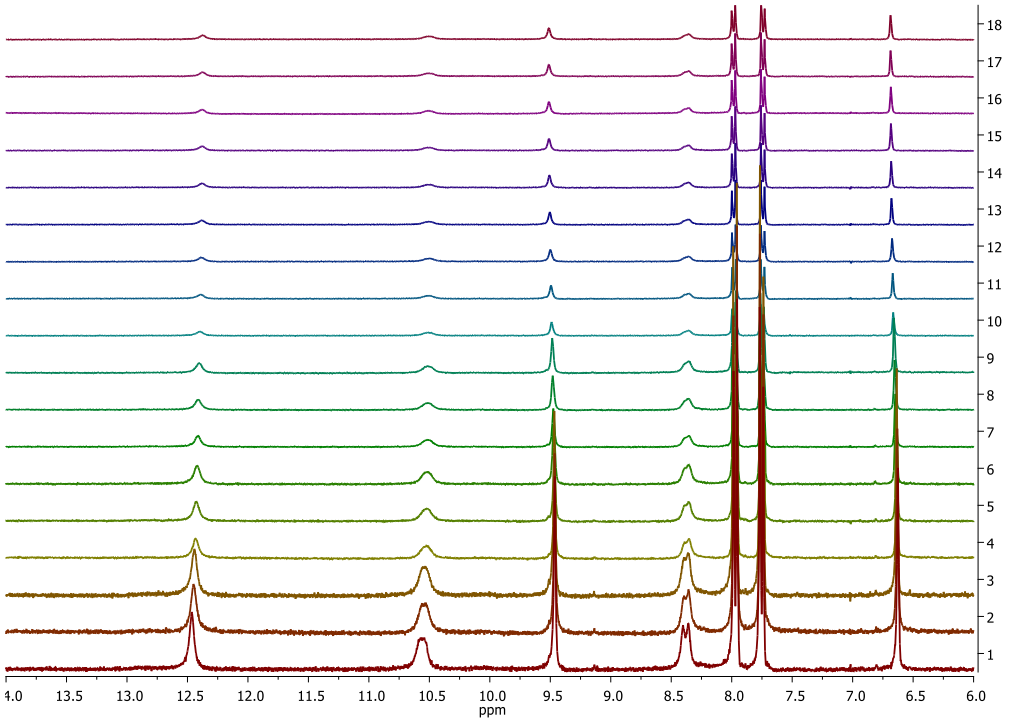

Figure S72. Excerpt of the ^{1}H NMR spectra (300 MHz, DMSO-d_6) obtained upon addition of different aliquots of a 0.6 M solution of $TBANO_3$, prepared with a 0.01 M solution of **1**·$HClO_4$, to a 0.01 M solution of **1**·$HClO_4$.

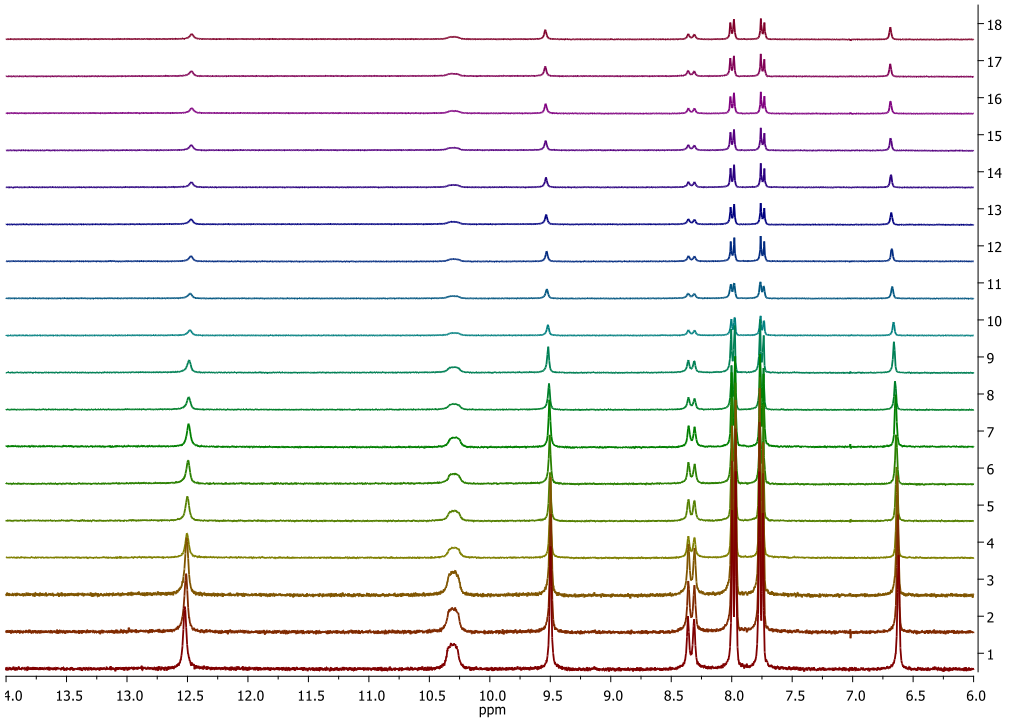

Figure S73. Excerpt of the ^{1}H NMR spectra (300 MHz, DMSO-d_6) obtained upon addition of different aliquots of a 0.6 M solution of $TBANO_3$, prepared with a 0.01 M solution of **2**·$HClO_4$, to a 0.01 M solution of **2**·$HClO_4$.

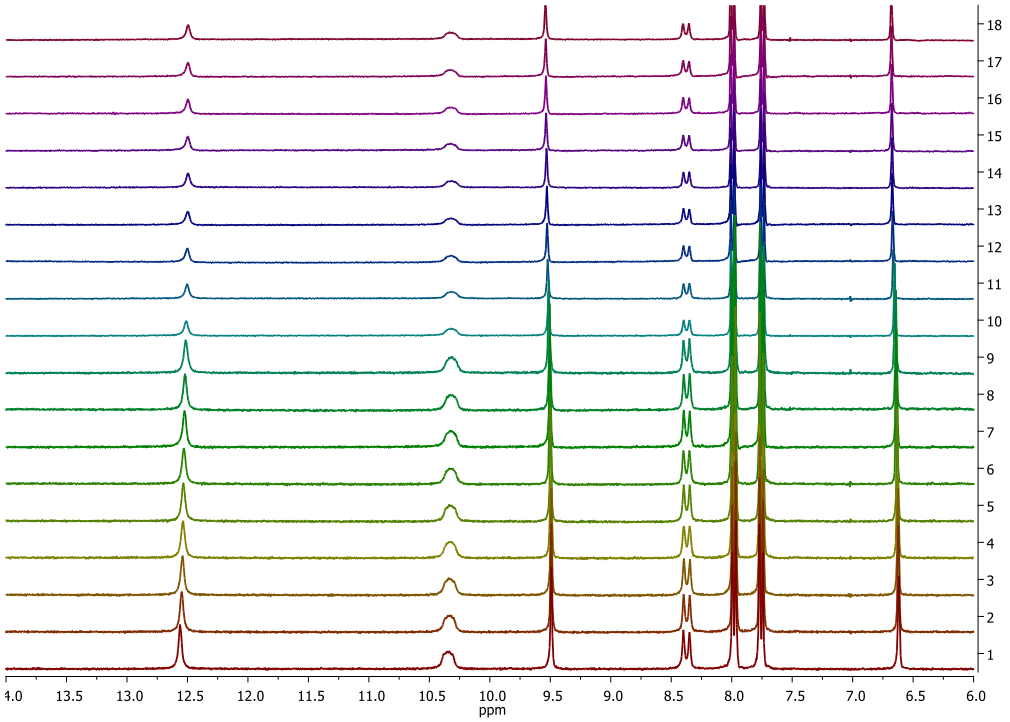

Figure S74. Excerpt of the ^{1}H NMR spectra (300 MHz, DMSO-d_6) obtained upon addition of different aliquots of a 0.6 M solution of $TBANO_3$, prepared with a 0.01 M solution of **3**·$HClO_4$, to a 0.01 M solution of **3**·$HClO_4$.

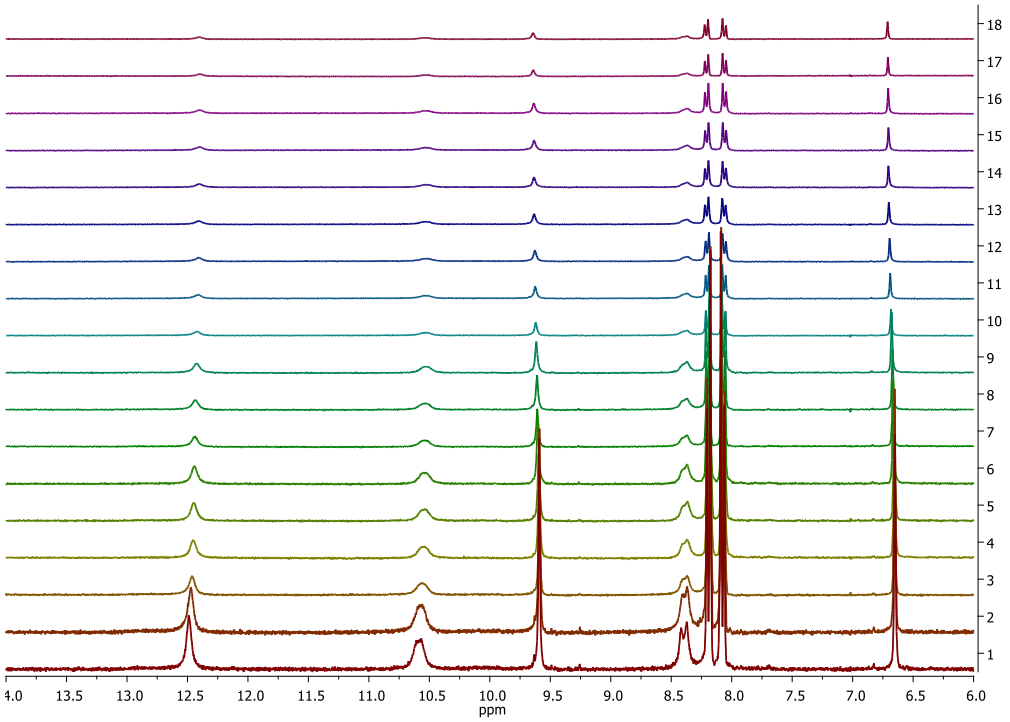

Figure S75. Excerpt of the ^{1}H NMR spectra (300 MHz, DMSO-d_6) obtained upon addition of different aliquots of a 0.6 M solution of $TBANO_3$, prepared with a 0.01 M solution of **4**·$HClO_4$, to a 0.01 M solution of **4**·$HClO_4$.

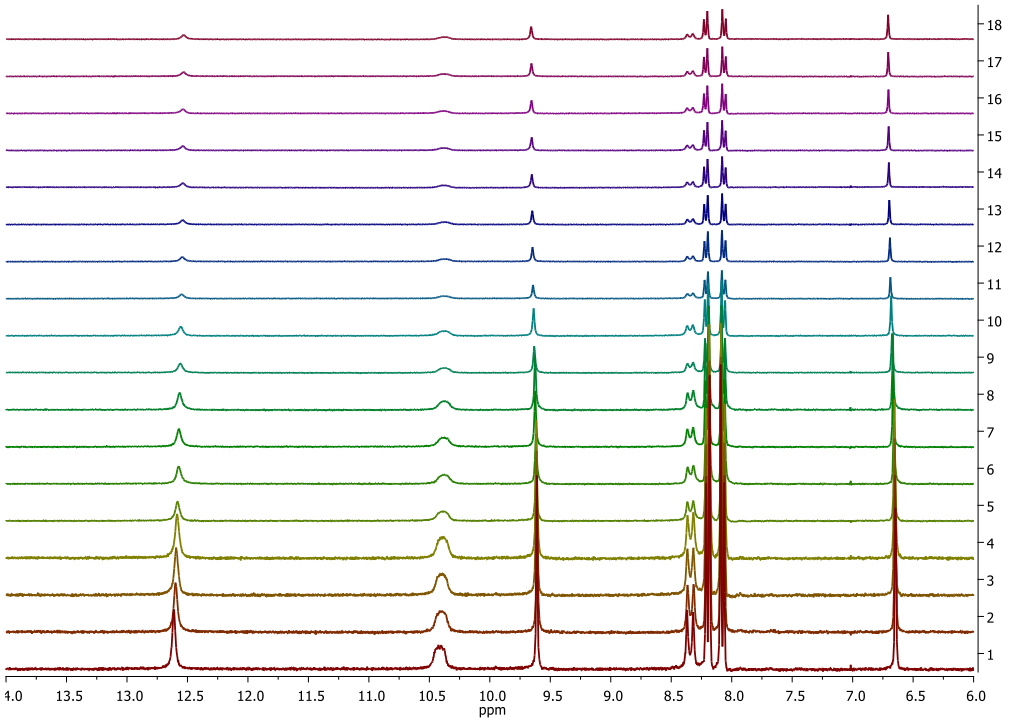

Figure S76. Excerpt of the ^{1}H NMR spectra (300 MHz, DMSO-d_6) obtained upon addition of different aliquots of a 0.6 M solution of $TBANO_3$, prepared with a 0.01 M solution of **5**·$HClO_4$, to a 0.01 M solution of **5**·$HClO_4$.

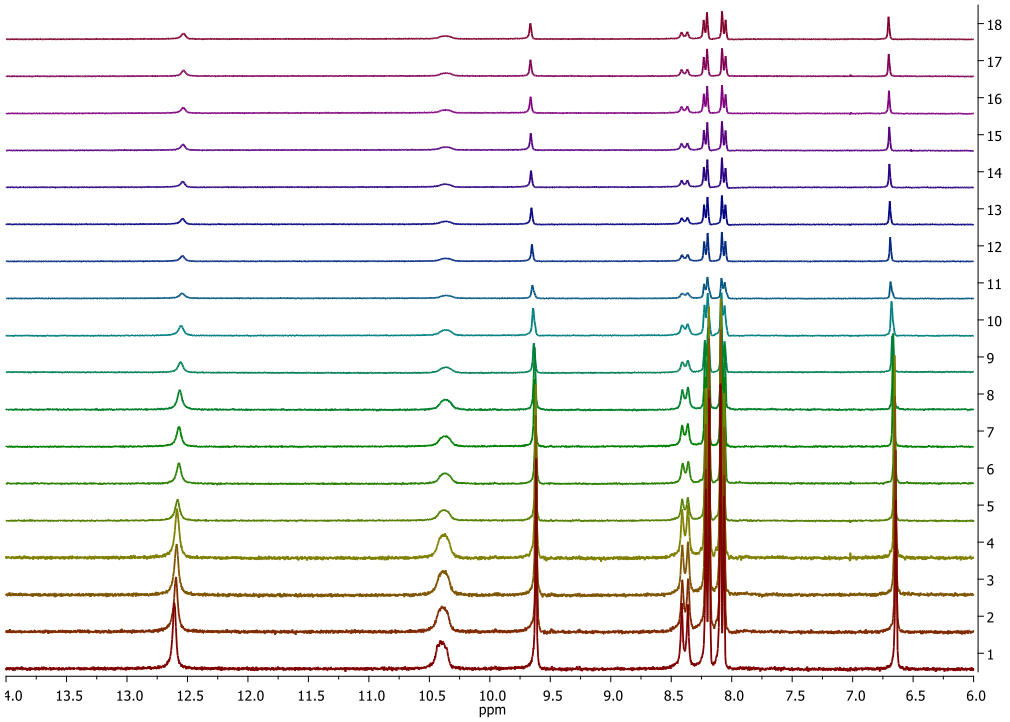

Figure S77. Excerpt of the ^{1}H NMR spectra (300 MHz, DMSO-d_6) obtained upon addition of different aliquots of a 0.6 M solution of $TBANO_3$, prepared with a 0.01 M solution of **6**·$HClO_4$, to a 0.01 M solution of **6**·$HClO_4$.

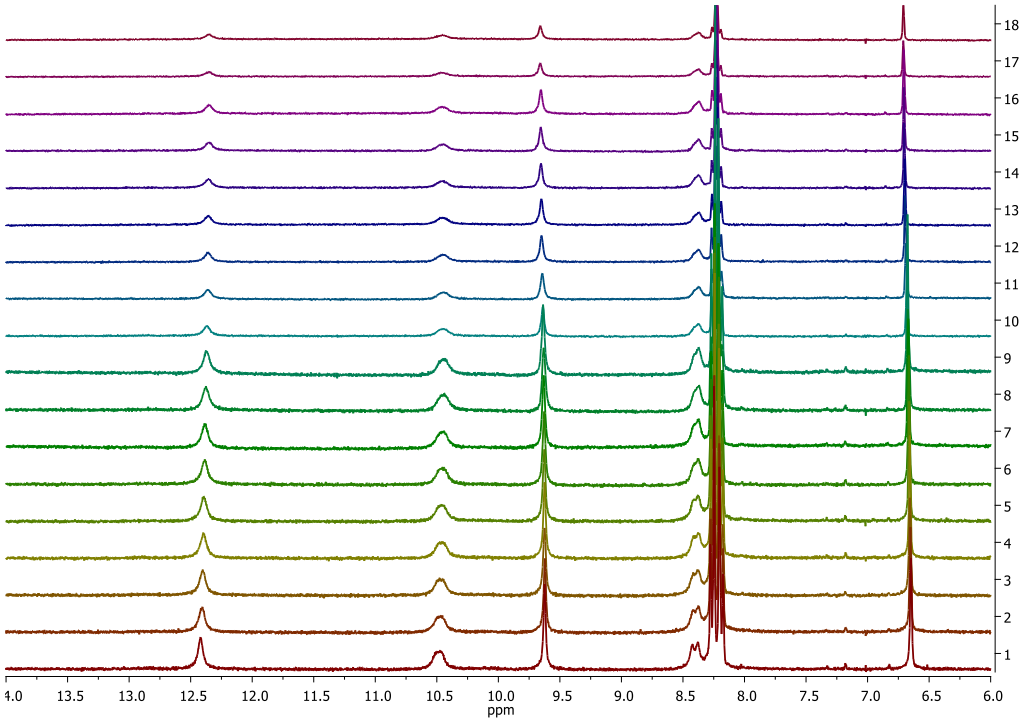

Figure S78. Excerpt of the ^{1}H NMR spectra (300 MHz, DMSO-d_6) obtained upon addition of different aliquots of a 0.6 M solution of $TBANO_3$, prepared with a 0.01 M solution of **7**·$HClO_4$, to a 0.01 M solution of **7**·$HClO_4$.

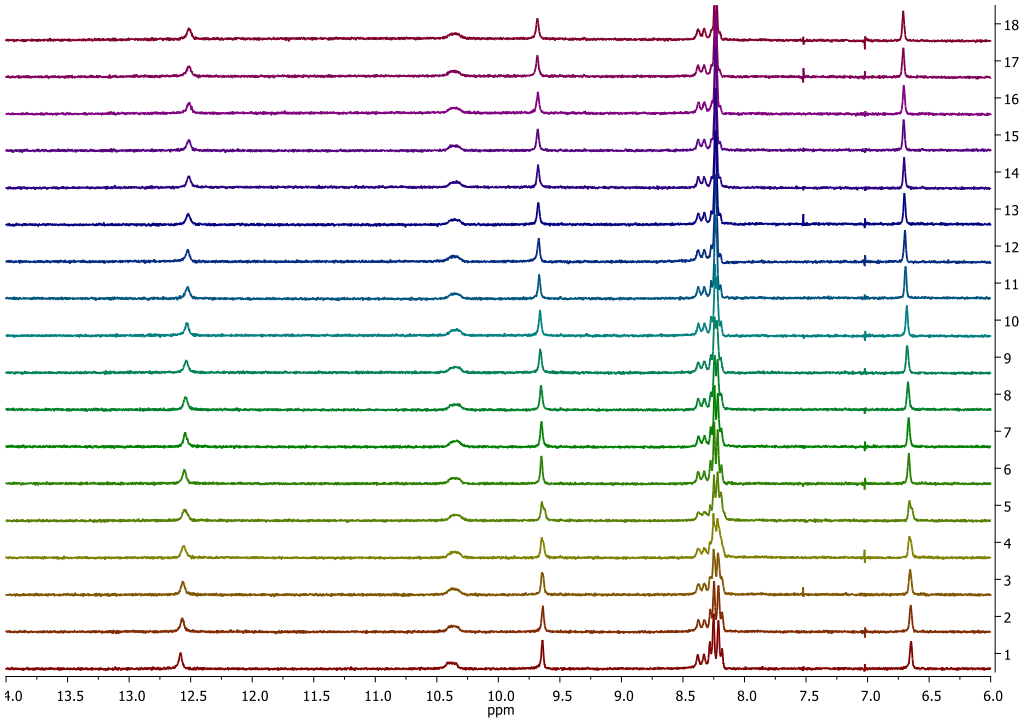

Figure S79. Excerpt of the ^{1}H NMR spectra (300 MHz, DMSO-d_6) obtained upon addition of different aliquots of a 0.6 M solution of $TBANO_3$, prepared with a 0.01 M solution of **8**·$HClO_4$, to a 0.01 M solution of **8**·$HClO_4$.

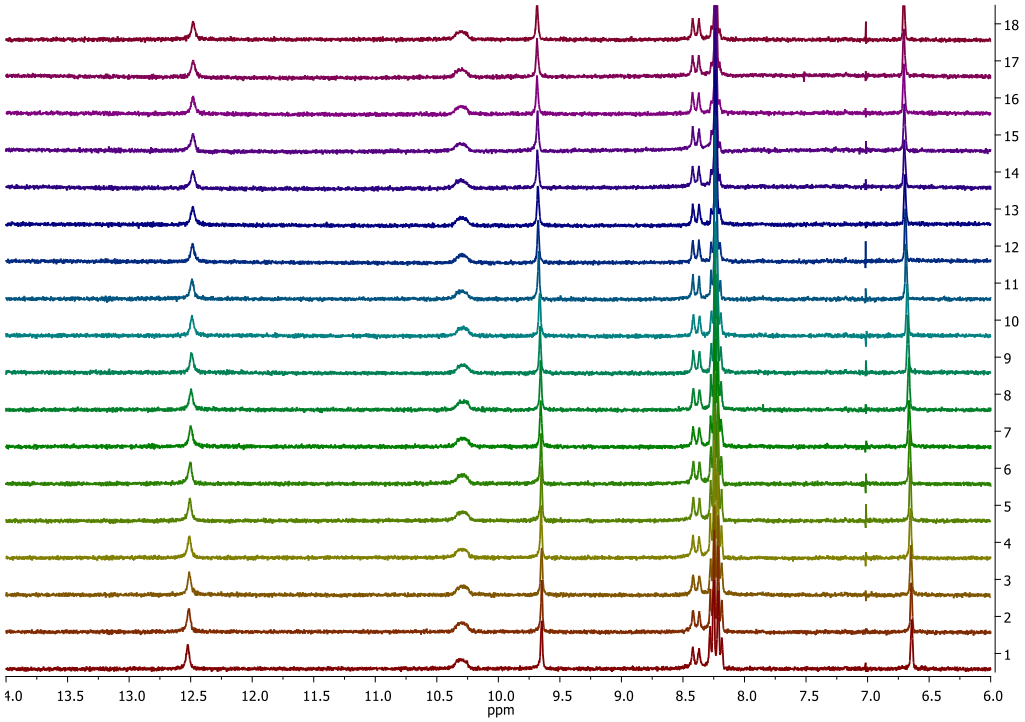

Figure S80. Excerpt of the ^{1}H NMR spectra (300 MHz, DMSO-d_6) obtained upon addition of different aliquots of a 0.6 M solution of $TBANO_3$, prepared with a 0.01 M solution of **9**·$HClO_4$, to a 0.01 M solution of **9**·$HClO_4$.

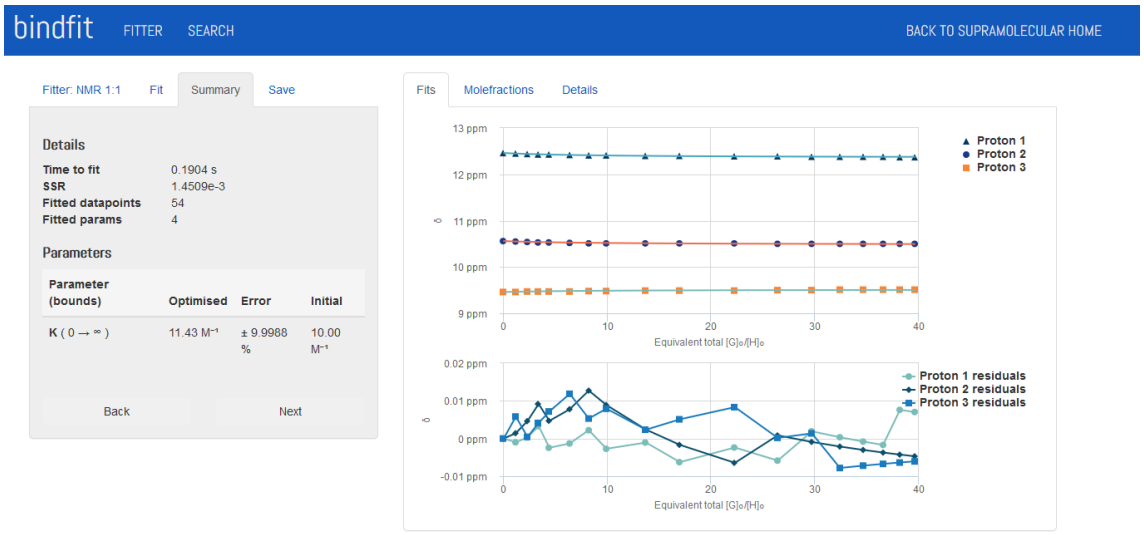

Figure S81. Fitted binding isotherm obtained for the titration of a 0.01 M solution of compound **1**·$HClO_4$ with a 0.6 M solution of $TBANO_3$ (DMSO-d_6). In order to avoid the dilution effect, the latter was prepared with the former. The graph shows the change in chemical shift of the signals due to the pyrrole and imine NH protons and the triazole CH proton of the molecule, fitted to the 1:1 (LH:NO_3) binding model. K_a = 11 ± 1 M^{-1}.

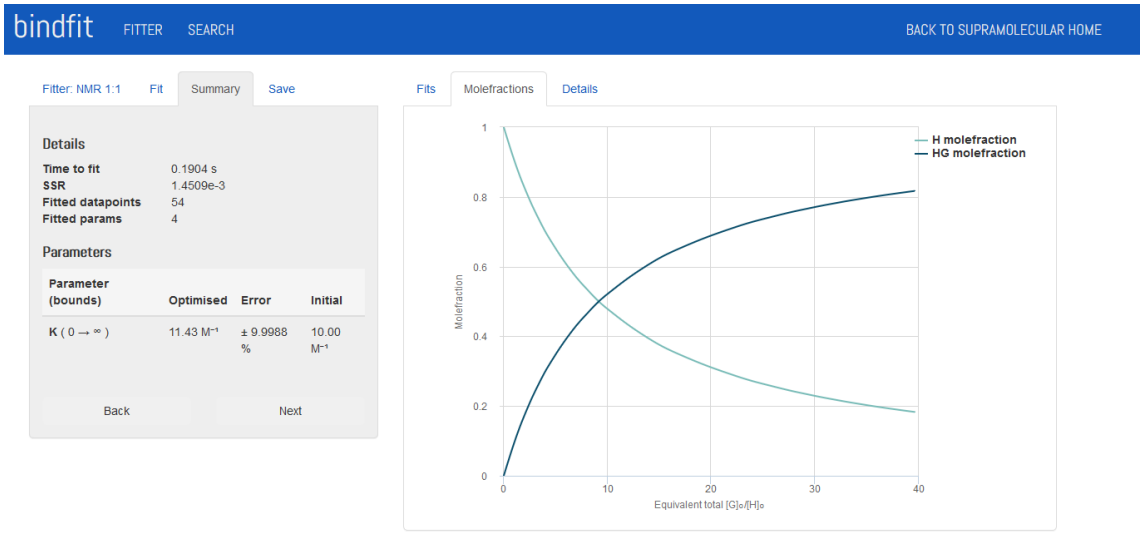

Figure S82. Species distribution diagram obtained for the titration of a 0.01 M solution of compound **1**·$HClO_4$ with a 0.6 M solution of $TBANO_3$ (DMSO-d_6), to show how the composition of the mixture changes over the course of the titration. *H* corresponds to the host, the protonated click tambjamine, and *G* to the guest, the nitrate anion.

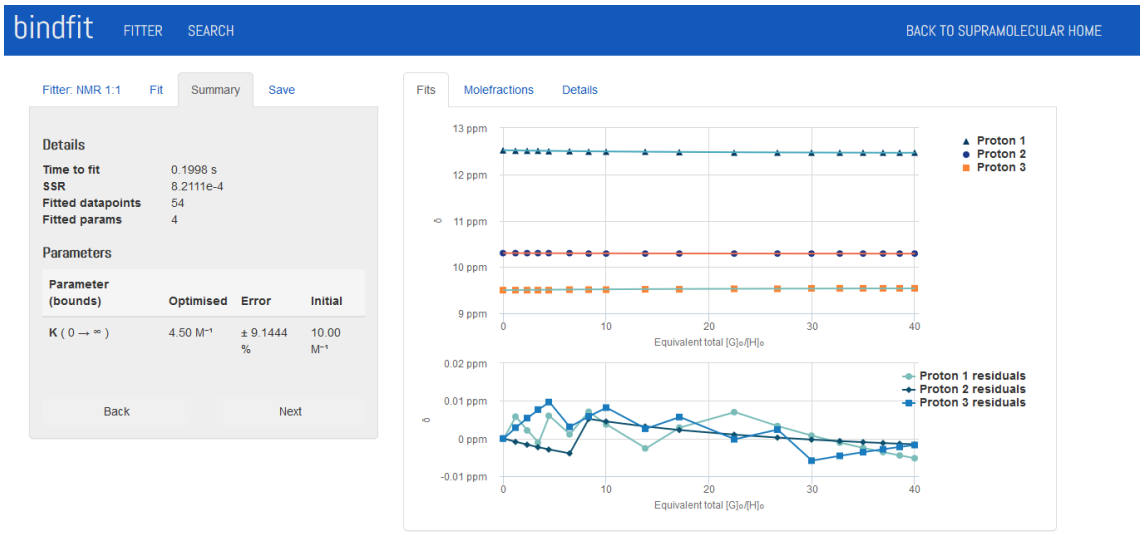

Figure S83. Fitted binding isotherm obtained for the titration of a 0.01 M solution of compound **2**·$HClO_4$ with a 0.6 M solution of $TBANO_3$ (DMSO-d_6). In order to avoid the dilution effect, the latter was prepared with the former. The graph shows the change in chemical shift of the signals due to the pyrrole and imine NH protons and the triazole CH proton of the molecule, fitted to the 1:1 (LH:NO_3) binding model. K_a = 4.5 ± 0.4 M^{-1}.

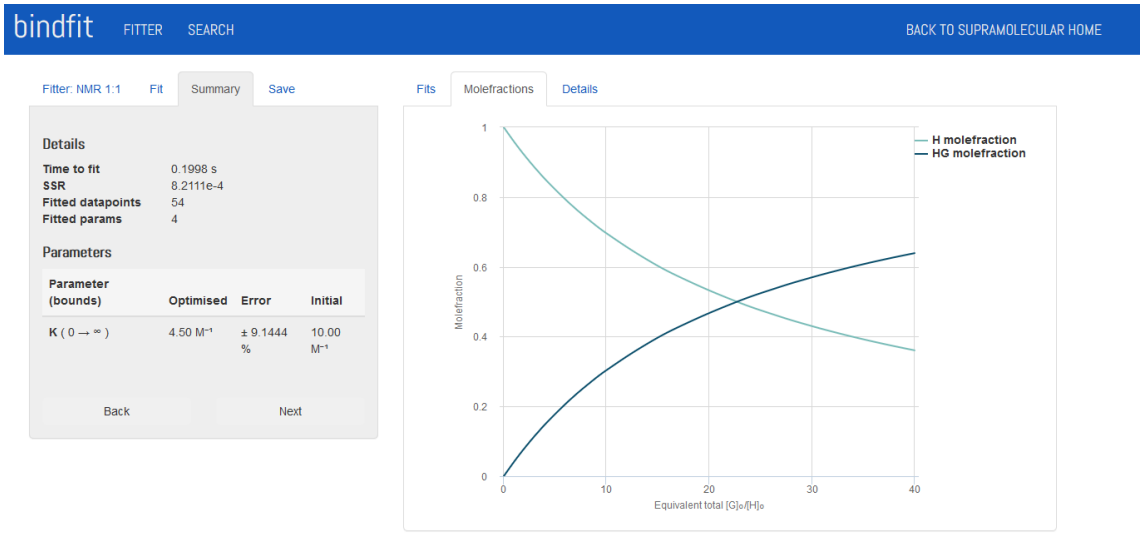

Figure S84. Species distribution diagram obtained for the titration of a 0.01 M solution of compound **2**·$HClO_4$ with a 0.6 M solution of $TBANO_3$ (DMSO-d_6), to show how the composition of the mixture changes over the course of the titration. *H* corresponds to the host, the protonated click tambjamine, and *G* to the guest, the nitrate anion.

Figure S85. Fitted binding isotherm obtained for the titration of a 0.01 M solution of compound **3**·$HClO_4$ with a 0.6 M solution of $TBANO_3$ (DMSO-d_6). In order to avoid the dilution effect, the latter was prepared with the former. The graph shows the change in chemical shift of the signals due to the pyrrole and imine NH protons and the triazole CH proton of the molecule, fitted to the 1:1 (LH:NO_3) binding model. K_a = 11 ± 1 M^{-1}.

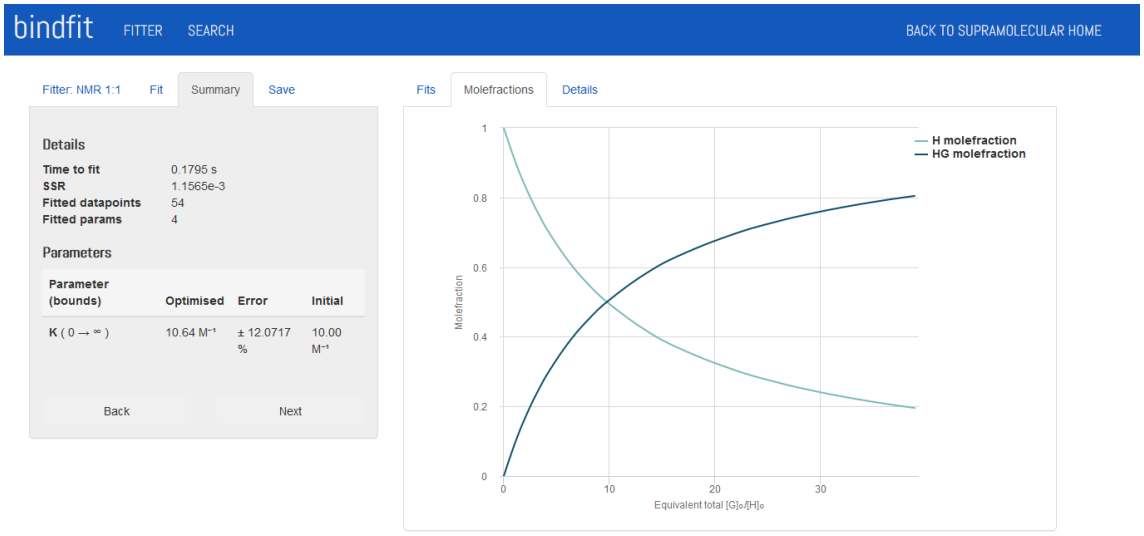

Figure S86. Species distribution diagram obtained for the titration of a 0.01 M solution of compound **3**·$HClO_4$ with a 0.6 M solution of $TBANO_3$ (DMSO-d_6), to show how the composition of the mixture changes over the course of the titration. *H* corresponds to the host, the protonated click tambjamine, and *G* to the guest, the nitrate anion.

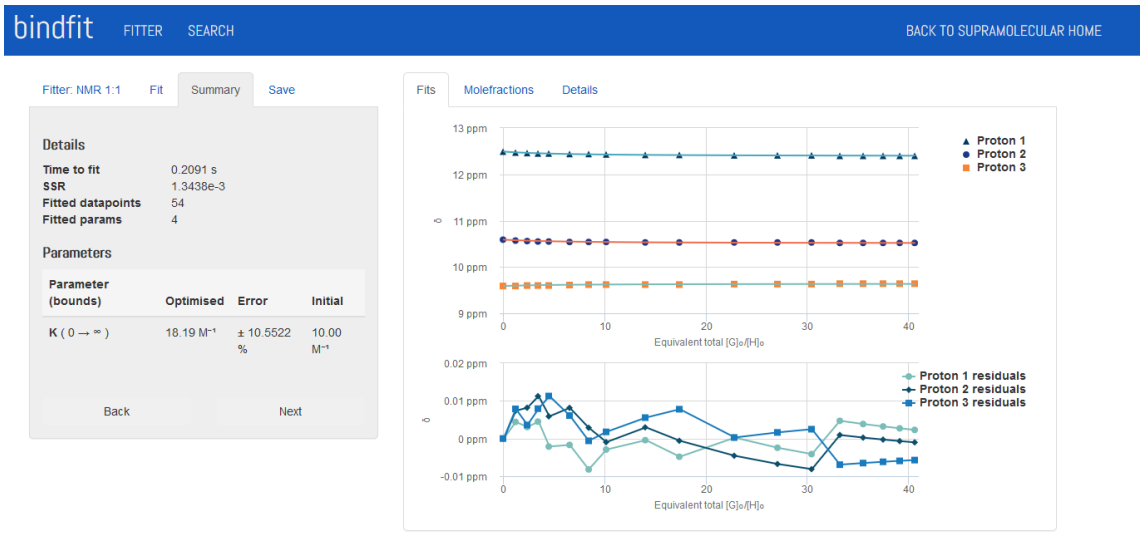

Figure S87. Fitted binding isotherm obtained for the titration of a 0.01 M solution of compound **4**·$HClO_4$ with a 0.6 M solution of $TBANO_3$ (DMSO-d_6). In order to avoid the dilution effect, the latter was prepared with the former. The graph shows the change in chemical shift of the signals due to the pyrrole and imine NH protons and the triazole CH proton of the molecule, fitted to the 1:1 (LH:NO_3) binding model. K_a = 18 ± 2 M^{-1}.

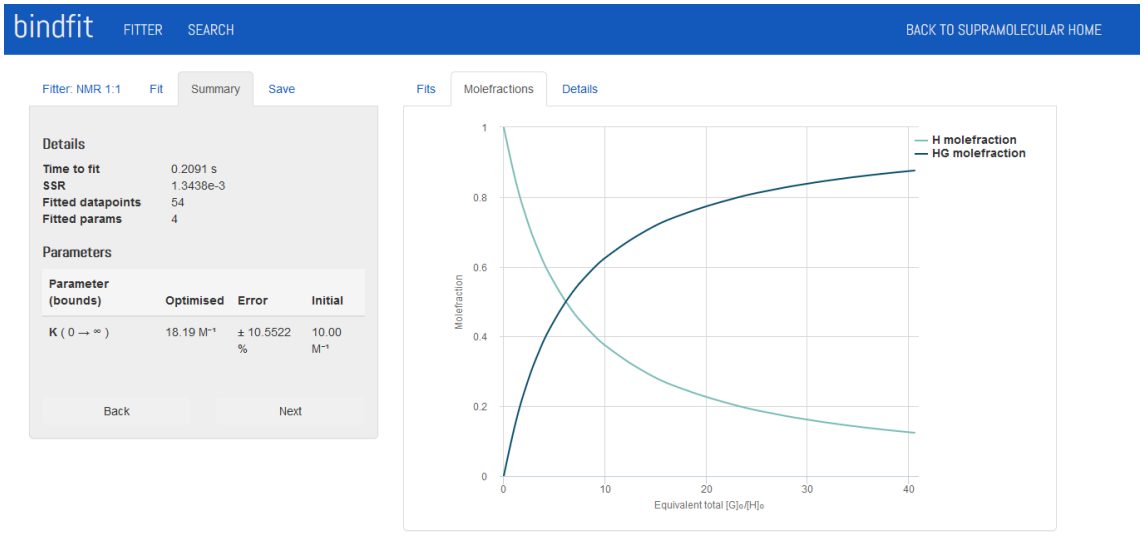

Figure S88. Species distribution diagram obtained for the titration of a 0.01 M solution of compound **4**·$HClO_4$ with a 0.6 M solution of $TBANO_3$ (DMSO-d_6), to show how the composition of the mixture changes over the course of the titration. *H* corresponds to the host, the protonated click tambjamine, and *G* to the guest, the nitrate anion.

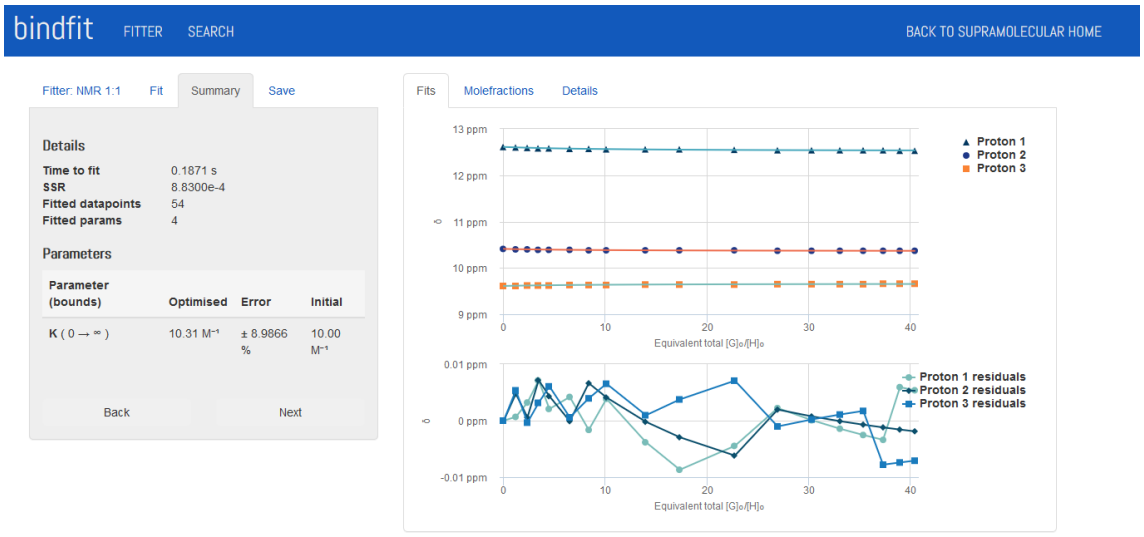

Figure S89. Fitted binding isotherm obtained for the titration of a 0.01 M solution of compound **5**·$HClO_4$ with a 0.6 M solution of $TBANO_3$ (DMSO-d_6). In order to avoid the dilution effect, the latter was prepared with the former. The graph shows the change in chemical shift of the signals due to the pyrrole and imine NH protons and the triazole CH proton of the molecule, fitted to the 1:1 (LH:NO_3) binding model. K_a = 10.3 ± 0.9 M^{-1}.

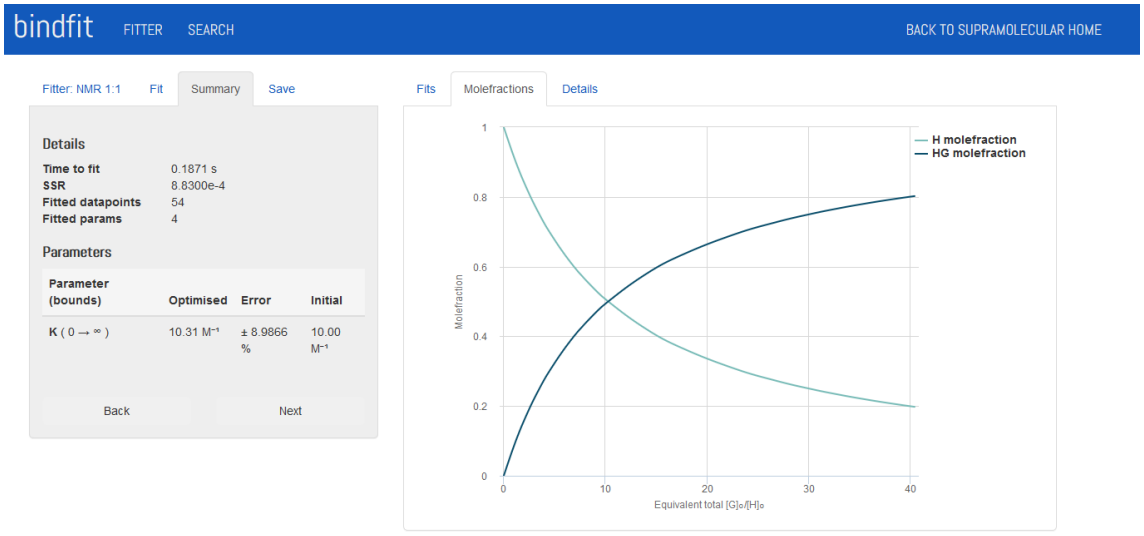

Figure S90. Species distribution diagram obtained for the titration of a 0.01 M solution of compound **5**·$HClO_4$ with a 0.6 M solution of $TBANO_3$ (DMSO-d_6), to show how the composition of the mixture changes over the course of the titration. *H* corresponds to the host, the protonated click tambjamine, and *G* to the guest, the nitrate anion.

Figure S91. Fitted binding isotherm obtained for the titration of a 0.01 M solution of compound **6**·$HClO_4$ with a 0.6 M solution of $TBANO_3$ (DMSO-d_6). In order to avoid the dilution effect, the latter was prepared with the former. The graph shows the change in chemical shift of the signals due to the pyrrole and imine NH protons and the triazole CH proton of the molecule, fitted to the 1:1 ($LH:NO_3$) binding model. K_a = 6.6 ± 0.6 M^{-1}.

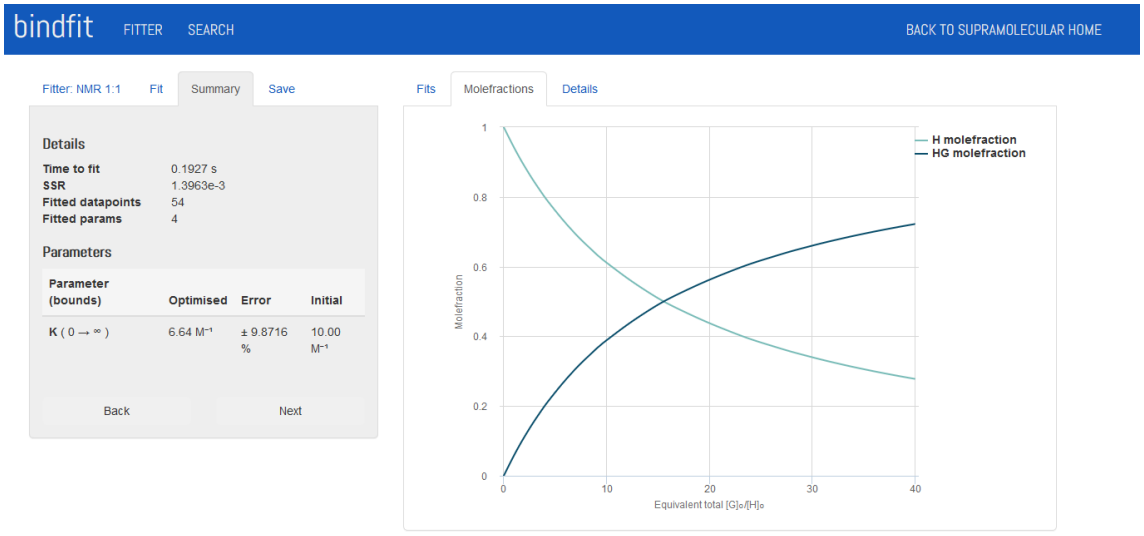

Figure S92. Species distribution diagram obtained for the titration of a 0.01 M solution of compound **6**·$HClO_4$ with a 0.6 M solution of $TBANO_3$ (DMSO-d_6), to show how the composition of the mixture changes over the course of the titration. *H* corresponds to the host, the protonated click tambjamine, and *G* to the guest, the nitrate anion.

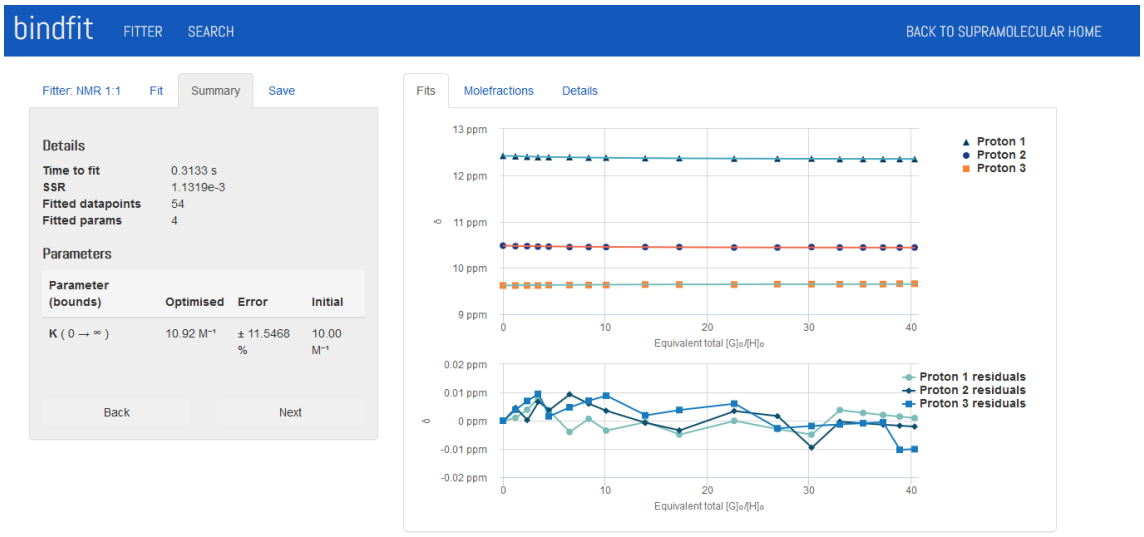

Figure S93. Fitted binding isotherm obtained for the titration of a 0.01 M solution of compound **7**·$HClO_4$ with a 0.6 M solution of $TBANO_3$ (DMSO-d_6). In order to avoid the dilution effect, the latter was prepared with the former. The graph shows the change in chemical shift of the signals due to the pyrrole and imine NH protons and the triazole CH proton of the molecule, fitted to the 1:1 (LH:NO_3) binding model. K_a = 11 ± 1 M^{-1}.

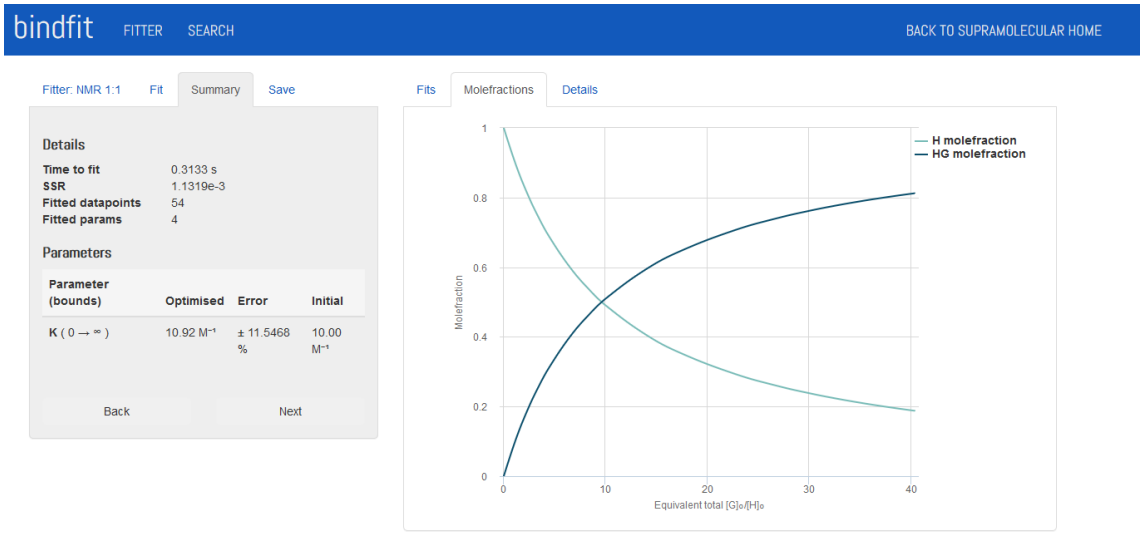

Figure S94. Species distribution diagram obtained for the titration of a 0.01 M solution of compound **7**·$HClO_4$ with a 0.6 M solution of $TBANO_3$ (DMSO-d_6), to show how the composition of the mixture changes over the course of the titration. *H* corresponds to the host, the protonated click tambjamine, and *G* to the guest, the nitrate anion.

Figure S95. Fitted binding isotherm obtained for the titration of a 0.01 M solution of compound **8**·$HClO_4$ with a 0.6 M solution of $TBANO_3$ (DMSO-d_6). In order to avoid the dilution effect, the latter was prepared with the former. The graph shows the change in chemical shift of the signals due to the pyrrole and imine NH protons and the triazole CH proton of the molecule, fitted to the 1:1 (LH:NO_3) binding model. K_a = 12 ± 1 M^{-1}.

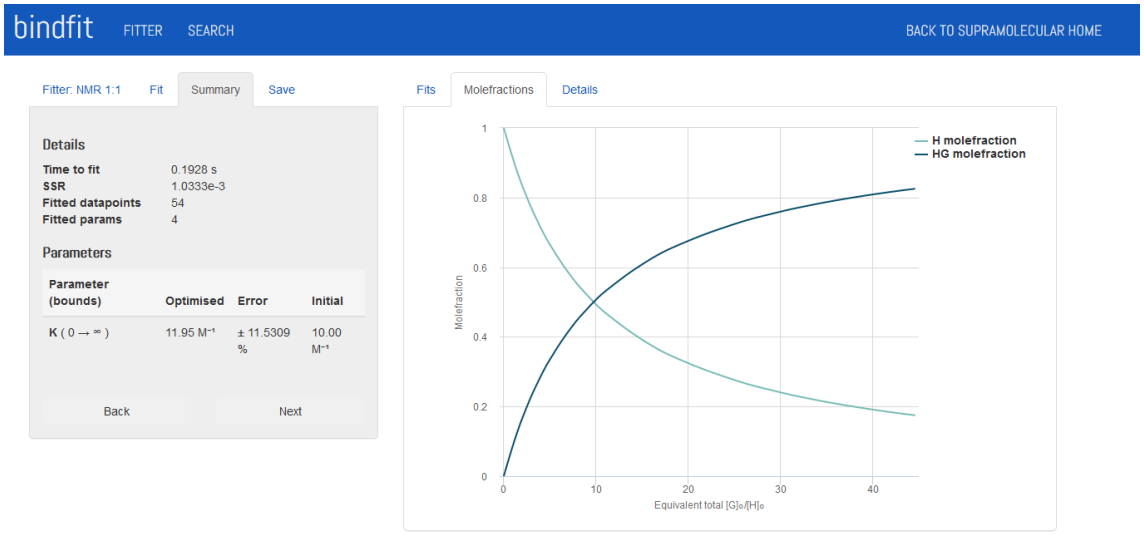

Figure S96. Species distribution diagram obtained for the titration of a 0.01 M solution of compound **8**·$HClO_4$ with a 0.6 M solution of $TBANO_3$ (DMSO-d_6), to show how the composition of the mixture changes over the course of the titration. *H* corresponds to the host, the protonated click tambjamine, and *G* to the guest, the nitrate anion.

Figure S97. Fitted binding isotherm obtained for the titration of a 0.01 M solution of compound **9**·$HClO_4$ with a 0.6 M solution of $TBANO_3$ (DMSO-d_6). In order to avoid the dilution effect, the latter was prepared with the former. The graph shows the change in chemical shift of the signals due to the pyrrole and imine NH protons and the triazole CH proton of the molecule, fitted to the 1:1 (LH:NO_3) binding model. K_a = 4.5 ± 0.5 M^{-1}.

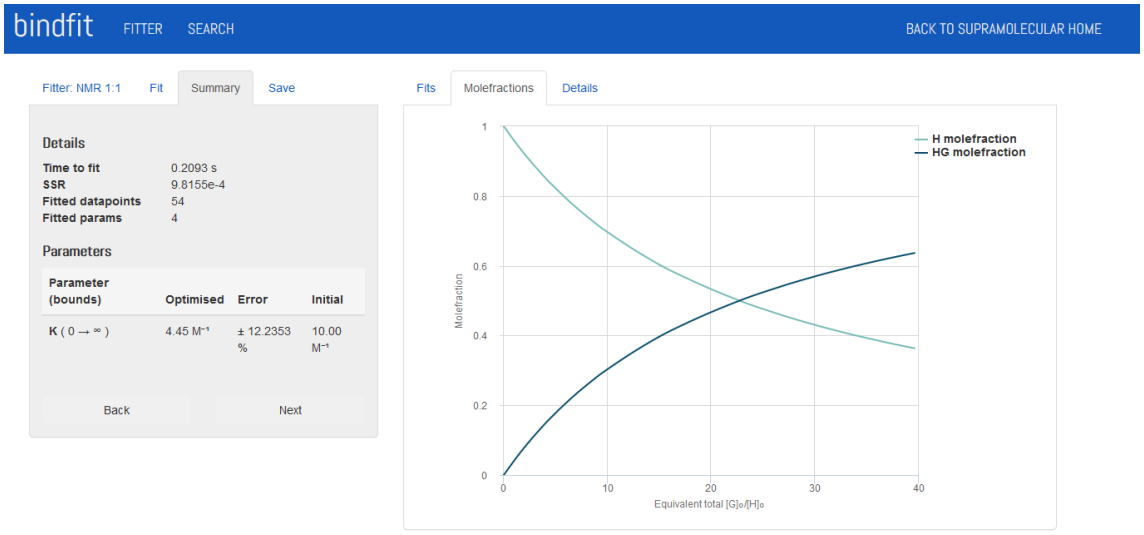

Figure S98. Species distribution diagram obtained for the titration of a 0.01 M solution of compound **9**·$HClO_4$ with a 0.6 M solution of $TBANO_3$ (DMSO-d_6), to show how the composition of the mixture changes over the course of the titration. *H* corresponds to the host, the protonated click tambjamine, and *G* to the guest, the nitrate anion.

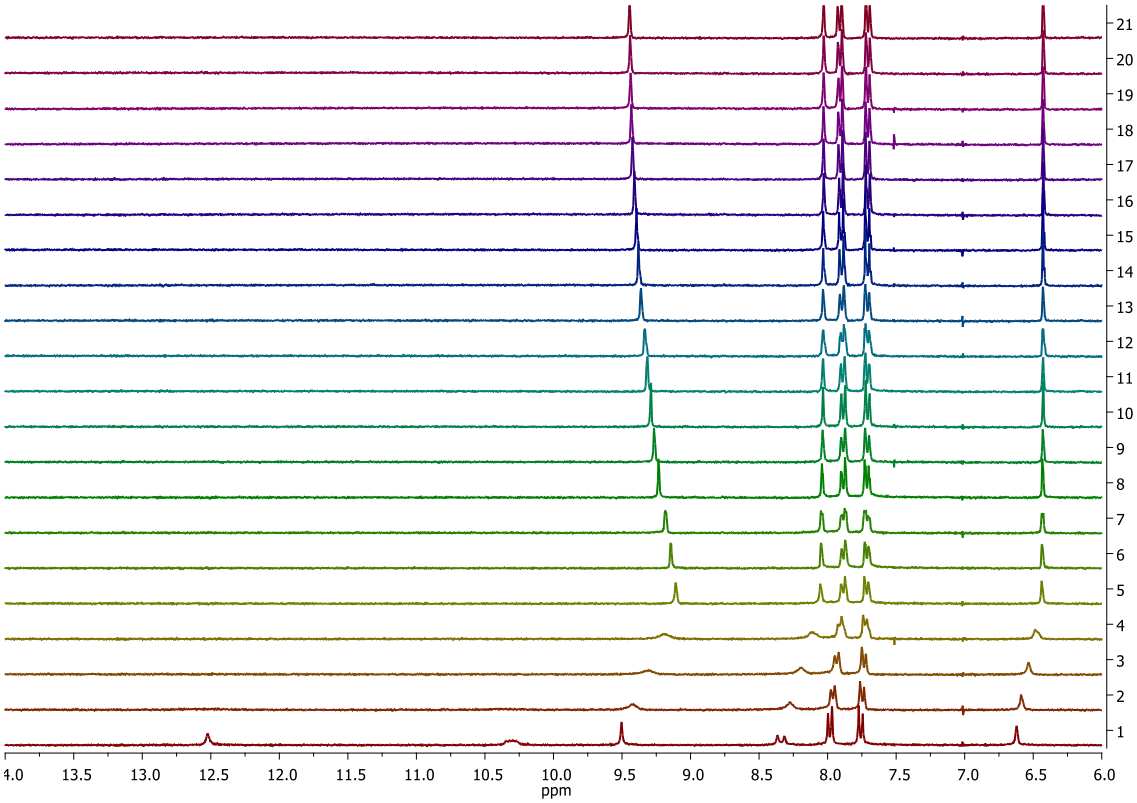

Figure S99. Excerpt of the ^{1}H NMR spectra (300 MHz, DMSO-d_6) obtained upon addition of different aliquots of a 0.2 M solution of $TEAHCO_3$, prepared with a 0.01 M solution of **2**·$HClO_4$, to a 0.01 M solution of **2**·$HClO_4$.

Table S2. Association constants K_a (M^{-1}) calculated for the chloride and nitrate adducts derived from the studied compounds.

Compound	Cl^-	NO_3^-
1	220 ± 5	11 ± 1
2	240 ± 8	4.5 ± 0.4
3	397 ± 23	11 ± 1
4	283 ± 9	18 ± 2
5	197 ± 6	10.3 ± 0.9
6	281 ± 7	6.6 ± 0.6
7	278 ± 8	11 ± 1
8	755 ± 87	12 ± 1
9	255 ± 8	4.5 ± 0.5

6. TRANSMEMBRANE ANION TRANSPORT EXPERIMENTS IN VESICLES

6.1. Preparation of phospholipid vesicles

A chloroform solution of 1-palmitoyl-2-oleoyl-*sn*-glycero-3-phosphocoline (POPC) (20 mg/mL) (Sigma Aldrich) was evaporated to dryness using a rotary evaporator and the resulting film was dried under high vacuum for, at least, two hours. A sodium chloride aqueous solution (489 mM and 5 mM phosphate buffer, pH 7.2, or 451 mM and 20 mM phosphate buffer, pH 7.2) was added to rehydrate the lipid film. The resulting suspension was vortexed and subjected to nine freeze-thaw cycles; subsequently, it was extruded twenty-nine times through a polycarbonate membrane (200 nm) employing a LiposoFast basic extruder (Avestin, Inc.). The resulting unilamellar vesicles were dialysed against a sodium nitrate (489 mM and 5 mM phosphate buffer, pH 7.2) or a sodium sulphate (150 mM and 20 mM phosphate buffer, pH 7.2) aqueous solutions, to remove unencapsulated chloride.

6.2. ISE transport experiments

Unilamellar vesicles (average diameter: 200 nm) made of POPC and containing a sodium chloride aqueous solution (489 mM and 5 mM phosphate buffer, pH 7.2, for chloride/nitrate exchange assays, or 451 mM and 20 mM phosphate buffer, pH 7.2, for chloride/bicarbonate exchange assays) were suspended in a sodium nitrate (489 mM and 5 mM phosphate buffer, pH 7.2) or a sodium sulphate (150 mM and 20 mM phosphate buffer, pH 7.2) aqueous solution, respectively, the final lipid concentration being 0.5 mM and the final volume 5 mL. A solution of the carrier in DMSO, usually 5 µL to avoid the influence of the organic solvent during the experiments, was added, and the chloride released was monitored employing a chloride-selective electrode (HACH 9652C). Once the experiment was finished, a surfactant (Triton-X, 10% dispersion in water, 20 µL) was added to lyse the vesicles and release all the encapsulated chloride. This value was regarded as 100% release and used as such. For the chloride/bicarbonate exchange assays, a sodium bicarbonate aqueous solution was added to the vesicles suspended in the sodium sulphate one (150 mM and 20 mM phosphate buffer, pH 7.2), the final bicarbonate concentration during the experiment being 40 mM. The chloride efflux was monitored for another five minutes, until the vesicles were lysed with the surfactant.

Cl^-/NO_3^- exchange assays

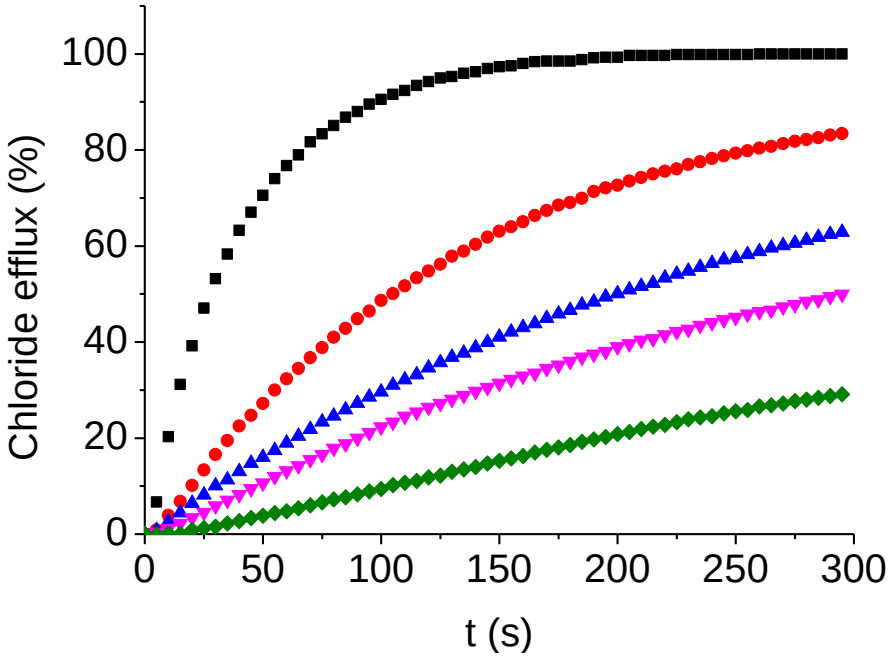

Figure S100. Chloride efflux promoted by **1** (5 μM, black; 0.5 μM, red; 0.25 μM, blue; 0.15 μM, pink; 0.05 μM, green) in unilamellar POPC vesicles. Vesicles loaded with 489 mM NaCl were buffered at pH 7.2 with 5 mM phosphate and dispersed in 489 mM $NaNO_3$ buffered at pH 7.2. Each trace represents the average of at least three trials.

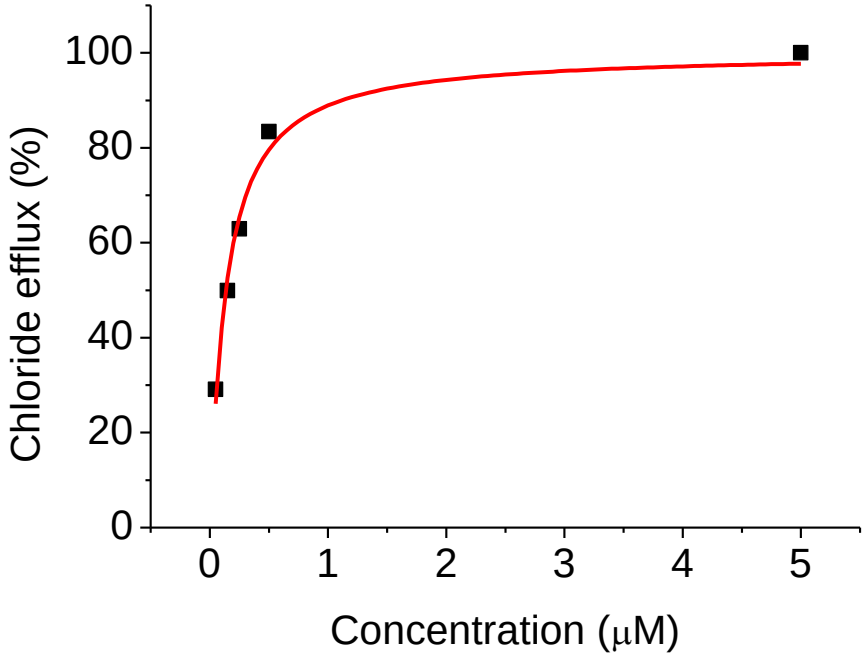

Figure S101. Hill analysis for compound **1**.

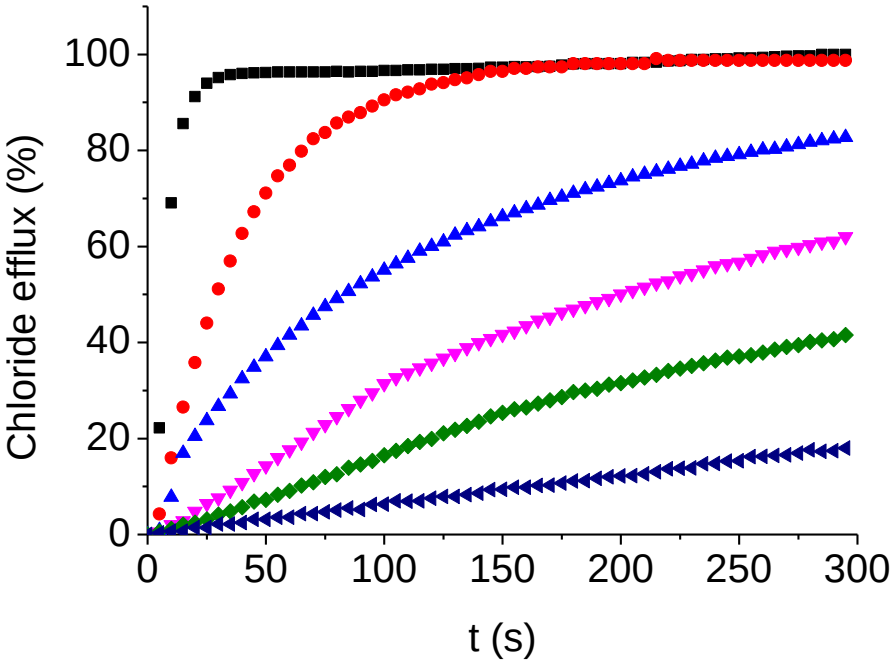

Figure S102. Chloride efflux promoted by **2** (5 μM, black; 0.5 μM, red; 0.1 μM, light blue; 0.05 μM, pink; 0.025 μM, green; 0.01 μM, dark blue) in unilamellar POPC vesicles. Vesicles loaded with 489 mM NaCl were buffered at pH 7.2 with 5 mM phosphate and dispersed in 489 mM $NaNO_3$ buffered at pH 7.2. Each trace represents the average of at least three trials.

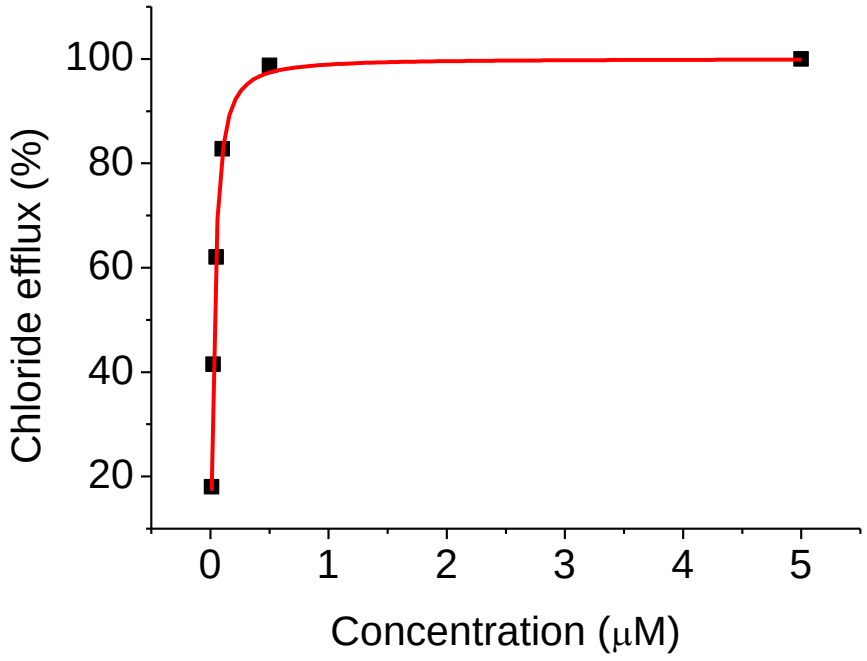

Figure S103. Hill analysis for compound **2**.

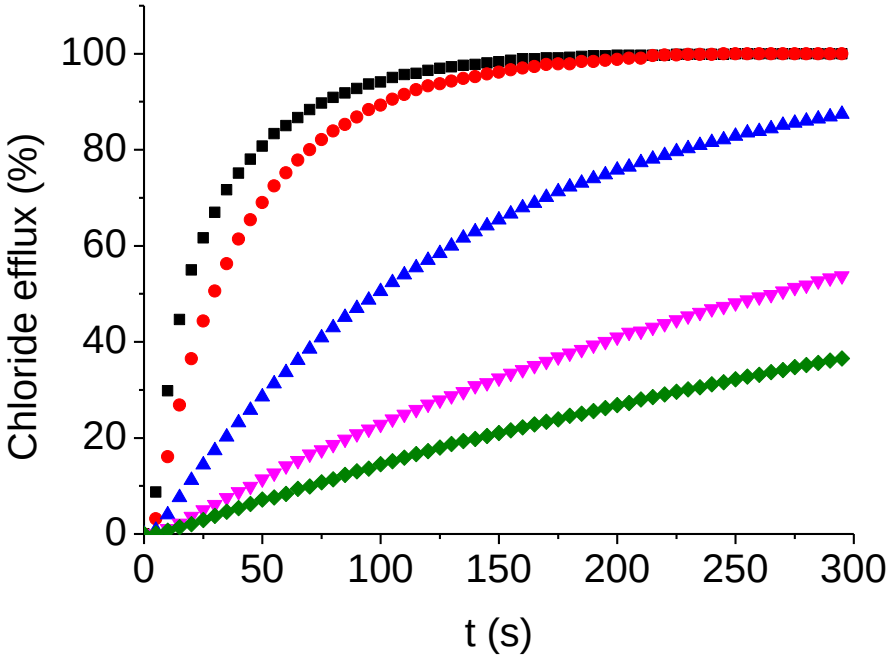

Figure S104. Chloride efflux promoted by **3** (5 μM, black; 0.5 μM, red; 0.05 μM, blue; 0.015 μM, pink; 0.005 μM, green) in unilamellar POPC vesicles. Vesicles loaded with 489 mM NaCl were buffered at pH 7.2 with 5 mM phosphate and dispersed in 489 mM $NaNO_3$ buffered at pH 7.2. Each trace represents the average of at least three trials.

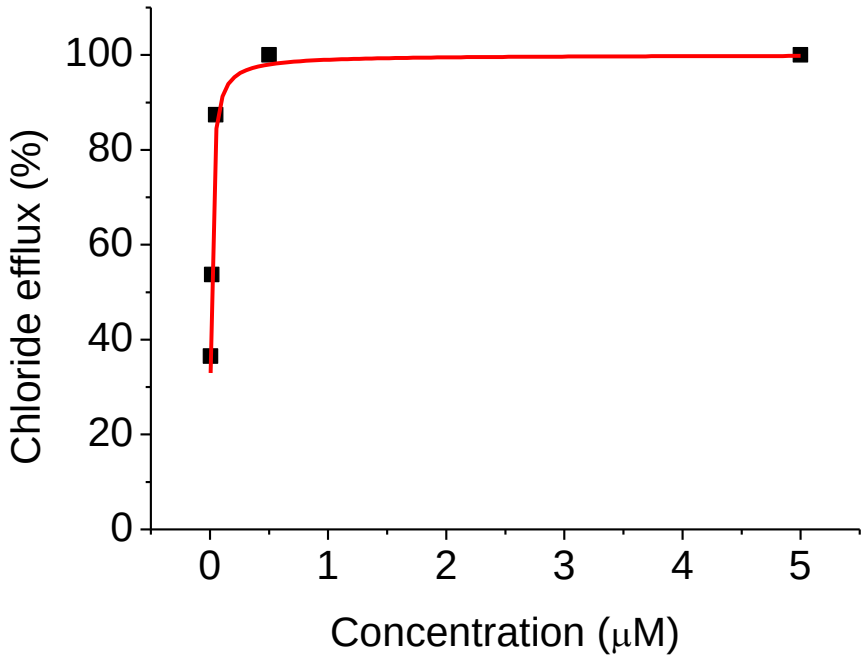

Figure S105. Hill analysis for compound **3**.

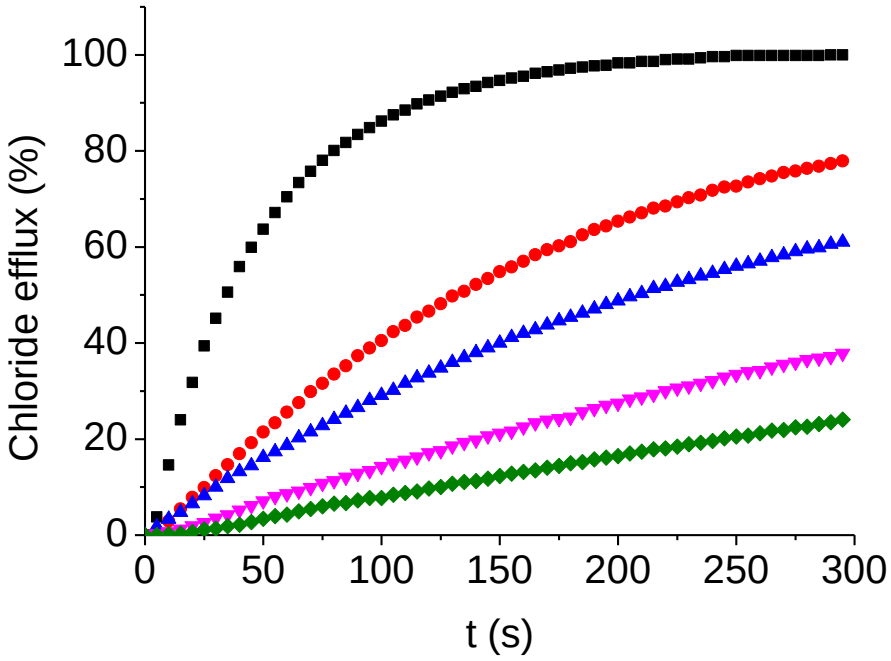

Figure S106. Chloride efflux promoted by **4** (5 μM, black; 0.5 μM, red; 0.25 μM, blue; 0.15 μM, pink; 0.05 μM, green) in unilamellar POPC vesicles. Vesicles loaded with 489 mM NaCl were buffered at pH 7.2 with 5 mM phosphate and dispersed in 489 mM $NaNO_3$ buffered at pH 7.2. Each trace represents the average of at least three trials.

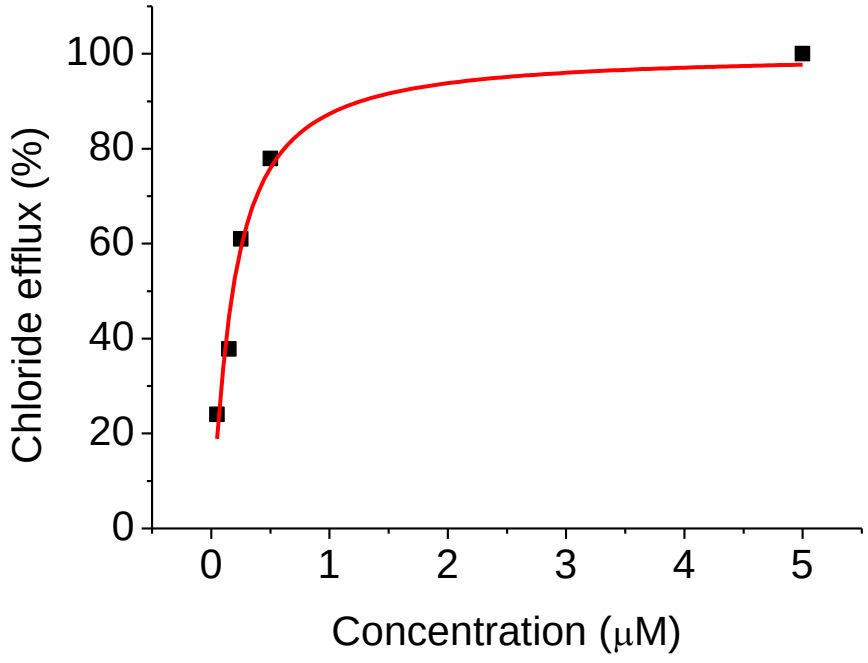

Figure S107. Hill analysis for compound **4**.

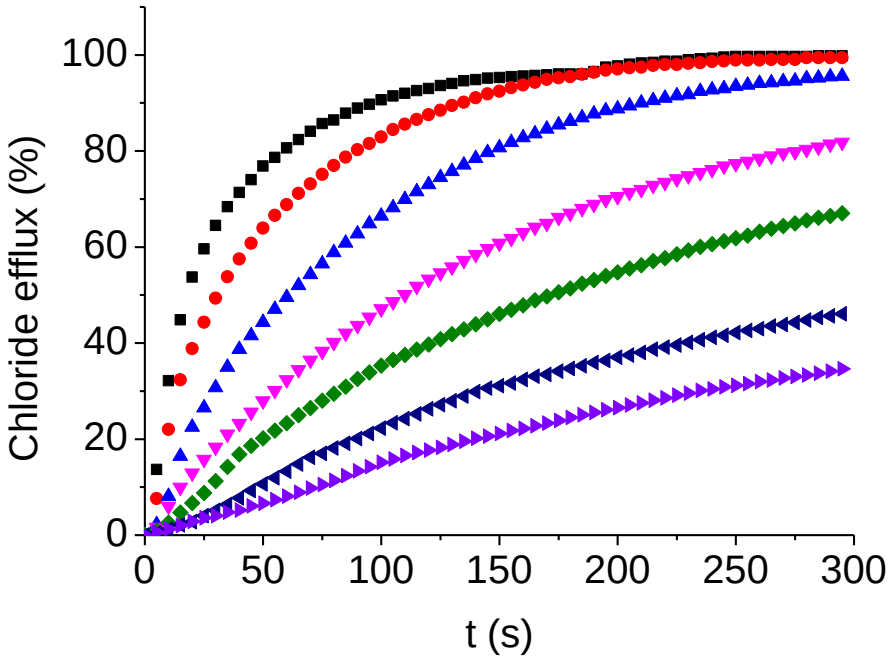

Figure S108. Chloride efflux promoted by **5** (5 μM, black; 1 μM, red; 0.25 μM, light blue; 0.15 μM, pink; 0.05 μM, green; 0.025 μM, dark blue; 0.015 μM, purple) in unilamellar POPC vesicles. Vesicles loaded with 489 mM NaCl were buffered at pH 7.2 with 5 mM phosphate and dispersed in 489 mM $NaNO_3$ buffered at pH 7.2. Each trace represents the average of at least three trials.

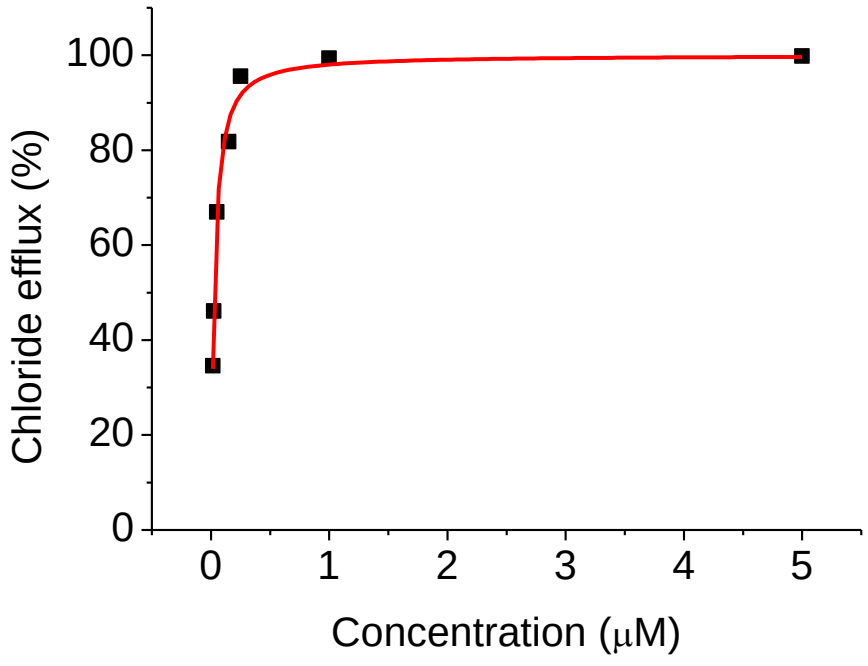

Figure S109. Hill analysis for compound **5**.

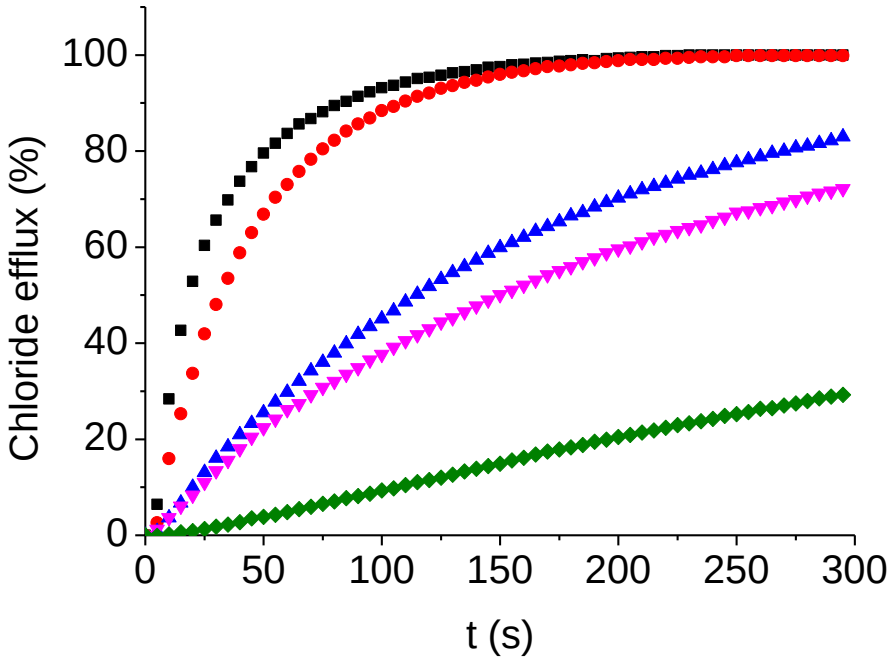

Figure S110. Chloride efflux promoted by **6** (5 μM, black; 0.5 μM, red; 0.05 μM, blue; 0.025 μM, pink; 0.005 μM, green) in unilamellar POPC vesicles. Vesicles loaded with 489 mM NaCl were buffered at pH 7.2 with 5 mM phosphate and dispersed in 489 mM $NaNO_3$ buffered at pH 7.2. Each trace represents the average of at least three trials.

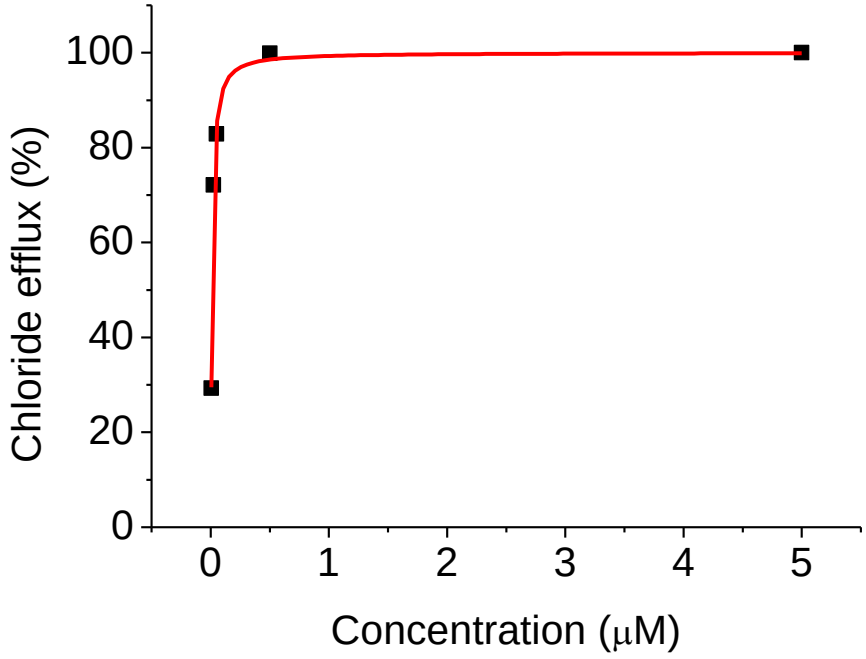

Figure S111. Hill analysis for compound **6**.

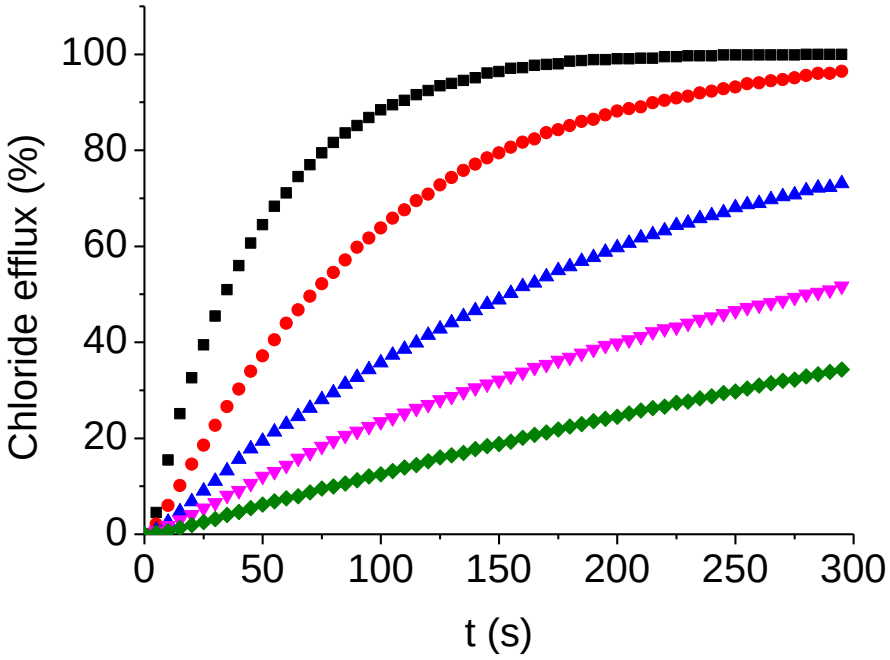

Figure S112. Chloride efflux promoted by **7** (5 μM, black; 1.5 μM, red; 0.5 μM, blue; 0.25 μM, pink; 0.15 μM, green) in unilamellar POPC vesicles. Vesicles loaded with 489 mM NaCl were buffered at pH 7.2 with 5 mM phosphate and dispersed in 489 mM $NaNO_3$ buffered at pH 7.2. Each trace represents the average of at least three trials.

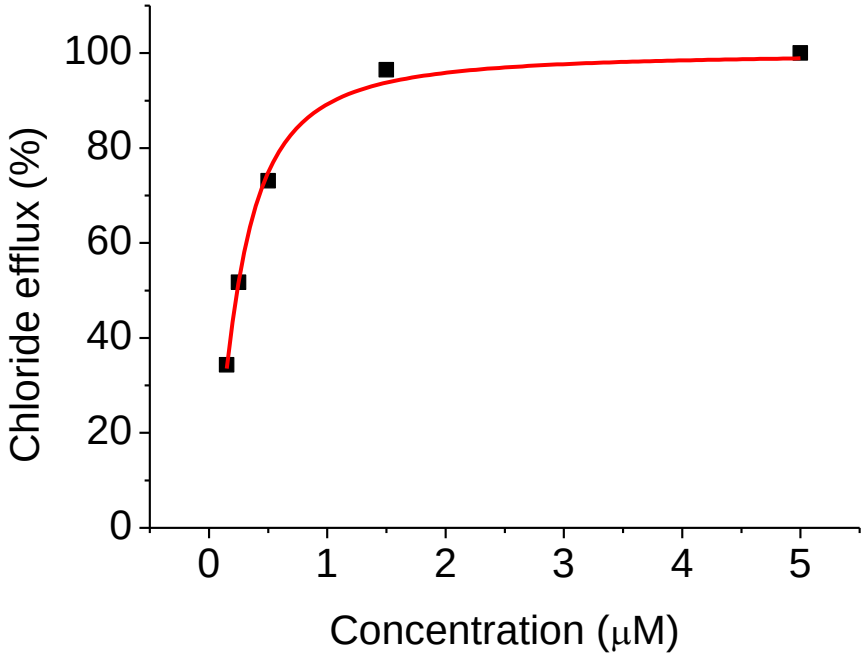

Figure S113. Hill analysis for compound **7**.

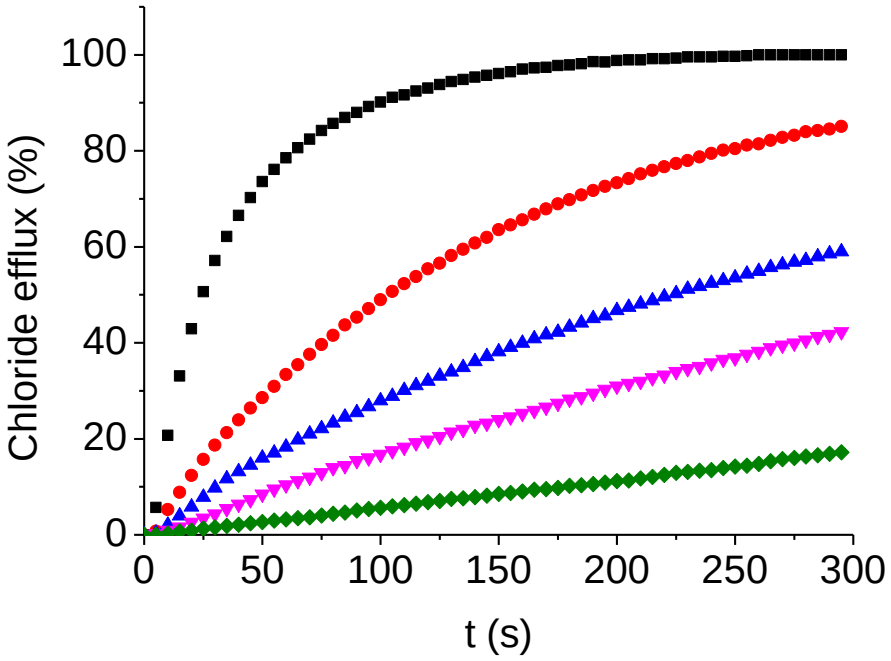

Figure S114. Chloride efflux promoted by **8** (5 μM, black; 0.15 μM, red; 0.05 μM, blue; 0.025 μM, pink; 0.005 μM, green) in unilamellar POPC vesicles. Vesicles loaded with 489 mM NaCl were buffered at pH 7.2 with 5 mM phosphate and dispersed in 489 mM $NaNO_3$ buffered at pH 7.2. Each trace represents the average of at least three trials.

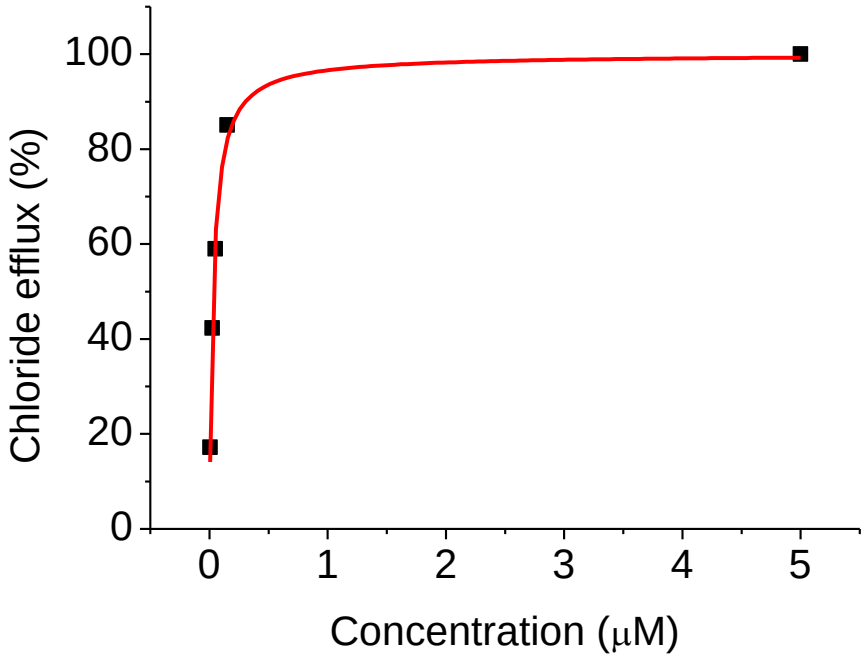

Figure S115. Hill analysis for compound **8**.

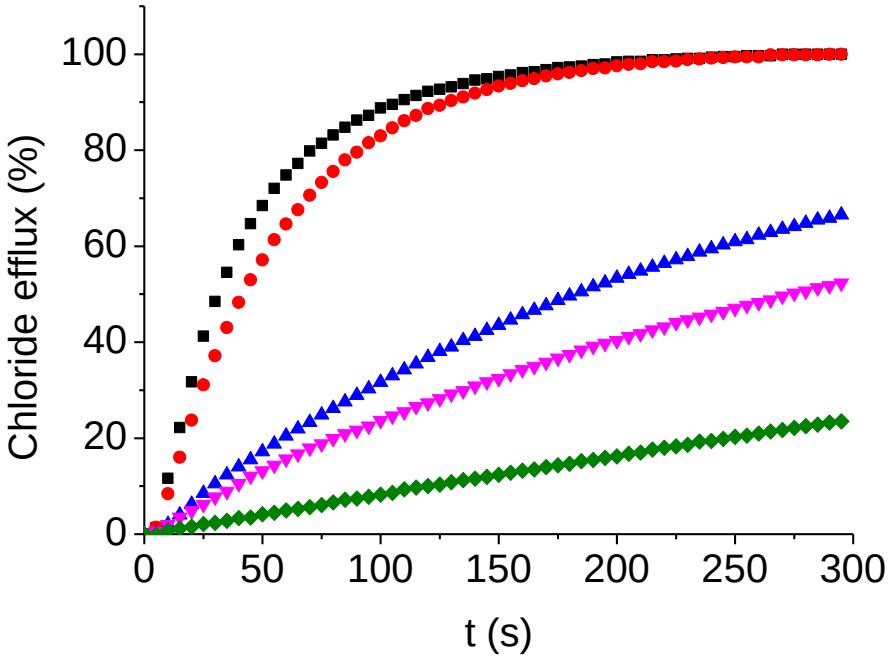

Figure S116. Chloride efflux promoted by **9** (5 μM, black; 0.5 μM, red; 0.05 μM, blue; 0.025 μM, pink; 0.005 μM, green) in unilamellar POPC vesicles. Vesicles loaded with 489 mM NaCl were buffered at pH 7.2 with 5 mM phosphate and dispersed in 489 mM $NaNO_3$ buffered at pH 7.2. Each trace represents the average of at least three trials.

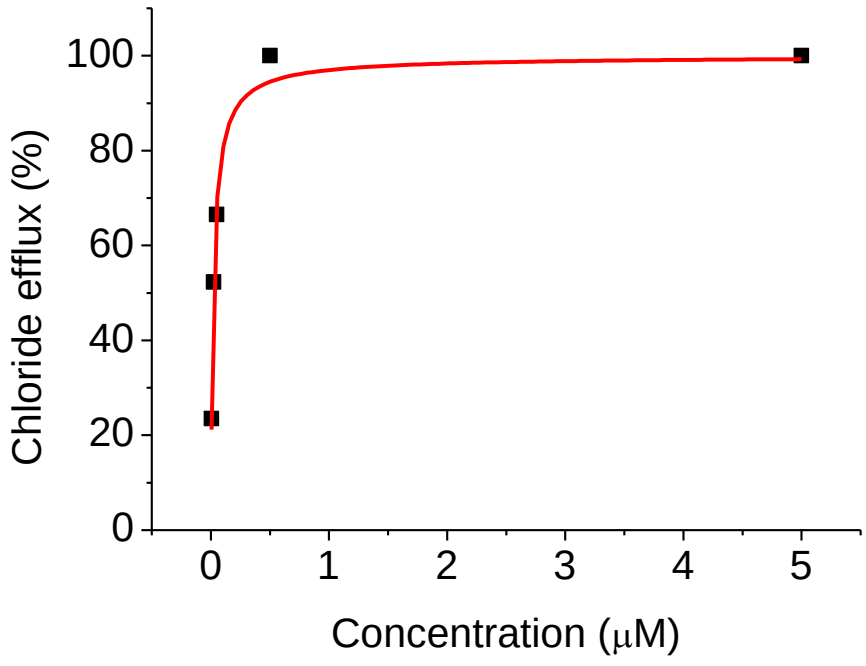

Figure S117. Hill analysis for compound **9**.

Cl^-/HCO_3^- exchange assays

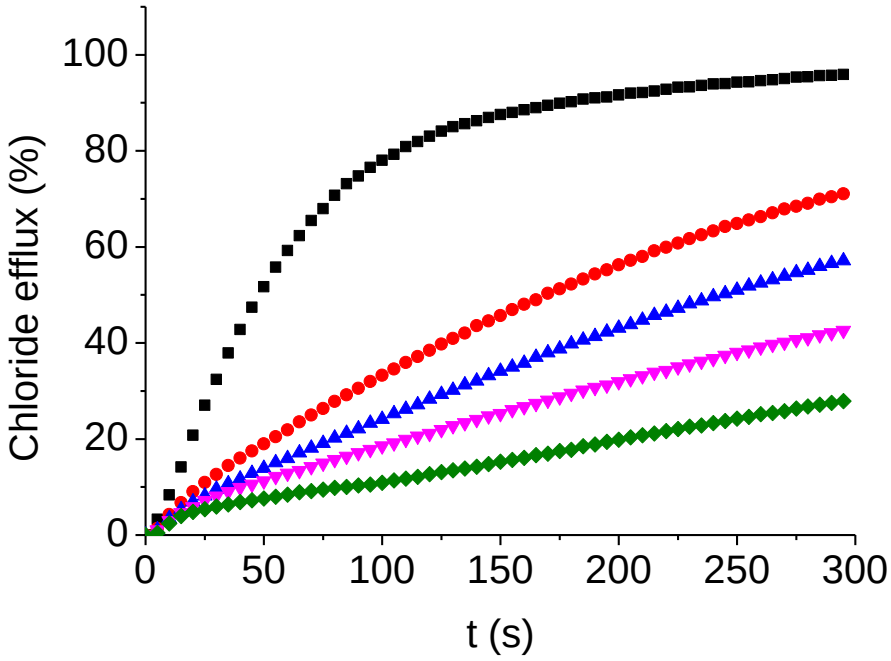

Figure S118. Chloride efflux promoted by **1** (20 μM, black; 5 μM, red; 3.5 μM, blue; 2.5 μM, pink; 1.5 μM, green) in unilamellar POPC vesicles. The vesicles, which contained NaCl (451 mM NaCl and 20 mM phosphate buffer, pH 7.2), were immersed in Na_2SO_4 (150 mM Na_2SO_4, 40 mM HCO_3^- and 20 mM phosphate buffer, pH 7.2). Each trace represents an average of at least three different experiments.

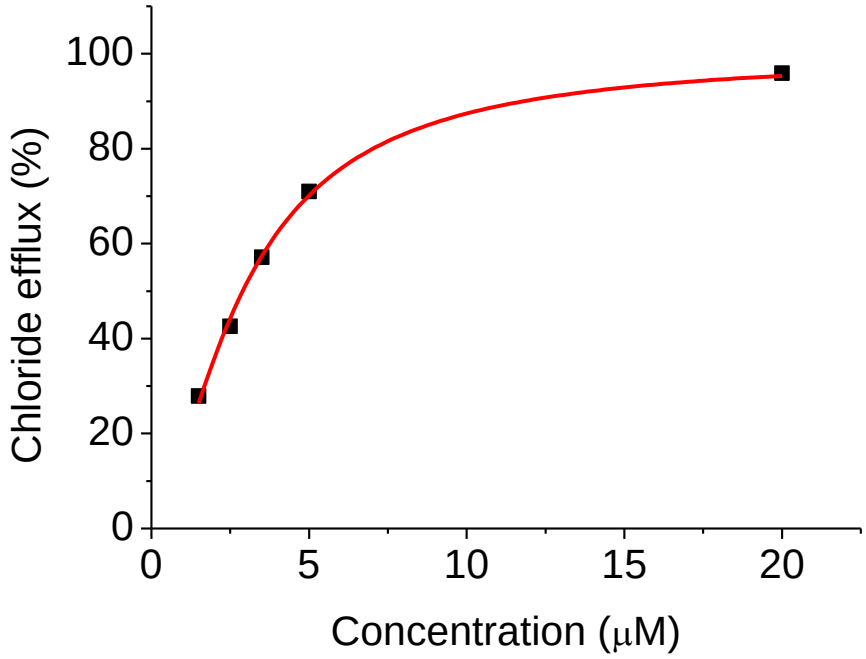

Figure S119. Hill analysis for compound **1**.

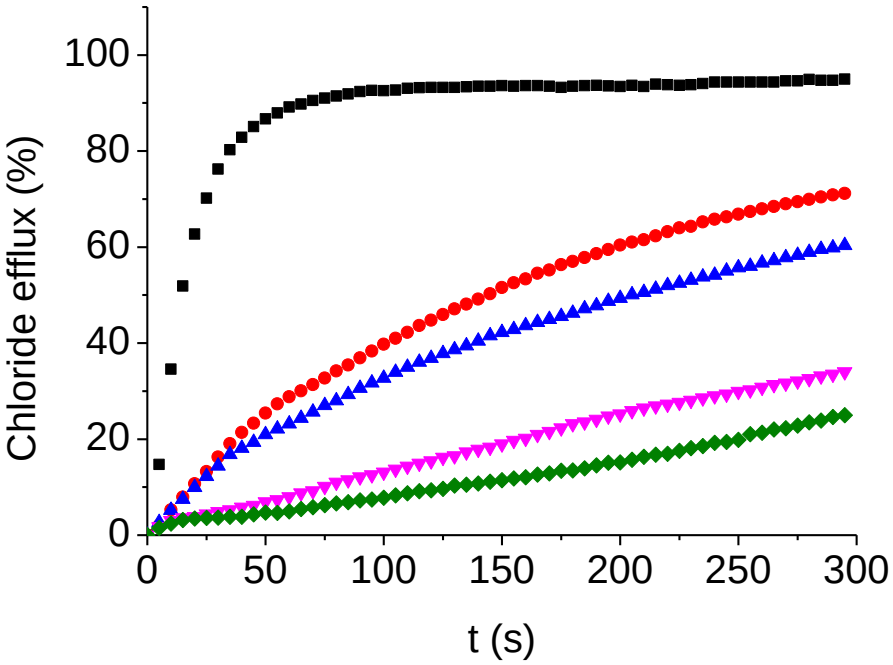

Figure S120. Chloride efflux promoted by **2** (5 μM, black; 0.5 μM, red; 0.25 μM, blue; 0.05 μM, pink; 0.025 μM, green) in unilamellar POPC vesicles. The vesicles, which contained NaCl (451 mM NaCl and 20 mM phosphate buffer, pH 7.2), were immersed in Na_2SO_4 (150 mM Na_2SO_4, 40 mM HCO_3^- and 20 mM phosphate buffer, pH 7.2). Each trace represents an average of at least three different experiments.

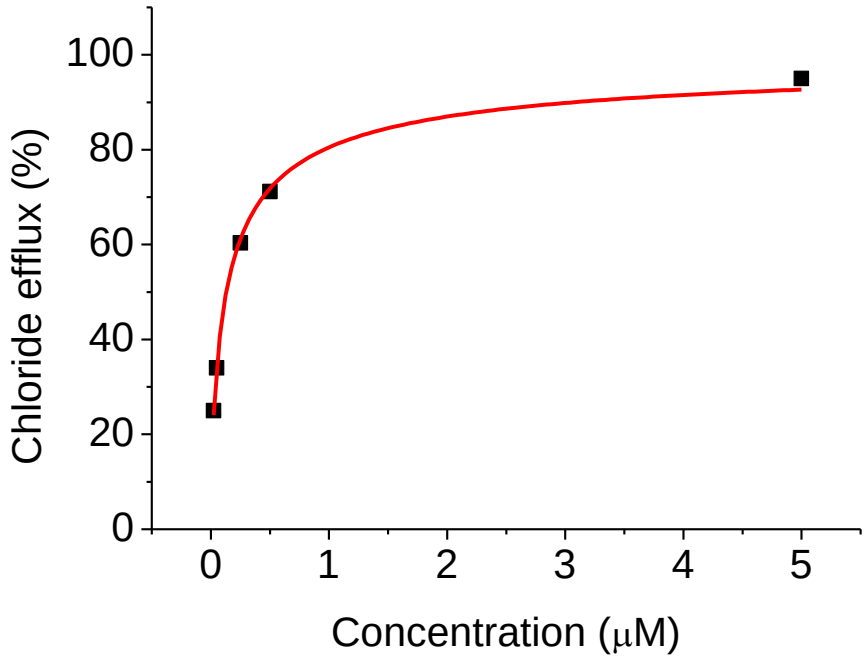

Figure S121. Hill analysis for compound **2**.

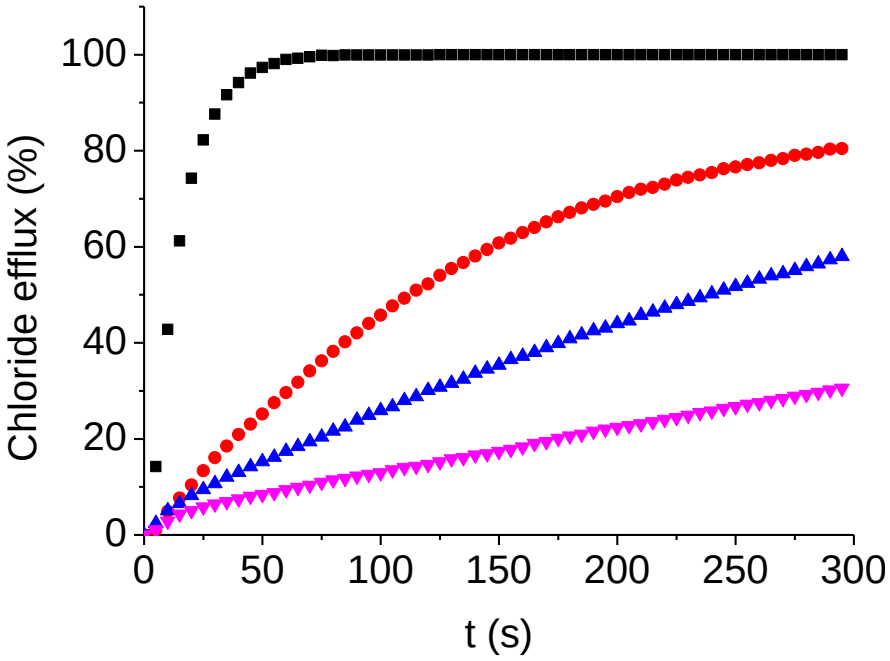

Figure S122. Chloride efflux promoted by **3** (5 μM, black; 0.5 μM, red; 0.15 μM, blue; 0.05 μM, pink) in unilamellar POPC vesicles. The vesicles, which contained NaCl (451 mM NaCl and 20 mM phosphate buffer, pH 7.2), were immersed in Na_2SO_4 (150 mM Na_2SO_4, 40 mM HCO_3^- and 20 mM phosphate buffer, pH 7.2). Each trace represents an average of at least three different experiments.

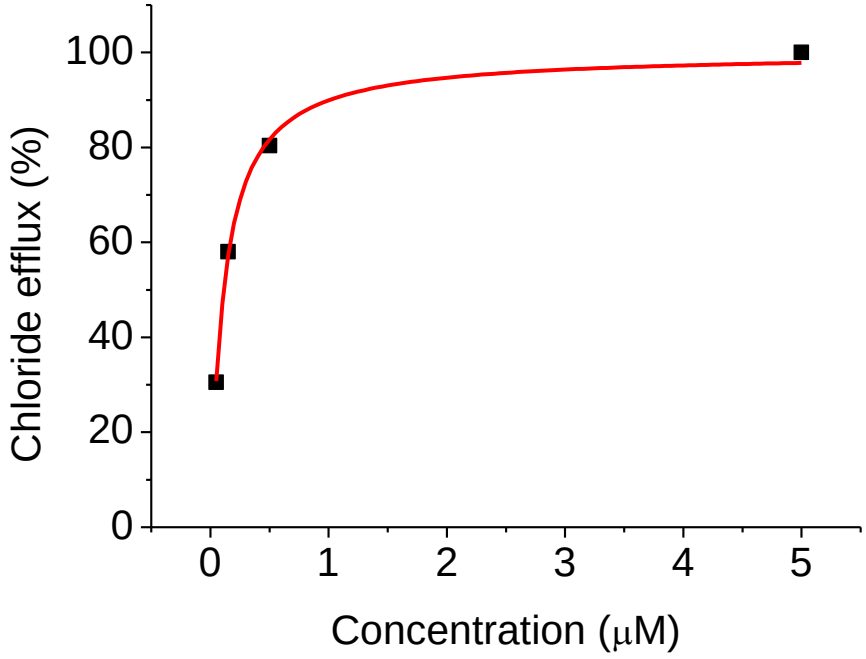

Figure S123. Hill analysis for compound **3**.

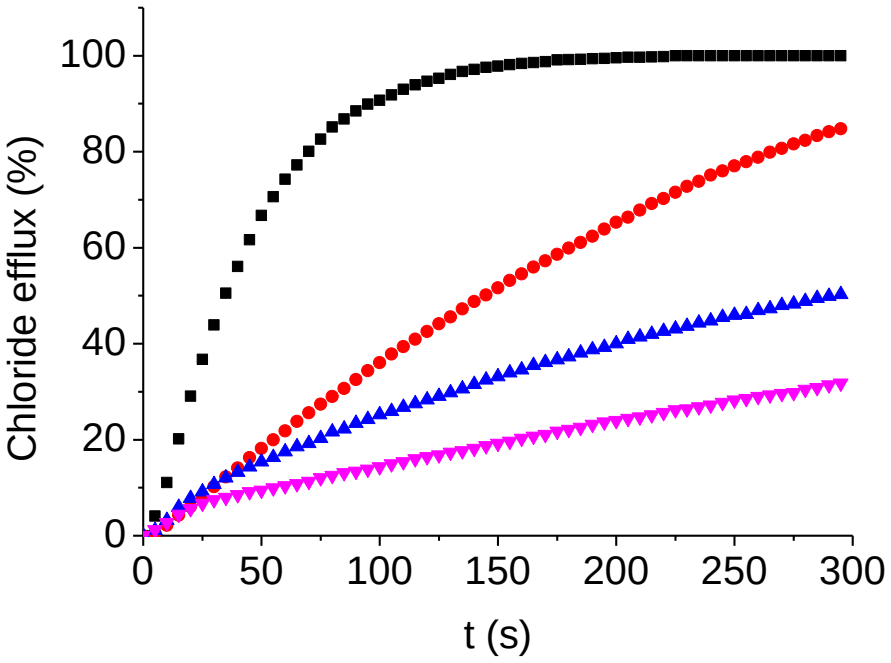

Figure S124. Chloride efflux promoted by **4** (25 μM, black; 5 μM, red; 2.5 μM, blue; 1.5 μM, pink) in unilamellar POPC vesicles. The vesicles, which contained NaCl (451 mM NaCl and 20 mM phosphate buffer, pH 7.2), were immersed in Na_2SO_4 (150 mM Na_2SO_4, 40 mM HCO_3^- and 20 mM phosphate buffer, pH 7.2). Each trace represents an average of at least three different experiments.

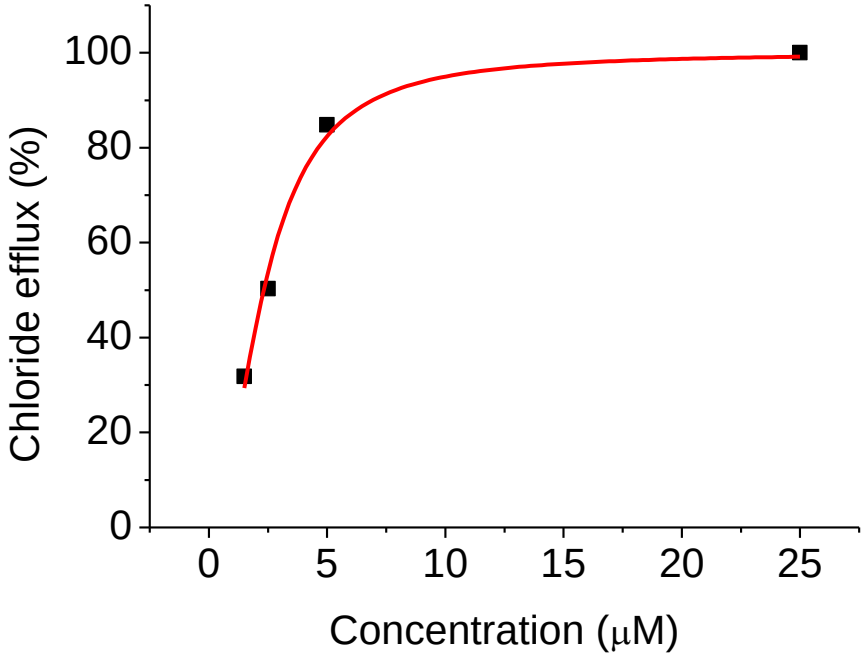

Figure S125. Hill analysis for compound **4**.

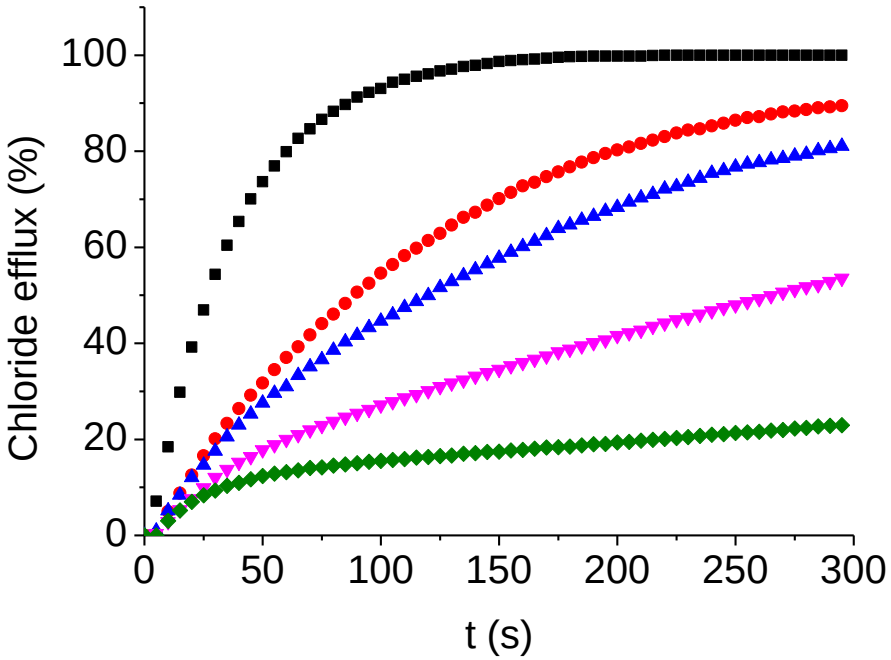

Figure S126. Chloride efflux promoted by **5** (5 μM, black; 1 μM, red; 0.5 μM, blue; 0.25 μM, pink; 0.025 μM, green) in unilamellar POPC vesicles. The vesicles, which contained NaCl (451 mM NaCl and 20 mM phosphate buffer, pH 7.2), were immersed in Na_2SO_4 (150 mM Na_2SO_4, 40 mM HCO_3^- and 20 mM phosphate buffer, pH 7.2). Each trace represents an average of at least three different experiments.

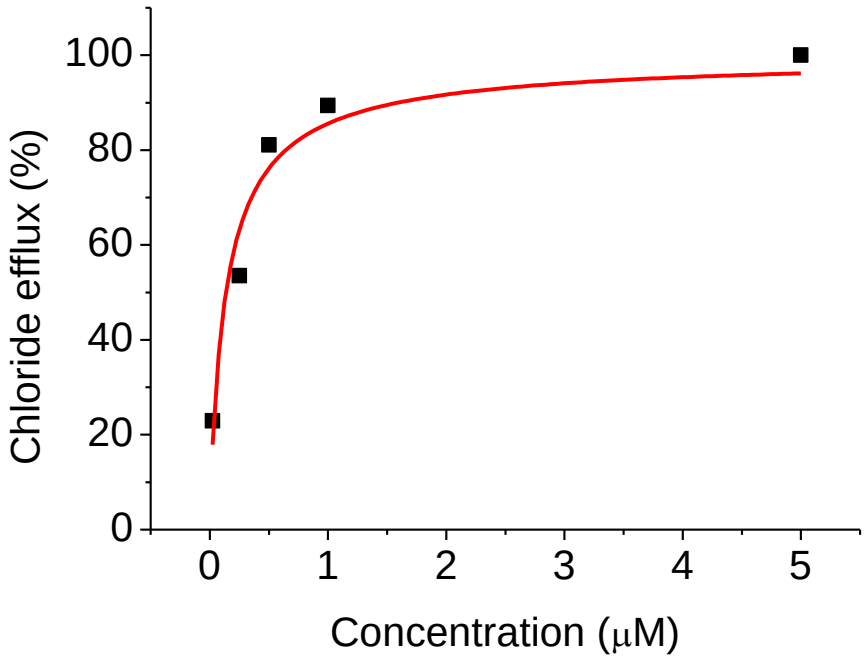

Figure S127. Hill analysis for compound **5**.

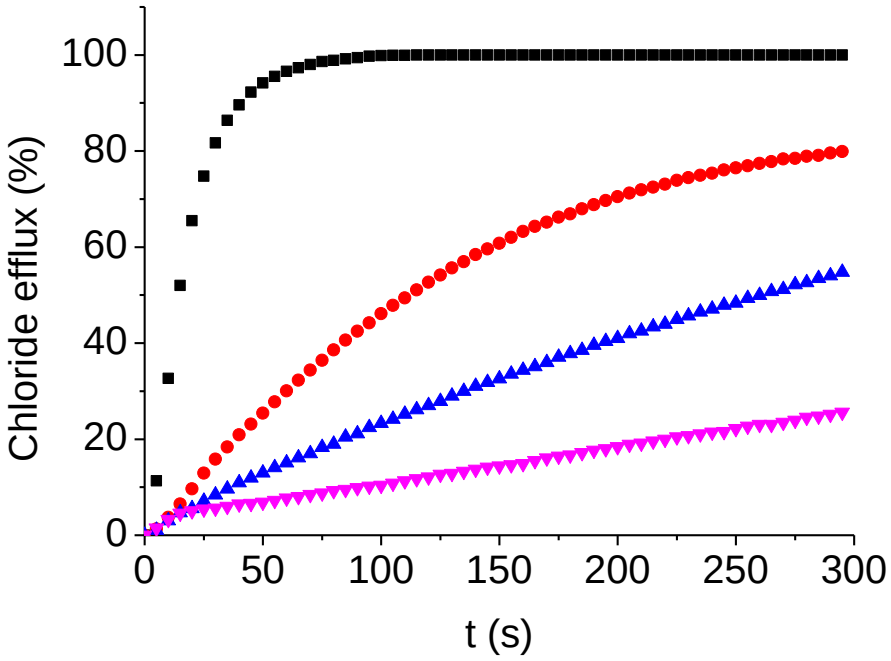

Figure S128. Chloride efflux promoted by **6** (5 μM, black; 0.5 μM, red; 0.15 μM, blue; 0.05 μM, pink) in unilamellar POPC vesicles. The vesicles, which contained NaCl (451 mM NaCl and 20 mM phosphate buffer, pH 7.2), were immersed in Na_2SO_4 (150 mM Na_2SO_4, 40 mM HCO_3^- and 20 mM phosphate buffer, pH 7.2). Each trace represents an average of at least three different experiments.

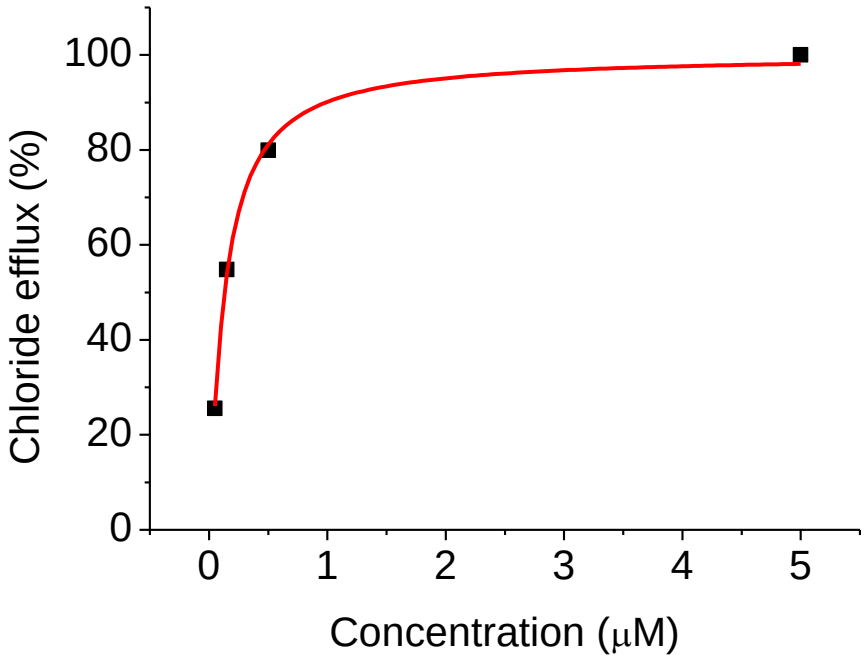

Figure S129. Hill analysis for compound **6**.

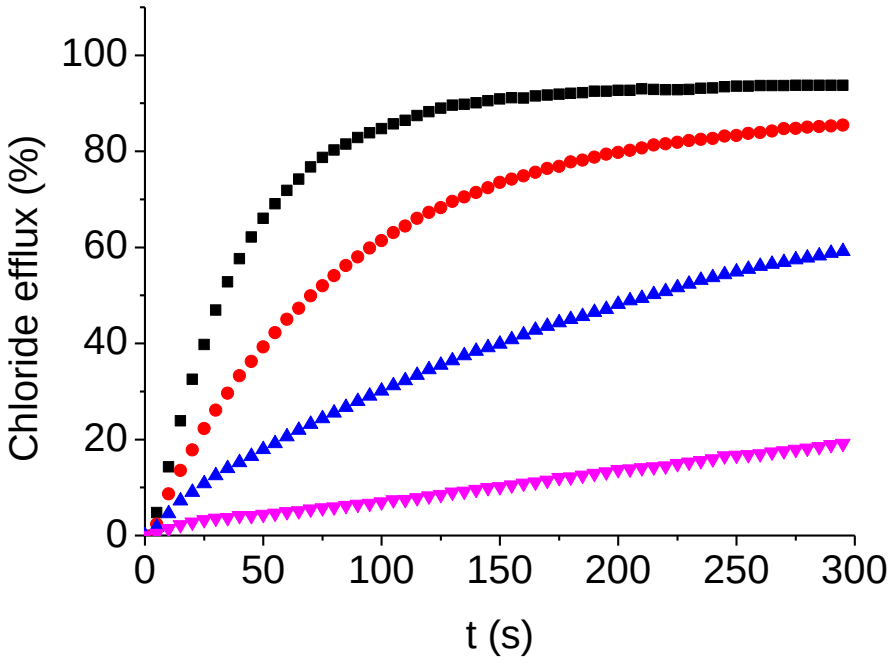

Figure S130. Chloride efflux promoted by **7** (25 μM, black; 15 μM, red; 5 μM, blue; 1 μM, pink) in unilamellar POPC vesicles. The vesicles, which contained NaCl (451 mM NaCl and 20 mM phosphate buffer, pH 7.2), were immersed in Na_2SO_4 (150 mM Na_2SO_4, 40 mM HCO_3^- and 20 mM phosphate buffer, pH 7.2). Each trace represents an average of at least three different experiments.

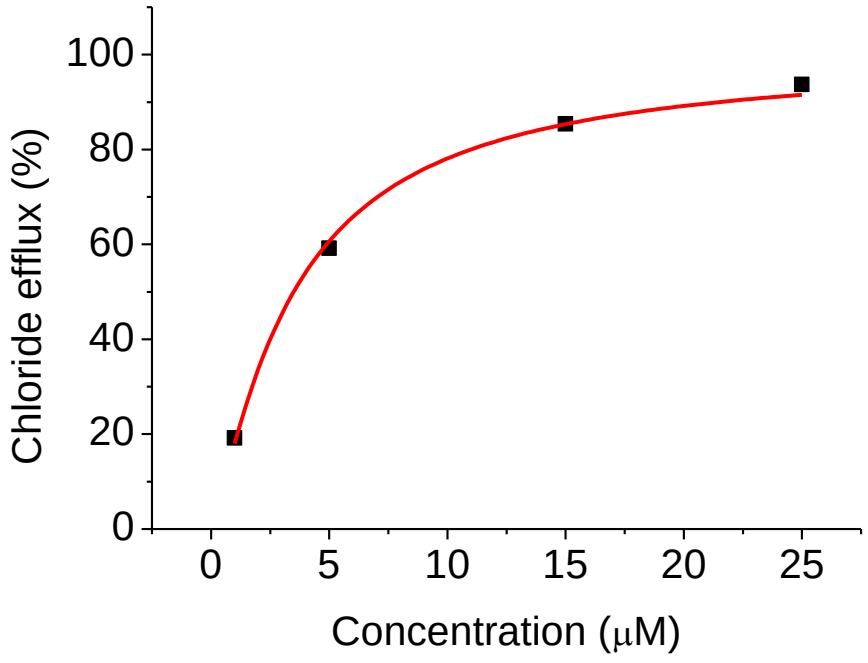

Figure S131. Hill analysis for compound **7**.

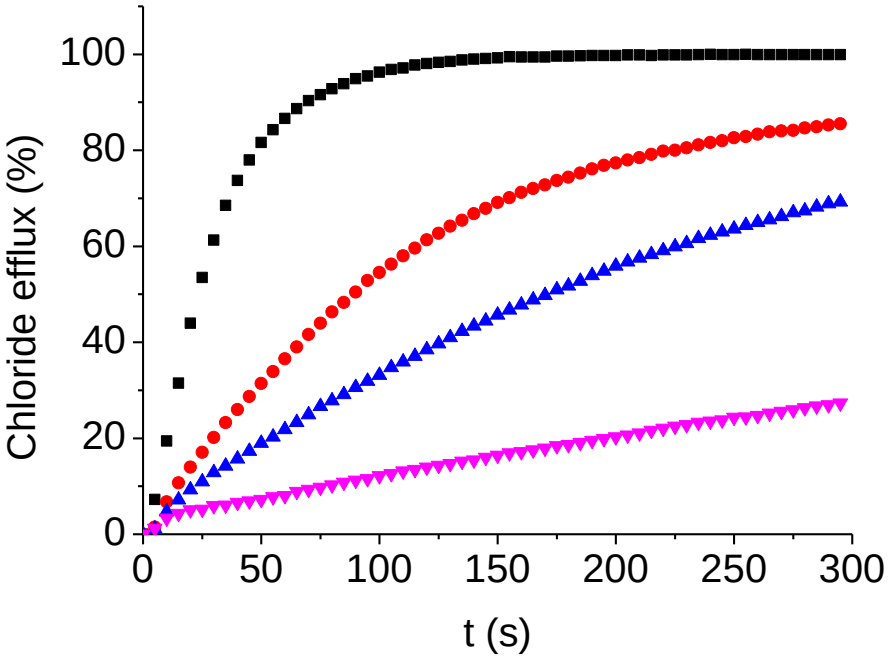

Figure S132. Chloride efflux promoted by **8** (5 μM, black; 1 μM, red; 0.5 μM, blue; 0.1 μM, pink) in unilamellar POPC vesicles. The vesicles, which contained NaCl (451 mM NaCl and 20 mM phosphate buffer, pH 7.2), were immersed in Na_2SO_4 (150 mM Na_2SO_4, 40 mM HCO_3^- and 20 mM phosphate buffer, pH 7.2). Each trace represents an average of at least three different experiments.

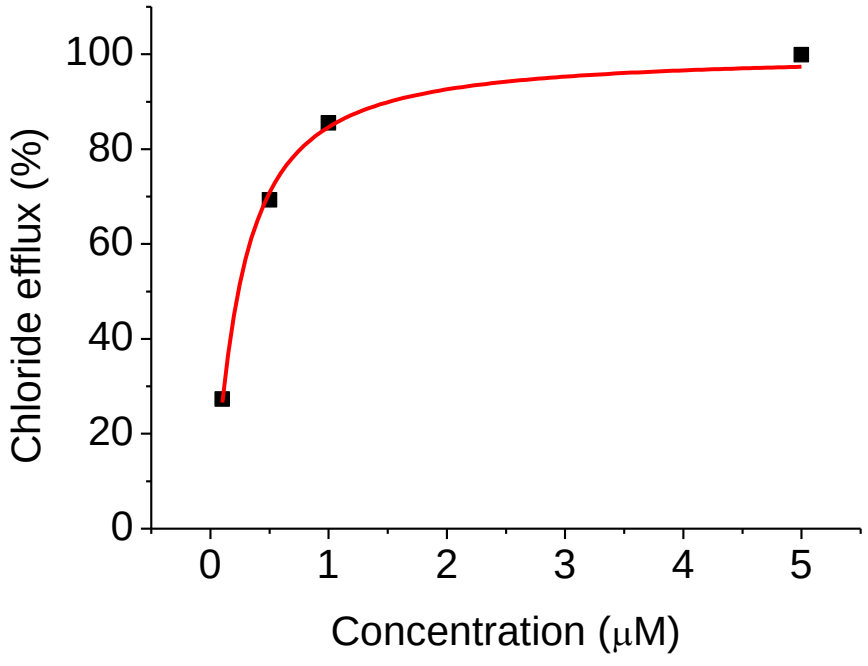

Figure S133. Hill analysis for compound **8**.

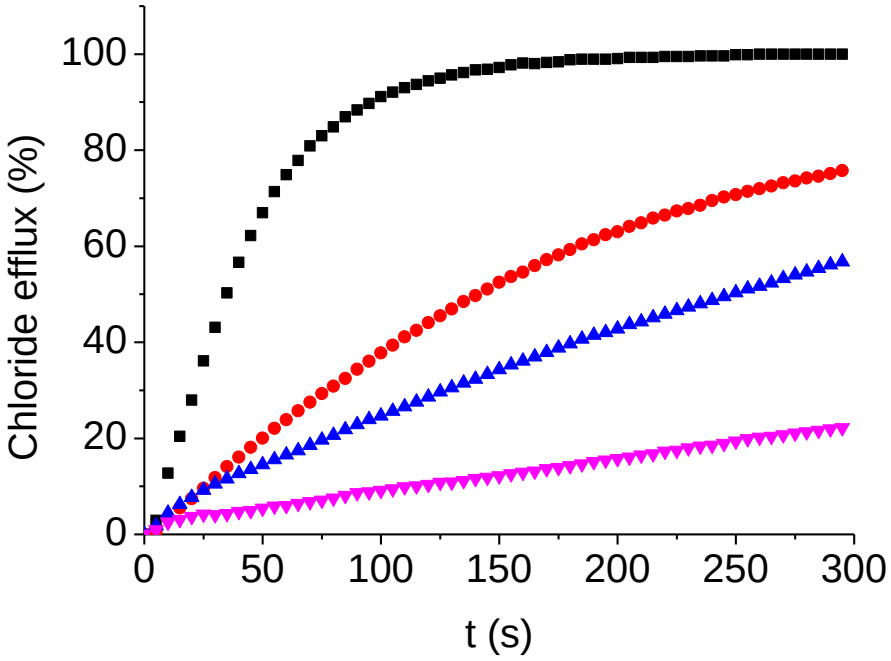

Figure S134. Chloride efflux promoted by **9** (5 μM, black; 0.5 μM, red; 0.25 μM, blue; 0.05 μM, pink) in unilamellar POPC vesicles. The vesicles, which contained NaCl (451 mM NaCl and 20 mM phosphate buffer, pH 7.2), were immersed in Na_2SO_4 (150 mM Na_2SO_4, 40 mM HCO_3^- and 20 mM phosphate buffer, pH 7.2). Each trace represents an average of at least three different experiments.

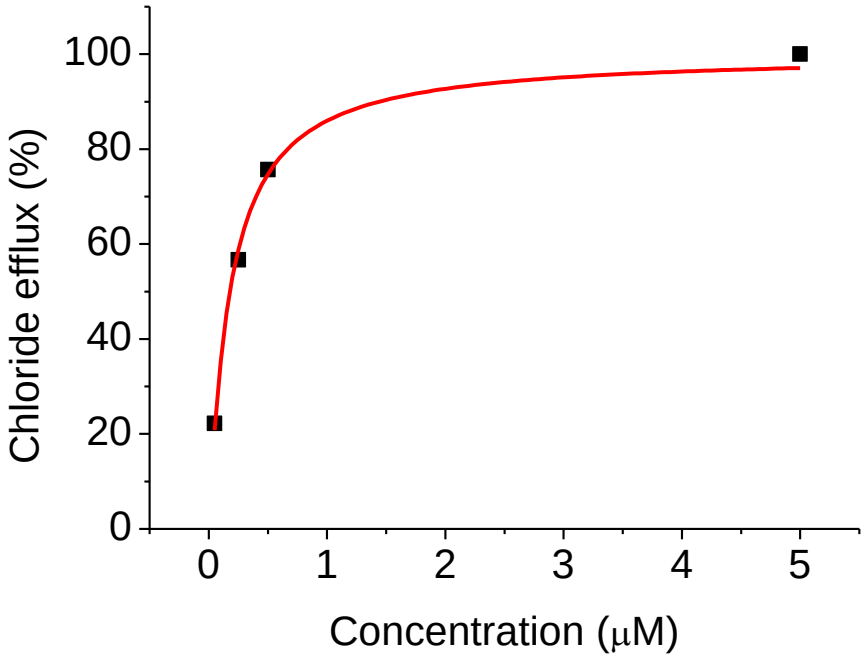

Figure S135. Hill analysis for compound **9**.

Table S3. Transport activities expressed as EC_{50} (nM) and Hill parameter for the studied compounds.

Compound	EC_{50} (nM) NO_3^-/Cl^-	Hill parameter, *n* NO_3^-/Cl^-	EC_{50} (nM) HCO_3^-/Cl^-	Hill parameter, *n* HCO_3^-/Cl^-	logP[a]
1	136 ± 12	1.0 ± 0.1	2893 ± 60	1.56 ± 0.07	3.09
2	32.6 ± 0.8	1.32 ± 0.05	130 ± 7	0.69 ± 0.03	4.22
3	10 ± 1	1.0 ± 0.2	112 ± 6	1.00 ± 0.06	5.20
4	181 ± 20	1.1 ± 0.2	2320 ± 113	2.0 ± 0.2	3.36
5	28 ± 2	1.09 ± 0.09	137 ± 37	0.9 ± 0.2	4.48
6	11.0 ± 0.4	1.10 ± 0.04	130 ± 6	1.08 ± 0.06	5.39
7	238 ± 9	1.5 ± 0.1	3496 ± 192	1.21 ± 0.07	4.25
8	32 ± 2	0.98 ± 0.09	236 ± 15	1.18 ± 0.07	5.29
9	21 ± 2	0.9 ± 0.1	178 ± 14	1.05 ± 0.09	6.22

[a] Determined for the deprotonated form of the compounds through Virtual Computational Chemistry Laboratory.

6.3. Emission spectroscopy transport experiments

6.3.1. Carboxyfluorescein-based assays

POPC vesicles were loaded with a sodium chloride aqueous solution (451 mM NaCl and 20 mM phosphate buffer, 50 mM carboxyfluorescein, pH 7.2) and treated according to the procedure described in *Section 6.1*. After being subjected to extrusion, liposomes were suspended in a sodium sulphate aqueous solution (150 mM Na_2SO_4 and 20 mM phosphate buffer, pH 7.2). The unencapsulated carboxyfluorescein was removed by size-exclusion chromatography, using Sephadex G-25 as the stationary phase and the external solution as the mobile phase. The experiments were performed in 1-cm disposable cells, the final POPC concentration in the cuvette being 0.05 mM and the total volume 2.5 mL. At t = 60 s the anion carrier was added and the emission changes were recorded during five minutes. At t = 300 s a pulse of the detergent Triton-X (10%) was added to lyse the vesicles and release all entrapped carboxyfluorescein.

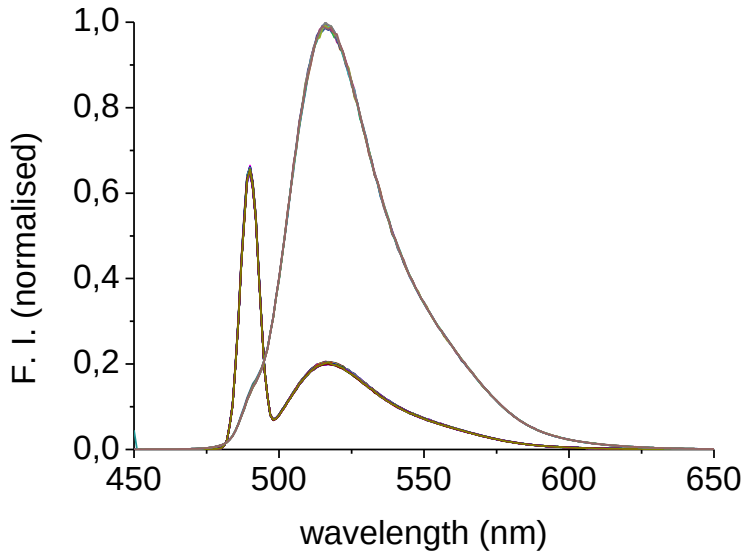

Figure S136. Carboxyfluorescein normalised fluorescence intensity recorded upon addition of **1** to POPC vesicles (0.05 mM). Vesicles (loaded with 451 mM NaCl buffered at pH 7.2 with 20 mM phosphate, and containing 50 mM CF; I.S. 500 mM) were suspended in Na_2SO_4 (150 mM, buffered at pH 7.2 with 20 mM phosphate; I.S. 500 mM). At t = 60 s the anion carrier was added (0.1% mol carrier to lipid), while at t = 360 s the detergent (20 μL) was added. Each trace represents the average of at least three different trials, done with at least two different batches of vesicles.

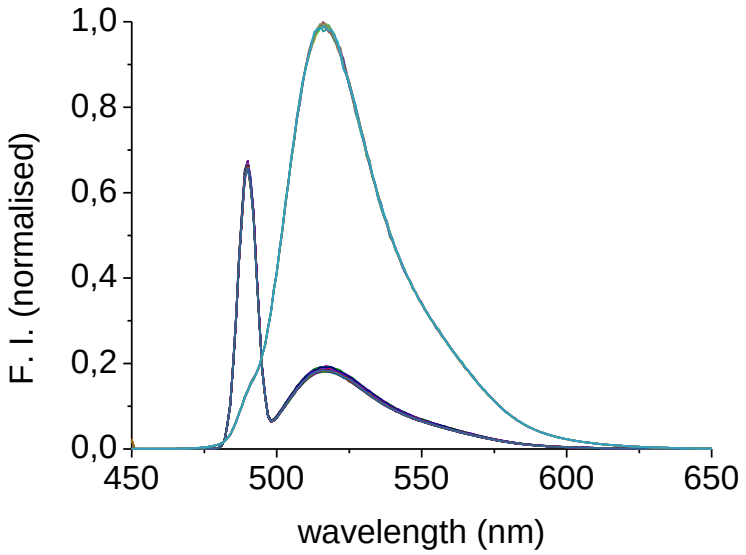

Figure S137. Carboxyfluorescein normalised fluorescence intensity recorded upon addition of **2** to POPC vesicles (0.05 mM). Vesicles (loaded with 451 mM NaCl buffered at pH 7.2 with 20 mM phosphate, and containing 50 mM CF; I.S. 500 mM) were suspended in Na_2SO_4 (150 mM, buffered at pH 7.2 with 20 mM phosphate; I.S. 500 mM). At t = 60 s the anion carrier was added (0.1% mol carrier to lipid), while at t = 360 s the detergent (20 μL) was added. Each trace represents the average of at least three different trials, done with at least two different batches of vesicles.

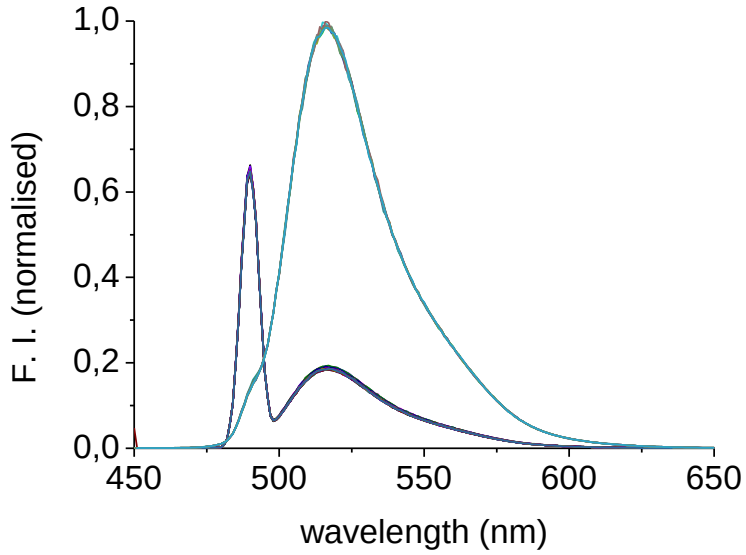

Figure S138. Carboxyfluorescein normalised fluorescence intensity recorded upon addition of **3** to POPC vesicles (0.05 mM). Vesicles (loaded with 451 mM NaCl buffered at pH 7.2 with 20 mM phosphate, and containing 50 mM CF; I.S. 500 mM) were suspended in Na_2SO_4 (150 mM, buffered at pH 7.2 with 20 mM phosphate; I.S. 500 mM). At t = 60 s the anion carrier was added (0.1% mol carrier to lipid), while at t = 360 s the detergent (20 μL) was added. Each trace represents the average of at least three different trials, done with at least two different batches of vesicles.

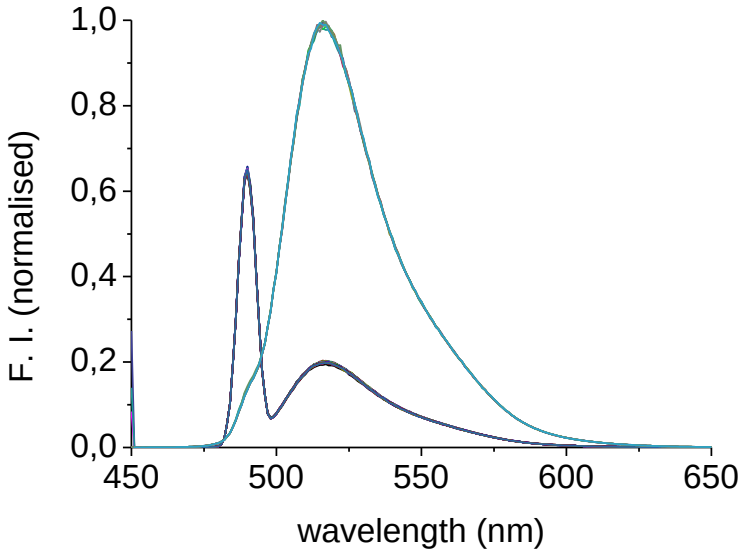

Figure S139. Carboxyfluorescein normalised fluorescence intensity recorded upon addition of **4** to POPC vesicles (0.05 mM). Vesicles (loaded with 451 mM NaCl buffered at pH 7.2 with 20 mM phosphate, and containing 50 mM CF; I.S. 500 mM) were suspended in Na_2SO_4 (150 mM, buffered at pH 7.2 with 20 mM phosphate; I.S. 500 mM). At t = 60 s the anion carrier was added (0.1% mol carrier to lipid), while at t = 360 s the detergent (20 μL) was added. Each trace represents the average of at least three different trials, done with at least two different batches of vesicles.

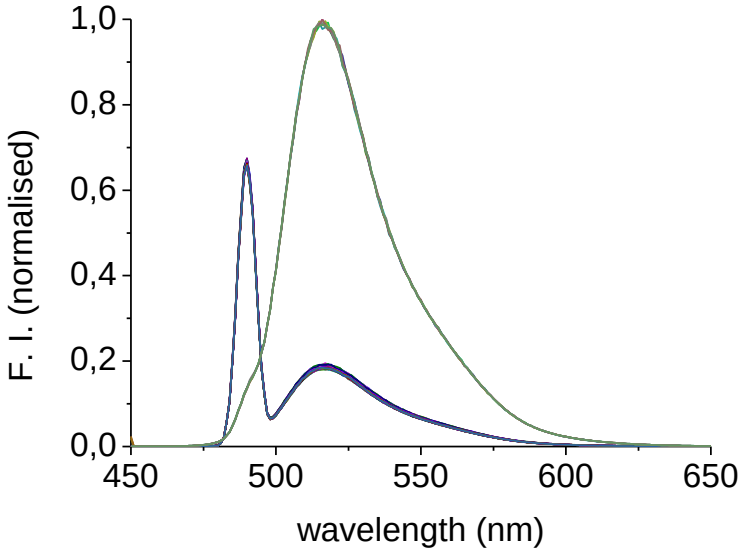

Figure S140. Carboxyfluorescein normalised fluorescence intensity recorded upon addition of **5** to POPC vesicles (0.05 mM). Vesicles (loaded with 451 mM NaCl buffered at pH 7.2 with 20 mM phosphate, and containing 50 mM CF; I.S. 500 mM) were suspended in Na_2SO_4 (150 mM, buffered at pH 7.2 with 20 mM phosphate; I.S. 500 mM). At t = 60 s the anion carrier was added (0.1% mol carrier to lipid), while at t = 360 s the detergent (20 μL) was added. Each trace represents the average of at least three different trials, done with at least two different batches of vesicles.

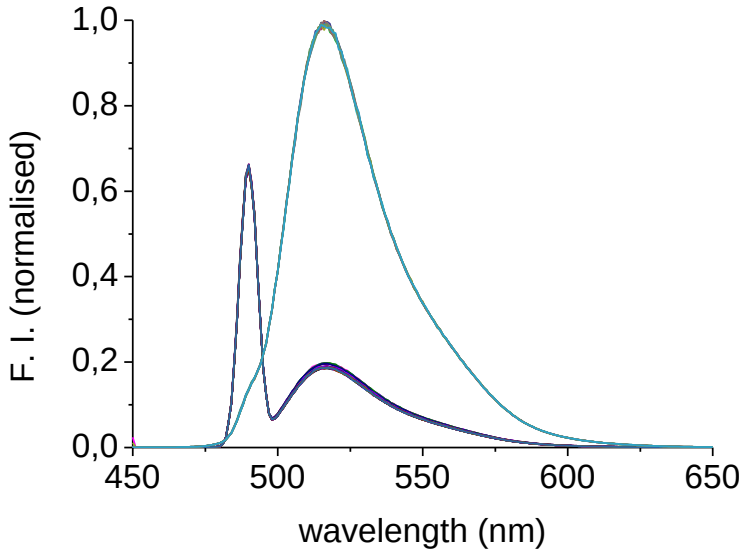

Figure S141. Carboxyfluorescein normalised fluorescence intensity recorded upon addition of **6** to POPC vesicles (0.05 mM). Vesicles (loaded with 451 mM NaCl buffered at pH 7.2 with 20 mM phosphate, and containing 50 mM CF; I.S. 500 mM) were suspended in Na_2SO_4 (150 mM, buffered at pH 7.2 with 20 mM phosphate; I.S. 500 mM). At t = 60 s the anion carrier was added (0.1% mol carrier to lipid), while at t = 360 s the detergent (20 μL) was added. Each trace represents the average of at least three different trials, done with at least two different batches of vesicles.

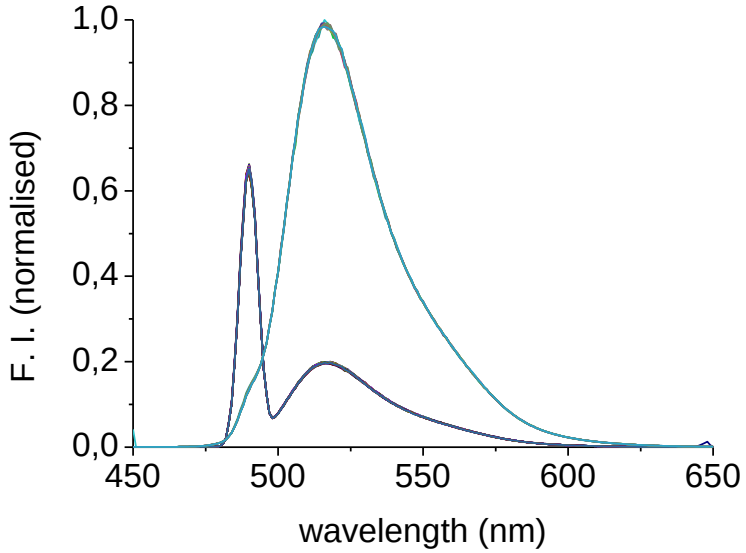

Figure S142. Carboxyfluorescein normalised fluorescence intensity recorded upon addition of **7** to POPC vesicles (0.05 mM). Vesicles (loaded with 451 mM NaCl buffered at pH 7.2 with 20 mM phosphate, and containing 50 mM CF; I.S. 500 mM) were suspended in Na_2SO_4 (150 mM, buffered at pH 7.2 with 20 mM phosphate; I.S. 500 mM). At t = 60 s the anion carrier was added (0.1% mol carrier to lipid), while at t = 360 s the detergent (20 μL) was added. Each trace represents the average of at least three different trials, done with at least two different batches of vesicles.

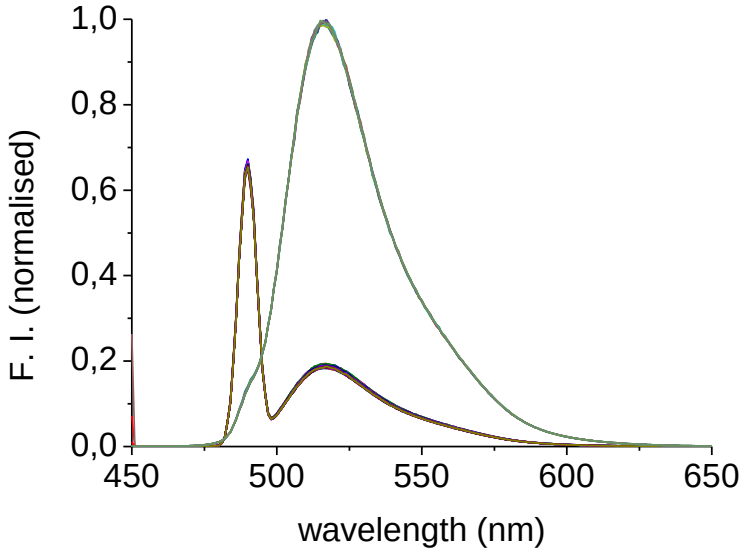

Figure S143. Carboxyfluorescein normalised fluorescence intensity recorded upon addition of **8** to POPC vesicles (0.05 mM). Vesicles (loaded with 451 mM NaCl buffered at pH 7.2 with 20 mM phosphate, and containing 50 mM CF; I.S. 500 mM) were suspended in Na_2SO_4 (150 mM, buffered at pH 7.2 with 20 mM phosphate; I.S. 500 mM). At t = 60 s the anion carrier was added (0.1% mol carrier to lipid), while at t = 360 s the detergent (20 μL) was added. Each trace represents the average of at least three different trials, done with at least two different batches of vesicles.

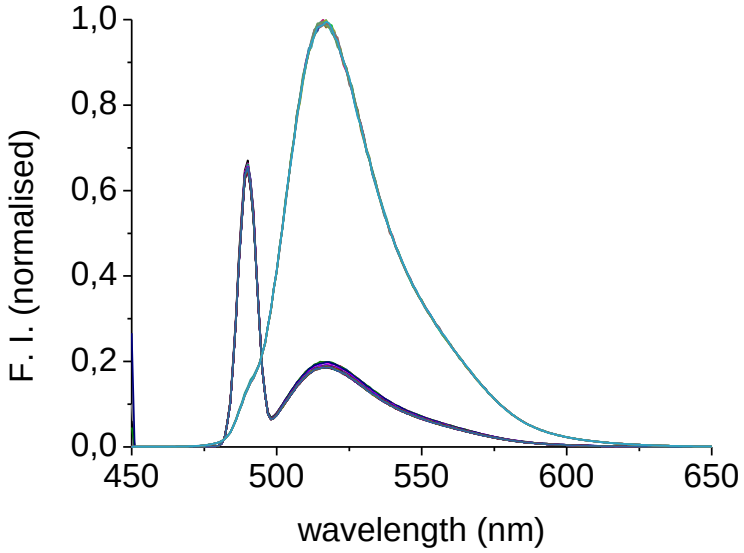

Figure S144. Carboxyfluorescein normalised fluorescence intensity recorded upon addition of **9** to POPC vesicles (0.05 mM). Vesicles (loaded with 451 mM NaCl buffered at pH 7.2 with 20 mM phosphate, and containing 50 mM CF; I.S. 500 mM) were suspended in Na_2SO_4 (150 mM, buffered at pH 7.2 with 20 mM phosphate; I.S. 500 mM). At t = 60 s the anion carrier was added (0.1% mol carrier to lipid), while at t = 360 s the detergent (20 μL) was added. Each trace represents the average of at least three different trials, done with at least two different batches of vesicles.

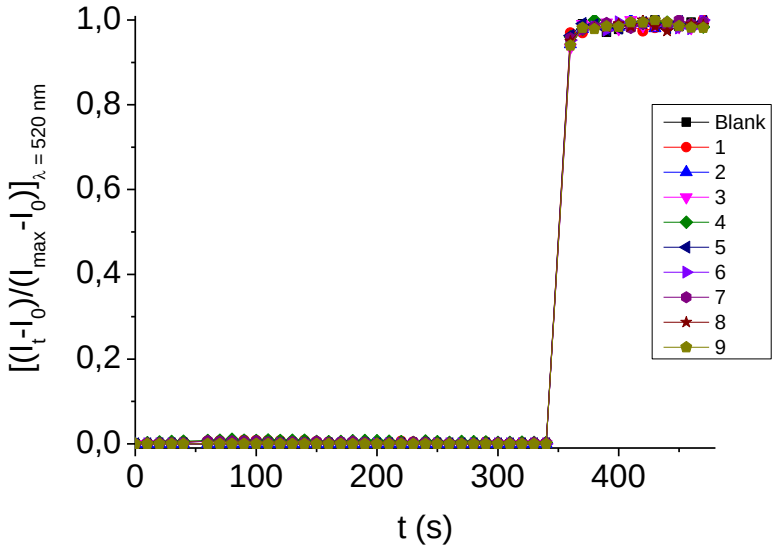

Figure S145. Carboxyfluorescein leakage observed upon addition of the studied compounds to POPC vesicles (0.05 mM). Vesicles (loaded with 451 mM NaCl buffered at pH 7.2 with 20 mM phosphate, and containing 50 mM CF; I.S. 500 mM) were suspended in Na_2SO_4 (150 mM, buffered at pH 7.2 with 20 mM phosphate; I.S. 500 mM). At t = 60 s the anion carrier was added (0.1% mol carrier to lipid), while at t = 360 s the detergent (20 μL) was added. The blank is DMSO (10 μL). Each trace represents the average of at least three trials, performed with at least two different batches of vesicles.

6.3.2. HPTS-based assays

First of all, a calibration curve matching I_{460}/I_{403}, the relationship between the emission intensity at 460 nm and that at 403 nm (corresponding to the excitation wavelengths of the dye's deprotonated and protonated forms, respectively) of an HPTS aqueous solution (15 nM), prepared with a sodium nitrate aqueous solution (126.2 mM $NaNO_3$ and 10 mM phosphate buffer), and the pH was built. In order to do it, aliquots of a sodium hydroxide aqueous solution (0.5 M), prepared with a sodium nitrate aqueous solution (126.2 mM $NaNO_3$ and 10 mM phosphate buffer), were succesively added to the HPTS solution, and after each addition the emission spectra at 403 and 460 nm and the pH value of the solution were recorded. Data were fitted to an *S*-logistic model, which provided an $R^2 > 0.99$.

7:3 POPC:cholesterol vesicles were loaded with a sodium nitrate aqueous solution (126.2 mM and 10 mM phosphate buffer, 10 μM HPTS, pH 7.2) and treated according to the procedure described in *Section 6.1*. The unencapsulated HPTS was removed by size-exclusion chromatography, using Sephadex G-25 as the stationary phase and the external solution as the mobile phase. The collected vesicles were suspended in the sodium nitrate aqueous solution to a final volume of 10 mL. The experiments were performed in 1-cm disposable cells, the final POPC concentration in the cuvette being 0.5 mM. At t = 30 s a pulse of a sodium hydroxide aqueous solution (20 μL of a 0.5 M solution) was added to obtain a final concentration of 4 mM of the base in the cuvette. At t = 60 s an aliquot of the corresponding click tambjamine in DMSO (or DMSO, in the case of the blank) was added and the emission spectra at λ_{exc} = 403 and 460 nm were recorded for five more minutes.

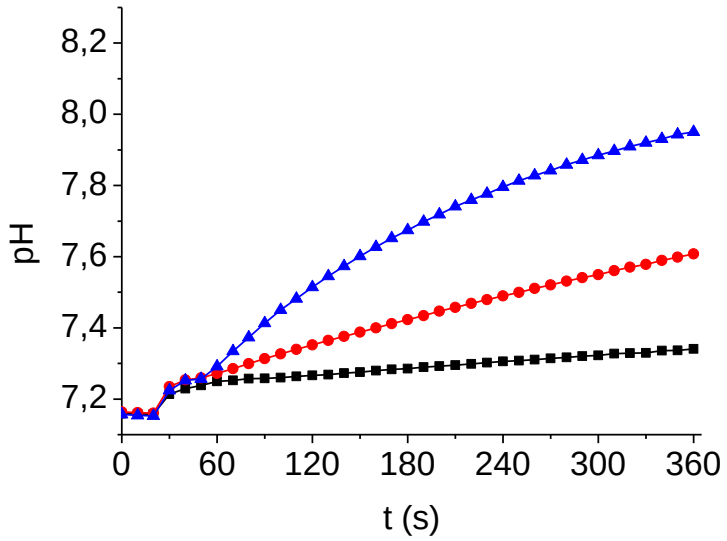

Figure S146. Variation of pH upon addition of **1** to 7:3 POPC:cholesterol vesicles (0.5 mM POPC). Vesicles (loaded with 126.2 mM $NaNO_3$ buffered at pH 7.2 with 10 mM phosphate, and containing 10 µM HPTS; I.S. 150 mM) were suspended in a $NaNO_3$ solution (126.2 mM $NaNO_3$ buffered at pH 7.2 with 10 mM phosphate; I.S. 150 mM). At t = 30 s an aliquot of a NaOH solution (20 µL, 0.5 M) was added, and at t = 60 s the anion carrier was added (0.0005% mol carrier to lipid concentration, blue; 0.0001%, red; blank, black). The blank is DMSO (10 µL). Each trace represents the average of at least three trials, performed with three different batches of vesicles.

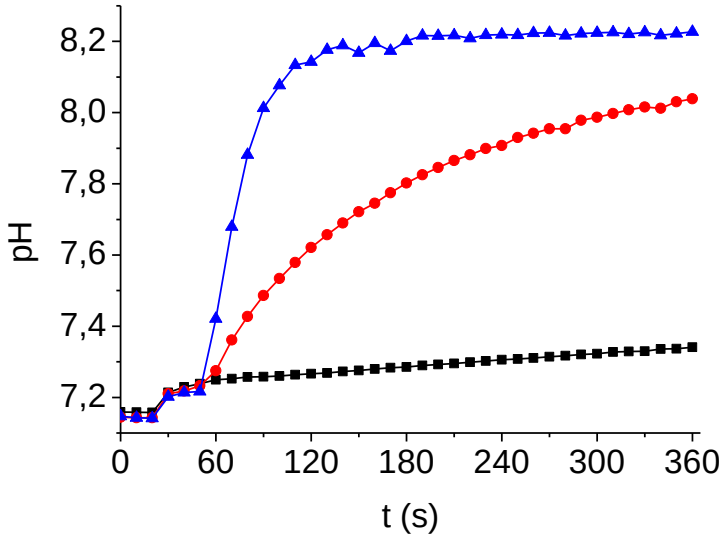

Figure S147. Variation of pH upon addition of **2** to 7:3 POPC:cholesterol vesicles (0.5 mM POPC). Vesicles (loaded with 126.2 mM $NaNO_3$ buffered at pH 7.2 with 10 mM phosphate, and containing 10 µM HPTS; I.S. 150 mM) were suspended in a $NaNO_3$ solution (126.2 mM $NaNO_3$ buffered at pH 7.2 with 10 mM phosphate; I.S. 150 mM). At t = 30 s an aliquot of a NaOH solution (20 µL, 0.5 M) was added, and at t = 60 s the anion carrier was added (0.0005% mol carrier to lipid concentration, blue; 0.0001%, red; blank, black). The blank is DMSO (10 µL). Each trace represents the average of at least three trials, performed with three different batches of vesicles.

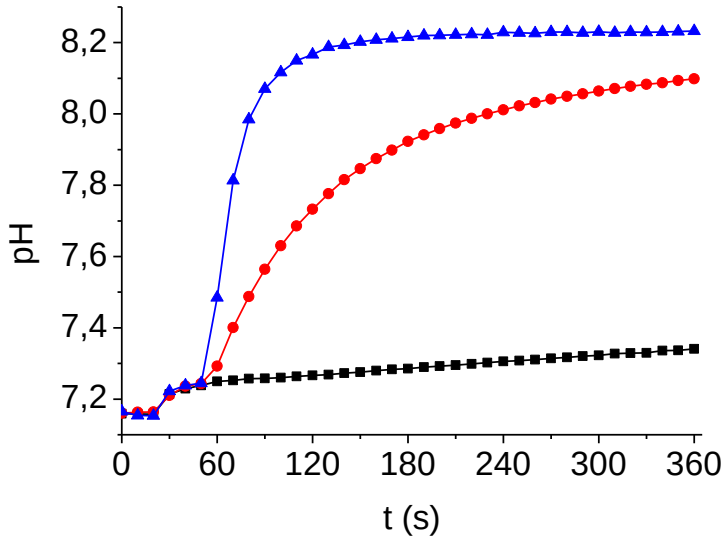

Figure S148. Variation of pH upon addition of **3** to 7:3 POPC:cholesterol vesicles (0.5 mM POPC). Vesicles (loaded with 126.2 mM $NaNO_3$ buffered at pH 7.2 with 10 mM phosphate, and containing 10 µM HPTS; I.S. 150 mM) were suspended in a $NaNO_3$ solution (126.2 mM $NaNO_3$ buffered at pH 7.2 with 10 mM phosphate; I.S. 150 mM). At t = 30 s an aliquot of a NaOH solution (20 µL, 0.5 M) was added, and at t = 60 s the anion carrier was added (0.0005% mol carrier to lipid concentration, blue; 0.0001%, red; blank, black). The blank is DMSO (10 µL). Each trace represents the average of at least three trials, performed with three different batches of vesicles.

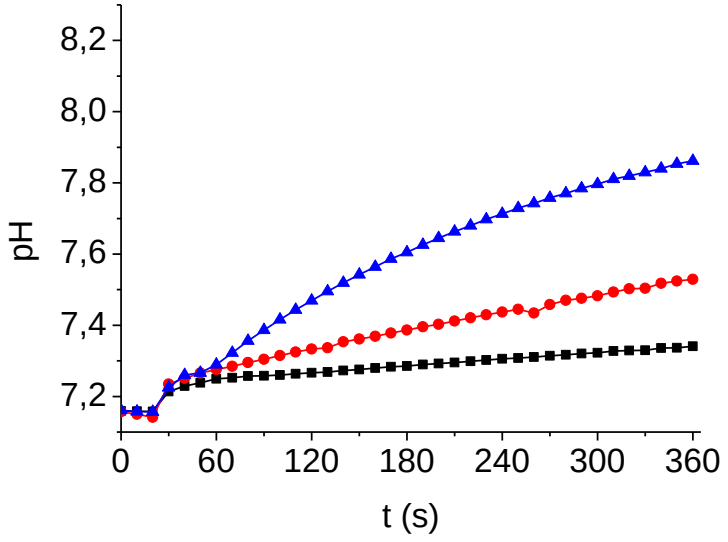

Figure S149. Variation of pH upon addition of **4** to 7:3 POPC:cholesterol vesicles (0.5 mM POPC). Vesicles (loaded with 126.2 mM $NaNO_3$ buffered at pH 7.2 with 10 mM phosphate, and containing 10 µM HPTS; I.S. 150 mM) were suspended in a $NaNO_3$ solution (126.2 mM $NaNO_3$ buffered at pH 7.2 with 10 mM phosphate; I.S. 150 mM). At t = 30 s an aliquot of a NaOH solution (20 µL, 0.5 M) was added, and at t = 60 s the anion carrier was added (0.0005% mol carrier to lipid concentration, blue; 0.0001%, red; blank, black). The blank is DMSO (10 µL). Each trace represents the average of at least three trials, performed with three different batches of vesicles.

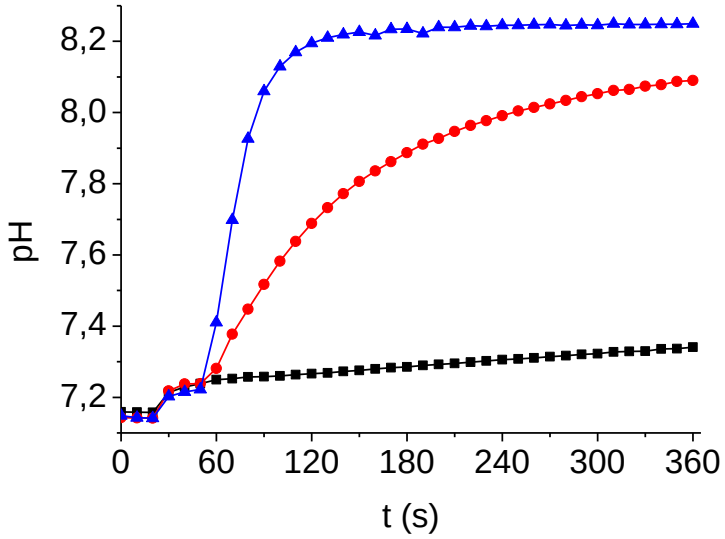

Figure S150. Variation of pH upon addition of **5** to 7:3 POPC:cholesterol vesicles (0.5 mM POPC). Vesicles (loaded with 126.2 mM $NaNO_3$ buffered at pH 7.2 with 10 mM phosphate, and containing 10 µM HPTS; I.S. 150 mM) were suspended in a $NaNO_3$ solution (126.2 mM $NaNO_3$ buffered at pH 7.2 with 10 mM phosphate; I.S. 150 mM). At t = 30 s an aliquot of a NaOH solution (20 µL, 0.5 M) was added, and at t = 60 s the anion carrier was added (0.0005% mol carrier to lipid concentration, blue; 0.0001%, red; blank, black). The blank is DMSO (10 µL). Each trace represents the average of at least three trials, performed with three different batches of vesicles.

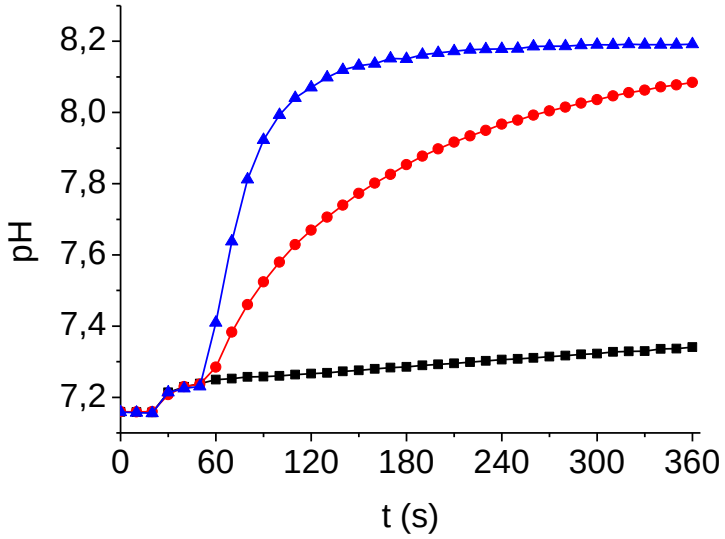

Figure S151. Variation of pH upon addition of **6** to 7:3 POPC:cholesterol vesicles (0.5 mM POPC). Vesicles (loaded with 126.2 mM $NaNO_3$ buffered at pH 7.2 with 10 mM phosphate, and containing 10 µM HPTS; I.S. 150 mM) were suspended in a $NaNO_3$ solution (126.2 mM $NaNO_3$ buffered at pH 7.2 with 10 mM phosphate; I.S. 150 mM). At t = 30 s an aliquot of a NaOH solution (20 µL, 0.5 M) was added, and at t = 60 s the anion carrier was added (0.0005% mol carrier to lipid concentration, blue; 0.0001%, red; blank, black). The blank is DMSO (10 µL). Each trace represents the average of at least three trials, performed with three different batches of vesicles.

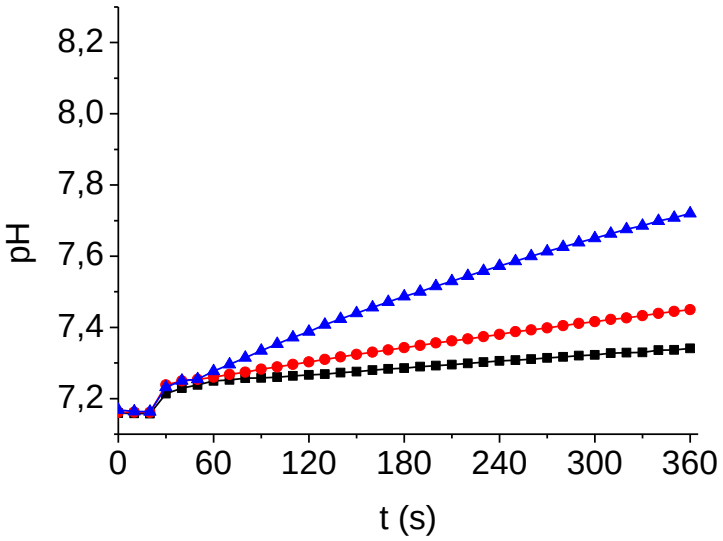

Figure S152. Variation of pH upon addition of **7** to 7:3 POPC:cholesterol vesicles (0.5 mM POPC). Vesicles (loaded with 126.2 mM $NaNO_3$ buffered at pH 7.2 with 10 mM phosphate, and containing 10 µM HPTS; I.S. 150 mM) were suspended in a $NaNO_3$ solution (126.2 mM $NaNO_3$ buffered at pH 7.2 with 10 mM phosphate; I.S. 150 mM). At t = 30 s an aliquot of a NaOH solution (20 µL, 0.5 M) was added, and at t = 60 s the anion carrier was added (0.0005% mol carrier to lipid concentration, blue; 0.0001%, red; blank, black). The blank is DMSO (10 µL). Each trace represents the average of at least three trials, performed with three different batches of vesicles.

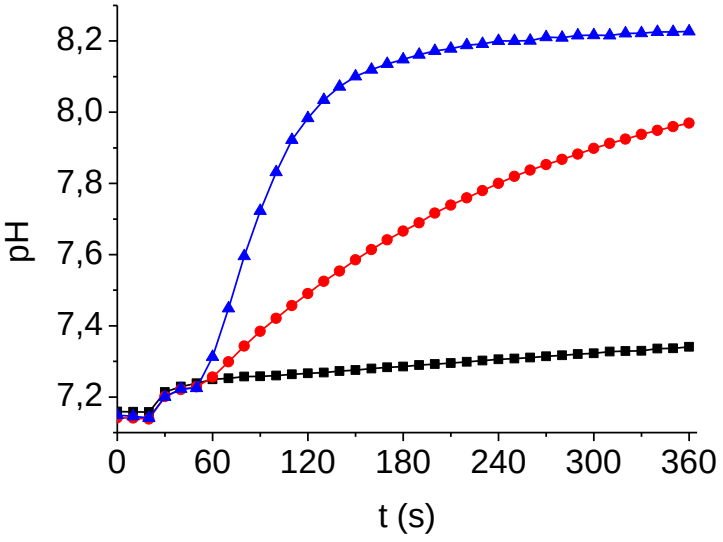

Figure S153. Variation of pH upon addition of **8** to 7:3 POPC:cholesterol vesicles (0.5 mM POPC). Vesicles (loaded with 126.2 mM $NaNO_3$ buffered at pH 7.2 with 10 mM phosphate, and containing 10 µM HPTS; I.S. 150 mM) were suspended in a $NaNO_3$ solution (126.2 mM $NaNO_3$ buffered at pH 7.2 with 10 mM phosphate; I.S. 150 mM). At t = 30 s an aliquot of a NaOH solution (20 µL, 0.5 M) was added, and at t = 60 s the anion carrier was added (0.0005% mol carrier to lipid concentration, blue; 0.0001%, red; blank, black). The blank is DMSO (10 µL). Each trace represents the average of at least three trials, performed with three different batches of vesicles.

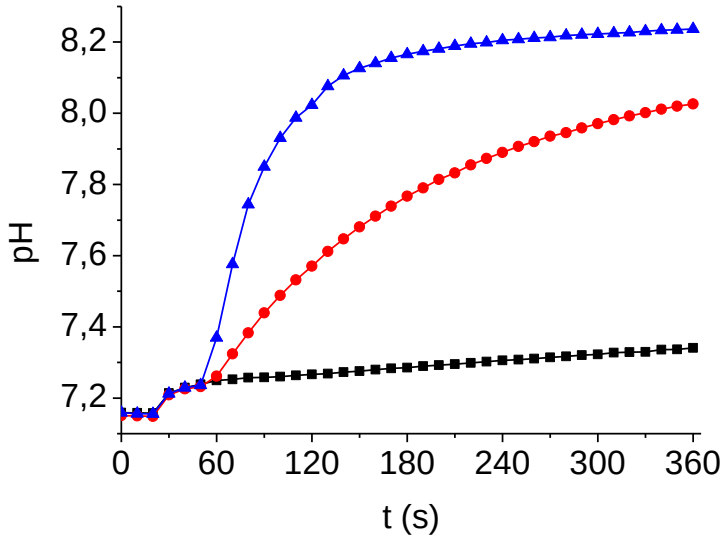

Figure S154. Variation of pH upon addition of **9** to 7:3 POPC:cholesterol vesicles (0.5 mM POPC). Vesicles (loaded with 126.2 mM $NaNO_3$ buffered at pH 7.2 with 10 mM phosphate, and containing 10 µM HPTS; I.S. 150 mM) were suspended in a $NaNO_3$ solution (126.2 mM $NaNO_3$ buffered at pH 7.2 with 10 mM phosphate; I.S. 150 mM). At t = 30 s an aliquot of a NaOH solution (20 µL, 0.5 M) was added, and at t = 60 s the anion carrier was added (0.0005% mol carrier to lipid concentration, blue; 0.0001%, red; blank, black). The blank is DMSO (10 µL). Each trace represents the average of at least three trials, performed with three different batches of vesicles.

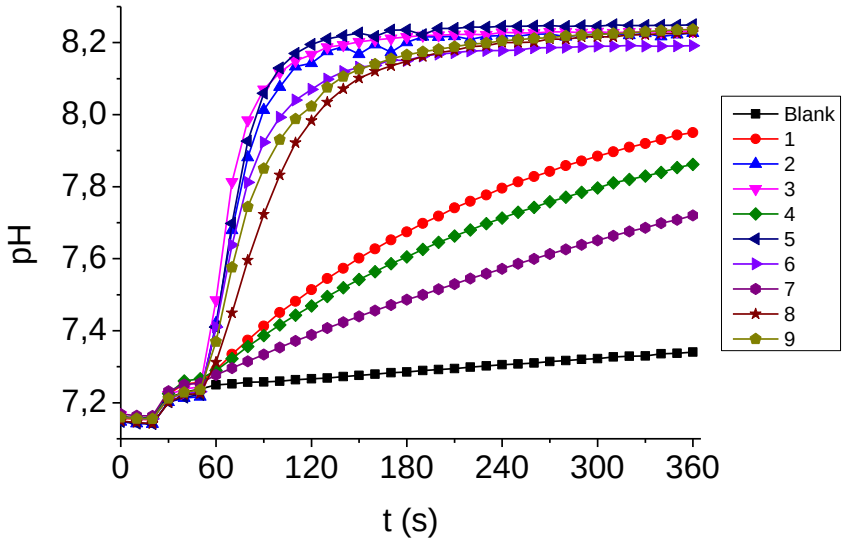

Figure S155. Variation of pH upon addition of the studied compounds to 7:3 POPC:cholesterol vesicles (0.5 mM POPC). Vesicles (loaded with 126.2 mM $NaNO_3$ buffered at pH 7.2 with 10 mM phosphate, and containing 10 µM HPTS; I.S. 150 mM) were suspended in a $NaNO_3$ aqueous solution (126.2 mM $NaNO_3$ buffered at pH 7.2 with 10 mM phosphate; I.S. 150 mM). At t = 30 s an aliquot of a NaOH solution (11 µL, 0.5 M) was added, and at t = 60 s the anion carrier was added (0.0005% mol carrier to lipid concentration). The blank is DMSO (10 µL). Each trace represents the average of at least three trials, performed with three different batches of vesicles.

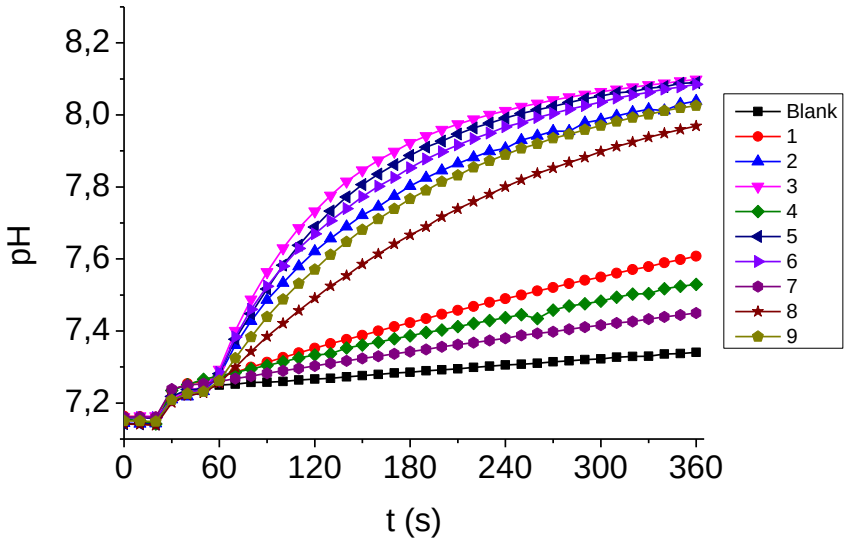

Figure S156. Variation of pH upon addition of the studied compounds to 7:3 POPC:cholesterol vesicles (0.5 mM POPC). Vesicles (loaded with 126.2 mM $NaNO_3$ buffered at pH 7.2 with 10 mM phosphate, and containing 10 µM HPTS; I.S. 150 mM) were suspended in a $NaNO_3$ aqueous solution (126.2 mM $NaNO_3$ buffered at pH 7.2 with 10 mM phosphate; I.S. 150 mM). At t = 30 s an aliquot of a NaOH solution (11 µL, 0.5 M) was added, and at t = 60 s the anion carrier was added (0.0001% mol carrier to lipid concentration). The blank is DMSO (10 µL). Each trace represents the average of at least three trials, performed with three different batches of vesicles.

7. BIOLOGICAL ASSAYS

7.1. Transmembrane anion transport experiments in cells

The transport activity of the nine compounds in cells was determined using Fisher Rat Thyroid (FRT) cells expressing a variant of the halide-sensitive yellow fluorescent protein (YFP-H148Q/I152L) as previously described.[10] This variant has a higher affinity for iodide than for chloride, allowing to detect iodide concentration changes without significant interferences from small chloride changes.[11]

FRT cells stably transfected with this YFP variant were plated on 96-well micro-plates at a density of 40,000 cells/well in Coon's modified medium supplemented with 10% serum, 2 mM L-glutamine, 1 mg/mL penicillin, 100 µg/mL treptomycin and 0.5 mg/mL hygromycin, the last one as selection agent for the YFP. Cells were kept at 37 °C in a 5%/95% CO_2/air atmosphere. Functional experiments were conducted 48 hours after cell seeding.

Cells were washed twice with an external solution containing 137 mM NaCl, 2.7 mM KCl, 8.1 mM Na_2HPO_4, 1.5 mM KH_2PO_4, 1 mM $CaCl_2$ and 0.5 mM $MgCl_2$ and buffered at pH 7.3 with HEPES. Subsequently, they were incubated in 60 µL of this solution, at 37 °C for 30 minutes, in the presence of the compounds (2, 8.3 and 20 µM) or of DMSO (control). After incubation, the fluorescence baseline was recorded for 2 seconds and then 165 µL of a NaI solution (137 mM, at pH 6.6 or 7.3 depending on the experiment; in the case of the former the pH was adjusted with MES, whereas HEPES was employed for the latter) were injected; in this way, the final concentration of NaI in the well was 100 mM. The iodide influx was observed as a fluorescence quenching, as the anion binds to the intracellular YFP.

The initial rate of fluorescence decay (QR) was derived by fitting the signal to a double exponential function, after background substraction and normalisation to obtain the average emission before the addition of the NaI solution.[10,11b,12] The QR parameter is a direct indication of the tested compound's activity. The curves resulting from plotting the quenching rate in front of the compound's concentration were fitted to a Hill-like equation.

The YFP fluorescence was measured with a plate reader (FLUOstar Galaxy, BMG) equipped with 500 nm excitation and 535 emission filters.

---

[10] E. Caci, A. Caputo, A. Hinzpeter, N. Arous, P. Fanen, N. Sonawane, A. S. Verkman, R. Ravazzolo, O. Zegarra-Moran and L. J. V. Galietta, *Biochem. J.*, 2008, **413**, 135-142.

[11] (a) L. J. V. Galietta, M. F. Springsteel, M. Eda, E. J. Niedzinski, K. By, M. J. Haddadin, M. J. Kurth, M. H. Nantz and A. S. Verkman, *J. Biol. Chem.*, 2001, **276**, 19723-19728; (b) L. J. V. Galietta, P. M. Haggie and A. S. Verkman, *FEBS Lett.*, 2001, **499**, 220-224.

[12] L. V. J. Galietta, S. Jayaraman and A. S. Verkman, *Am. J. Physiol., Cell Physiol.*, 2001, **281**, C1734-C1742.

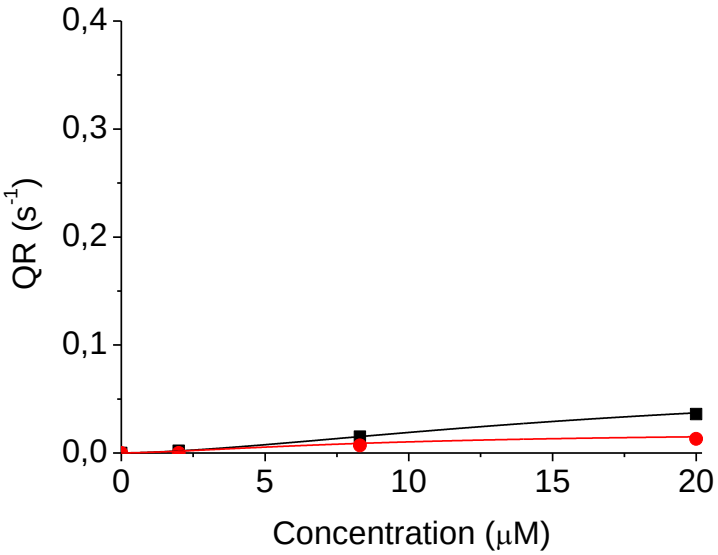

Figure S157. Representation of the QR values obtained at different pH values (6.6 and 7.3) and different concentrations of **1** in FRT cells against such concentrations. The plots were fitted to a first-order binding model. The black dots and line are the experimental data and the fitting, respectively, of the assays performed at pH 6.6, whereas the red ones correspond to those conducted at pH 7.3.

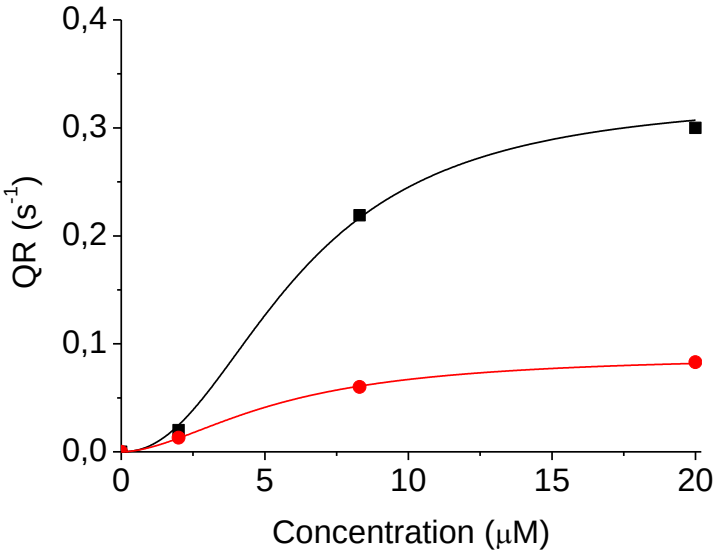

Figure S158. Representation of the QR values obtained at different pH values (6.6 and 7.3) and different concentrations of **2** in FRT cells against such concentrations. The plots were fitted to a first-order binding model. The black dots and line are the experimental data and the fitting, respectively, of the assays performed at pH 6.6, whereas the red ones correspond to those conducted at pH 7.3.

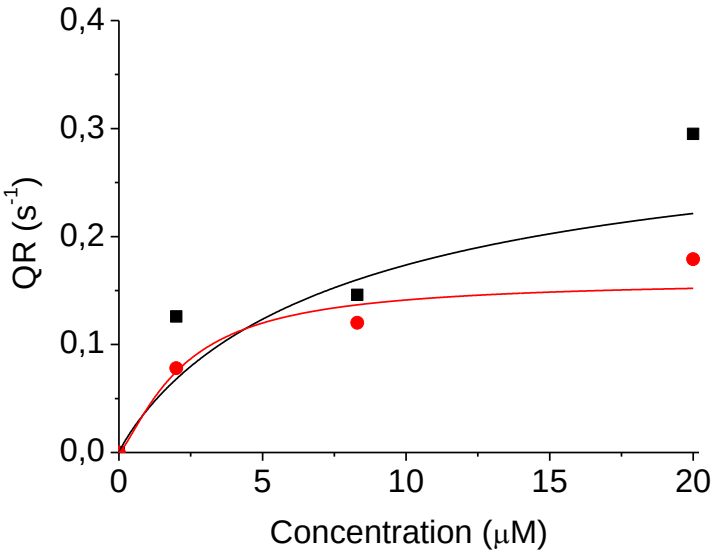

Figure S159. Representation of the QR values obtained at different pH values (6.6 and 7.3) and different concentrations of **3** in FRT cells against such concentrations. The plots were fitted to a first-order binding model. The black dots and line are the experimental data and the fitting, respectively, of the assays performed at pH 6.6, whereas the red ones correspond to those conducted at pH 7.3.

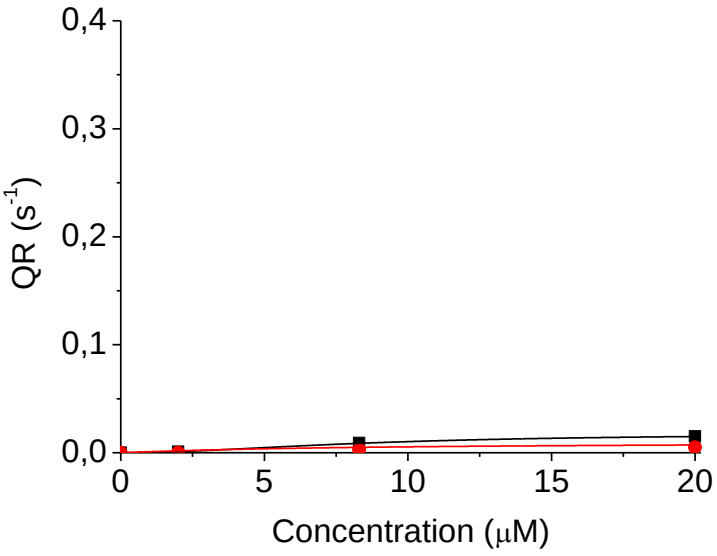

Figure S160. Representation of the QR values obtained at different pH values (6.6 and 7.3) and different concentrations of **4** in FRT cells against such concentrations. The plots were fitted to a first-order binding model. The black dots and line are the experimental data and the fitting, respectively, of the assays performed at pH 6.6, whereas the red ones correspond to those conducted at pH 7.3.

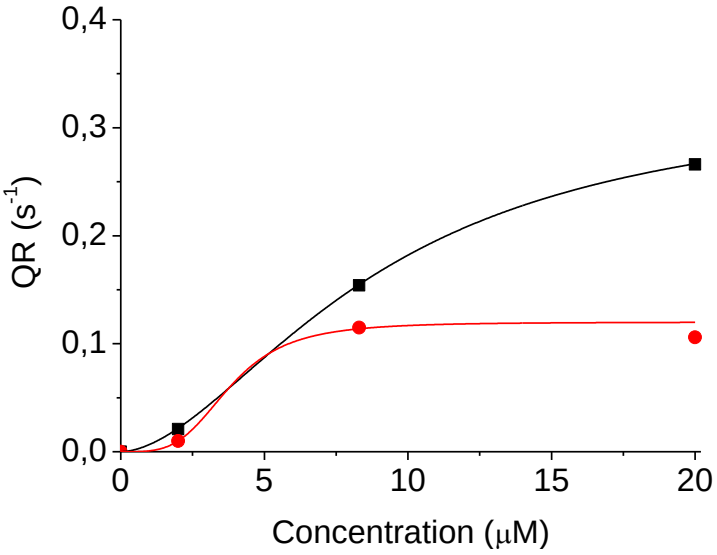

Figure S161. Representation of the QR values obtained at different pH values (6.6 and 7.3) and different concentrations of **5** in FRT cells against such concentrations. The plots were fitted to a first-order binding model. The black dots and line are the experimental data and the fitting, respectively, of the assays performed at pH 6.6, whereas the red ones correspond to those conducted at pH 7.3.

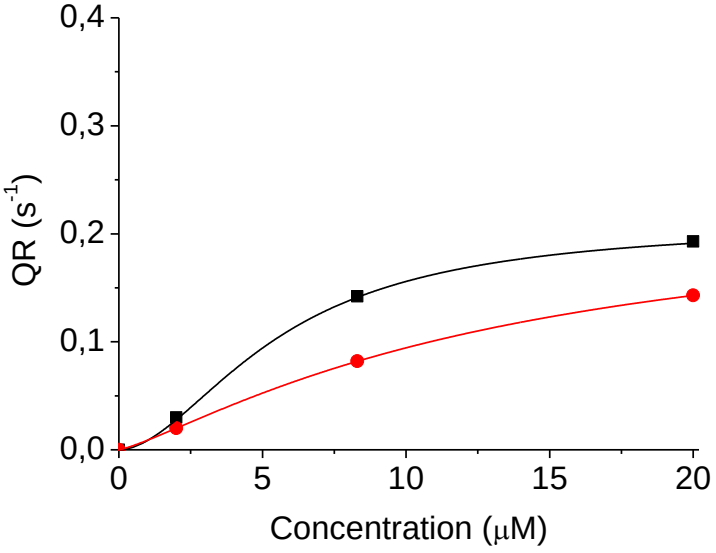

Figure S162. Representation of the QR values obtained at different pH values (6.6 and 7.3) and different concentrations of **6** in FRT cells against such concentrations. The plots were fitted to a first-order binding model. The black dots and line are the experimental data and the fitting, respectively, of the assays performed at pH 6.6, whereas the red ones correspond to those conducted at pH 7.3.

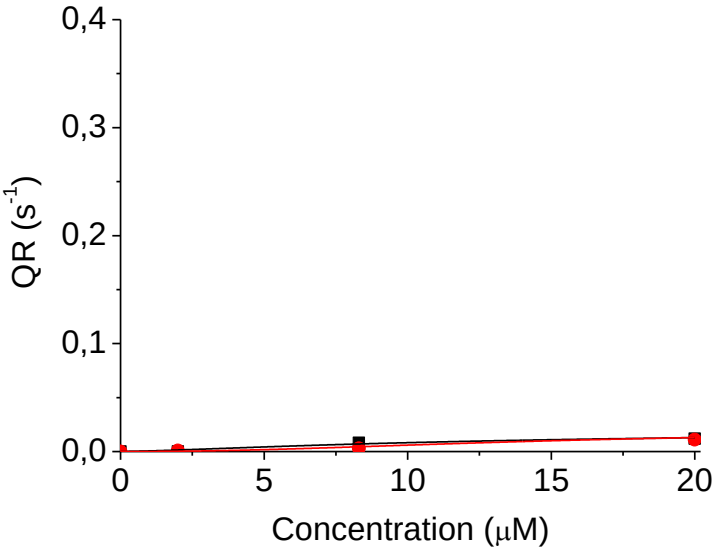

Figure S163. Representation of the QR values obtained at different pH values (6.6 and 7.3) and different concentrations of **7** in FRT cells against such concentrations. The plots were fitted to a first-order binding model. The black dots and line are the experimental data and the fitting, respectively, of the assays performed at pH 6.6, whereas the red ones correspond to those conducted at pH 7.3.

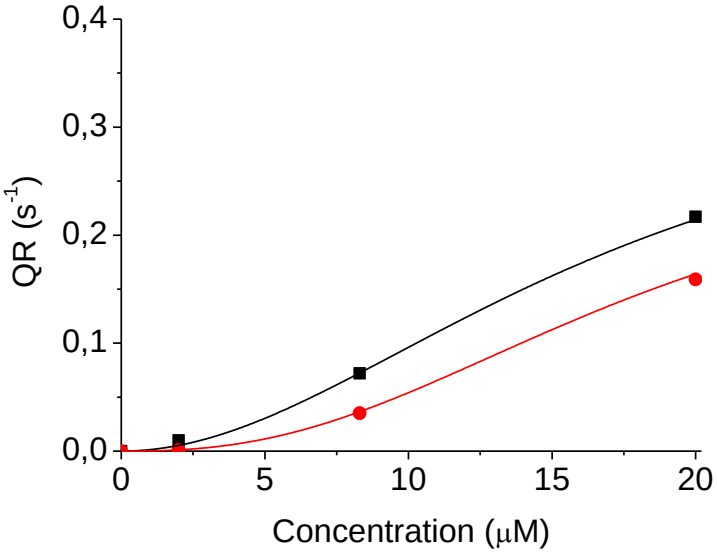

Figure S164. Representation of the QR values obtained at different pH values (6.6 and 7.3) and different concentrations of **8** in FRT cells against such concentrations. The plots were fitted to a first-order binding model. The black dots and line are the experimental data and the fitting, respectively, of the assays performed at pH 6.6, whereas the red ones correspond to those conducted at pH 7.3.

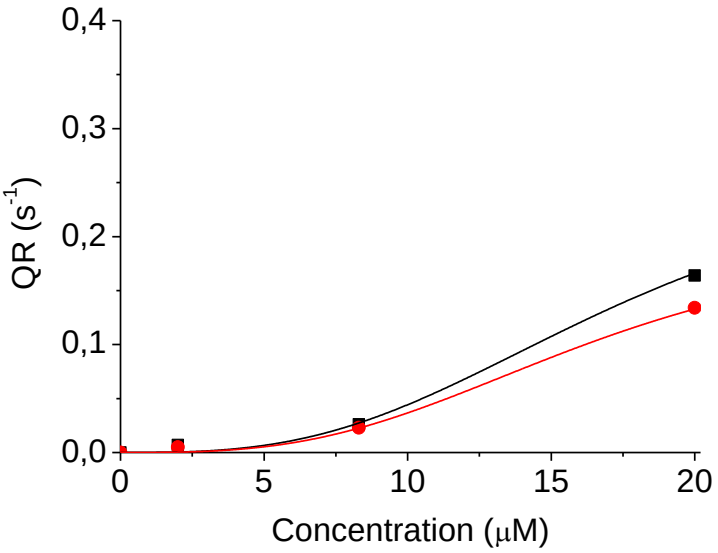

Figure S165. Representation of the QR values obtained at different pH values (6.6 and 7.3) and different concentrations of **9** in FRT cells against such concentrations. The plots were fitted to a first-order binding model. The black dots and line are the experimental data and the fitting, respectively, of the assays performed at pH 6.6, whereas the red ones correspond to those conducted at pH 7.3.

7.2. Cytotoxicity studies

Cell culture

Human lung adenocarcinoma A549, breast adenocarcinoma MCF-7 and MCF-10A cell lines were obtained from the American Type Culture Collection (ATCC, Manassas, VA, USA). A549 cells were cultured in DMEM medium with 10% heat-inactivated fetal bovine serum (FBS; Life Technologies, Carlsbad, CA, USA), 100 U/mL penicillin, 100 µg/mL streptomycin and 2.0 mM glutamine. The MCF-7 cell line was cultured in DMEM-F12 (HAM) media (1:1) with 10% FBS, 50 µM sodium pyruvate, 10 µg/mL insulin (Sigma-Aldrich Chemical Co., St. Louis, MO, USA), 100 U/mL penicillin, 100 µg/mL streptomycin and 2 mM glutamine. MCF10A cells were cultured in DMEM-F12 (HAM) media (1:1) with 5% horse serum (Life Technologies), 100 U/mL penicillin, 100 µg/mL streptomycin, 2.0 mM glutamine, 10 µg/mL insulin, 0.5 µg/mL hydrocortisone (Sigma-Aldrich), 20 ng/mL epidermal growth factor (EGF, Sigma-Aldrich) and 100 ng/mL choleric toxin (Calbiochem, San Diego, CA, USA). All reagents not specified were obtained from Biological Industries, Beit Haemek, Israel. Cells were grown at 37 °C in a 5% CO_2 atmosphere.

Cell viability assays

Cell viability assays were conducted using the MTT (3-(4,5-dimethylthiazol-2-yl) -2,5-diphenyl-tetrazolium bromide) assay. For that purpose, 10^4 cells were seeded in 96-well plates (10^5 cells/mL) and allowed to grow for 24 h. Dose-response experiments were performed and cells were treated with different concentrations of the compounds (ranging from 0.8 to 100 µM) or diluent (control cells, 1% DMSO) for 24 h. After treatment, a 10-µM solution of MTT was added to each well and assay plates were incubated for 2 h at 37 °C. The medium was removed and purple formazan crystals were dissolved in 100 µL of DMSO. The absorbance was measured at 570 nm using a multi-well plate reader (Multiskan FC, Thermo Scientific). The cell viability was calculated according to the formula: viability (%) = [(absorbance of treated wells) / (absorbance of control wells)] × 100. The inhibitory concentration (IC_{50}) values (corresponding to the compound concentrations that produce 50% reduction in cell viability) were obtained from the dose-response curves using GraphPad Prism V5.0 for Windows™ (GraphPad Software, San Diego, CA, USA). All data are shown as the mean value ± S.D. of at least three independent experiments performed in duplicate.

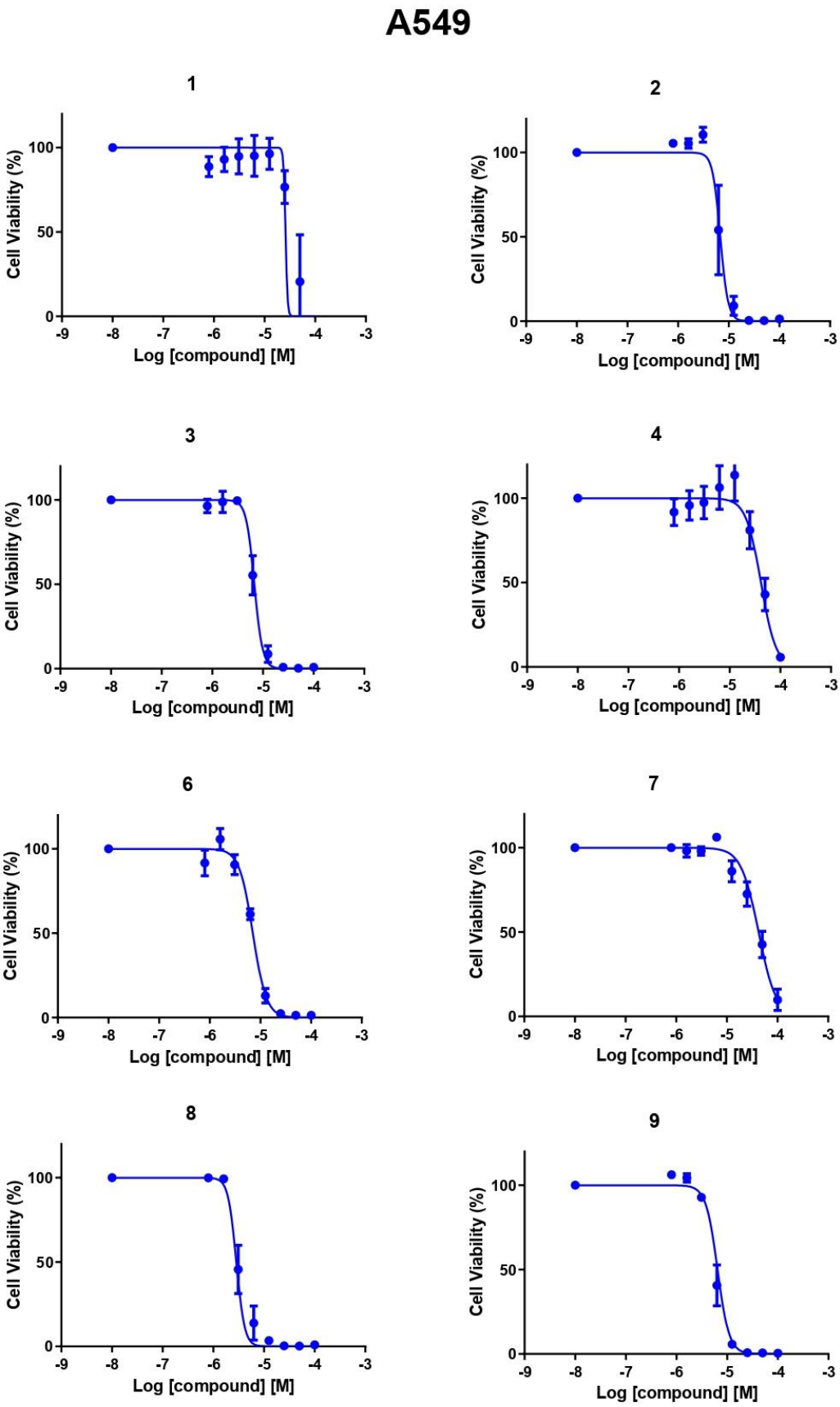

Figure S166. Cell viability in the A549 human lung adenocarcinoma cell line in the presence of different concentrations of compounds **1**-**4** and **6**-**9**.

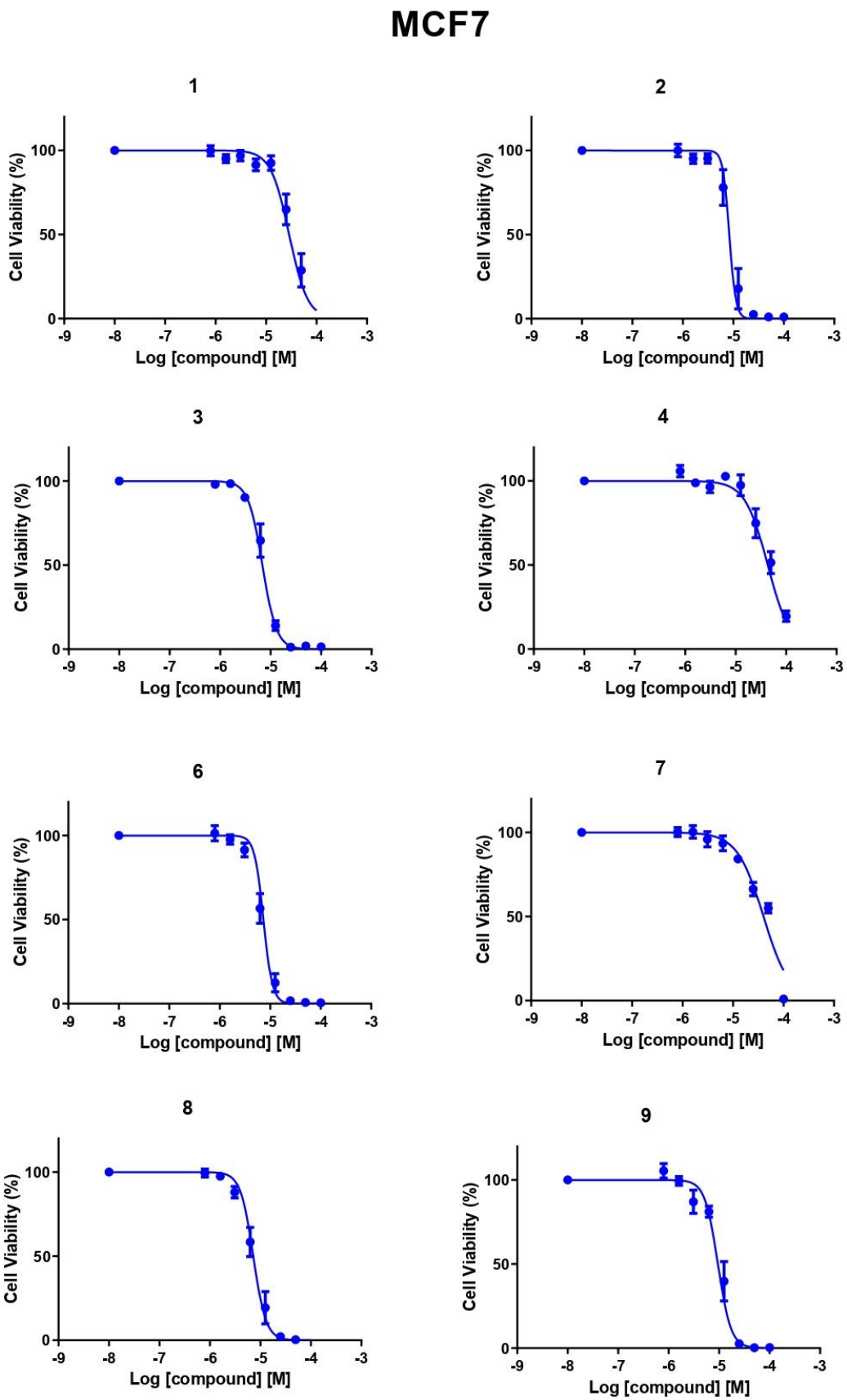

Figure S167. Cell viability in the MCF-7 breast adenocarcinoma cell line in the presence of different concentrations of compounds **1**-**4** and **6**-**9**.

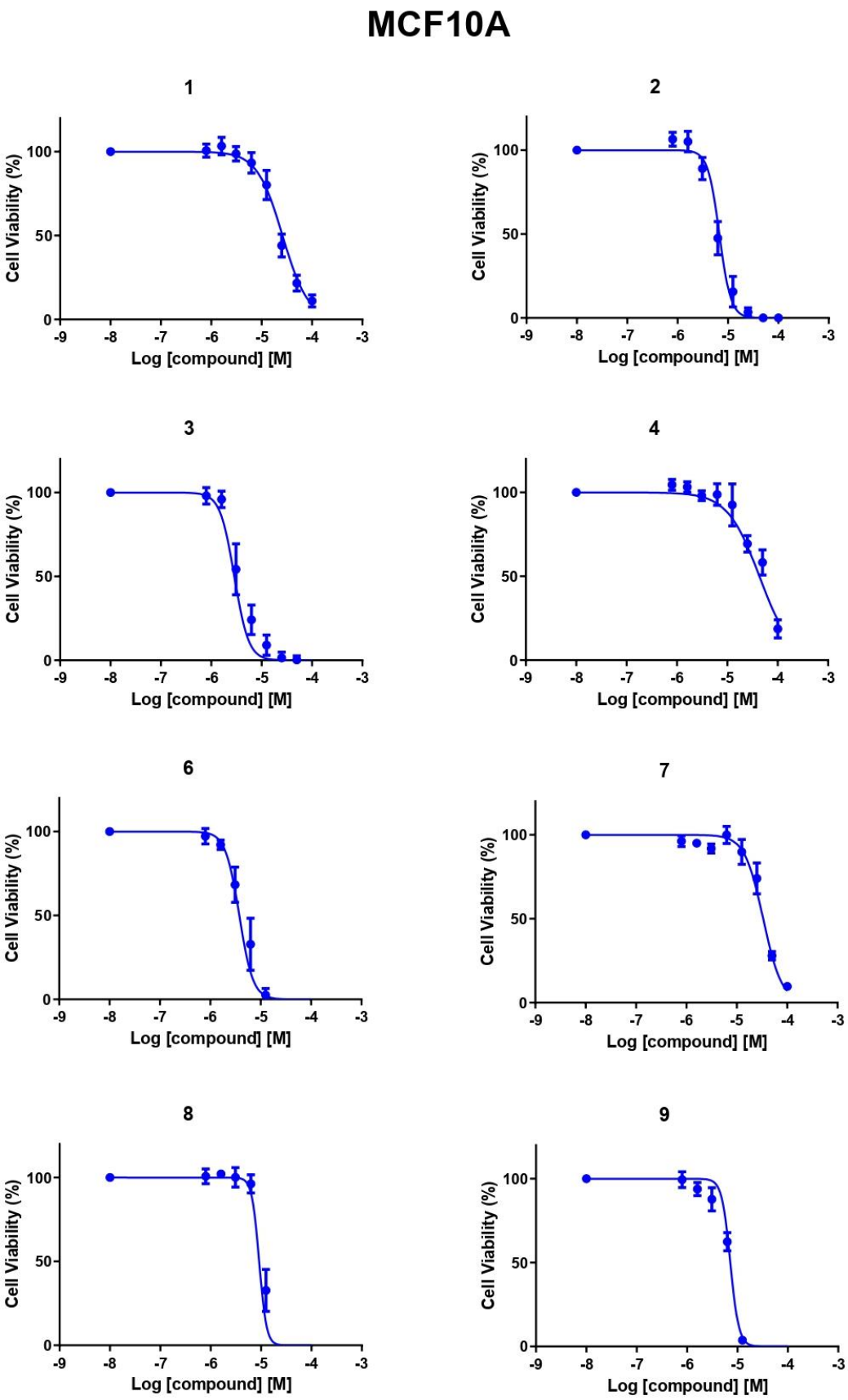

Figure S168. Cell viability in the MCF-10A human mammary epithelial cell line in the presence of different concentrations of compounds **1**-**4** and **6**-**9**.